

Department of Mathematics
University of Fribourg (Switzerland)

On the existence and growth properties of hyperbolic Coxeter groups

THESIS

presented to the Faculty of Science and Medicine of the University of
Fribourg (Switzerland)
in consideration for the award of the academic grade of
Doctor of Philosophy in Mathematics

by

Naomi Bredon

from

France

Thesis No: 8046
Uniprint Fribourg
2024

Accepted by the Faculty of Science and Medicine of the University of Fribourg (Switzerland) upon the recommendation of the jury:

Prof. Dr. Anand Dessai
University of Fribourg (Switzerland), President of the jury

Prof. Dr. Ruth Kellerhals
University of Fribourg (Switzerland), Thesis supervisor

Prof. Dr. Yohei Komori
Waseda University (Japan), External expert

Dr. Jean Raimbault
University of Aix- Marseille (France), External expert

Prof. Dr. Pavel Tumarkin
Durham University (United Kingdom), External expert

Fribourg, 12.09.2024

Thesis supervisor

Dean

Prof. Dr. Ruth Kellerhals

Prof. Dr. Ulrich Ultes-Nitsche

ABSTRACT

A Coxeter polyhedron in \mathbb{H}^n is a convex polyhedron of finite volume all of whose dihedral angles are integral submultiples of π . The group generated by the reflections in the facets of a hyperbolic Coxeter polyhedron is called a hyperbolic Coxeter group. While hyperbolic Coxeter polyhedra exist only for $n \leq 995$, they are far from being classified for dimensions beyond 3.

In this thesis, we study hyperbolic Coxeter polyhedra and their reflection groups from two different point of views.

In the first part of our work, we consider Coxeter polyhedra with mutually intersecting facets all of whose dihedral angles are $\frac{\pi}{2}$, $\frac{\pi}{3}$ and (at least one) $\frac{\pi}{6}$. Since their associated hyperbolic Coxeter groups satisfy a crystallographic condition, we call them ADEG-polyhedra. Our first main result provides the classification of all ADEG-polyhedra in \mathbb{H}^n . We discover a new polyhedron P_\star in \mathbb{H}^9 , and present various of its properties. Furthermore, for $n \geq 7$, we show that Coxeter polyhedra in \mathbb{H}^n with mutually intersecting facets have dihedral angles of the form $\frac{\pi}{m}$ with $m \leq 6$, only.

In the second part of our work, we study growth minimality properties of Coxeter groups acting on \mathbb{H}^n for dimensions $n \geq 4$. To this end, we establish a new method to identify the groups realizing smallest growth rate and exploit it subsequently by distinguishing between the cocompact and the non-cocompact cases. One of our results concerns the cocompact case and dimensions $n = 4$ and 5 while the other result describes the non-cocompact case and dimensions $4 \leq n \leq 9$. In both settings, we are able to identify the Coxeter groups of minimal growth rate. It turns out that they are all intimately related to the fundamental groups of (compact arithmetic resp. cusped) hyperbolic n -orbifolds of minimal volume.

RÉSUMÉ

Un polyèdre de Coxeter dans \mathbb{H}^n est un polyèdre convexe de volume fini dont tous les angles dièdres sont des sous-multiples entiers de π . Le groupe engendré par les réflexions par rapport aux facettes d'un polyèdre de Coxeter hyperbolique est appelé un groupe de Coxeter hyperbolique. Bien qu'il soit établi que les polyèdres de Coxeter hyperboliques existent seulement pour $n \leq 995$, ils sont loin d'être classifiés au delà de la dimension 3.

Cette thèse porte sur l'étude des polyèdres de Coxeter hyperboliques et leurs groupes de réflexions selon deux points de vue différents.

Dans la première partie de notre travail, nous considérons des polyèdres de Coxeter hyperboliques dont toutes les facettes s'intersectent, et ce, en des angles dièdres $\frac{\pi}{2}$, $\frac{\pi}{3}$ et (au moins un) $\frac{\pi}{6}$. Les groupes de Coxeter associés à de tels polyèdres satisfont une condition crystallographique, et nous les baptisons polyèdres ADEG. Notre premier résultat principal établit la classification complète des polyèdres ADEG. Nous découvrons un nouveau polyèdre P_\star dans \mathbb{H}^9 , et présentons plusieurs de ses propriétés. De plus, nous montrons que, pour $n \geq 7$, les polyèdres de Coxeter dont toutes les facettes s'intersectent ont des angles dièdres de la forme $\frac{\pi}{m}$ pour $m \leq 6$ seulement.

Dans la seconde partie de notre travail, nous étudions la propriété de croissance minimale des groupes de Coxeter de covolume fini agissant sur \mathbb{H}^n pour $n \geq 4$. Pour cela, nous établissons une nouvelle méthode pour identifier les groupes dont le taux de croissance est minimal. Nous exploitons cette méthode en distinguant les cas cocompact et non-cocompact.

Un de nos résultats concerne le cas cocompact en dimension $n = 4$ et 5, tandis que notre autre résultat porte sur le cas non-cocompact pour $4 \leq n \leq 9$. Dans les deux cas, nous identifions les groupes de Coxeter de plus petit taux de croissance. Ces derniers sont en fait étroitement liés aux groupes fondamentaux des n -orbivariétés (compactes arithmétiques, respectivement cuspidées) hyperboliques de volume minimal.

ZUSAMMENFASSUNG

Ein Coxeter-Polyeder in \mathbb{H}^n ist ein konvexes Polyeder von endlichem Volumen, dessen Diederwinkel ganzzahlige Teiler von π sind. Die Gruppe, die durch die Spiegelungen in den Facetten eines hyperbolischen Coxeter-Polyeders erzeugt wird, heisst eine hyperbolische Coxeter-Gruppe. Während hyperbolische Coxeter-Polyeder nur für $n \leq 995$ existieren, ist man dennoch weit entfernt von deren Klassifikation jenseits der Dimension drei.

In dieser Arbeit untersuchen wir hyperbolische Coxeter-Polyeder und deren Spiegelungsgruppen aus zwei verschiedenen Blickwinkeln. Im ersten Teil unserer Arbeit betrachten wir Coxeter-Polyeder mit sich gegenseitig schneidenden Facetten, deren Diederwinkel alle gleich $\frac{\pi}{2}$, $\frac{\pi}{3}$ und (mindestens einem) $\frac{\pi}{6}$ sind. Da ihre zugehörigen hyperbolischen Coxeter-Gruppen eine kristallographische Bedingung erfüllen, nennen wir sie ADEG-Polyeder. Unser erstes Hauptergebnis liefert die Klassifikation aller ADEG-Polyeder in \mathbb{H}^n . Dabei entdecken wir ein neues Polyeder P_* in \mathbb{H}^9 und präsentieren verschiedene seiner Eigenschaften. Ausserdem zeigen wir für $n \geq 7$, dass Coxeter-Polyeder in \mathbb{H}^n mit sich gegenseitig schneidenden Facetten nur Diederwinkel der Form $\frac{\pi}{m}$ mit $m \leq 6$ haben können.

Im zweiten Teil unserer Arbeit untersuchen wir die Eigenschaft des minimalen Wachstums für Coxeter-Gruppen, die auf \mathbb{H}^n für Dimensionen $n \geq 4$ operieren. Zu diesem Zweck etablieren wir eine neue Methode, um die Gruppen mit minimaler Wachstumsrate zu identifizieren, und wenden diese anschliessend an, indem wir zwischen dem kokompakten und dem nicht kokompakten Fall unterscheiden.

Eines unserer beiden Ergebnisse betrifft den kokompakten Fall und die Dimensionen $n = 4$ und 5 , während das andere Ergebnis den nicht-kokompakten Fall und die Dimensionen $4 \leq n \leq 9$ behandelt. In beiden Fällen sind wir in der Lage, die Coxeter-Gruppen mit minimaler Wachstumsrate zu identifizieren. Es stellt sich heraus, dass sie alle eng mit den Fundamentalgruppen von (kompakten arithmetischen bzw. gespitzten) hyperbolischen n -Orbifolds von minimalem Volumen verknüpft sind.

REMERCIEMENTS

Je tiens à exprimer ma profonde gratitude envers Ruth Kellerhals pour son soutien et ses conseils avisés tout au long de l'écriture de ce manuscrit. Ce fût un honneur de travailler avec elle, et je garderai en mémoire nos nombreux échanges stimulants, nos excursions mathématiques, et tout ce que j'ai appris à ses côtés. Son expérience a grandement contribué au développement de mes compétences ces dernières années, sur les plans académique, professionnel, et même personnel. Pour tout cela, je lui suis infiniment reconnaissante.

Je remercie les membres du jury Yohei Komori, Jean Raimbault et Pavel Tumarkin d'avoir accepté de constituer le jury et pour leur soutien dans mon projet. J'aimerais aussi remercier Anand Dessai qui préside le jury.

Ma gratitude s'étend également envers ma famille pour leur écoute et leurs nombreux encouragements. Merci à vous mes chers parents, mes chères sœurs et mon cher frère, pour votre soutien inébranlable. Plus largement, je remercie mes amis, d'ici et d'ailleurs, et tous ceux qui m'ont accompagnée dans cette aventure.

Quant à chacun des membres du département, et à ceux d'autres instituts, qui ont croisé ma route, merci pour ces moments de convivialité. Finalement, merci à mes étudiants pour leur dynamisme et leur investissement, vos questionnements m'ont moi-même souvent enrichie. Vous tous avez contribué à rendre chaque étape de ce voyage mémorable et significative.

Merci à chacun d'entre vous

TABLE OF CONTENTS

INTRODUCTION		1
I	PRELIMINARIES	5
1	COXETER GROUPS AND COXETER POLYHEDRA	6
1	Geometric spaces of constant curvature	6
2	Hyperplanes, polyhedra and Gram matrix	9
3	Abstract and geometric Coxeter groups	14
3.1	The Coxeter diagram of a Coxeter group	16
3.2	Spherical and Euclidean Coxeter groups	17
3.3	Hyperbolic Coxeter groups	18
2	ROOT SYSTEMS AND FUNDAMENTAL WEIGHTS	24
1	Root systems and Weyl groups	24
2	Dynkin diagrams and extended Dynkin diagrams	27
3	Classification of root systems of type A , D , E and G_2	27
II	ON THE EXISTENCE OF HYPERBOLIC COXETER GROUPS	32
3	SOME CLASSIFICATION RESULTS	33
1	In low dimensions	34
2	In higher dimensions	37
2.1	Coxeter polyhedra with a small number of facets	37
2.2	Coxeter polyhedra with mutually intersecting facets	42

4	COXETER POLYHEDRA WITH DIHEDRAL ANGLES $\frac{\pi}{2}, \frac{\pi}{3}$ AND $\frac{\pi}{6}$	45
1	The general strategy	48
2	Proof of the main theorem	49
	2.1 First steps	49
	2.2 Existence of a component \tilde{G}_2	50
	2.3 From a G_2 -face to an admissible set of vectors	50
	2.4 The classification of ADEG-polyhedra	55
3	Further results and comments	69
	3.1 Properties of the polyhedron P_\star	69
	3.2 An angular obstruction	73
III ON THE GROWTH RATES OF HYPERBOLIC COXETER GROUPS		74
5	THE GROWTH RATES OF COXETER GROUPS	75
1	Growth series and growth rates	75
2	About the arithmetic nature of growth rates	80
3	Comparing growth rates	82
	3.1 Partial order and growth monotonicity	82
	3.2 A useful lemma	85
6	MINIMAL GROWTH RATES FOR HYPERBOLIC COXETER GROUPS	87
1	In low dimensions	88
2	In higher dimensions	89
3	Proofs of the two main results	90
	3.1 The cocompact case	91
	3.2 The non-cocompact case	92
IV APPENDICES		95
A DATA FOR PROKHOROV'S FORMULA		96
B ADMISSIBLE PAIRS		98
C NORMAL VECTORS AND VINBERG FORM		114
D THE TWO REPRINTS		119
BIBLIOGRAPHY		148

INTRODUCTION

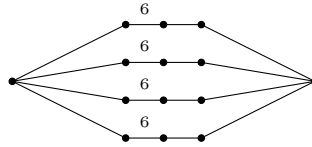
Let \mathbb{H}^n be the hyperbolic space of dimension $n \geq 2$. A Coxeter polyhedron $P \subset \mathbb{H}^n$ is a convex polyhedron of finite volume all of whose dihedral angles are integer submultiples of π . Associated with P is the discrete group $\Gamma(P)$ in $\text{Isom}\mathbb{H}^n$ generated by the reflections in the facets of P . Such groups are called hyperbolic Coxeter groups and form a natural but important family of transformation groups arising in several different contexts, ranging from algebra, geometry to topology. However, in contrast to the Euclidean and the spherical cases, hyperbolic Coxeter polyhedra are far from being entirely understood.

Our thesis is devoted to this theme and consists of three parts. While Part I contains the preparatory material, our two key achievements are presented in Part II and in Part III.

Firstly, we consider a class of Coxeter polyhedra in \mathbb{H}^n with prescribed combinatorial and angular structure. In fact, instead of fixing the number of their facets in terms of the dimension n , as happened often in works of other authors, we suppose that the polyhedra have mutually intersecting facets and dihedral angles given by $\frac{\pi}{2}$, $\frac{\pi}{3}$ and (at least one) $\frac{\pi}{6}$. Motivated by work of Prokhorov, and in view of their relation to crystallographic Coxeter groups of type A, D, E and G_2 , we call them ADEG-polyhedra. Our central result can be stated as follows.

Theorem. *Let $P \subset \mathbb{H}^n$ be an ADEG-polyhedron. Then, P is one of the 24 Coxeter polyhedra depicted in Table 4.0.1. In particular, P is non-compact for $n > 2$, non-simple for $n > 3$, and P is of dimension $n \leq 11$. Furthermore, P is combinatorially equal to one of the following polyhedra.*

-
- ✧ P is a triangle.
 - ✧ P is a tetrahedron.
 - ✧ P is a doubly-truncated 5-simplex.
 - ✧ P is a pyramid over a product of two or three simplices.
 - ✧ P is the polyhedron $P_\star \subset \mathbb{H}^9$ with 14 facets depicted as follows.



The polyhedron $P_\star \subset \mathbb{H}^9$ is a new discovery, and it is given here by its Coxeter diagram. Such a diagram can be read as follows. The nodes correspond to facets, and they are joined by a simple edge or an edge with label $m \geq 4$ if the facets are not orthogonal but intersect under the angle $\frac{\pi}{3}$ or $\frac{\pi}{m}$, respectively.

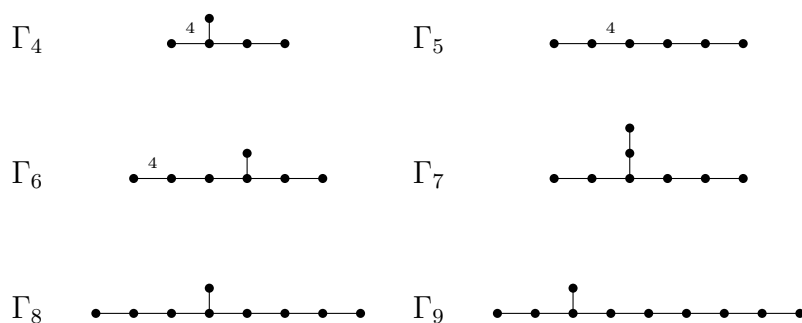
The proof of the classification theorem above is in parts based on Prokhorov's work in the ADE-case and given in Chapter 4. Of fundamental importance to us are the results of Felikson and Tumarkin characterizing the combinatorics of Coxeter polyhedra with mutually intersecting facets, as well as Borcherds' theorem helping us to identify faces of codimension two as Coxeter polyhedra.

At the end of Part II, we present a few properties of P_\star and of its associated Coxeter group $\Gamma_\star = \Gamma(P_\star)$. We show that its volume is a rational multiple q of $\zeta(5)/22, 295, 347, 200$ with $q \in \mathbb{Q}_{>1}$. Moreover, the group Γ_\star is arithmetic (over \mathbb{Q}), and its commensurability class contains all Coxeter simplex groups and all Coxeter pyramid groups as well as the group related to Prokhorov's ADE-polyhedron.

Let us add that our proof methods are general and can be applied to Coxeter polyhedra with mutually intersecting facets and for any set of dihedral angles. However, as we proved in Proposition 4.3.3, the dihedral angles of Coxeter polyhedra with mutually intersecting facets of dimensions beyond 6 must be of the form $\frac{\pi}{m}$ with $m \leq 6$. Although a complete classification of these polyhedra can therefore be realized in finite time and for all dimensions, we did not pursue this direction of research.

Secondly, we present in Part III our results about hyperbolic Coxeter groups of minimal growth rate in dimensions beyond three. Since these results have

already been published at an earlier stage of this thesis work, we are content to summarize them in a condensed but nevertheless complete way. The first result¹ in this context is given by Theorem 6.2.1 and identifies the cocompact hyperbolic Coxeter groups of minimal growth rate in dimensions $n = 4$ and 5. More precisely, for dimension 4, it is the group Γ_4^c associated with the compact simplex with Coxeter symbol $[5, 3, 3, 3]$ while for dimension 5, it is the group Γ_5^c associated with the compact prism with Coxeter symbol $[5, 3, 3, 3, 3, \infty]$. The second result², given by Theorem 6.2.2, identifies the non-cocompact hyperbolic Coxeter groups of minimal growth rate in dimensions $4 \leq n \leq 9$. The minimizing groups Γ_n are depicted below.



In both cases, the minimizers are unique and closely related to the fundamental groups of compact arithmetic and cusped hyperbolic n -orbifolds of minimal volume, respectively.

The work finishes with several appendices. Appendix A and Appendix B display some material and lists in connection with the proof of the above Theorem. Appendix C contains the technical details relevant for the proof of Proposition 4.3.1 about the commensurability class of Γ_* . Lastly, the two articles mentioned above constitute Appendix D. Let us indicate that we contributed significantly to the research in our joint work with Ruth Kellerhals.

¹N. Bredon, R. Kellerhals, *Hyperbolic Coxeter groups and minimal growth rates in dimensions four and five*, Groups Geom. Dynamics 16 (2022), 725–741.

²N. Bredon, *Hyperbolic Coxeter groups of minimal growth rates in higher dimensions*, Canad. Math. Bull. 66 (2023), 232–242.

PART I:

PRELIMINARIES

In our times, geometers are still exploring those new Wonderlands, partly for the sake of their applications to cosmology and other branches of science, but much more for the sheer joy of passing through the looking glass into a land where the familiar lines, planes, triangles, circles and spheres are seen to behave in strange but precisely determined ways.

H. S. M. COXETER

CHAPTER 1

COXETER GROUPS AND COXETER POLYHEDRA

Let \mathbb{X}^n be a geometric space of dimension $n \geq 2$ and of constant sectional curvature $0, 1$ or -1 . Let $\text{Isom}\mathbb{X}^n$ be the isometry group of \mathbb{X}^n . We are interested in discrete groups in $\text{Isom}\mathbb{H}^n$ generated by finitely many reflections with respect to hyperplanes of \mathbb{X}^n .

For their characterization, we first present vector models for the spaces \mathbb{X}^n . Our interest lies especially in the case $\mathbb{X}^n = \mathbb{H}^n$. After that, we describe hyperplanes and polyhedra in \mathbb{X}^n . Then, we introduce the important notion of Coxeter groups. We first consider them as abstract objects, and then represent some of them as *geometric* Coxeter groups, that is, Coxeter groups realized as discrete subgroups of $\text{Isom}\mathbb{X}^n$ generated by reflections in hyperplanes in \mathbb{X}^n . We characterize geometric Coxeter groups in terms of their Coxeter diagrams and by means of the Gram matrix of their fundamental polyhedra.

As general references for this chapter, we quote [16, 37, 82, 83, 84].

1 Geometric spaces of constant curvature

Let $n \geq 2$. The only simply connected complete Riemannian manifolds of constant sectional curvature of dimension n are, up to isometry, the Euclidean space \mathbb{E}^n , the sphere \mathbb{S}^n and the hyperbolic space \mathbb{H}^n . In what follows, we consider each of these spaces as a metric space.

Denote by $K \in \{0, 1, -1\}$ the constant sectional curvature of the space \mathbb{X}^n .

1. Geometric spaces of constant curvature

For $x = (x_1, x_2, \dots, x_{n+1})$ and $y = (y_1, y_2, \dots, y_{n+1}) \in \mathbb{R}^{n+1}$, define the bilinear form

$$\langle x, y \rangle_K := \sum_{i=1}^n x_i y_i + K x_{n+1} y_{n+1} .$$

We denote by $\|\cdot\|_K$ the associated (pseudo-)norm. If the context is clear, we simply write $\langle \cdot, \cdot \rangle := \langle \cdot, \cdot \rangle_K$ and $\|\cdot\| := \|\cdot\|_K$.

The bilinear form $\langle \cdot, \cdot \rangle_0$ is positive semidefinite, and the bilinear form $\langle \cdot, \cdot \rangle_1$ is positive definite. The bilinear form $\langle \cdot, \cdot \rangle_{-1}$ is indefinite of signature $(n, 1)$, and it is called the *Lorentzian form*.

The spaces \mathbb{X}^n admit the following linear models.

(i) We identify the space \mathbb{E}^n with the hyperplane

$$\mathbb{E}^n = \{x \in \mathbb{R}^{n+1} \mid x_{n+1} = 0\}$$

in \mathbb{R}^{n+1} . It is naturally endowed with the metric $d_{\mathbb{E}}(x, y) = \sqrt{\langle x - y, x - y \rangle_0}$ for any $x, y \in \mathbb{E}^n$.

(ii) The space \mathbb{S}^n is given by

$$\mathbb{S}^n = \{x \in \mathbb{R}^{n+1} \mid \langle x, x \rangle_1 = 1\} ,$$

together with the usual angular metric $d_{\mathbb{S}}(x, y) = \arccos \langle x, y \rangle_1$ for $x, y \in \mathbb{S}^n$.

(iii) Denote by $\mathbb{R}^{n,1}$ the Lorentz-Minkowski space, that is, the space \mathbb{R}^{n+1} endowed with the Lorentzian product $\langle \cdot, \cdot \rangle_{-1}$; see Figure 1.1.1.

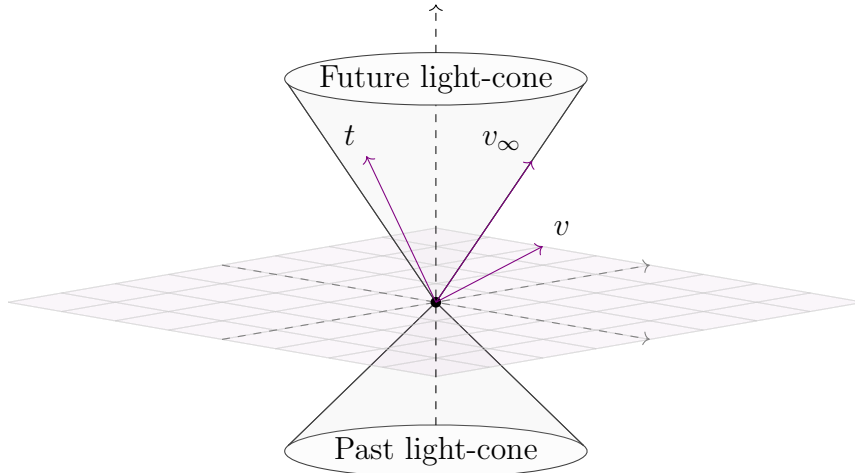


Figure 1.1.1: The Lorentz-Minkowski space $\mathbb{R}^{n,1}$

A vector $v \in \mathbb{R}^{n,1} \setminus \{0\}$ is said to be

- *spacelike* if $\langle v, v \rangle_{-1} > 0$,
- *timelike* if $\langle v, v \rangle_{-1} < 0$,
- *lightlike* if $\langle v, v \rangle_{-1} = 0$.

In Figure 1.1.1, we depict a spacelike vector v , a timelike vector t , and a lightlike vector v_∞ in the Lorentz-Minkowski space $\mathbb{R}^{n,1}$.

We usually identify the hyperbolic space \mathbb{H}^n as the upper shell \mathcal{H}^n of the two-sheeted hyperboloid in \mathbb{R}^{n+1} , that is,

$$\mathbb{H}^n = \{x \in \mathbb{R}^{n+1} \mid \langle x, x \rangle_{-1} = -1, x_{n+1} > 0\}, \quad (1.1)$$

with the metric $d(x, y) = d_{\mathbb{H}}(x, y) = \operatorname{arccosh}(-\langle x, y \rangle_{-1})$ for any $x, y \in \mathbb{H}^n$.

The *boundary* of \mathbb{H}^n , denoted by $\partial\mathbb{H}^n$, can then be identified with

$$\partial\mathbb{H}^n = \{x \in \mathbb{R}^{n+1} \mid \langle x, x \rangle_1 = 1, \langle x, x \rangle_{-1} = 0, x_{n+1} \geq 0\}. \quad (1.2)$$

We denote the compactification of \mathbb{H}^n by $\overline{\mathbb{H}^n} = \mathbb{H}^n \cup \partial\mathbb{H}^n$.

Let us mention that in this linear model, the volume element of \mathbb{H}^n is given by

$$\operatorname{dvol}_n = \frac{dx_1 \cdots dx_n}{\sqrt{1 + x_1^2 + \dots + x_n^2}}.$$

A point $p \in \mathbb{H}^n$ is called an *ordinary* point, and a point $q \in \partial\mathbb{H}^n$ is called an *ideal* point. A metric sphere centered at an ordinary point p carries a spherical structure in a natural way. A metric sphere internally tangent to an ideal point q carries a Euclidean structure and is called a *horosphere* S_q centered at q . Horospheres as Euclidean spaces are best treated in the upper half space model $\mathcal{U}^n = \{x \in \mathbb{R}^n \mid x_n = 0\}$ endowed with the metric $ds_{\mathcal{U}}^2 = \frac{dx_1^2 + \dots + dx_n^2}{x_n^2}$. Indeed, a horosphere centered at $q = \infty$ is a hyperplane $H_t = \{x_n = t\}$, $t > 0$, with induced metric $ds_{\mathcal{U}}^2|_{H_t} = \frac{1}{t^2}(dx_1^2 + \dots + dx_{n-1}^2)$.

Let us emphasize that the group $O(n, 1)$ of Lorentzian matrices acting by isometries on $\mathbb{R}^{n,1}$ admits four connected components. Among them, the subgroup $O^+(n, 1)$ of *positive* Lorentz-matrices preserves each of the two sheets of the hyperboloid. It can be verified that the group $\operatorname{Isom}\mathbb{H}^n$ is isomorphic to $O^+(n, 1)$.

In order to complete the picture, let us mention the well-known projective model that will also be useful to describe \mathbb{H}^n . For

$$\mathcal{C} := \{x \in \mathbb{R}^{n+1} \mid \langle x, x \rangle_{-1} < 0, x_{n+1} > 0\}, \quad (1.3)$$

we have the isometry

$$\mathbb{H}^n \cong \mathcal{C}/\mathbb{R}_+ . \quad (1.4)$$

In this way, we interpret \mathbb{H}^n as space of classes represented by timelike rays of the future light-cone \mathcal{C} of $\mathbb{R}^{n,1}$. Similarly, any point on the boundary $\partial\mathbb{H}^n$ can be identified with a lightlike ray belonging to $\partial\mathcal{C}$.

2 Hyperplanes, polyhedra and Gram matrix

Assume that $\mathbb{X}^n = \mathbb{E}^n, \mathbb{S}^n$ or \mathbb{H}^n . It is well known that any element of $\text{Isom}\mathbb{X}^n$ can be written as a finite product of hyperplane reflections. Any hyperplane in \mathbb{X}^n separates the space into two closed convex half-spaces, and there is a reflection which fixes the hyperplane and exchanges the two half spaces. In this section, we start with the description of hyperplanes in \mathbb{X}^n , and then characterize convex polyhedra in \mathbb{X}^n .

In \mathbb{E}^n , a hyperplane is an affine hyperplane given by a normal vector $v \in \mathbb{S}^{n-1}$ and a translational vector $u \in \mathbb{E}^n$ as follows.

$$H_{u,v} = \{x \in \mathbb{E}^n \mid \langle x, v \rangle_1 = 0\} + u .$$

Observe that each $H_{u,v}$ is isomorphic to $H_v := H_{0,v}$.

For a hyperplane H_v in \mathbb{E}^n , the reflection s_v with respect to H_v is given by

$$s_v(x) = x - 2 \frac{\langle v, x \rangle}{\|v\|^2} v , \quad x \in \mathbb{E}^n . \quad (1.5)$$

For any two unit vectors $v_1, v_2 \in \mathbb{E}^n$, we say that the hyperplanes H_{v_1} and H_{v_2} are *parallel* if and only if $\langle v_1, v_2 \rangle_1 = -1$. For $H_{v_1} \cap H_{v_2} \neq \emptyset$, the dihedral angle $\angle(H_{v_1}, H_{v_2})$ is given by

$$\cos \angle(H_{v_1}, H_{v_2}) = -\langle v_1, v_2 \rangle_1 .$$

In the case of constant curvature $K \neq 0$, given a vector $v \in \mathbb{R}^{n+1}$ such that $\langle v, v \rangle_K = 1$, its *orthogonal complement* is given by

$$X_v = v^\perp := \{x \in \mathbb{R}^{n+1} \mid \langle x, v \rangle_K = 0\} . \quad (1.6)$$

The intersection $H_v := X_v \cap \mathbb{X}^n$ gives a hyperplane in \mathbb{X}^n with normal vector v . Any hyperplane of \mathbb{X}^n is obtained in such a way. If not otherwise stated, we always assume v to be a unit vector. For a hyperplane H_v in \mathbb{X}^n , we can associate the (oriented) closed half-space

$$H_v^- := \{x \in \mathbb{X}^n \mid \langle x, v \rangle_K \leq 0\} ,$$

bounded by H_v , and where v is pointing outwards.

The reflection s_v with respect to H_v given by

$$s_v(x) = x - 2\langle v, x \rangle v \quad , x \in \mathbb{X}^n \quad ,$$

is an isometry of \mathbb{X}^n .

◇ If $\mathbb{X}^n = \mathbb{S}^n$, any two spherical hyperplanes H_{v_1}, H_{v_2} intersect in \mathbb{S}^n . Their dihedral angle is given by

$$\cos \angle(H_{v_1}, H_{v_2}) = -\langle v_1, v_2 \rangle_1 \quad .$$

◇ If $\mathbb{X}^n = \mathbb{H}^n$, two hyperbolic hyperplanes H_{v_1}, H_{v_2} intersect inside \mathbb{H}^n if and only if

$$|\langle v_1, v_2 \rangle_{-1}| < 1 \quad .$$

Furthermore, their dihedral angle is given by

$$\cos \angle(H_{v_1}, H_{v_2}) = -\langle v_1, v_2 \rangle_{-1} \quad . \tag{1.7}$$

Two hyperbolic hyperplanes H_{v_1}, H_{v_2} intersect at a point on the boundary $\partial\mathbb{H}^n$, and are called (hyperbolic-) *parallel*, if and only if $|\langle v_1, v_2 \rangle_{-1}| = 1$. This condition is equivalent to the fact that H_{v_1} and H_{v_2} intersect at a dihedral angle 0.

Lastly, two hyperplanes H_{v_1} and H_{v_2} do not intersect in $\overline{\mathbb{H}^n} = \partial\mathbb{H}^n \cup \mathbb{H}^n$ if and only if $|\langle v_1, v_2 \rangle_{-1}| > 1$. In this case, they are called *ultraparallel*, and they give rise to a unique hyperbolic line L orthogonal to both of them. The distance between H_{v_1} and H_{v_2} is then given by

$$\cosh d(H_{v_1}, H_{v_2}) = |\langle v_1, v_2 \rangle_{-1}| \quad .$$

Observe that we have $\langle v_1, v_2 \rangle_{-1} < 0$ if and only if v_1 and v_2 are of opposite orientation.

Let k be a positive integer. For a k -dimensional vector subspace $V \subset \mathbb{R}^{n,1}$, V is called *hyperbolic* if it has nonempty intersection with \mathbb{H}^n . More specifically, the intersection $V \cap \overline{\mathbb{H}^n}$ is a hyperbolic $(k - 1)$ -plane. In a similar way, $V \subset \mathbb{R}^{n,1}$ is *elliptic* if $V \cap \mathbb{H}^n$ is empty, and it is *parabolic* in the remaining case.

It is not difficult to see but important to note that the orthogonal complement of V is elliptic if and only if V is hyperbolic. In particular, a hyperplane H_v is hyperbolic if and only if the normal vector v is spacelike.

The following elementary lemma will be useful later on.

Lemma 1.2.1. *Any two Lorentz-orthogonal lightlike vectors are collinear.*

Proof. Assume that $v, v' \in \mathbb{R}^{n,1}$ are two Lorentz-orthogonal lightlike vectors. Let w be a timelike vector of squared norm -1 . Then, the Lorentz-Minkowski space $\mathbb{R}^{n,1}$ decomposes as $\mathbb{R}w \oplus w^\perp$. Hence, there exist $\lambda, \lambda' \in \mathbb{R} \setminus \{0\}$ and two spacelike vectors $x, x' \in \mathbb{R}^{n,1}$ such that $v = \lambda w + x$ and $v' = \lambda' w + x'$. Since $\langle v, w \rangle = \lambda \langle w, w \rangle + \langle x, w \rangle = -\lambda$, we derive that

$$\begin{aligned} \langle x, x \rangle &= \langle v - \lambda w, v - \lambda w \rangle \\ &= \langle v, v \rangle - \lambda^2 \langle w, w \rangle \\ &= \lambda^2 \end{aligned}$$

and, similarly, $\langle x', x' \rangle = \lambda'^2$ and $\langle x, x' \rangle = \lambda \lambda'$. Now, one has

$$\langle \lambda' x - \lambda x', \lambda' x - \lambda x' \rangle = \lambda'^2 \langle x, x \rangle + \lambda^2 \langle x', x' \rangle - 2\lambda \lambda' \langle x, x' \rangle = 0 .$$

It follows that $\lambda' x - \lambda x' = 0$, as $\lambda' x - \lambda x'$ belongs to the elliptic subspace w^\perp . Therefore,

$$\lambda' v - \lambda v' = \lambda x' - \lambda' x = 0 .$$

□

Now, we introduce the important concept of (convex) polyhedra in \mathbb{X}^n as follows.

Definition 1.2.2. A *polyhedron* of dimension n or an *n-polyhedron* $P \subset \mathbb{X}^n$ is the non-empty intersection of finitely many closed half spaces $H_{v_i}^-$ in \mathbb{X}^n bounded by $N \geq n + 1$ hyperplanes H_{v_i} in \mathbb{X}^n , that is,

$$P = \bigcap_{i=1}^N H_{v_i}^- . \tag{1.8}$$

In the sequel, we often suppose $P \subset \mathbb{X}^n$ to be of dimension n . By construction, P is convex and entirely determined by its normal vectors up to isometry.

The *dihedral angles* of P are the angles associated with the normal vectors of two intersecting hyperplanes in the boundary of P ; see (1.7).

Depending on whether $\mathbb{X}^n = \mathbb{E}^n, \mathbb{S}^n$ or \mathbb{H}^n , a polyhedron $P \subset \mathbb{X}^n$ given by (1.8) is said to be *Euclidean*, *spherical*, or *hyperbolic*. In what follows, we assume polyhedra to have finite volume, except if mentioned otherwise. Observe that a polyhedron $P \subset \mathbb{H}^n$ is of finite volume if and only if P is the (hyperbolically) convex hull of finitely many points in $\overline{\mathbb{H}^n}$.

Definition 1.2.3. For $0 \leq k \leq n - 1$, a k -face of P is the non-empty intersection of $n - k$ bounding hyperplanes of P with \mathbb{H}^n . A *facet* of P is a $(n - 1)$ -face of P , an *edge* is a 1-face of P , and an *ordinary vertex* is a 0-face of P .

Definition 1.2.4. An ideal point $q \in \partial\mathbb{H}^n$ is an *ideal vertex* of $P \subset \mathbb{H}^n$ if $q \in \overline{P}$ and the intersection $P \cap S_q$ of P with a sufficiently small horosphere S_q centered at q is compact when considered as an $(n - 1)$ -dimensional Euclidean polyhedron.

Remark 1.2.5. As a consequence of the famous volume differential formula of Schläfli, the volume of a hyperbolic polyhedron P is a monotonously decreasing function with respect to each dihedral angle of P ; see [47] for example.

For completeness, let us introduce the f -vector of a polyhedron $P \subset \mathbb{X}^n$.

Definition 1.2.6. Let $P \subset \mathbb{X}^n$ be a polyhedron, and let f_k be the number of k -faces of P . The f -vector of P is the vector given by

$$(f_0, \dots, f_{n-1}) .$$

By the celebrated formula of Euler-Schläfli, we have the following result.

Proposition 1.2.7. *Let $P \subset \mathbb{X}^n$ be a polyhedron. Then,*

$$\sum_{k=0}^{n-1} (-1)^k f_k = 1 - (-1)^n .$$

Next, we introduce a very useful tool for the characterization of a polyhedron in \mathbb{X}^n , its *Gram matrix*.

Definition 1.2.8. Let $P \subset \mathbb{X}^n$ be a polyhedron as given by (1.8). The *Gram matrix* $Gr(P)$ of P is the Gram matrix of the system of unit normal vectors $\{v_1, \dots, v_N\}$ given by

$$Gr(P) = (g_{ij})_{1 \leq i, j \leq N} \text{ where } g_{ij} := \langle v_i, v_j \rangle_K .$$

Remark 1.2.9. As defined above, $Gr(P)$ is a real symmetric matrix with diagonal entries equal to 1. At times, we use a different normalization of the vectors v_i in order to get a matrix with integer coefficients.

A polyhedron P is said to be *non-degenerate* if its bounding hyperplanes do not share a common point, and there is no hyperplane orthogonal to all of them. A non-degenerate polyhedron is said to be *indecomposable* if and only if its Gram matrix $Gr(P)$ is indecomposable in the classical sense. Observe that any hyperbolic polyhedron of finite volume is indecomposable.

From now on we focus on *acute-angled* polyhedra, that is, polyhedra whose bounding hyperplanes either intersect at a dihedral angle not exceeding $\frac{\pi}{2}$ or are disjoint.

Assume that $P \subset \mathbb{X}^n$ is a non-degenerate indecomposable acute-angled polyhedron. Depending on \mathbb{X}^n , we have the following characterization of the Gram matrix $Gr(P)$.

- For $\mathbb{X}^n = \mathbb{E}^n$, $Gr(P)$ is positive semi-definite of rank n .
- For $\mathbb{X}^n = \mathbb{S}^n$, $Gr(P)$ is positive definite of rank $n + 1$.
- For $\mathbb{X}^n = \mathbb{H}^n$, $Gr(P)$ is indefinite of signature $(n, 1)$.

Observe that in the hyperbolic case, only, the matrix $Gr(P)$ of $P \subset \mathbb{H}^n$ can be *arbitrarily large* in comparison with n .

Assume that $P \subset \mathbb{X}^n$ is decomposable. For $\mathbb{X}^n = \mathbb{E}^n$, $Gr(P)$ is made of several block matrices, each one positive semi-definite of rank k_i , say, but such that $\sum_i k_i = n$. For $\mathbb{X}^n = \mathbb{S}^n$, the Gram matrix $Gr(P)$ is made of several positive definite block matrices of rank k_i such that $\sum_i k_i = n + 1$.

If a polyhedron $P \subset \mathbb{X}^n$ is bounded by precisely $N = n + 1$ hyperplanes, P is called a *simplex*.

As a consequence of the Perron-Frobenius theory, we have the following result.

Theorem 1.2.10. *Let n be a positive integer. Let $G = (g_{ij})_{1 \leq i, j \leq n+1} \in \text{Mat}(n+1, \mathbb{R})$ be an indecomposable symmetric matrix such that $g_{ii} = 1$ for $i = 1, \dots, n+1$ and such that $-1 \leq g_{ij} \leq 0$ for $1 \leq i \neq j \leq n+1$. Then, one has the following properties.*

- *If G is positive semi-definite of rank n such that, for all $1 \leq i, j \leq n+1$, the (i, j) -th cofactor of G is positive, then G is the Gram matrix of a Euclidean simplex in \mathbb{E}^n which is unique up to isometry.*
- *If $g_{ij} \neq -1$ for all $1 \leq i, j \leq n+1$, $i \neq j$, and G is positive definite, then G is the Gram matrix of a spherical simplex in \mathbb{S}^n which is unique up to isometry.*

- If G has signature $(n, 1)$ such that, for all $1 \leq i, j \leq n + 1$, the (i, j) -th cofactor of G is positive, then G is the Gram matrix of a compact hyperbolic simplex in \mathbb{H}^n which is unique up to isometry.

For the cases $\mathbb{X}^n = \mathbb{S}^n$ and \mathbb{E}^n , we cite the following additional results.

Theorem 1.2.11. *Any acute-angled non-degenerate spherical (respectively, Euclidean) polyhedron P is a simplex (respectively, a direct product of simplices).*

Let $P \subset \mathbb{H}^n$ be a polyhedron and $k \geq 1$. Each k -face F of P gives rise to a principal submatrix $Gr(F)$ of the matrix $Gr(P)$. Here, $Gr(F)$ is the matrix formed by the columns and rows corresponding to the facets of P containing F . As a consequence, there is a one-to-one correspondence between the set of k -faces of P and the set of positive definite principal submatrices of $Gr(P)$ of rank k . A similar result holds for ordinary vertices as they correspond to positive definite principal submatrices of rank n of $Gr(P)$.

Let $P \subset \mathbb{H}^n$ be acute-angled and of finite volume. An ideal vertex of P gives rise to a neighbourhood in \overline{P} that is a cone over a direct product of simplices. As a consequence, there is a one-to-one correspondence between the set of ideal vertices of P and the set of positive semi-definite principal submatrices of rank $n - 1$ of $Gr(P)$.

Finally, a vertex of a polyhedron $P \subset \mathbb{X}^n$ is said to be *simple* if it is the intersection of precisely n bounding hyperplanes of P . The polyhedron P is called *simple* if all of its vertices are simple. It follows from the above that any compact acute-angled hyperbolic polyhedron is simple.

3 Abstract and geometric Coxeter groups

Definition 1.3.1. An *abstract Coxeter group* $\Gamma = (W, S)$ of rank N is a finitely generated group W with generating set S of cardinality N and a presentation according to

$$W = \langle s_i \in S \mid s_i^2 = 1, (s_i s_j)^{m_{ij}} = 1 \rangle, \tag{1.9}$$

where $m_{ij} = m_{ji} \in \{2, 3, \dots, \infty\}$ for all $i \neq j$.

Observe that the set S of generators of a Coxeter group is symmetric, that is, $S = S^{-1}$.

Let $\Gamma = (W, S)$ be an abstract Coxeter group. For any subset $T \subset S$, the group W_T generated by the elements of T is a subgroup of W , and W_T is itself a Coxeter group. We say that W_T is a *parabolic* subgroup of W .

We are interested in Coxeter groups that admit a geometric representation as discrete subgroups of $\text{Isom}\mathbb{X}^n$ generated by hyperplane reflections.

A natural approach is to consider a polyhedral arrangement of hyperplanes as follows.

Definition 1.3.2. A *Coxeter polyhedron* $P = \bigcap_{i=1}^N H_{v_i}^- \subset \mathbb{X}^n$ is a polyhedron all of whose dihedral angles are zero or of the form $\frac{\pi}{k}$ for $k \in \mathbb{Z}_{\geq 2}$.

Given a Coxeter polyhedron $P \subset \mathbb{X}^n$ as in Definition 1.3.2, we denote by $s_1, \dots, s_N \in \text{Isom}\mathbb{X}^n$ the reflections with respect to the hyperplanes H_{v_1}, \dots, H_{v_N} bounding P . Let Γ be the group generated by $S = \{s_1, \dots, s_N\}$. If two hyperplanes H_{v_i}, H_{v_j} intersect at a dihedral angle $\frac{\pi}{m_{ij}}$, then the composition $s_i s_j$ is a rotation of angle $\frac{2\pi}{m_{ij}}$. Furthermore, if two hyperplanes do not intersect in \mathbb{H}^n (that is, they are parallel or ultraparallel), the composition $s_i s_j$ has infinite order. In this way, we deduce that Γ admits a presentation as a Coxeter group

$$\Gamma = \langle s_1, \dots, s_N \mid s_i^2 = 1, (s_i s_j)^{m_{ij}} = 1 \rangle. \quad (1.10)$$

Definition 1.3.3. Let $P \subset \mathbb{X}^n$ be a Coxeter polyhedron. The Coxeter group $\Gamma \subset \text{Isom}\mathbb{H}^n$ generated by reflections with respect to the bounding hyperplanes of P is called the *geometric Coxeter group associated with P* . The Gram matrix $Gr(\Gamma)$ of Γ is defined to be the Gram matrix $Gr(P)$ of P .

Depending on whether $\mathbb{X}^n = \mathbb{E}^n, \mathbb{S}^n$ or \mathbb{H}^n , the geometric Coxeter group Γ is said to be *Euclidean*, *spherical*, or *hyperbolic*. Observe that a spherical Coxeter group is always finite.

The Coxeter group $\Gamma \subset \text{Isom}\mathbb{X}^n$ is called *cocompact* if the associated Coxeter polyhedron $P \subset \mathbb{X}^n$ is compact, and *non-cocompact* otherwise. In addition, Γ is called *cofinite* if the associated Coxeter polyhedron P has finite volume.

In what follows, we assume hyperbolic Coxeter groups to be cofinite, except if mentioned otherwise.

3.1 The Coxeter diagram of a Coxeter group

Now, we introduce the notion of Coxeter diagram for an abstract Coxeter group $\Gamma = (W, S)$ of rank N presented by

$$W = \langle s_i \in S \mid s_i^2 = 1, (s_i s_j)^{m_{ij}} = 1 \rangle.$$

Definition 1.3.4. The *Coxeter diagram* Σ of Γ is the (non-oriented) graph whose nodes correspond to the generators s_1, \dots, s_N of Γ . Any two nodes ν_i and ν_j in the graph are connected by an edge labelled by m_{ij} when the corresponding generators satisfy $(s_i s_j)^{m_{ij}} = 1$ for $m_{ij} \in \{3, \dots, \infty\}$. In other words, two nodes are not connected if the corresponding generators commute. We omit the label when $m_{ij} = 3$ since it occurs frequently.

If a Coxeter diagram is a linear graph with consecutive edges labelled by k_1, \dots, k_r , we describe the corresponding Coxeter group (or Coxeter polyhedron) by its *Coxeter symbol* $[k_1, \dots, k_r]$.

Each parabolic subgroup of (W, S) gives rise to a *subdiagram* σ of Σ . Note that Coxeter diagrams and/or some of their subdiagrams need not to be connected graphs. However, a Coxeter diagram Σ is connected if and only if its Coxeter group (W, S) is irreducible.

In the case of a geometric Coxeter group $\Gamma \subset \text{Isom}\mathbb{X}^n$, its Coxeter diagram Σ is called *affine*, *spherical*, or *hyperbolic*, depending on whether $\mathbb{X}^n = \mathbb{E}^n, \mathbb{S}^n$ or \mathbb{H}^n .

Furthermore, in this geometric context and by (1.8) and (1.9), the Coxeter diagram Σ coincides with the graph whose nodes correspond to the bounding hyperplanes of the associated Coxeter polyhedron $P \subset \mathbb{X}^n$, where two nodes are joined by an edge labelled by m_{ij} when the corresponding hyperplanes share a dihedral angle $\frac{\pi}{m_{ij}}$ for $m_{ij} \geq 3$. An edge is labelled by ∞ when the corresponding hyperplanes are disjoint inside \mathbb{X}^n for $\mathbb{X}^n \neq \mathbb{S}^n$.

Example 1.3.5. A simple but prominent example is given by the Coxeter group Γ with Coxeter symbol $[7, 3]$ based on the hyperbolic Coxeter triangle $\Delta(\frac{\pi}{2}, \frac{\pi}{3}, \frac{\pi}{7})$. In fact, the group Γ is of minimal co-area among all discrete groups in $\text{Isom}\mathbb{H}^2$, and has minimal growth rate given by Lehmer's number; see Chapters 3 and 5.

In the sequel, for a geometric Coxeter group Γ , we do not distinguish between Γ , its Coxeter polyhedron P , the Coxeter diagram Σ , and the Gram matrix $Gr(\Gamma)$.

The number N of nodes is called the *order* of the Coxeter diagram Σ , and it coincides with the rank of Γ . The rank of the Gram matrix $Gr(\Gamma)$ is called the *rank* of Σ .

Note that if the polyhedron P is indecomposable, its Coxeter diagram Σ is connected and the group Γ is irreducible, and vice versa.

3.2 Spherical and Euclidean Coxeter groups

In the fundamental work [16], H. S. M. Coxeter classified all spherical and Euclidean Coxeter groups. In Tables 1.3.1 and 1.3.2, we give the list of all irreducible spherical and Euclidean Coxeter groups in terms of their Coxeter diagrams.

$n \geq 1$	A_n		$n = 3$	H_3	
$n \geq 2$	B_n		$n = 4$	H_4	
$n \geq 3$	D_n		$n = 6$	E_6	
$n = 2$	$G_2^{(m)}$		$n = 7$	E_7	
$n = 4$	F_4		$n = 8$	E_8	

Table 1.3.1: The irreducible spherical Coxeter groups of rank n

The following theorems have been established by Coxeter [16]; see also the work of Vinberg [84].

Theorem 1.3.6. *Let $P \subset \mathbb{S}^{n-1}$ be a spherical Coxeter polyhedron with associated Coxeter group Γ . Then, P is a simplex, and its Coxeter diagram is a disjoint union of Coxeter diagrams of irreducible spherical Coxeter groups of rank k_i such that $\sum k_i = n$.*

In contrast to the spherical case, by Theorem 1.2.10, any connected affine Coxeter diagram of rank n has order $n + 1$.

Theorem 1.3.7. *Let $P \subset \mathbb{E}^n$ be a Euclidean Coxeter polyhedron of finite volume with associated Coxeter group Γ . Then, P is a product of simplices, and its Coxeter diagram is a disjoint union of Coxeter diagrams of irreducible affine Coxeter groups of rank k_i such that $\sum k_i = n$.*

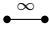
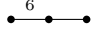

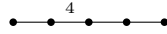
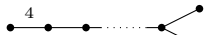



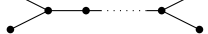

$n = 1$	\tilde{A}_1		$n = 2$	\tilde{G}_2	
$n \geq 2$	\tilde{A}_n		$n = 4$	\tilde{F}_4	
$n \geq 3$	\tilde{B}_n		$n = 6$	\tilde{E}_6	
$n \geq 2$	\tilde{C}_n		$n = 7$	\tilde{E}_7	
$n \geq 4$	\tilde{D}_n		$n = 8$	\tilde{E}_8	

Table 1.3.2: The irreducible affine Coxeter groups of rank n

3.3 Hyperbolic Coxeter groups

Let $P = \bigcap_{i=1}^N H_{v_i}^-$ be a Coxeter polyhedron in \mathbb{H}^n and Γ its associated Coxeter group of rank N . Assume that all the vectors v_i normal to the bounding hyperplanes $H_i = H_{v_i}$ of P have Lorentzian norm 1.

The Gram matrix $Gr(\Gamma) \in \text{Mat}(N, \mathbb{R})$ of Γ (and of the polyhedron P) has the following coefficients off the diagonal; see Section 2.

$$\langle v_i, v_j \rangle_{-1} = \begin{cases} -\cos \frac{\pi}{m_{ij}} & \text{if } \angle(H_i, H_j) = \frac{\pi}{m_{ij}} \neq 0 \\ -1 & \text{if } H_i, H_j \text{ are parallel} \\ -\cosh l & \text{if } d_{\mathbb{H}}(H_i, H_j) = l > 0 \end{cases} \quad (1.11)$$

Vertices and faces

In what follows we describe vertices and faces of a hyperbolic Coxeter polyhedron and cite important correspondences at the level of its Coxeter diagram.

Theorem 1.3.8. *Let P be a Coxeter polyhedron in \mathbb{H}^n , and let Σ be its Coxeter diagram. Then, for $1 \leq k \leq n$, there is a one-to-one correspondence between $(n - k)$ -faces of P and spherical subdiagrams σ of Σ of rank k .*

In particular, any ordinary vertex corresponds to a spherical subdiagram of rank n . In addition, ideal vertices of P correspond to affine subdiagrams σ_∞ of rank $n - 1$.

Let us add that an ideal vertex of a hyperbolic Coxeter polyhedron is non-simple if and only if σ_∞ is made of at least two affine components.

By Theorem 1.3.8, a spherical subdiagram σ of rank k of Σ corresponds to an $(n - k)$ -face $F = F(\sigma)$ of P ; see Table 1.3.1. The face F itself is an acute-angled polyhedron of finite volume, but it is *not* necessarily a Coxeter polyhedron in \mathbb{H}^{n-k} .

The following important theorem provides a condition for the face F to be a Coxeter polyhedron. It was first proven by Borchers [5] in a more general context, and has been reformulated by Allcock [1] as follows.

Theorem 1.3.9. *Let P be a hyperbolic Coxeter polyhedron with Coxeter diagram Σ . Let $F = F(\sigma)$ be a face of P corresponding to a spherical subdiagram σ of Σ . Assume that σ does not contain any component of type A_l , for $l \geq 1$, or D_5 . Then, F is itself a Coxeter polyhedron.*

The facets of $F \subset P$ correspond to all those nodes of Σ that, together with σ , form a spherical subdiagram of Σ . We say that a node $\nu \in \Sigma \setminus \sigma$ is a *good neighbour* of σ if the subdiagram spanned by σ and ν is spherical. Otherwise, ν is said to be a *bad neighbour*. As a consequence, the facets of F correspond to the good neighbours of σ .

Let ν_1, ν_2 be two good neighbours of σ . Then, the nodes ν_1, ν_2 correspond to facets $f_1 = F_1 \cap F, f_2 = F_2 \cap F$ of F , where F_1, F_2 are facets of P . Their dihedral angle $\angle(f_1, f_2)$ is less than or equal to $\angle(F_1, F_2)$.

More precisely, according to Allcock [1], the dihedral angles $\angle(f_1, f_2)$ of the facets f_1, f_2 of F are given as follows.

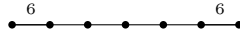
Theorem 1.3.10. *Let P be a Coxeter polyhedron, and let $F = F(\sigma)$ be a face of P with facets f_1, f_2 as above. Assume that σ does not contain any component of type A_l , for $l \geq 1$, or D_5 . Then, one has the following characterization.*

1. *If neither ν_1 nor ν_2 attaches to σ , then $\angle(f_1, f_2) = \angle(F_1, F_2)$.*
2. *Assume ν_1, ν_2 attach to different components of σ . If $\angle(F_1, F_2) = \frac{\pi}{2}$, then $\angle(f_1, f_2) = \frac{\pi}{2}$. Otherwise, f_1 and f_2 are disjoint.*
3. *Assume ν_1, ν_2 attach to the same component σ_0 of σ . If ν_1 and ν_2 are not joined by an edge and $\{\sigma_0, \nu_1, \nu_2\}$ yields a diagram E_6 (respectively, E_8 or F_4), then $\angle(f_1, f_2) = \frac{\pi}{3}$ (respectively, $\frac{\pi}{4}$). Otherwise, f_1 and f_2 are disjoint.*
4. *Assume ν_1 attaches to a component σ_0 of σ , and ν_2 does not attach to σ . If $\angle(F_1, F_2) = \frac{\pi}{2}$, then $\angle(f_1, f_2) = \frac{\pi}{2}$. If ν_1 and ν_2 are joined by a simple edge and $\{\sigma_0, \nu_i, \nu_j\}$ yields a diagram B_k (respectively, D_k, E_8*

or H_4), then $\angle(f_1, f_2) = \frac{\pi}{4}$ (respectively, $\frac{\pi}{4}$, $\frac{\pi}{6}$ or $\frac{\pi}{10}$). Otherwise, f_1 and f_2 are disjoint.

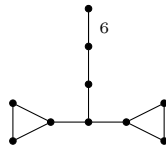
Remark 1.3.11. Let $m \geq 6$ be an integer. Then, any node connected to the subdiagram $G_2^{(m)} = [m]$ of Σ is a bad neighbour. As a result of Theorem 1.3.9, it is easy to identify each $(n - 2)$ -face $F(G_2^{(m)})$ of a hyperbolic Coxeter polyhedron $P \subset \mathbb{H}^n$. Furthermore, by Theorem 1.3.10, its dihedral angles are precisely given by the dihedral angles of P .

Example 1.3.12. Let $P \subset \mathbb{H}^5$ be the Coxeter pyramid depicted below.



By Theorem 1.3.9 and Remark 1.3.11, each 3-face of P corresponding to one of the two subdiagrams $G_2 = G_2^{(6)} = [6]$ is a Coxeter tetrahedron with Coxeter symbol $[6, 3, 3]$ (or $[3, 3, 6]$).

Example 1.3.13. For the Coxeter 7-pyramid depicted below, the 5-face $F(G_2)$ is a pyramid over a product of two simplices of type \tilde{A}_2 ; see also Table 3.2.2.



Criteria for compactness and finite volume

Recall that a hyperbolic Coxeter n -polyhedron P has finite volume if it is the convex hull of a finite number of points in $\overline{\mathbb{H}^n}$. The polyhedron P is compact if all of its vertices are ordinary points in \mathbb{H}^n . Otherwise, P is non-compact (but of finite volume) and has at least one ideal vertex; see Definition 1.2.4.

The following criteria were established by Vinberg [82].

Theorem 1.3.14 (Compactness criterion). *A polyhedron $P \subset \mathbb{H}^n$ is compact if and only if the following holds.*

1. P has at least one ordinary vertex.
2. For every vertex v of P and every edge of P emanating from v , there is precisely one other vertex of P on that edge.

Theorem 1.3.15 (Finite-volume criterion). *A polyhedron $P \subset \mathbb{H}^n$ has finite volume if and only if the following holds.*

1. P has at least one (ordinary or ideal) vertex.
2. For every (ordinary or ideal) vertex v of P and every edge of P emanating from v , there is precisely one other (ordinary or ideal) vertex of P on that edge.

For a Coxeter polyhedron P with Coxeter diagram Σ , Theorem 1.3.15 can be reformulated as follows.

1. Σ contains at least one spherical subdiagram of rank n or one affine subdiagram of rank $n - 1$.
2. Each spherical subdiagram of rank $n - 1$ of Σ can be extended in exactly two ways to a spherical subdiagram of rank n or to an affine subdiagram of rank $n - 1$.

Remark 1.3.16. By exploiting Theorems 1.3.14 and 1.3.15, Guglielmetti [30, 31] developed the software CoxIter, which, for a given hyperbolic Coxeter diagram $\Sigma = \Sigma(P)$, indicates whether the polyhedron P is compact or of finite volume. The software CoxIter provides some more important information. For example, the Euler characteristic of the group $\Gamma(P)$ is displayed, which, in the even dimensional case, is well known to be proportional to the volume of P .

Finally, let us add another non-trivial result, due to Felikson and Tumarkin [25], which will be very useful for us in the sequel; see Chapter 4.

Proposition 1.3.17. *Let P be a hyperbolic Coxeter n -polyhedron (of finite volume), and let Σ be its Coxeter diagram. Then, no proper subdiagram of Σ is the Coxeter diagram of a finite-volume Coxeter n -polyhedron.*

Arithmeticity of hyperbolic Coxeter groups

The general theory of arithmetic groups is a broad field which we present here only briefly and this in the restricted case of hyperbolic Coxeter groups. We refer to [57, 58, 81], for example.

We begin by the following definition, comparing two discrete groups Γ_1, Γ_2 in $\text{Isom}\mathbb{H}^n$. The groups Γ_1 and Γ_2 are *commensurable (in the wide sense)* if there is an element $\gamma \in \text{Isom}\mathbb{H}^n$ such that $\Gamma_1 \cap \gamma\Gamma_2\gamma^{-1}$ has finite index in both

Γ_1 and $\gamma\Gamma_2\gamma^{-1}$. Commensurability preserves properties such as discreteness and finite covolume.

A fundamental theorem of Margulis states that a cofinite group Γ in $\text{Isom}\mathbb{H}^n$, $n \geq 3$ is non-arithmetic if and only if its commensurator

$$\text{Comm}(\Gamma) = \{ \gamma \in \text{Isom}\mathbb{H}^n \mid \Gamma \text{ and } \gamma\Gamma\gamma^{-1} \text{ are commensurable} \}$$

is a discrete subgroup of finite covolume in $\text{Isom}\mathbb{H}^n$; see [87], for example.

Margulis' result can be taken as a definition of a cofinite discrete group $\Gamma \subset \text{Isom}\mathbb{H}^n$ to be (non-)arithmetic.

There are several arithmeticity criteria and results. For instance, in dimension $n = 2$, Takeuchi [58, Appendix 13.3] classified all discrete triangle groups up to arithmeticity.

Example 1.3.18. The four cocompact triangle groups (p, q, r) where $p, q, r \in \{2, 3, 6\}$ and with at least one entry equal to 6, are all arithmetic.

Let $\Gamma \subset \text{Isom}\mathbb{H}^n$ be a non-cocompact Coxeter group of finite covolume. In this restricted context, the arithmeticity property can be characterized in an easy way. For its formulation, we consider the Gram matrix $\text{Gr}(\Gamma)$ of Γ and its related *cycles*.

Definition 1.3.19. For an arbitrary matrix $A = (a_{ij})_{i,j \in \{1, \dots, N\}}$, a *cycle* in A is an element of the form

$$a_{i_1 i_2} \cdots a_{i_{k-1} i_k} a_{i_k i_1} \quad \text{for } i_1, \dots, i_k \in \{1, \dots, N\}, \quad k \geq 2.$$

A cycle in A is said to be *irreducible* if all i_1, \dots, i_k are distinct.

The following arithmeticity criterion is due to Vinberg [84].

Theorem 1.3.20 (Arithmeticity criterion). *Let $\Gamma \subset \text{Isom}\mathbb{H}^n$ be a non-cocompact Coxeter group of finite covolume. Denote its Gram matrix by $G = \text{Gr}(\Gamma)$. Then, Γ is arithmetic (and defined over \mathbb{Q}) if and only if all cycles in $2G$ are rational integers.*

In view of Chapter 4, we specialize the context even more, and consider hyperbolic Coxeter groups Γ as in (1.9) which satisfy the conditions of Theorem 1.3.20, and whose Coxeter polyhedra $P \subset \mathbb{H}^n$ have no pair of ultraparallel facets. Then, Guglielmetti [32] added the following characterization.

Theorem 1.3.21. *Let $P \subset \mathbb{H}^n$ be a non-compact Coxeter polyhedron with no pair of ultraparallel facets. Then, its Coxeter group Γ is arithmetic if and only if $m_{ij} \in \{2, 3, 4, 6, \infty\}$ for all distinct i, j , and any irreducible cycle in $2G$ of length at least 3 is an integer.*

The following example gives an illustration of Theorem 1.3.21.

Example 1.3.22. The Coxeter pyramid group $[6, 3, 3, 3, 3, 6]$ in $\text{Isom}\mathbb{H}^5$ is arithmetic. However, the Coxeter 5-simplex group depicted in Figure 1.3.22 is non-arithmetic.



Figure 1.3.2: The non-arithmetic Coxeter simplex group in $\text{Isom}\mathbb{H}^5$

CHAPTER 2

ROOT SYSTEMS AND FUNDAMENTAL WEIGHTS

In this chapter, we provide a brief survey of the classical theory of root systems in Euclidean vector spaces. Their classification including details about their simple root systems, highest root and fundamental weights will play an important role in Chapter 4.

As references for this chapter, we quote [6, 37].

1 Root systems and Weyl groups

From now on, we denote by V a Euclidean vector space of finite dimension.

Definition 2.1.1. A *root system* R is a finite subset of V made of non-zero vectors, called *roots*, such that the following conditions hold.

1. R generates V .
2. $R \cap \mathbb{R}\alpha = \{\alpha, -\alpha\}$.
3. For any root $\alpha \in R$, the reflection s_α along $\alpha \in R$ as given by (1.5) permutes the elements of R , that is, $s_\alpha(\beta) \in R$ for all $\beta \in R$.

The *rank* of the root system R is defined to be the dimension of V . The root system R is *reducible* if there exist non-empty, disjoint root systems R_1, R_2 such that $R = R_1 \cup R_2$ and $\text{span}(R) = \text{span}(R_1) \oplus \text{span}(R_2)$. Otherwise, the root system R is said to be *irreducible*.

We often impose the *crystallographic* condition for R , ensuring that the vector $s_\alpha(\beta)$ is obtained from β by adding an *integral* multiple of α .

Definition 2.1.2 (Crystallographic condition). A root system R is said to be *crystallographic* if for any roots $\alpha, \beta \in R$ one has

$$k_{\alpha,\beta} := 2 \frac{\langle \alpha, \beta \rangle}{\langle \alpha, \alpha \rangle} \in \mathbb{Z} . \quad (2.1)$$

In fact, it is sufficient to require the condition (2.1) for a set of *simple* roots in R as follows. Let us first introduce the notion of *positive* roots.

Let $R^+ \subset R$ satisfy the following properties.

1. For each $\alpha \in R$, exactly one of α and $-\alpha$ belongs to R^+ ;
2. For any distinct $\alpha, \beta \in R^+$ such that $\alpha + \beta \in R$, one has $\alpha + \beta \in R^+$.

The elements of R^+ are called *positive roots*.

Definition 2.1.3. A *simple* root is a positive root that cannot be decomposed as the sum of two positive roots. We denote by $B = B(R)$ the set of simple roots.

Note that every system R^+ of positive roots contains a unique set B of simple roots. Furthermore, the set B of simple roots is a basis of V .

Definition 2.1.4. The group $W = W(R)$ generated by the reflections s_α through the hyperplanes α^\perp associated with the roots $\alpha \in B$ is called the *Weyl group* of R .

Proposition 2.1.5. *The Weyl group W is finite.*

For a fixed system B of simple roots in R , the Weyl group W satisfies the relations

$$(s_\alpha s_\beta)^{m_{\alpha,\beta}} = 1 \quad \text{for } \alpha, \beta \in B, \quad (2.2)$$

where $m_{\alpha,\beta}$ is the order of the composition $s_\alpha s_\beta$ in W . Hence, W can be identified with a spherical Coxeter group; see Section 3.2 in Chapter 1.

Let us mention the following two well-known results.

Proposition 2.1.6. *Any positive root $\beta \in R^+$ can be written as a linear combination of simple roots, that is,*

$$\beta = \sum_{\alpha \in B} m_\alpha \alpha , \quad (2.3)$$

where each m_α is a non-negative integer.

Proposition 2.1.7. *For any two distinct simple roots $\alpha, \beta \in B$, one has*

$$\langle \alpha, \beta \rangle \leq 0 . \tag{2.4}$$

We consider the following natural partial ordering on R with respect to R^+ . For two roots $\alpha, \beta \in R$, one says that $\alpha \leq \beta$ if and only if $\beta - \alpha$ is a sum of simple roots with non-negative coefficients; see Proposition 2.1.6.

If R is an irreducible root system, there exists a unique *highest root* with respect to this ordering, and we will denote it by $\bar{\alpha}$. In view of Proposition 2.1.7, the highest root $\bar{\alpha}$ forms a non-obtuse angle with every simple root $\beta \in B$.

From now on, we consider a crystallographic root system R ; see (4).

As $\langle \alpha, \beta \rangle = \|\alpha\| \cdot \|\beta\| \cos \angle(\alpha, \beta)$, it follows that

$$k_{\alpha, \beta} k_{\beta, \alpha} = 4 \cos^2 \angle(\alpha, \beta) \in \mathbb{Z}_{\geq 0} . \tag{2.5}$$

Since $k_{\alpha, \beta}$ and $k_{\beta, \alpha}$ are integers, one gets

$$k_{\alpha, \beta} k_{\beta, \alpha} \in \{0, 1, 2, 3, 4\} . \tag{2.6}$$

The crystallographic condition for R implies that its simple roots can be of at most two different lengths, and they are called *short* and *long* roots. In fact, the quotient of the squared lengths of two simple roots can be equal to 2 or 3, only.

Furthermore, the Weyl group W generated by s_α , $\alpha \in B$, is a finite reflection group with $m_{\alpha, \beta} \in \{2, 3, 4, 6\}$ for any two distinct simple roots $\alpha, \beta \in B$; see (2.2). The group W is said to be *crystallographic*, and W stabilizes the \mathbb{Z} -lattice spanned by B .

Definition 2.1.8. Let Λ be the set of vectors $w \in V$ such that $k_{w, \alpha} \in \mathbb{Z}$ for all $\alpha \in R$. The elements of Λ are called *weights*, and a weight $w \in \Lambda$ is *dominant* if all the integers $k_{w, \alpha}$ are nonnegative for all $\alpha \in R^+$.

Lastly, we define the notion of *fundamental* weights as follows. Let n be the rank of R , and write $B = \{\alpha_1, \dots, \alpha_n\}$.

Definition 2.1.9. The *fundamental* weights $w_1, \dots, w_n \in \Lambda$ are the dominant weights defined by the condition $k_{w_i, \alpha_j} = \delta_{ij}$ for all $1 \leq i, j \leq n$, where δ_{ij} is the Kronecker symbol.

2 Dynkin diagrams and extended Dynkin diagrams

Let R be an irreducible crystallographic root system in V , and let $W = W(R)$ be its Weyl group.

The *Dynkin diagram* of such a root system encodes all the information about the relative root lengths of simple roots of R and their angles. In the following, we restrict the context to the subfamily of Weyl groups used in this work, that is, the Weyl groups of type A, D, E and G_2 .

In this context, the Dynkin diagram of R will coincide with the Coxeter diagram of W except for the case G_2 .

Definition 2.2.1. The *Dynkin diagram* of R is the graph whose nodes correspond to the simple roots of R , and where two nodes are joined as follows. If the roots are orthogonal, there is no edge between the corresponding nodes. If the angle between the two roots is $\frac{2\pi}{3}$, there is a simple edge between the nodes. If the angle is $\frac{5\pi}{6}$, the two nodes are joined by a triple edge, and there is an arrow on the edge pointing from the long root to the short root.

When all roots have the same length, the Dynkin diagram has simple edges and is called *simply laced*. It corresponds to one of the Coxeter diagrams occurring in Figure 1.3.1.

Note that a root system is irreducible if and only if its Dynkin diagram is connected.

The *extended Dynkin diagram* of R contains additional information in view of an extra root added to the set B of simple roots of R as follows.

Definition 2.2.2. The *extended Dynkin diagram* of R is the diagram obtained by adding the node to the Dynkin diagram of R that corresponds to the inverse $-\bar{\alpha}$ of the highest root $\bar{\alpha}$.

Since $\bar{\alpha}$ is a linear combination of the simple roots of R , the extended Dynkin diagram is closely related to a connected affine Coxeter diagram; see Table 1.3.2.

3 Classification of root systems of type A, D, E and G_2

In this section, we consider some particular irreducible crystallographic root systems. We choose a *natural* system of simple roots, establish the highest root and provide the fundamental weights. In addition, we depict the associated extended Dynkin diagram decorated by the corresponding root at each node.

Let us first introduce the *ADE*-root systems. Their Dynkin diagrams are simply laced.

Denote by ϵ_i the i -th vector of the standard basis of \mathbb{R}^k .

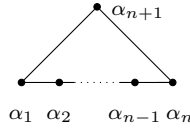
Definition 2.3.1. Let V be the subspace of vectors in \mathbb{R}^{n+1} whose coordinates sum up to 0. The A_n -root system \mathcal{A}_n is the set of vectors in V of length $\sqrt{2}$ with integer coordinates given by

$$\mathcal{A}_n = \{\epsilon_i - \epsilon_j \mid 1 \leq i \neq j \leq n+1\} .$$

The natural simple roots are $\alpha_1 = \epsilon_1 - \epsilon_2, \dots, \alpha_n = \epsilon_n - \epsilon_{n+1}$. Then, the highest root is given by $\bar{\alpha} = \alpha_1 + \dots + \alpha_n = \epsilon_{n+1} - \epsilon_1 =: -\alpha_{n+1}$. The notation $\alpha_{n+1} = -\bar{\alpha}$ will also be used in the subsequent cases. The fundamental weights of \mathcal{A}_n can be expressed as

$$w_i = \epsilon_1 + \dots + \epsilon_i - \frac{i}{n+1} \sum_{j=1}^{n+1} \epsilon_j \quad \text{for } 1 \leq i \leq n .$$

The extended Dynkin diagram is given as follows, where each node is indexed by the corresponding root.



Definition 2.3.2. Let $V = \mathbb{R}^n$. The D_n -root system \mathcal{D}_n is the set of vectors in V of length $\sqrt{2}$ with integer coordinates given by

$$\mathcal{D}_n = \{\epsilon_i - \epsilon_j \mid 1 \leq i \neq j \leq n\} \cup \{\pm(\epsilon_i + \epsilon_j) \mid 1 \leq i < j \leq n\} ,$$

and the natural simple roots are $\alpha_1 = \epsilon_1 - \epsilon_2, \dots, \alpha_{n-1} = \epsilon_{n-1} - \epsilon_n, \alpha_n = \epsilon_{n-1} + \epsilon_n$. The highest root satisfies

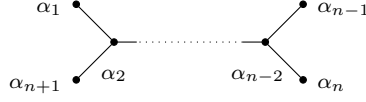
$$\bar{\alpha} = \alpha_1 + 2\alpha_2 + \dots + 2\alpha_{n-2} + \alpha_{n-1} + \alpha_n = \epsilon_1 + \epsilon_2 ,$$

and the fundamental weights are given by

$$\begin{cases} w_i & = \epsilon_1 + \dots + \epsilon_i \quad \text{for } i < n-1 \\ w_{n-1} & = \frac{1}{2}(\epsilon_1 + \dots + \epsilon_{n-1} - \epsilon_n) \\ w_n & = \frac{1}{2}(\epsilon_1 + \dots + \epsilon_{n-1} + \epsilon_n) \end{cases}$$

3. Classification of root systems of type A , D , E and G_2

The extended Dynkin diagram is given as follows.



Definition 2.3.3. Let $V = \mathbb{R}^8$, and consider the lattice $L = L_0 + \mathbb{Z}(\frac{1}{2} \sum_{1 \leq i \leq 8} \epsilon_i)$ where L_0 consists of all vectors $\sum_{1 \leq i \leq 8} c_i \epsilon_i$ with $c_i \in \mathbb{Z}$ and $\sum_{1 \leq i \leq 8} c_i$ even.

The E_8 -root system \mathcal{E}_8 is the set of vectors of length $\sqrt{2}$ in L . One has

$$\mathcal{E}_8 = \{ \pm \epsilon_i \pm \epsilon_j \mid i < j \} \cup \left\{ \frac{1}{2} \sum_{i=1}^8 (-1)^{\eta_i} \epsilon_i \mid \sum_{i=1}^8 \eta_i \text{ is even} \right\},$$

and the natural simple roots are given by

$$\begin{cases} \alpha_1 &= \frac{1}{2}(\epsilon_1 - \epsilon_2 - \cdots - \epsilon_7 + \epsilon_8) \\ \alpha_2 &= \epsilon_1 + \epsilon_2 \\ \alpha_i &= \epsilon_{i-1} - \epsilon_{i-2} \text{ for } 3 \leq i \leq 8 \end{cases}$$

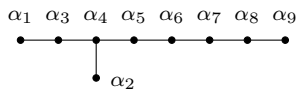
The highest root can be expressed as

$$\bar{\alpha} = 2\alpha_1 + 3\alpha_2 + 4\alpha_3 + 6\alpha_4 + 5\alpha_5 + 4\alpha_6 + 3\alpha_7 + 2\alpha_8 = \epsilon_7 + \epsilon_8,$$

and the fundamental weights are

$$\begin{cases} w_1 = 2\epsilon_8 \\ w_2 = \frac{1}{2}(\epsilon_1 + \epsilon_2 + \epsilon_3 + \epsilon_4 + \epsilon_5 + \epsilon_6 + \epsilon_7 + 5\epsilon_8) \\ w_3 = \frac{1}{2}(-\epsilon_1 + \epsilon_2 + \epsilon_3 + \epsilon_4 + \epsilon_5 + \epsilon_6 + \epsilon_7 + 7\epsilon_8) \\ w_4 = \epsilon_3 + \epsilon_4 + \epsilon_5 + \epsilon_6 + \epsilon_7 + 5\epsilon_8 \\ w_5 = \epsilon_4 + \epsilon_5 + \epsilon_6 + \epsilon_7 + 4\epsilon_8 \\ w_6 = \epsilon_5 + \epsilon_6 + \epsilon_7 + 3\epsilon_8 \\ w_7 = \epsilon_6 + \epsilon_7 + 2\epsilon_8 \\ w_8 = \epsilon_7 + \epsilon_8 \end{cases}$$

The extended Dynkin diagram is given as follows.



Definition 2.3.4. Let V be the hyperplane in \mathbb{R}^8 generated by the first seven simple roots $\alpha_1, \dots, \alpha_7$ of \mathcal{E}_8 ; see Definition 2.3.3. Then, V is orthogonal to w_8 . The E_7 -root system \mathcal{E}_7 is defined as $\mathcal{E}_7 = \mathcal{E}_8 \cap V$. One has

$$\mathcal{E}_7 = \{\pm\epsilon_i \pm \epsilon_j \mid 1 \leq i < j \leq 6\} \cup \{\pm(\epsilon_7 - \epsilon_8)\} \cup \left\{ \frac{1}{2} \sum_{i=1}^6 (-1)^{\eta_i} \epsilon_i + \epsilon_7 - \epsilon_8 \mid \sum_{i=1}^6 \eta_i \text{ is odd} \right\},$$

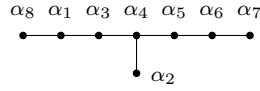
and the natural simple roots are $\alpha_1, \dots, \alpha_7$. The highest root is given by

$$\bar{\alpha} = 2\alpha_1 + 2\alpha_2 + 3\alpha_3 + 4\alpha_4 + 3\alpha_5 + 2\alpha_6 + \alpha_7 = \epsilon_8 - \epsilon_7,$$

and the fundamental weights are

$$\begin{cases} w_1 = -\epsilon_7 + \epsilon_8 \\ w_2 = \frac{1}{2}(\epsilon_1 + \epsilon_2 + \epsilon_3 + \epsilon_4 + \epsilon_5 + \epsilon_6 - 2\epsilon_7 + 2\epsilon_8) \\ w_3 = \frac{1}{2}(-\epsilon_1 + \epsilon_2 + \epsilon_3 + \epsilon_4 + \epsilon_5 + \epsilon_6 - 3\epsilon_7 + 3\epsilon_8) \\ w_4 = \epsilon_3 + \epsilon_4 + \epsilon_5 + \epsilon_6 - 2\epsilon_7 + 2\epsilon_8 \\ w_5 = \epsilon_4 + \epsilon_5 + \epsilon_6 - \frac{3}{2}\epsilon_7 + \frac{3}{2}\epsilon_8 \\ w_6 = \epsilon_5 + \epsilon_6 - \epsilon_7 + \epsilon_8 \\ w_7 = \epsilon_6 - \frac{1}{2}\epsilon_7 + \frac{1}{2}\epsilon_8 \end{cases}$$

The extended Dynkin diagram is given as follows.



Definition 2.3.5. Let V be the hyperplane generated by $\alpha_1, \dots, \alpha_6$ in \mathbb{R}^8 . Then, V is orthogonal to w_7 and w_8 . The E_6 -root system \mathcal{E}_6 is defined as $\mathcal{E}_6 = \mathcal{E}_8 \cap V$ and has the natural simple roots $\alpha_1, \dots, \alpha_6$.

The highest root is given by

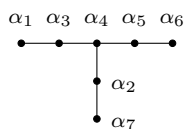
$$\bar{\alpha} = \alpha_1 + 2\alpha_2 + 2\alpha_3 + 4\alpha_4 + 2\alpha_5 + \alpha_6,$$

and the fundamental weights are

$$\begin{cases} w_1 = \frac{2}{3}(-\epsilon_6 - \epsilon_7 + \epsilon_8) \\ w_2 = \frac{1}{2}(\epsilon_1 + \epsilon_2 + \epsilon_3 + \epsilon_4 + \epsilon_5 - \epsilon_6 - \epsilon_7 + \epsilon_8) \\ w_3 = \frac{1}{2}(-\epsilon_1 + \epsilon_2 + \epsilon_3 + \epsilon_4 + \epsilon_5) + \frac{5}{6}(-\epsilon_6 - \epsilon_7 + \epsilon_8) \\ w_4 = \epsilon_3 + \epsilon_4 + \epsilon_5 - \epsilon_6 - \epsilon_7 + \epsilon_8 \\ w_5 = \epsilon_4 + \epsilon_5 + \frac{2}{3}(-\epsilon_6 - \epsilon_7 + \epsilon_8) \\ w_6 = \epsilon_5 + \frac{1}{3}(-\epsilon_6 - \epsilon_7 + \epsilon_8) \end{cases}$$

3. Classification of root systems of type A , D , E and G_2

The extended Dynkin diagram is given as follows.



Lastly, we introduce the G_2 -root system \mathcal{G}_2 , whose natural simple roots will have *different* lengths.

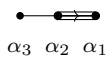
Definition 2.3.6. Let V be the hyperplane in \mathbb{R}^3 consisting of all vectors whose coordinates add up to 0. The G_2 -root system \mathcal{G}_2 is the set of vectors in V with integer coordinates and of length $\sqrt{2}$ or $\sqrt{6}$ given by

$$\mathcal{G}_2 = \{\pm(\epsilon_i - \epsilon_j) \mid 1 \leq i < j \leq 3\} \cup \{\pm(2\epsilon_i - \epsilon_j - \epsilon_k) \mid 1 \leq i, j, k \leq 3\},$$

and the natural simple roots are $\alpha_1 = \epsilon_1 - \epsilon_2$, $\alpha_2 = -2\epsilon_1 + \epsilon_2 + \epsilon_3$. Then, the highest root can be written according to

$$\bar{\alpha} = 3\alpha_1 + 2\alpha_2 = -\epsilon_1 - \epsilon_2 + 2\epsilon_3,$$

and the fundamental weights are given by $w_1 = 2\alpha_1 + \alpha_2$ and $w_2 = 3\alpha_1 + 2\alpha_2$.



We do not discuss the crystallographic root systems of type F_4 , B_n and C_n as they will not be used in this work; for more details about them, see [37].

PART II:

ON THE EXISTENCE OF HYPERBOLIC COXETER GROUPS

We adore chaos because we love to
produce order.

M.C. ESCHER

CHAPTER 3

SOME CLASSIFICATION RESULTS

The classification of hyperbolic Coxeter polyhedra is far from being complete. In fact, for dimensions beyond 3, only a comparatively small quantity of them is known.

We begin this chapter by quoting some general non-existence results for hyperbolic Coxeter polyhedra of finite volume. Then, we present the most important classification results for hyperbolic Coxeter polyhedra serving for our purposes. The first section is a brief survey of some of the results in dimensions 2 and 3. The second section is devoted to hyperbolic Coxeter polyhedra in higher dimensions.

Main references for this chapter are [6, 15, 21, 24, 37, 70, 84]; see also the webpage survey of Felikson [23].

The following non-existence results for hyperbolic Coxeter polyhedra have been established by Khovanski [49] and Prokhorov [69] for the finite-volume case, and by Vinberg [83] in the compact case.

Theorem 3.0.1. *Hyperbolic Coxeter polyhedra of finite volume do not exist in dimensions bigger than 995.*

Theorem 3.0.2. *Compact hyperbolic Coxeter polyhedra do not exist in dimensions bigger than 29.*

However, in dimensions beyond 3, examples of hyperbolic Coxeter polyhedra are known for dimensions ≤ 19 and in dimension 21 in the finite volume case, and for dimensions ≤ 8 in the compact case, only.

Note that throughout this chapter, and as usually, Coxeter polyhedra are considered to have *finite volume*.

1 In low dimensions

In dimensions 2 and 3, there exist infinitely many Coxeter polyhedra. There are fundamental results, proven by Poincaré and Andreev, that characterize their existence.

In dimension 2

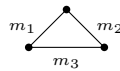
Theorem 3.1.1 (Poincaré [68]). *Let $N \in \mathbb{Z}_{\geq 3}$. A hyperbolic (convex) N -gon $P \subset \mathbb{H}^2$ with angles α_i exists if and only if*

$$\sum_{1 \leq i \leq N} \alpha_i < \pi(N - 2).$$

From Theorem 3.1.1, we deduce the following for Coxeter polygons. For $N = 3$, there exist infinitely many Coxeter triangles in \mathbb{H}^2 , as there are infinitely many integers $m_1, m_2, m_3 \geq 2$ such that

$$\frac{1}{m_1} + \frac{1}{m_2} + \frac{1}{m_3} < 1.$$

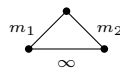
The Coxeter diagram of a compact Coxeter triangle is then given by



where

$$\frac{1}{m_1} + \frac{1}{m_2} + \frac{1}{m_3} < 1.$$

For a non-compact Coxeter triangle, the Coxeter diagram has the form



for (arbitrarily large) $m_1 \geq 2$ and $m_2 \geq 3$.

Example 3.1.2. As a consequence of Theorem 3.1.1, there exist no compact hyperbolic squares, as the sum of the angles should not exceed 2π . However, there exist right-angled N -gons in \mathbb{H}^2 for any $N \geq 5$.

Remark 3.1.3. Observe that for $N \geq 4$, a Coxeter N -gon admits at least one pair of ultraparallel edges.

Let P be a hyperbolic triangle with angles α_1, α_2 and α_3 . Then, the well-known defect formula for the area of P yields

$$\text{area}(P) = \pi - (\alpha_1 + \alpha_2 + \alpha_3) .$$

Let us situate hyperbolic Coxeter triangles in the context of fundamental polygons of discrete groups in $\text{Isom}\mathbb{H}^2$. It is a classical result due to C. L. Siegel [73] that the smallest co-area of a discrete group in $\text{Isom}\mathbb{H}^2$ is achieved by the Coxeter triangle group $[7, 3]$. Furthermore, one has

$$\text{area}([7, 3]) = \pi - \left(\frac{\pi}{2} + \frac{\pi}{3} + \frac{\pi}{7}\right) = \frac{\pi}{42} .$$

In the non-cocompact case, the smallest co-area is realised by the Coxeter triangle group $[\infty, 3]$ closely related to the modular group $\text{SL}_2(\mathbb{Z})$. One has

$$\text{area}([\infty, 3]) = \pi - \left(\frac{\pi}{2} + \frac{\pi}{3}\right) = \frac{\pi}{6} .$$

In dimension 3

By a fundamental result of Andreev [2], we dispose of a complete description of Coxeter polyhedra in \mathbb{H}^3 . In fact, the existence of an acute-angled polyhedron of finite volume in \mathbb{H}^3 can be deduced from the mutual intersection behaviour of its facets and the resulting angular inequalities. As a consequence, any family of Coxeter polyhedra of fixed combinatorial type in \mathbb{H}^3 can be listed in detail. In what follows, we give an overview of the most important families of interest for our work.

All hyperbolic Coxeter tetrahedra have been classified. This result is mainly due to Lannér [54] in the compact case, and to Chein [15] and Koszul [53] in the non-compact case. They are listed in Figures 3.1.1 and 3.1.2.

In addition, all Coxeter 3-pyramids have been established by Tumarkin [78]. Their Coxeter diagrams are given in Figure 3.1.3. Note that all of them admit a pair of disjoint facets.

Observe that for all Coxeter polyhedra mentioned above, their dihedral angles are bigger than or equal to $\frac{\pi}{6}$. This phenomenon holds for all Coxeter polyhedra with at most 5 facets in \mathbb{H}^3 ; see [23].

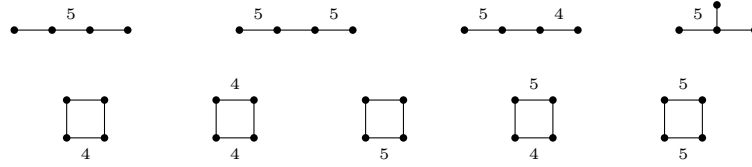


Figure 3.1.1: The compact Coxeter tetrahedra

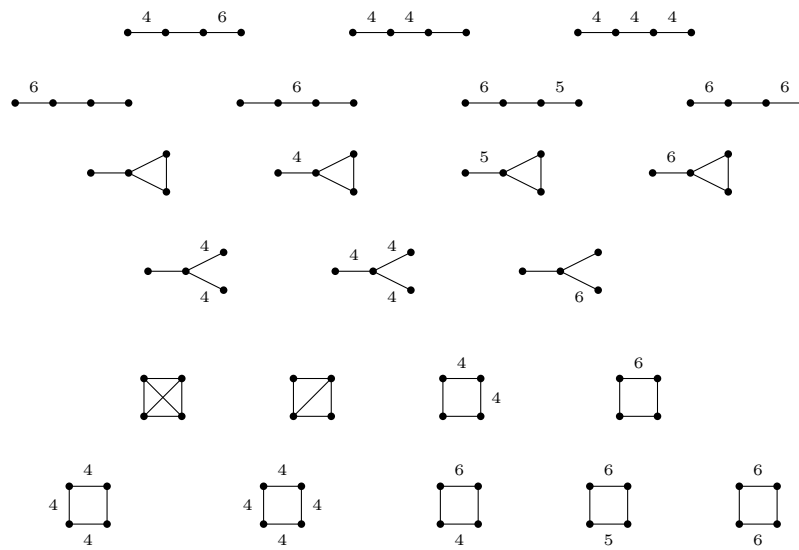


Figure 3.1.2: The non-compact Coxeter tetrahedra

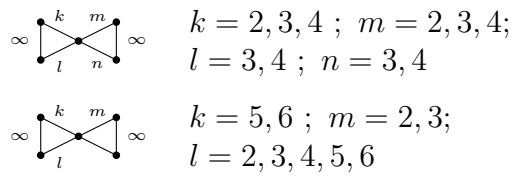


Figure 3.1.3: The Coxeter pyramids in \mathbb{H}^3

2 In higher dimensions

In dimensions beyond 3, only a few essentially different examples are known. In this section, we summarize the classification results of interest to us.

2.1 Coxeter polyhedra with a small number of facets

The compact Coxeter simplices were classified by Lannér, and they exist only in dimensions $n \leq 4$, while non-compact Coxeter simplices were classified by Chein [15] and Koszul [53], and exist in dimensions $n \leq 9$. The latter simplices are sometimes called *quasi-Lannér*. Moreover, all Coxeter polyhedra in \mathbb{H}^n with precisely $n + 2$ facets (respectively, $n + 3$ facets in the compact case) are known due to the works of Esselmann [20, 21], Kaplinskaya [42] and Tumarkin [78, 79, 80].

This section contains the lists of all Coxeter polyhedra in \mathbb{H}^n for $n \geq 4$ with facet number $f_{n-1} = n + 1$, together with classification results and sublists relevant for this thesis when the facet number satisfies $f_{n-1} \geq n + 2$.

The case $f_{n-1} = n + 1$

As mention above, compact Coxeter simplices exist for dimensions $n \leq 4$ only; see Figure 3.2.4.

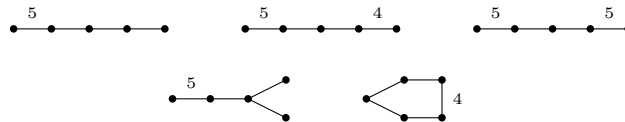


Figure 3.2.4: The compact Coxeter simplices in \mathbb{H}^4

In the non-compact case, we know that simplices exist up to dimension $n = 9$. We give their Coxeter diagrams in Table 3.2.1. Observe that all of them have dihedral angles $\frac{\pi}{2}$, $\frac{\pi}{3}$, $\frac{\pi}{4}$ or $\frac{\pi}{6}$, only.

Let us add that the covolumes of all hyperbolic Coxeter simplex groups have been determined by Johnson, Kellerhals, Ratcliffe and Tschantz [40].

The case $f_{n-1} = n + 2$

Let now P be a Coxeter polyhedron in \mathbb{H}^n with precisely $n + 2$ facets. Then, P is combinatorially a product of two simplices or a pyramid over a product of two simplices.

n			
4			
5			
6			
7			
8			
9			

Table 3.2.1: The non-compact Coxeter simplices in \mathbb{H}^n for $n \geq 4$

Let us first consider products of simplices. All simplicial prisms have been classified by Kaplinskaya [42] and exist up to dimension $n = 5$. We emphasize that all of them contain one pair of disjoint facets.

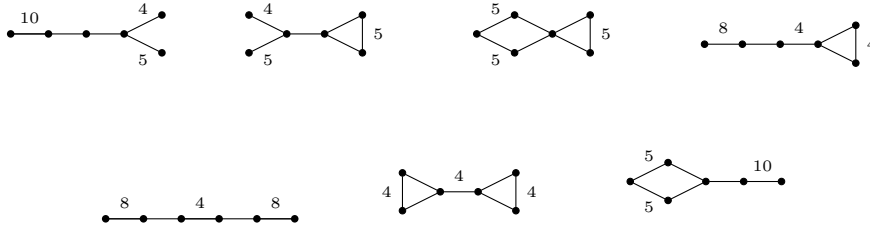


Figure 3.2.5: The Esselmann polyhedra

Assume that P is combinatorially a product of two simplices each of dimension greater than 1. If P is compact, then P is one of the polyhedra listed in Figure 3.2.5. They were found by Esselmann [21] and are called *Esselmann polyhedra*. There are exactly seven Esselmann polyhedra, and they are all of dimension 4.

The unique non-compact Coxeter polyhedron being a product of two simplices is the Coxeter polyhedron $P_0 \subset \mathbb{H}^4$ found by Tumarkin [78] and depicted in Figure 3.2.6.

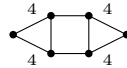


Figure 3.2.6: The Coxeter polyhedron $P_0 \subset \mathbb{H}^4$

All Coxeter pyramids over a product of two simplices have been classified by Tumarkin [78]. They are non-compact and exist in \mathbb{H}^n for dimensions $n \leq 13$ and $n = 17$. In dimension $n = 4$, all of them contain one pair of parallel facets, and in particular, their Coxeter diagrams contain a subdiagram of type $\tilde{A}_1 = [\infty]$.

In dimension beyond 4, we emphasize that all of their dihedral angles are equal to $\frac{\pi}{2}$, $\frac{\pi}{3}$, $\frac{\pi}{4}$ or $\frac{\pi}{6}$ only.

Table 3.2.2 contains all Coxeter pyramids over a product of simplices in \mathbb{H}^n having *no pair of disjoint facets* and *no dihedral angle $\frac{\pi}{4}$* . These pyramids exist only for $5 \leq n \leq 17$. They will play a crucial role in Chapter 4.

Chapter 3. Some classification results

n	
5	
6	
7	
8	
9	
11	
12	
13	
17	

Table 3.2.2: The Coxeter pyramids with mutually intersecting facets and having only dihedral angles of the form $\frac{\pi}{2}$, $\frac{\pi}{3}$ or $\frac{\pi}{6}$ in \mathbb{H}^n

The case $f_{n-1} = n + 3$

For a Coxeter polyhedron $P \subset \mathbb{H}^n$ with $n + 3$ facets, the classification is complete in the compact case (see [21, 79]), but it is *not* complete in the non-compact finite volume case. In fact, Coxeter polyhedra with $n + 3$ facets and non-simple vertices are not entirely known; see also [72].

In the compact case, Esselmann [20] showed that Coxeter n -polyhedra with $n + 3$ facets do not exist in dimensions $n > 8$, and Tumarkin [80] classified all of them. The unique polyhedron in dimension $n = 8$ is the one found earlier by Bugaenko [11].

In the non-compact case, Coxeter n -pyramids with $n + 3$ facets are pyramids over a product of three simplices and have been classified by Tumarkin [79] as well. They exist for dimensions $n \leq 13$. Table 3.2.2 contains the examples of Coxeter pyramids with mutually intersecting facets and having dihedral angles $\frac{\pi}{2}$, $\frac{\pi}{3}$ or $\frac{\pi}{6}$, only. Observe that they exist only for $n = 7$.

Another class of non-compact Coxeter polyhedra with $n + 3$ facets of interest to us are special *Napier cycles* found by Im Hof [38]. These are doubly-truncated orthogonal simplices, all of whose dihedral angles are bigger than or equal to $\frac{\pi}{6}$.

Finally, Tumarkin [80] proved that Coxeter polyhedra with $n + 3$ facets do not exist in dimensions $n \geq 17$, and that there exists a unique one in dimension $n = 16$.

As for Coxeter polyhedra with at most $n + 3$ facets, there are the following results.

All *compact* hyperbolic Coxeter polyhedra with at most $n + 3$ facets are classified; see the above sections.

In [26], Felikson and Tumarkin consider compact Coxeter polyhedra with ultraparallel facets and proved the following result.

Theorem 3.2.1. *A compact Coxeter polyhedron in \mathbb{H}^n with exactly one pair of ultraparallel facets has at most $n + 3$ facets.*

As a consequence, all compact hyperbolic Coxeter polyhedra with a unique pair of disjoint facets are known, and compact Coxeter polyhedra with more than $n + 3$ facets admit at least two pairs of non-intersecting facets.

About $f_{n-1} \geq n + 4$

Let us first mention that, in general, Coxeter n -polyhedra with at least $n + 4 \geq 8$ facets and no further restrictions are not well understood.

One result which we would like to cite here is due to Jacquemet and Tschantz [39]. They classified all the Coxeter hypercubes in \mathbb{H}^n and showed that they exist up to dimension $n = 5$.

A second and important observation concerns the result on pyramids of McLeod [61], who completed the classification as follows. A pyramid over a product of more than three simplices is necessarily a pyramid over a product of four simplices, and they exist only in dimension 5. Again, each of them admits a pair of disjoint facets. This fact will be used later on.

For dimensions $n = 4$ and 5, Coxeter polyhedra with precisely $n + 4$ facets are classified by works of Burcroff [12] and Ma-Zheng [55, 56]. For dimension $n = 7$, there is a unique Coxeter polyhedron with $n + 4$ facets, and there are no such polyhedra for $n \geq 8$, as proven by Felikson and Tumarkin in [27].

2.2 Coxeter polyhedra with mutually intersecting facets

In this section, we consider Coxeter polyhedra with *mutually intersecting facets*, that is, admitting no pair of disjoint facets in $\mathbb{H}^n \cup \partial\mathbb{H}^n$. In other words, their Coxeter diagrams have only finite labels.

In the following, we provide some important results due to Felikson and Tumarkin concerning the minimal number of pairs of non-intersecting facets in the subclass of *simple* Coxeter polyhedra. Then, we discuss the classification result due to Prokhorov [70] who considered Coxeter polyhedra with mutually intersecting facets and dihedral angles $\frac{\pi}{2}$ and $\frac{\pi}{3}$, only.

Some important results

Let $P \subset \mathbb{H}^n$ be a (finite-volume) Coxeter polyhedron all of whose facets are mutually intersecting.

The following results due to Felikson and Tumarkin [24] are of fundamental importance for this thesis.

Theorem 3.2.2. *Let $P \subset \mathbb{H}^n$ be a compact Coxeter polyhedron. If all facets of P are mutually intersecting, then P is either a simplex, or it is an Esselmann polyhedron.*

In the non-compact case, a similar result holds for simple polyhedra; see [24].

Theorem 3.2.3. *Let $P \subset \mathbb{H}^n$ be a non-compact simple Coxeter polyhedron. Assume that all facets of P are mutually intersecting. Then, P is either a simplex, or it is isometric to the polyhedron P_0 whose Coxeter graph is depicted in Figure 3.2.7.*

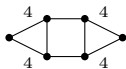


Figure 3.2.7: The Coxeter polyhedron $P_0 \subset \mathbb{H}^4$

As a consequence of Theorem 3.2.2 and Theorem 3.2.3, we deduce the following by-product. In fact, for $n \leq 4$, one can drop the simplicity condition from the combinatorial structure of ideal vertices.

Corollary 3.2.4. *Let $n \leq 4$. If $P \subset \mathbb{H}^n$ is a finite-volume Coxeter polyhedron with mutually intersecting facets, then P is a simplex, an Esselmann polyhedron, or P is isometric to the polyhedron P_0 depicted in Figure 3.2.7.*

Proof. Let $P \subset \mathbb{H}^n$ be a Coxeter polyhedron with mutually intersecting facets for $2 \leq n \leq 4$. If P is simple, by Theorems 3.2.2 and 3.2.3, P is either a simplex, an Esselmann polyhedron, or P_0 , and we are done. Suppose therefore that P has a non-simple vertex v_∞ , that is, v_∞ is the intersection of at least $n + 1$ facets. As any Coxeter polygon is simple, we can assume that $n > 2$.

In the Coxeter diagram Σ of P , the vertex v_∞ corresponds to an affine Coxeter subdiagram σ_∞ of rank $n - 1$ satisfying

$$\text{rank}(\sigma_\infty) = \text{order}(\sigma_\infty) - m, \quad (3.1)$$

where m is the number of connected affine components of σ_∞ ; see Theorem 1.3.8. Since v_∞ is non-simple, one has that $\text{order}(\sigma_\infty) \geq n + 1$. By means of (3.1), we deduce that the subdiagram σ_∞ admits at least $m \geq 2$ affine components. Since $n \leq 4$, it follows that σ_∞ has at least one affine component of rank 1. More precisely, for $n = 3$, $\sigma_\infty = \tilde{A}_1 \cup \tilde{A}_1$, and for $n = 4$, σ_∞ is either $\tilde{A}_1 \cup \tilde{A}_2$, $\tilde{A}_1 \cup \tilde{G}_2$, or $\tilde{A}_1 \cup \tilde{A}_1 \cup \tilde{A}_1$. Therefore, we derive that P admits at least one pair of parallel facets. \square

By Corollary 3.2.4, all Coxeter polyhedra in \mathbb{H}^n with mutually intersecting facets are known for $n \leq 4$.

The classification of ADE-polyhedra

Among all Coxeter polyhedra with mutually intersecting facets, a specific subfamily - very important for our research - has been classified by Prokhorov in [70]. This family comprises the so-called *ADE*-polyhedra.

Definition 3.2.5. An *ADE-polyhedron* is a Coxeter polyhedron $P \subset \mathbb{H}^n$ of finite volume satisfying the following properties.

1. All facets of P are mutually intersecting.
2. All dihedral angles of P are equal to $\frac{\pi}{2}$ or $\frac{\pi}{3}$.

The terminology is inspired by the spherical and affine cases where Coxeter polyhedra with mutually intersecting facets and with dihedral angles $\frac{\pi}{2}$ or $\frac{\pi}{3}$ are of type A_n , D_n or E_6, E_7, E_8 , as well as of type \tilde{A}_n , for $n > 1$, \tilde{D}_n , for $n \geq 3$, or $\tilde{E}_6, \tilde{E}_7, \tilde{E}_8$; see Tables 1.3.1 and 1.3.2.

By use of the classification results for ADE-lattices due to Nikulin [64], Prokhorov [70] derived that ADE-polyhedra do not exist in \mathbb{H}^n for $n > 17$, and he proved the following classification result.

Theorem 3.2.6 (Prokhorov [70]). *Let P be an ADE-polyhedron. Then, P is either a simplex, a pyramid, or one of the Coxeter polyhedra depicted in Figure 3.2.8.*

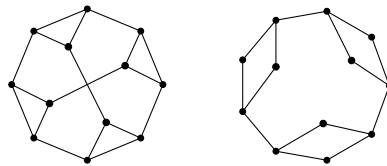


Figure 3.2.8: The ADE-polyhedra $P_1 \subset \mathbb{H}^8$ and $P_2 \subset \mathbb{H}^9$

In total, there are 34 hyperbolic ADE-polyhedra. The 32 ADE-simplices and ADE-pyramids can be found in the previous sections; see Figure 3.1.2, Table 3.2.1 and Table 3.2.2. The highest dimensional ADE-polyhedron is the Coxeter pyramid in \mathbb{H}^{17} depicted Table 3.2.2.

In the following chapter, we shall extend substantially Prokhorov's algorithm and develop further strategies in order to classify so-called ADEG-polyhedra. These are Coxeter polyhedra with mutually intersecting facets all of whose dihedral angles are $\frac{\pi}{2}$, $\frac{\pi}{3}$ and (at least one) $\frac{\pi}{6}$.

CHAPTER 4

COXETER POLYHEDRA WITH MUTUALLY INTERSECTING FACETS AND DIHEDRAL ANGLES $\frac{\pi}{2}$, $\frac{\pi}{3}$ AND $\frac{\pi}{6}$

In this chapter, we provide the complete classification of the following family of hyperbolic Coxeter polyhedra.

Definition 4.0.1. A polyhedron $P \subset \mathbb{H}^n$ is an *ADEG-polyhedron* if P is of finite volume and satisfies the following properties.

1. All facets of P are mutually intersecting.
2. All dihedral angles of P are equal to $\frac{\pi}{2}$, $\frac{\pi}{3}$ or $\frac{\pi}{6}$.
3. P has at least one dihedral angle $\frac{\pi}{6}$.

The terminology is inspired by Prokhorov's work [70] on the classification of ADE-polyhedra.

Let $P \subset \mathbb{H}^n$ be an ADEG-polyhedron and consider the Coxeter group Γ associated with P with its natural presentation given by (1.9), that is,

$$\langle s_1, \dots, s_N \mid s_i^2 = 1, (s_i s_j)^{m_{ij}} = 1 \rangle.$$

The ADEG-property of P implies that Γ satisfies the crystallographic condition which says that $m_{ij} \in \{2, 3, 4, 6\}$ for all $i, j \in \{1, \dots, N\}$; see Chapter 2. The irreducible spherical and affine subgroups of Γ and the related root systems are hence well understood.

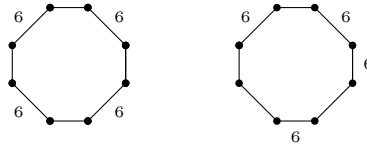


Figure 4.0.1: Two Napier cycles in \mathbb{H}^5

In Chapter 3, we already mentioned some examples of ADEG-polyhedra. For instance, the two special Napier cycles depicted in Figure 4.0.1 describe ADEG-polyhedra in \mathbb{H}^5 ; see [38].

We state now our main result providing the complete classification of ADEG-polyhedra; see [10].

Theorem 4.0.2. *Let $P \subset \mathbb{H}^n$ be an ADEG-polyhedron. Then, P is one of the 24 Coxeter polyhedra depicted in Table 4.0.1. In particular, P is non-compact for $n > 2$, non-simple for $n > 3$, and P is of dimension $n \leq 11$. Furthermore, P is combinatorially equivalent to one of the following polyhedra.*

- ✧ P is a triangle.
- ✧ P is a tetrahedron.
- ✧ P is a doubly-truncated 5-simplex.
- ✧ P is a pyramid over a product of two or three simplices.
- ✧ P is the polyhedron $P_\star \subset \mathbb{H}^9$ with 14 facets depicted in Figure 4.0.2.

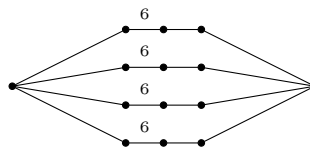


Figure 4.0.2: The Coxeter polyhedron $P_\star \subset \mathbb{H}^9$

Remark 4.0.3. Apart from the two-dimensional case and one tetrahedron, all ADEG-polyhedra give rise to Coxeter groups which are arithmetic over \mathbb{Q} ; see Chapter 1. The four compact ADEG-triangle groups are arithmetic as well, but their field of definition is $\mathbb{Q}(\sqrt{3})$; see Example 1.3.18.

n	
2	
3	
5	
6	
7	
9	
11	

Table 4.0.1: The ADEG-polyhedra in \mathbb{H}^n

Remark 4.0.4. The Coxeter polyhedron $P_\star \subset \mathbb{H}^9$ is a new discovery. It has 14 facets and 134 vertices with 6 of them being ideal. It will turn out that the group $\Gamma_\star = \Gamma(P_\star)$ is commensurable to the group associated with the ADE-polyhedron P_2 found by Prokhorov, as well as to all Coxeter simplex groups and all Coxeter pyramid groups in \mathbb{H}^9 ; see Figure 3.2.8 and Proposition 4.3.1. In particular, we will see that the volumes of all these polyhedra are of the form $q \cdot \frac{\zeta(5)}{22,295,347,200}$ with $q \in \mathbb{Q}_{\geq 1}$.

1 The general strategy

The proof of our main result as stated in Theorem 4.0.2 is very involved and has several ingredients of structural and of quite technical nature. In this section, we provide a rough overview and the different ideas which will show up. Later on, we will give all details. Some auxiliary data are collected in the two Appendices A and B.

Let $P \subset \mathbb{H}^n$ be a candidate for an ADEG-polyhedron, and let Σ be its Coxeter diagram.

- As P must have mutually intersecting facets, we have full control if P is simple or of dimension $n \leq 4$, in view of the results of Felikson and Tumarkin. Therefore, we will henceforth assume that P is a non-simple (and hence non-compact) polyhedron of dimension $n \geq 5$.
- As P must have at least one dihedral angle equal to $\frac{\pi}{6}$, the diagram Σ contains a subdiagram $\sigma = [6]$ of type G_2 . This property has two fundamental consequences.
- A first consequence is of combinatorial-metrical nature. By Borchers' theorem, σ corresponds to a face $F(\sigma)$ of codimension 2 in P which is itself an ADE- or an ADEG-polyhedron. We shall call $F(\sigma) = F(G_2)$ a G_2 -face.
- The second consequence is of algebraic nature. We show that $\sigma = [6]$ gives rise to an affine subdiagram $[6, 3]$ of type \tilde{G}_2 in Σ .
- The subdiagram \tilde{G}_2 can be completed to an affine subdiagram σ_∞ of rank $n - 1$ in Σ , and σ_∞ describes a non-simple ideal vertex v_∞ of P .
- The vertex v_∞ appears as the apex of a polyhedral cone $C_\infty \subset \mathbb{H}^n$ over a product of several simplices, each of dimension ≥ 2 .

- The cone C_∞ is of infinite volume and has to be truncated by additional hyperplanes $H_x, x \in \mathbb{R}^{n,1}$, not passing through v_∞ , in order to yield P . For two such hyperplanes H_x, H_y , one has $\angle(H_x, H_y) \in \{\frac{\pi}{2}, \frac{\pi}{3}, \frac{\pi}{6}\}$.
- The first hyperplanes H_x which we detect have to belong to the boundary of the G_2 -face $F(\sigma)$. This set is completed by hyperplanes H_y subject to the imposed angular condition.
- The related Lorentzian product $\langle x, y \rangle$ is controlled by Prokhorov's formula in terms of the (reducible) root lattice corresponding to σ_∞ . In this way, one finds several but finitely many so-called *admissible* pairs of vectors $\{x, y\}$.
- By truncating the cone C_∞ with all hyperplanes indexed by pairwise admissible vectors, one obtains a polyhedral object P . Finally, it remains to test if P is the realisation of a finite-volume hyperbolic n -polyhedron.

The above procedure is constructive relating P to its G_2 -faces, and it yields all but finitely many polyhedral candidates in each dimension.

Obviously, by the non-existence result stated in Theorem 3.0.1, the algorithm will not furnish ADEG-polyhedra of dimensions $n \geq 996$. In fact, it stops much earlier, namely for $n = 20$.

2 Proof of the main theorem

2.1 First steps

By the results of Felikson and Tumarkin, and by Corollary 3.2.4, all ADEG-polyhedra in \mathbb{H}^n are known for $n \leq 4$, and they are all simple. In fact, all simple ADEG-polyhedra are known in *any* dimension, and they are given by certain Coxeter simplices. They exist up to dimension 3. More precisely, in dimension 2, there are four compact triangles, and in dimension 3, there are seven non-compact tetrahedra, all depicted in Table 3.2.1.

Moreover, all Coxeter pyramids are classified, and we can extract all ten ADEG-pyramids from Table 3.2.2.

In the sequel we will consider ADEG-polyhedra of dimensions $n \geq 5$, only. They are non-simple, and we can suppose that they are different from (the known) Coxeter pyramids. We point out that all of their G_2 -faces are non-compact.

2.2 Existence of a component \tilde{G}_2

Let P be an ADEG-polyhedron in \mathbb{H}^n for $n \geq 5$. Let Σ be its Coxeter diagram. By hypothesis, it contains a subdiagram $\sigma = [6]$ of type G_2 in Σ . We show that Σ contains in fact a subdiagram $[6, 3]$ of type \tilde{G}_2 . This result will be essential.

Lemma 4.2.1. *Let $n \geq 5$, and let $P \subset \mathbb{H}^n$ be an ADEG-polyhedron. Then, the Coxeter diagram of P contains at least one subdiagram of type \tilde{G}_2 .*

Proof. Let $n \geq 5$, and let $P \subset \mathbb{H}^n$ be an ADEG-polyhedron. Denote by Σ its Coxeter diagram. Since P is an ADEG-polyhedron, Σ contains a subdiagram $\sigma = [6]$.

By Borchers' result stated in Theorem 1.3.9, σ yields a G_2 -face $F = F(G_2)$ of dimension $n - 2$ which is an ADE- or an ADEG-polyhedron. As $n - 2 \geq 3$, F is non-compact. Denote by σ_F the Coxeter diagram of F , and notice that σ_F is disjoint from σ .

Now, σ_F contains an affine subdiagram σ_F^∞ of rank $n - 3$ which appears as a component in an affine diagram of rank $n - 1$ in Σ . As the complement $\Sigma \setminus \sigma_F$ contains σ , the affine subdiagram of $\Sigma \setminus \sigma_F^\infty$ coincides with the diagram $[6, 3]$ of type \tilde{G}_2 . □

2.3 From a G_2 -face to an admissible set of vectors

Let $P \subset \mathbb{H}^n$ be an ADEG-polyhedron for $n \geq 5$, and let Σ be its Coxeter diagram.

By Lemma 4.2.1, there is an affine subdiagram in Σ of the form

$$\sigma_\infty = \sigma_1 \cup \sigma_2 \cup \cdots \cup \sigma_m = \tilde{G}_2 \cup \sigma_2 \cup \cdots \cup \sigma_m, \quad m \geq 2.$$

As before, denote by r_i the rank of σ_i so that $\sum_{i=1}^m r_i = n - 1$.

In our setting, each affine component σ_i can be interpreted as the extended Dynkin diagram of a root system R_i of type A, D, E or G_2 ; see Chapter 2.

Denote by $e_1^i, \dots, e_{r_i}^i$ the natural simple roots (with their prescribed lengths), together with $e_{r_i+1}^i$ given by the opposite of the highest root of R_i .

The diagram σ_∞ corresponds to a non-simple ideal vertex v_∞ of the polyhedron P . The vectors e_j^i associated with σ_i can be interpreted as spacelike vectors normal to hyperplanes $H_{e_j^i}$ passing through v_∞ . Furthermore, we treat v_∞ as a lightlike vector in $\mathbb{R}^{n,1}$. In particular, v_∞ is Lorentz-orthogonal

to all e_j^i , and it can be expressed in terms of certain lightlike vectors v_∞^i related to the affine components σ_i for $i = 1, \dots, m$ as follows.

Lemma 4.2.2. *For each $1 \leq i \leq m$, there exist positive integers $c_1^i, \dots, c_{r_i+1}^i$ with $c_{r_i+1}^i = 1$ such that the vector $v_\infty^i := c_1^i e_1^i + \dots + c_{r_i+1}^i e_{r_i+1}^i \in \mathbb{R}^{n,1}$ is collinear with v_∞ .*

Proof. Let $c_1^i, \dots, c_{r_i}^i \in \mathbb{Z}$ be the integers such that

$$-e_{r_i+1} = c_1^i e_1^i + \dots + c_{r_i}^i e_{r_i}^i \in \mathbb{R}^{r_i}; \quad (4.1)$$

see Chapter 2 for their explicit form. The vector $v_\infty^i = c_1^i e_1^i + \dots + c_{r_i}^i e_{r_i}^i + e_{r_i+1}^i$ (suitably extended to a non-zero vector in $\mathbb{R}^{n,1}$) satisfies $\langle v_\infty^i, v_\infty^i \rangle = 0$ by properties of the highest root. In addition, $\langle v_\infty^i, v_\infty \rangle = 0$ as $\langle e_j^i, v_\infty \rangle = 0$ for all $j = 1, \dots, r_i + 1$. Now, we conclude by means of Lemma 1.2.1. \square

As a consequence of Lemma 4.2.2, and for each i , the vectors v_∞ and v_∞^i are collinear and define the same lightlike ray, symbolized by $v_\infty \sim v_\infty^i$. In particular, for $i = 1$ and $\sigma_1 = \tilde{G}_2$, we derive that

$$v_\infty \sim v_\infty^1 = 3e_1^1 + 2e_2^1 + e_3^1; \quad (4.2)$$

see Definition 2.3.6.

Let us come back to the set of hyperplanes $H_{e_j^i}$ with $1 \leq j \leq r_i + 1$ and $1 \leq i \leq m$. The goal is to complete this set by at least two additional hyperplanes H_x, H_y , where $x, y \in \mathbb{R}^{n,1}$ are spacelike vectors, in order to form the boundary of an ADEG-polyhedron.

In what follows, we will always consider x and y to have squared norm 2.

We characterize the vectors $x, y \in \mathbb{R}^{n,1}$ in terms of their Lorentzian products $k_j^i := \langle x, e_j^i \rangle$ and $l_j^i := \langle y, e_j^i \rangle$ with the vectors e_j^i .

More precisely, we encode x and y by strings in the following way.

$$x \leftrightarrow (k_1^1, k_2^1, k_3^1; k_1^2, \dots, k_{r_2+1}^2; \dots; k_1^m, \dots, k_{r_m+1}^m) \quad (4.3)$$

$$y \leftrightarrow (l_1^1, l_2^1, l_3^1; l_1^2, \dots, l_{r_2+1}^2; \dots; l_1^m, \dots, l_{r_m+1}^m)$$

Since $\angle(H_x, H_{e_j^i})$ and $\angle(H_y, H_{e_j^i})$ vary within the set $\{\frac{\pi}{2}, \frac{\pi}{3}, \frac{\pi}{6}\}$, one has $k_j^i, l_j^i \in \{0, -1, -\sqrt{3}, -3\}$. More specifically, the quantities $k_j^i = \langle x, e_j^i \rangle$ are

as follows.

$$\langle x, e_j^i \rangle = \begin{cases} 0 & \text{if } \angle(H_x, H_{e_j^i}) = \frac{\pi}{2} \\ -1 & \text{if } \angle(H_x, H_{e_j^i}) = \frac{\pi}{3} \text{ and } \|e_j^i\|^2 = 2 \\ -\sqrt{3} & \text{if } \angle(H_x, H_{e_j^i}) = \frac{\pi}{6} \text{ and } \|e_j^i\|^2 = 2 \\ -\sqrt{3} & \text{if } \angle(H_x, H_{e_j^i}) = \frac{\pi}{3} \text{ and } \|e_j^i\|^2 = 6 \\ -3 & \text{if } \angle(H_x, H_{e_j^i}) = \frac{\pi}{6} \text{ and } \|e_j^i\|^2 = 6 \end{cases} \quad (4.4)$$

Similar expressions hold for $l_j^i = \langle y, e_j^i \rangle$.

In this setting, the Lorentzian product $\langle x, y \rangle$ can be expressed in terms of the string coefficients of x and y given by (4.3). This point of view is taken from work of Nikulin [65] and Prokhorov [70], and we provide the technical details in what follows.

Fix two spacelike vectors $x, y \in \mathbb{R}^{n,1}$ such that $\langle x, v_\infty \rangle \neq 0$, $\langle y, v_\infty \rangle \neq 0$, that is, the hyperplanes H_x and H_y do not pass through the vertex v_∞ .

Consider now the quantities Λ and Λ_i , $1 \leq i \leq m$, defined as follows.

$$\Lambda = \Lambda_{xy} := \frac{\langle x, v_\infty \rangle}{\langle y, v_\infty \rangle} \quad \text{and} \quad \Lambda_i := \frac{\langle x, v_\infty^i \rangle}{\langle y, v_\infty^i \rangle} = \frac{\langle x, \sum_{k=1}^{r_i+1} c_k^i e_k^i \rangle}{\langle y, \sum_{k=1}^{r_i+1} c_k^i e_k^i \rangle},$$

where the lightlike vectors v_∞^i are defined in Lemma 4.2.2.

In particular, in our setting where $\sigma_1 = \tilde{G}_2$, one has

$$\Lambda_1 = \frac{3k_1^1 + 2k_2^1 + k_3^1}{3l_1^1 + 2l_2^1 + l_3^1}. \quad (4.5)$$

Since $v_\infty^i \sim v_\infty$ by Lemma 4.2.2, one immediately deduces that

$$\Lambda_i = \Lambda \quad \text{for } i = 1, \dots, m. \quad (4.6)$$

With these preparations, we are able to write down Prokhorov's formula [70] for the Lorentzian product $\langle x, y \rangle$.

Prokhorov's formula.

$$\langle x, y \rangle = \frac{\langle x, x \rangle}{2\Lambda} + \frac{\langle y, y \rangle}{2}\Lambda - (\Delta_1 + \dots + \Delta_m), \quad (4.7)$$

with

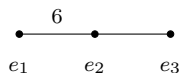
$$\Delta_p = \sum_{1 \leq i < j \leq r_p+1} (k_i^p l_j^p + k_j^p l_i^p - \frac{k_i^p k_j^p}{\Lambda} - l_i^p l_j^p \Lambda) s_{ij}^p. \quad (4.8)$$

The quantities s_{ij}^p in (4.8) depend on the fundamental weights of the root system R_p as follows; see [70]. Let w_1, \dots, w_{r_p} be the fundamental weights of the root system R_p as described in Chapter 2, and let c_j^p be the integers according to (4.1). Then,

$$\begin{cases} s_{ij}^p = \langle w_i, w_j \rangle - \frac{\langle w_i, w_i \rangle c_j^p}{2c_i^p} - \frac{\langle w_j, w_j \rangle c_i^p}{2c_j^p} & \text{for } 1 \leq i, j \leq r_p, \\ s_{ir_p}^p = \frac{\langle w_i, w_i \rangle}{2c_i^p} & \text{for } i = 1, \dots, r_p, \\ s_{ii}^p = 0 & \text{for } i = 1, \dots, r_p + 1. \end{cases} \quad (4.9)$$

In the following example we give the explicit form of these quantities for a component of type \tilde{G}_2 . For the affine components of type \tilde{A} , \tilde{D} or \tilde{E} , we refer to Appendix A.

Example 4.2.3. For the root system G_2 underlying \tilde{G}_2 , the roots indexing the nodes of the diagram \tilde{G}_2 , as depicted below, are such that $\|e_1\|^2 = 2$, and $\|e_2\|^2 = \|e_3\|^2 = 6$; see Definition 2.3.6. One has $\langle e_1, e_2 \rangle = \langle e_2, e_3 \rangle = -3$ and $\langle e_1, e_3 \rangle = 0$.



Furthermore, $c_1 = 3, c_2 = 2$ and $c_3 = 1$, and the fundamental weights for G_2 are given by

$$\begin{cases} w_1 = 2e_1 + e_2 \\ w_2 = 3e_1 + 2e_2. \end{cases}$$

Hence $\langle w_1, w_1 \rangle = 2, \langle w_2, w_2 \rangle = 6, \langle w_1, w_2 \rangle = 3$. From (4.9), it follows that

$$s_{12} = \frac{13}{6}, \quad s_{23} = \frac{1}{3} \quad \text{and} \quad s_{13} = \frac{3}{2}.$$

Let us return to the non-simple ideal vertex v_∞ of the ADEG-polyhedron $P \subset \mathbb{H}^n$ and its associated affine diagram

$$\sigma_\infty = \tilde{G}_2 \cup \sigma_2 \cup \dots \cup \sigma_m, \quad m \geq 2.$$

In this context, consider two spacelike vectors x, y of squared norm 2 such that $\langle x, v_\infty \rangle \neq 0, \langle y, v_\infty \rangle \neq 0$, together with their strings (4.3).

Definition 4.2.4. The vectors x, y form an *admissible pair*, denoted by $\{x, y\}$, if they fulfil the following conditions.

$$\Lambda_1 = \frac{3k_1^1 + 2k_2^1 + k_3^1}{3l_1^1 + 2l_2^1 + l_3^1} = \frac{\sum_j c_j^2 k_j^2}{\sum_j c_j^2 l_j^2} = \dots = \frac{\sum_j c_j^m k_j^m}{\sum_j c_j^m l_j^m} = \Lambda_m = \Lambda, \quad (4.10)$$

and

$$\langle x, y \rangle = \Lambda + \frac{1}{\Lambda} - (\Delta_1 + \dots + \Delta_m) \in \{0, -1, -\sqrt{3}\}, \quad (4.11)$$

where $\Delta_1, \dots, \Delta_m$ are given by (4.8).

A set of vectors $\{z_1, \dots, z_t\}$ is said to be *admissible* if its elements are pairwise admissible, that is, $\{z_i, z_j\}$ is an admissible pair for all $i, j \in \{1, \dots, t\}$, $i \neq j$.

Now, consider the subdiagram $\sigma = [6]$ of the component \tilde{G}_2 in σ_∞ , and let $F = F(\sigma)$ be the G_2 -face with Coxeter diagram σ_F . By Borchers' result, σ_F contains the affine diagram $\sigma_2 \cup \dots \cup \sigma_m$, and it is hyperbolic.

Denote by x_1, \dots, x_t all the nodes in $\sigma_F \setminus (\sigma_2 \cup \dots \cup \sigma_m)$. They represent hyperplanes H_{x_1}, \dots, H_{x_t} not containing v_∞ , and we take them of squared norm 2. Furthermore, they are *good* neighbours of σ implying that

$$\langle x_i, e_1^1 \rangle = \langle x_i, e_2^1 \rangle = 0 \quad \text{for } i = 1, \dots, t.$$

To begin with, suppose that $t = 1$, and write $x = x_1$. Since x is a good neighbour of σ , its string can be written as

$$x \leftrightarrow (0, 0, a; k_1^2, \dots, k_{r_2+1}^2; \dots; k_1^m, \dots, k_{r_m+1}^m), \quad (4.12)$$

where we abbreviate $a := k_3^1 = \langle x, e_3^1 \rangle \in \{0, -\sqrt{3}, -3\}$; see (4.4). Observe that $a \neq 0$, since otherwise the complement of σ_F in Σ is not equal to σ .

By assumption, the ADEG-polyhedron P is not a pyramid; see Section 2.1. Therefore, there is at least one additional hyperplane H_y that is not passing through v_∞ . The corresponding node is a *bad* neighbour of σ , and obviously outside of σ_F .

Suppose that y is of squared norm 2, and put

$$y \leftrightarrow (l_1^1, l_2^1, l_3^1; l_1^2, \dots, l_{r_2+1}^2; \dots; l_1^m, \dots, l_{r_m+1}^m)$$

for its string. As y is a bad neighbour of σ , l_1^1 and l_2^1 are not simultaneously zero.

Notation. In what follows, for simplicity, we replace k_j^i by its opposite and write $k_j^i = -\langle x, e_j^i \rangle$ from now on. Similarly, we denote $l_j^i = -\langle y, e_j^i \rangle$.

Since P should be an ADEG-polyhedron, the vectors x and y form an admissible pair $\{x, y\}$. If the hyperplanes H_x and H_y combined with the hyperplanes $H_{e_j^i}, 1 \leq j \leq r_i + 1, 1 \leq i \leq m$, bound a finite-volume polyhedron in \mathbb{H}^n , we realised an ADEG-polyhedron whose combinatorial-metrical structure is explicit. Otherwise, for $t = 1$, we have to search for additional vectors y_i such that $\{x, y_i\}$ and $\{y_i, y_j\}, i \neq j$, are admissible pairs.

Next, suppose that $t \geq 2$. The vectors x_1, \dots, x_t are all encoded by strings according to (4.12) where

$$a_i := -\langle x_i, e_3^1 \rangle \in \{\sqrt{3}, 3\}. \quad (4.13)$$

Since P is an ADEG-polyhedron, the set $\{x_1, \dots, x_t\}$ is admissible. As above, either the hyperplanes H_{x_i} , together with the hyperplanes $H_{e_j^i}$, bound a finite-volume polyhedron in \mathbb{H}^n , or one has to add vectors y_i to $\{x_1, \dots, x_t\}$ to produce an admissible set.

Remark 4.2.5. Each G_2 -face $F \subset P$ is an ADE- or ADEG-polyhedron of dimension $n - 2 \geq 3$. By fixing one such polyhedron, we fix the string coefficients of the corresponding vectors x_1, \dots, x_t up to the terms given by (4.13). In this way, and by comparing with Prokhorov's way, our classification procedure in the ADEG-case is more efficient.

2.4 The classification of ADEG-polyhedra

Let $n \geq 5$, and let $P \subset \mathbb{H}^n$ be an ADEG-polyhedron with Coxeter diagram Σ . Assume that P is not a pyramid. As in the previous sections, denote by v_∞ a non-simple vertex of P whose associated subdiagram is of the form

$$\sigma_\infty = \tilde{G}_2 \cup \sigma_2 \cup \dots \cup \sigma_m, \quad m \geq 2.$$

Recall that the G_2 -face $F = F(\sigma) \subset \mathbb{H}^{n-2}$, where $\sigma = [6] \subset \tilde{G}_2$, is a non-compact ADE- or ADEG-polyhedron. Denote by σ_F its Coxeter diagram.

We work inductively on the dimension $n \geq 5$ by taking into account the knowledge of all ADE- and ADEG-polyhedra of dimensions 3 and 4.

This induction process finishes in dimension n if there exists neither an ADE-polyhedron nor an ADEG-polyhedra in \mathbb{H}^{n-2} which could serve as a G_2 -face of an ADEG-polyhedron in \mathbb{H}^n . A priori, the procedure has to be performed at least up to dimension $n = 19$, as there exists one ADE-pyramid in \mathbb{H}^{17} .

In practice, we fix a face G_2 -face F , and denote by x_1, \dots, x_t the nodes which, together with $\sigma_2 \cup \dots \cup \sigma_m$, constitute the diagram σ_F .

Observe that in the case where F is a simplex or a pyramid, one necessarily has $t = 1$, and one has $t \geq 2$ otherwise.

By means of Prokhorov's formula, and with the help of the software Mathematica [85], we find all the vectors y which together with the vectors corresponding to x_1, \dots, x_t form an admissible set; see Section 2.3.

Then, for each admissible set, we verify if the arrangement of the different hyperplanes of the form $H_{e_j^i}$, H_x and H_y give rise to a finite-volume polyhedron in \mathbb{H}^n . To this end, we apply one of the following three criteria.

- ✧ The signature of the Gram matrix is $(n, 1)$.
- ✧ Vinberg's finite-volume criterion stated in Theorem 1.3.15.
- ✧ Each $(n - 2)$ -face has to be of finite volume.

For example, spherical subdiagrams of rank $> n$ cannot appear, and any affine subdiagram is a component of an affine subdiagram of rank $n - 1$.

We are now ready to start the induction procedure.

Assume that $n = 5$

By Lemma 4.2.1, the affine diagram $\sigma_\infty = \sigma_1 \cup \sigma_2$ of rank 4 is either $\tilde{G}_2 \cup \tilde{G}_2$ or $\tilde{G}_2 \cup \tilde{A}_2$. In addition, we know that the 3-face $F = F(G_2)$ is a finite-volume Coxeter polyhedron whose Coxeter diagram σ_F contains σ_2 . Therefore, F is an ADE- or ADEG-tetrahedron, and there are ten possibilities for σ_F ; see Figure 3.1.2.

Consider the vector $x \in \mathbb{R}^{5,1}$, $\|x\|^2 = 2$, that together with e_1^2, e_2^2 and e_3^2 forms σ_F . For the string of x , we have

$$x \leftrightarrow (0, 0, a; k_1^2, k_2^2, k_3^2) \tag{4.14}$$

where $a = -\langle x, e_3^1 \rangle \in \{\sqrt{3}, 3\}$ and $k_j^2 = -\langle x, e_j^2 \rangle \in \{0, 1, \sqrt{3}, 3\}$.

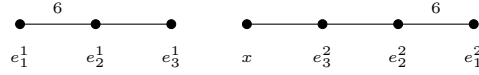
Table 4.2.2 contains all relevant strings for x to be considered, written as in (4.14). In fact, we omit the ones that lead to symmetric configurations. Notice also that in some cases the coefficient $a = \sqrt{3}$ for x can be excluded. The reason will become clear in part (i) below; see Remark 4.2.6.

◇ Suppose that $\sigma_\infty = \tilde{G}_2 \cup \tilde{G}_2$. Then, F is one of the seven ADEG-tetrahedra; see Figure 3.1.2. In what follows, we describe the two most important cases, only. For all other cases, we give just a few details, but display all the admissible pairs in Table 4.2.3.

σ_∞	String for x	σ_∞	String for x
$\widetilde{G}_2 \cup \widetilde{G}_2$	$(0, 0, 3; 0, 0, \sqrt{3})$	$\widetilde{G}_2 \cup \widetilde{A}_2$	$(0, 0, 3; 1, 0, 0)$
	$(0, 0, a; 1, 0, 0)$		$(0, 0, a; 1, 0, 1)$
	$(0, 0, 3; 0, 0, 3)$		$(0, 0, a; 1, 1, 1)$
	$(0, 0, a; 0, \sqrt{3}, 0)$		$(0, 0, a; \sqrt{3}, 0, 0)$
	$(0, 0, a; 1, 0, \sqrt{3})$		
	$(0, 0, a; 1, 0, 3)$		

Table 4.2.2: Strings for dimension $n = 5$

(i) Assume that F is the Coxeter tetrahedron with Coxeter symbol $[3, 3, 6]$. The situation can be described with the following diagram.



We get $x \leftrightarrow (0, 0, a; 0, 0, \sqrt{3})$ for $a \in \{\sqrt{3}, 3\}$.

A vector $y \leftrightarrow (l_1^1, l_2^1, l_3^1; l_1^2, l_2^2, l_3^2)$, $\|y\|^2 = 2$, forms an admissible pair with x if

$$\Lambda_1 = \frac{a}{3l_1^1 + 2l_2^1 + l_3^1} = \frac{\sqrt{3}}{3l_1^2 + 3l_2^2 + l_3^2} = \Lambda_2 = \Lambda,$$

and if $\langle x, y \rangle = \Lambda + \frac{1}{\Lambda} - (\Delta_1 + \Delta_2) \in \{0, -1, -\sqrt{3}\}$ with Δ_1 and Δ_2 as in (4.8).

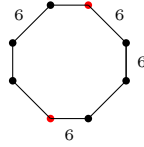
Remark 4.2.6. For $a = \sqrt{3}$, the Coxeter diagram of a 5-pyramid of finite-volume appears as a proper subdiagram of Σ which is impossible in view of Proposition 1.3.17.

As a consequence of Remark 4.2.6, we can assume that $a = 3$. There is a unique solution so that $\{x, y\}$ is admissible, and it is given by

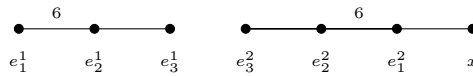
$$y \leftrightarrow (l_1^1, l_2^1, l_3^1; l_1^2, l_2^2, l_3^2) = (\sqrt{3}, 0, 0; 1, 0, 0)$$

for which $\Lambda = \frac{1}{\sqrt{3}}$, $\Delta_1 = \sqrt{3}$ and $\Delta_2 = \frac{1}{\sqrt{3}}$, and one gets $\langle x, y \rangle = 0$.

This configuration corresponds to the Napier cycle depicted below wherein the red nodes correspond to the vectors x and y .



(ii) Assume that F is the tetrahedron with Coxeter symbol $[3, 6, 3]$. The situation can be described with the following diagram.

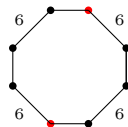


For $x \leftrightarrow (0, 0, \sqrt{3}; 1, 0, 0)$, there is unique vector y such that the pair $\{x, y\}$ is admissible. It is given by $y \leftrightarrow (0, \sqrt{3}, \sqrt{3}; 1, 0, 0)$ and yields $\langle x, y \rangle = 0$. This configuration, depicted below, does not correspond to a finite-volume 5-polyhedron.



In fact, this can be easily deduced from the Coxeter diagram as it contains an affine subdiagram \tilde{A}_2 which cannot be completed to yield an affine subdiagram of rank 4. This contradicts Theorem 1.3.15.

For $x \leftrightarrow (0, 0, 3; 1, 0, 0)$, there is again a unique solution $y \leftrightarrow (1, 0, 0; 0, 0, 3)$ which satisfies $\langle x, y \rangle = 0$. This gives rise to the Napier cycle depicted below.



For all of the remaining cases, the admissible pairs are listed in Table 4.2.3. However, none of them gives rise to a 5-polyhedron of finite volume. Furthermore, there exists no admissible set of cardinality > 2 .

◊ In the case where $\tilde{\sigma}_\infty = \tilde{G}_2 \cup \tilde{A}_2$, none of the admissible pairs yields a finite-volume polyhedron. In addition, we find one admissible set formed by three vectors. The set of their strings is as follows.

$$\{(0, 0, 3; 1, 0, 0), (\sqrt{3}, 0, 0; 0, 0, \sqrt{3}), (0, 0, 3; \sqrt{3}, 0, 0)\} .$$

However, also in this case, we do not obtain a finite-volume polyhedron.

This finishes the proof for $n = 5$.

σ_∞	x	y	$\langle x, y \rangle$
$\tilde{G}_2 \cup \tilde{G}_2$	$(0, 0, 3; 0, 0, \sqrt{3})$	$(\sqrt{3}, 0, 0; 1, 0, 0)$	0
	$(0, 0, \sqrt{3}; 1, 0, 0)$	$(1, 0, 0; 0, \sqrt{3}, \sqrt{3})$	0
	$(0, 0, 3; 1, 0, 0)$	$(1, 0, 0; 0, 0, 3)$	0
	$(0, 0, 3; 0, 0, 3)$	$(1, 0, 0; 1, 0, 0)$	0
	$(0, 0, 3; 0, \sqrt{3}, \sqrt{3})$	$(\sqrt{3}, 0, 0; 1, 3, 0)$	0
$\tilde{G}_2 \cup \tilde{A}_2$	$(0, 0, 3; 1, 0, 0)$	$(\sqrt{3}, 0, 0; 0, 0, \sqrt{3})$	0
	$(0, 0, 3; \sqrt{3}, 0, 0)$	$(\sqrt{3}, 0, 0; 0, 0, \sqrt{3})$	0
	$(0, 0, 3; \sqrt{3}, 0, 0)$	$(\sqrt{3}, 0, 0; 0, \sqrt{3}, 0)$	0

 Table 4.2.3: Admissible pairs $\{x, y\}$ for $n = 5$

Assume that $n = 6$

By means of Lemma 4.2.1, there is a unique case to consider given by $\sigma_\infty = \tilde{G}_2 \cup \tilde{A}_3$. Hence, there are two possibilities for F , since σ_F has to contain to component \tilde{A}_3 . More precisely, σ_F is one of the two corresponding ADE-simplices; see Table 3.2.1.

By Remark 4.2.6, we only have to consider the strings $x \leftrightarrow (0, 0, 3; 1, 0, 0, 0)$ and $x \leftrightarrow (0, 0, a; 1, 0, 1, 0)$ for $a \in \{\sqrt{3}, 3\}$. In both cases, we find that there is no admissible pair.

Hence, apart from a single pyramid, there are no further ADEG-polyhedra in \mathbb{H}^6 .

Assume that $n = 7$

There are eight possibilities for the diagram σ_F . Namely, F is one of the three ADE-simplices, the three ADEG-pyramids and the two Napier cycles in \mathbb{H}^5 given in Figure 4.0.1.

If F is a simplex or a pyramid, there is only one vector x to be added to the set $\{e_j^i\}_{i,j}$ in order to form σ_F . If F is a Napier cycle, two vectors x_1 and x_2 are added to $\{e_j^i\}_{i,j}$ to form σ_F . By taking into account Remark 4.2.6, we list all corresponding strings in Table 4.2.4.

In what follows, we only give the details for the case where $\sigma_\infty = \tilde{G}_2 \cup \tilde{G}_2 \cup \tilde{G}_2$. Hence, F is the pyramid with the Coxeter symbol $[6, 3, 3, 3, 3, 6]$, or one of the two Napier cycles.

For all the other cases, the admissible pairs are summarized in Table 4.2.5.

σ_∞	Strings for x
$\tilde{G}_2 \cup \tilde{A}_4$	$(0,0,3;1,0,0,0,0)$
$\tilde{G}_2 \cup \tilde{D}_4$	$(0,0,3;1,0,0,0,0)$ $(0,0,a;0,1,0,0,0)$
$\tilde{G}_2 \cup \tilde{A}_2 \cup \tilde{A}_2$	$(0,0,3;1,0,0;1,0,0)$
$\tilde{G}_2 \cup \tilde{G}_2 \cup \tilde{A}_2$	$(0,0,3;0,0,\sqrt{3};1,0,0)$
$\tilde{G}_2 \cup \tilde{G}_2 \cup \tilde{G}_2$	$(0,0,3;0,0,\sqrt{3};0,0,\sqrt{3})$ $\{x_1 \leftrightarrow (0,0,a_1;0,0,3;1,0,0),$ $x_2 \leftrightarrow (0,0,a_2;1,0,0;\sqrt{3},0,0)\}$ $\{x_1 \leftrightarrow (0,0,a_1;0,0,\sqrt{3};0,0,3),$ $x_2 \leftrightarrow (0,0,a_2;0,0,3;1,0,0)\}$

Table 4.2.4: Strings for dimension $n = 7$

(i) Assume that $\sigma_F = [6, 3, 3, 3, 3, 6]$. By Remark 4.2.6, we consider the vector x with the string

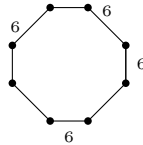
$$x \leftrightarrow (0, 0, 3; 0, 0, \sqrt{3}; 0, 0, \sqrt{3}) .$$

There are two vectors y_i such that $\{x, y_i\}$ is an admissible pair, namely

$$y_1 \leftrightarrow (\sqrt{3}, 0, 0; 0, 0, 3; 1, 0, 0) , \quad y_2 \leftrightarrow (\sqrt{3}, 0, 0; 1, 0, 0; 0, 0, 3),$$

and one has $\langle x, y_1 \rangle = \langle x, y_2 \rangle = 0$. Moreover, we verify that $\{y_1, y_2\}$ is also an admissible pair. However, there is no admissible set giving rise to a finite-volume 7-polyhedron.

(ii) Assume that F is the Napier cycle depicted below.



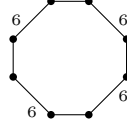
In this case, we can choose

$$x_1 \leftrightarrow (0, 0, a_1; 0, 0, \sqrt{3}; 0, 0, 3) \text{ and } x_2 \leftrightarrow (0, 0, a_2; 1, 0, 0; \sqrt{3}, 0, 0) .$$

Then, we determine the coefficients $a_1, a_2 \in \{\sqrt{3}, 3\}$ so that $\{x_1, x_2\}$ is an admissible pair. As $\Lambda_1 = \frac{a_1}{a_2}$ and $\Lambda_2 = \Lambda_3 = \frac{1}{\sqrt{3}}$, this yields $a_1 = \frac{a_2}{\sqrt{3}}$, that is, $a_1 = \sqrt{3}$ and $a_2 = 3$. It follows that $\langle x_1, x_2 \rangle = 0$. However, the resulting polyhedron does not have finite volume.

Next, we search for all vectors y such that $\{x_1, x_2, y\}$ is an admissible set. The only solution is given by $y \leftrightarrow (1, 0, 0; 0, 0, 3; \sqrt{3}, 0, 0)$, and again, we do not get a finite-volume polyhedron.

(iii) Assume that F is the Napier cycle given below.



We write $x_1 \leftrightarrow (0, 0, a_1; 1, 0, 0; 0, 0, 3)$ and $x_2 \leftrightarrow (0, 0, a_2; 0, 0, 3; 1, 0, 0)$.

As above, since $\Lambda_2 = \Lambda_3 = 1$, this amounts to $a_1 = a_2 \in \{\sqrt{3}, 3\}$. As a consequence, $\Delta_1 = 0$, and for each $a := a_1 = a_2 \in \{\sqrt{3}, 3\}$, $\{x_1, x_2\}$ is admissible and such that $\langle x_1, x_2 \rangle = 0$. None of the resulting configurations yields a finite-volume polyhedron.

For $a = \sqrt{3}$, we find one vector $y \leftrightarrow (1, 0, 0; \sqrt{3}, 0, 0; \sqrt{3}, 0, 0)$ such that $\{x_1, x_2, y\}$ is admissible. Also, this configuration does not give rise to a finite-volume polyhedron.

For $a = 3$, we find all the vectors z_i such that $\{x_1, x_2, z_i\}$ is admissible. They are given by

$$z_1 \leftrightarrow (1, 0, 0; 0, 0, 3; 0, 0, 3) , \quad z_2 \leftrightarrow (1, 0, 0; 1, 0, 0; 1, 0, 0) , \\ z_3 \leftrightarrow (\sqrt{3}, 0, \sqrt{3}; \sqrt{3}, 0, \sqrt{3}; \sqrt{3}, 0, \sqrt{3}) .$$

In addition, $\{z_1, z_2\}$ and $\{z_1, z_3\}$ are admissible pairs. However, for each of the different admissible sets, we do not obtain a finite-volume polyhedron.

σ_∞	x	y	$\langle x, y \rangle$
$\tilde{G}_2 \cup \tilde{D}_4$	$(0, 0, \sqrt{3}; 0, 1, 0, 0, 0)$	$(0, \sqrt{3}, \sqrt{3}; 1, 1, 1, 1, 1)$	0
$\tilde{G}_2 \cup \tilde{A}_2 \cup \tilde{A}_2$	$(0, 0, 3; 1, 0, 0; 1, 0, 0)$	$y_1 \leftrightarrow (\sqrt{3}, 0, 0; 0, 0, \sqrt{3}; \sqrt{3}, 0, 0)$	0
		$y_2 \leftrightarrow (\sqrt{3}, 0, 0; 0, \sqrt{3}, 0; \sqrt{3}, 0, 0)$	0
$\tilde{G}_2 \cup \tilde{G}_2 \cup \tilde{A}_2$	$(0, 0, 3; 0, 0, \sqrt{3}; 1, 0, 0)$	$(\sqrt{3}, 0, 0; 1, 0, 0; \sqrt{3}, 0, 0)$	0

Table 4.2.5: The remaining admissible pairs $\{x, y\}$ for $n = 7$

For the remaining cases, we list all admissible pairs in Table 4.2.5. Notice that there is no admissible pair for $\sigma_\infty = \tilde{G}_2 \cup \tilde{A}_4$.

The pair $\{y_1, y_2\}$ as given in Table 4.2.5 for $\sigma_\infty = \tilde{G}_2 \cup \tilde{A}_2 \cup \tilde{A}_2$ is not admissible. Again, none of the admissible pairs yields a finite-volume polyhedron in \mathbb{H}^7 .

Assume that $n = 8$

By means of Lemma 4.2.1, σ_F is either one of the two ADE-simplices or one of two ADEG-pyramids. The corresponding strings are listed in Table 4.2.6.

σ_∞	String for x
$\tilde{G}_2 \cup \tilde{A}_5$	$(0, 0, a; 1, 0, 0, 0, 0, 0)$
$\tilde{G}_2 \cup \tilde{D}_5$	$(0, 0, a; 1, 0, 0, 0, 0, 0)$
$\tilde{G}_2 \cup \tilde{A}_2 \cup \tilde{A}_3$	$(0, 0, a; 1, 0, 0; 1; 0, 0, 0)$
$\tilde{G}_2 \cup \tilde{G}_2 \cup \tilde{A}_3$	$(0, 0, a; 0, 0, \sqrt{3}; 1; 0, 0, 0)$

Table 4.2.6: Strings for dimension $n = 8$

Let us give some details for the case where $\sigma_\infty = \tilde{G}_2 \cup \tilde{A}_5$, only. By Table 4.2.7, there are six admissible pairs of the form $\{x, y_i\}$. We determine which of the vectors y_1, \dots, y_6 form admissible pairs and give their Lorentzian products $\langle y_i, y_j \rangle$ in Table 4.2.8. Empty boxes correspond to inadmissible pairs.

σ_∞	x	y	$\langle x, y \rangle$
$\tilde{G}_2 \cup \tilde{A}_5$	$(0, 0, \sqrt{3}; 1, 0, 0, 0, 0, 0)$	$y_1 \leftrightarrow (0, \sqrt{3}, \sqrt{3}; 0, 0, 0, 1, 1, 1)$	-1
		$y_2 \leftrightarrow (0, \sqrt{3}, \sqrt{3}; 0, 1, 1, 1, 0, 0)$	0
		$y_3 \leftrightarrow (0, \sqrt{3}, \sqrt{3}; 1, 1, 0, 0, 0, 1)$	0
		$y_4 \leftrightarrow (1, 3, 3; \sqrt{3}, 0, 0, \sqrt{3}, \sqrt{3}, \sqrt{3})$	0
		$y_5 \leftrightarrow (1, 3, 3; \sqrt{3}, \sqrt{3}, \sqrt{3}, \sqrt{3}, 0, 0)$	0
		$y_6 \leftrightarrow (\sqrt{3}, \sqrt{3}, 0; 1, 1, 1, 0, 0, 1)$	0
$\tilde{G}_2 \cup \tilde{D}_5$	$(0, 0, \sqrt{3}; 1, 0, 0, 0, 0, 0)$	$(0, \sqrt{3}, \sqrt{3}; 1, 1, 0, 0, 0, 0)$	0
		$(\sqrt{3}, \sqrt{3}, 0; 1, 1, 0, 1, 1, 0)$	0
$\tilde{G}_2 \cup \tilde{A}_2 \cup \tilde{A}_3$	$(0, 0, 3; 1, 0, 0; 1; 0, 0, 0)$	$(\sqrt{3}, 0, 0; 0, 0, \sqrt{3}; \sqrt{3}, 0, 0, 0)$	0
		$(\sqrt{3}, 0, 0; 0, \sqrt{3}, 0; \sqrt{3}, 0, 0, 0)$	0
$\tilde{G}_2 \cup \tilde{G}_2 \cup \tilde{A}_3$	$(0, 0, \sqrt{3}; 0, 0, \sqrt{3}; 1; 0, 0, 0)$	$(0, \sqrt{3}, \sqrt{3}; \sqrt{3}, 0, 0; 1, 1, 0, 1)$	-1
		$(\sqrt{3}, 0, 0; 0, \sqrt{3}, \sqrt{3}; 1, 1, 0, 1)$	-1
		$(\sqrt{3}, 0, 0; 1, 0, 0; \sqrt{3}, 0, 0, 0)$	0

Table 4.2.7: Admissible pairs $\{x, y\}$ for $n = 8$

By looking at each admissible set, we see that that none of them gives rise to a finite-volume polyhedron in \mathbb{H}^8 .

	y_2	y_3	y_4	y_5	y_6
y_1	0	0		$-\sqrt{3}$	0
y_2		0	$-\sqrt{3}$		0
y_3			0	0	
y_4					0
y_5					0

Table 4.2.8: The Lorentzian products $\langle y_i, y_j \rangle$

We proceed similarly for the other diagrams σ_∞ , with the difference that, in these cases, there are no admissible sets of cardinality > 2 . The conclusion remains the same, and the proof for $n = 8$ is finished.

Interlude. For $n \geq 9$, the number of admissible pairs increases and admissible sets of big cardinality show up. Despite the considerable amount of cases to test, only a single one will finally provide a realisation of a hyperbolic polyhedron of finite volume. As announced in Theorem 4.0.2, it will be the polyhedron $P_\star \subset \mathbb{H}^9$.

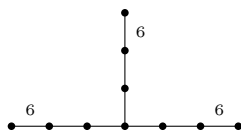
In view of all the lengthy work performed, we will just summarize our findings, apart from a few cases, in Appendix B. The cases which we explain in some more details are the ones where the G_2 -face $F \subset \mathbb{H}^{n-2}$, for $n \neq 9$, is neither a simplex nor a pyramid, and where $F \subset \mathbb{H}^7$ is the pyramid with apex v_∞ of type $\tilde{G}_2 \cup \tilde{G}_2 \cup \tilde{G}_2$.

In Appendix B, we list all admissible pairs $\{x, y_i\}$ for a given σ_∞ , together with the Lorentzian products $\langle x, y_j \rangle$, as well as the products $\langle y_i, y_j \rangle$ when the pair $\{y_i, y_j\}$ is admissible and of further relevance; see Table 4.2.8, for example.

Assume that $n = 9$

By means of Lemma 4.2.1, there are twelve possibilities for F . Namely, there are three simplices, five pyramids over a product of two simplices, and four pyramids over a product of three simplices; see Tables 3.2.1 and 3.2.2. The corresponding strings are listed in Table 4.2.9; see Remark 4.2.6.

Remarquable is the case where $\sigma_\infty = \tilde{G}_2 \cup \tilde{G}_2 \cup \tilde{G}_2 \cup \tilde{G}_2$, and where F is the 7-pyramid over a product of three simplices depicted below.



σ_∞	String for x
$\tilde{G}_2 \cup \tilde{A}_6$	$(0, 0, \sqrt{3}; 1, 0, 0, 0, 0, 0)$
$\tilde{G}_2 \cup \tilde{D}_6$	$(0, 0, a; 1, 0, 0, 0, 0, 0)$
$\tilde{G}_2 \cup \tilde{E}_6$	$(0, 0, a; 1, 0, 0, 0, 0, 0)$
$\tilde{G}_2 \cup \tilde{A}_3 \cup \tilde{A}_3$	$(0, 0, a; 1, 0, 0, 0; 1, 0, 0, 0)$
$\tilde{G}_2 \cup \tilde{A}_2 \cup \tilde{A}_4$	$(0, 0, a; 1, 0, 0; 1, 0, 0, 0)$
$\tilde{G}_2 \cup \tilde{G}_2 \cup \tilde{A}_4$	$(0, 0, a; 0, 0, \sqrt{3}; 1, 0, 0, 0, 0)$
$\tilde{G}_2 \cup \tilde{A}_2 \cup \tilde{D}_4$	$(0, 0, a; 1, 0, 0; 1, 0, 0, 0)$
$\tilde{G}_2 \cup \tilde{G}_2 \cup \tilde{D}_4$	$(0, 0, a; 0, 0, \sqrt{3}; 1, 0, 0, 0, 0)$
$\tilde{G}_2 \cup \tilde{A}_2 \cup \tilde{A}_2 \cup \tilde{A}_2$	$(0, 0, a; 0, 0, 1; 0, 0, 1; 0, 0, 1)$
$\tilde{G}_2 \cup \tilde{G}_2 \cup \tilde{A}_2 \cup \tilde{A}_2$	$(0, 0, a; 0, 0, \sqrt{3}; 0, 0, 1; 0, 0, 1)$
$\tilde{G}_2 \cup \tilde{G}_2 \cup \tilde{G}_2 \cup \tilde{A}_2$	$(0, 0, a; 0, 0, \sqrt{3}; 0, 0, \sqrt{3}; 1, 0, 0)$
$\tilde{G}_2 \cup \tilde{G}_2 \cup \tilde{G}_2 \cup \tilde{G}_2$	$(0, 0, a; 0, 0, \sqrt{3}; 0, 0, \sqrt{3}; 0, 0, \sqrt{3})$

Table 4.2.9: Strings for dimension $n = 9$

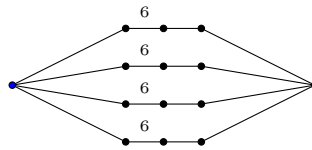
As before, we denote $x \leftrightarrow (0, 0, a; 0, 0, \sqrt{3}; 0, 0, \sqrt{3}; 0, 0, \sqrt{3})$ for $a \in \{\sqrt{3}, 3\}$.

By applying Borcherds' theorem to one of the subdiagrams [6] in (the symmetric) diagram σ_F , one immediately deduces that $a = \sqrt{3}$.

We find that there is a unique and beautiful admissible pair $\{x, y\}$ with y given by

$$y \leftrightarrow (1, 0, 0; 1, 0, 0; 1, 0, 0; 1, 0, 0) ,$$

and we have $\langle x, y \rangle = 0$. The corresponding diagram is depicted below.



By means of Theorem 1.3.15, we verify that this polyhedron is a Coxeter polyhedron of finite volume in \mathbb{H}^9 ! We call it P_\star . For more details and further results about P_\star , see Section 3.1.

For all other cases, see Tables 2.0.1, 2.0.2, 2.0.5, 2.0.6, 2.0.7, 2.0.3, 2.0.8, 2.0.9, 2.0.10, 2.0.11 and 2.0.12 in Appendix B.

Assume that $n = 10$

There are seven possibilities for F . Namely, there are three ADE-simplices, three ADEG-pyramids and the ADE-polyhedron P_1 of Prokhorov in \mathbb{H}^8 .

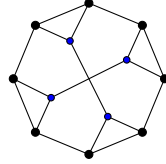
All corresponding strings are listed in Table 4.2.10.

σ_∞	String for x
$\tilde{G}_2 \cup \tilde{A}_7$	$(0, 0, a; 1, 0, 0, 0, 0, 0, 0)$ $\{x_1 \leftrightarrow (0, 0, a_1; 1, 1, 0, 0, 0, 0, 0),$ $x_2 \leftrightarrow (0, 0, a_2; 0, 0, 1, 1, 0, 0, 0),$ $x_3 \leftrightarrow (0, 0, a_3; 0, 0, 0, 0, 1, 1, 0),$ $x_4 \leftrightarrow (0, 0, a_4; 0, 0, 0, 0, 1, 1, 0)\}$
$\tilde{G}_2 \cup \tilde{D}_7$	$(0, 0, a; 1, 0, 0, 0, 0, 0, 0)$
$\tilde{G}_2 \cup \tilde{E}_7$	$(0, 0, a; 1, 0, 0, 0, 0, 0, 0)$
$\tilde{G}_2 \cup \tilde{A}_3 \cup \tilde{D}_4$	$(0, 0, a; 1, 0, 0, 0; 1, 0, 0, 0, 0)$
$\tilde{G}_2 \cup \tilde{A}_2 \cup \tilde{D}_5$	$(0, 0, a; 1, 0, 0; 1, 0, 0, 0, 0)$
$\tilde{G}_2 \cup \tilde{G}_2 \cup \tilde{D}_5$	$(0, 0, a; 0, 0, \sqrt{3}; 1, 0, 0, 0, 0)$

Table 4.2.10: Strings for dimension $n = 10$

Consider the case $\sigma_\infty = \tilde{G}_2 \cup \tilde{A}_7$. When the face F is an ADE-simplex, we refer to Table 2.0.13 in Appendix B.

Of interest here is the case where the face F is given by Prokhorov's polyhedron P_1 depicted below.



Let us denote

$$x_1 \leftrightarrow (0, 0, a_1; 1, 1, 0, 0, 0, 0, 0) , \quad x_2 \leftrightarrow (0, 0, a_2; 0, 0, 1, 1, 0, 0, 0) ,$$

$$x_3 \leftrightarrow (0, 0, a_3; 0, 0, 0, 0, 1, 1, 0) , \quad x_4 \leftrightarrow (0, 0, a_4; 0, 0, 0, 0, 0, 0, 1, 1) ,$$

where $a_i \in \{\sqrt{3}, 3\}$ for $i = 1, 2, 3, 4$. It is easy to see that the set $\{x_1, x_2, x_3, x_4\}$ is admissible if and only if $a_1 = a_2 = a_3 = a_4$. Let $a := a_i, 1 \leq i \leq 4$. In both cases, for $a = \sqrt{3}$ and $a = 3$, the corresponding diagram does not encode a finite-volume polyhedron. Furthermore, we do not find any additional vector y such that the set $\{x_1, x_2, x_3, x_4, y\}$ is admissible.

For all other cases, see Tables 2.0.14, 2.0.15, 2.0.16, 2.0.17 and 2.0.18 in Appendix B.

Assume that $n = 11$

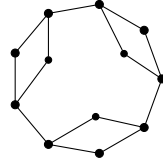
There are eight possibilities for F . Namely, there are three ADE-simplices, three ADEG-pyramids, the ADE-polyhedron P_2 of Prokhorov and the ADEG-polyhedron P_\star in \mathbb{H}^9 . The corresponding strings are listed in Table 4.2.11.

We provide details only for $F = P_2$ and $F = P_\star$.

σ_∞	String for x
$\tilde{G}_2 \cup \tilde{A}_8$	$(0, 0, a; 1, 0, 0, 0, 0, 0, 0, 0, 0)$ $\{x_1 \leftrightarrow (0, 0, a_1; 1, 0, 1, 0, 0, 0, 0, 0, 0),$ $x_2 \leftrightarrow (0, 0, a_2; 0, 0, 0, 1, 0, 1, 0, 0, 0),$ $x_3 \leftrightarrow (0, 0, a_3; 0, 0, 0, 0, 0, 0, 1, 0, 1)\},$
$\tilde{G}_2 \cup \tilde{D}_8$	$(0, 0, a; 1, 0, 0, 0, 0, 0, 0, 0, 0)$
$\tilde{G}_2 \cup \tilde{E}_8$	$(0, 0, a; 1, 0, 0, 0, 0, 0, 0, 0, 0)$
$\tilde{G}_2 \cup \tilde{D}_4 \cup \tilde{D}_4$	$(0, 0, a; 1, 0, 0, 0, 0; 1, 0, 0, 0, 0)$
$\tilde{G}_2 \cup \tilde{A}_2 \cup \tilde{E}_6$	$(0, 0, a; 1, 0, 0; 1, 0, 0, 0, 0, 0, 0)$
$\tilde{G}_2 \cup \tilde{G}_2 \cup \tilde{E}_6$	$(0, 0, a; 0, 0, \sqrt{3}; 1, 0, 0, 0, 0, 0, 0)$
$\tilde{G}_2 \cup \tilde{G}_2 \cup \tilde{G}_2 \cup \tilde{G}_2 \cup \tilde{G}_2$	$\{x_1 \leftrightarrow (0, 0, a_1; 0, 0, \sqrt{3}; 0, 0, \sqrt{3}; 0, 0, \sqrt{3}; 0, 0, \sqrt{3})$ $x_2 \leftrightarrow (0, 0, a_2; 1, 0, 0; 1, 0, 0; 1, 0, 0; 1, 0, 0)\}$

 Table 4.2.11: Strings for dimension $n = 11$

(i) Assume that $\sigma_\infty = \tilde{G}_2 \cup \tilde{A}_8$ and that $F = P_2$ is as depicted below.



For $a_1, a_2, a_3 \in \{\sqrt{3}, 3\}$, write

$$\begin{aligned} x_1 &\leftrightarrow (0, 0, a_1; 1, 0, 1, 0, 0, 0, 0, 0, 0), \\ x_2 &\leftrightarrow (0, 0, a_2; 0, 0, 0, 1, 0, 1, 0, 0, 0), \\ x_3 &\leftrightarrow (0, 0, a_3; 0, 0, 0, 0, 0, 0, 1, 0, 1). \end{aligned}$$

As we require $\{x_1, x_2, x_3\}$ to be an admissible set, we derive that $a := a_1 = a_2 = a_3$. For both $a = \sqrt{3}$ and $a = 3$, it turns out that the resulting polyhedron is not of finite volume.

Next, we search for vectors y_i such that the set $\{x_1, x_2, x_3, y\}$ is admissible.

For $a = \sqrt{3}$, we find eight vectors y_i listed in Table 4.2.12. In addition, we give the Lorentzian products $\langle y_i, y_j \rangle$ when $\{y_i, y_j\}$ is an admissible pair in the Table 4.2.13. However, we see that none of the admissible sets gives rise to a finite-volume polyhedron.

Admissible vectors for $a = \sqrt{3}$	$\langle x_1, y_i \rangle$	$\langle x_2, y_i \rangle$	$\langle x_3, y_i \rangle$
$y_1 \leftrightarrow (1, 0, 0; 0, 0, 0, 0, \sqrt{3}, 0, 0, \sqrt{3}, 0)$	$-\sqrt{3}$	0	0
$y_2 \leftrightarrow (1, 0, 0; 0, 0, 0, \sqrt{3}, 0, 0, 0, 0, \sqrt{3})$	0	0	0
$y_3 \leftrightarrow (1, 0, 0; 0, 0, \sqrt{3}, 0, 0, 0, \sqrt{3}, 0, 0)$	0	0	0
$y_4 \leftrightarrow (1, 0, 0; 0, \sqrt{3}, 0, 0, 0, 0, 0, \sqrt{3}, 0)$	0	$-\sqrt{3}$	0
$y_5 \leftrightarrow (1, 0, 0; 0, \sqrt{3}, 0, 0, \sqrt{3}, 0, 0, 0, 0)$	0	0	$-\sqrt{3}$
$y_6 \leftrightarrow (1, 0, 0; \sqrt{3}, 0, 0, 0, 0, 0, \sqrt{3}, 0, 0)$	0	0	0
$y_7 \leftrightarrow (\sqrt{3}, 0, 0; 0, 1, 1, 0, 1, 1, 0, 1, 1)$	0	0	0
$y_8 \leftrightarrow (\sqrt{3}, 0, 0; 1, 1, 0, 1, 1, 0, 1, 1, 0)$	0	0	0

Admissible vectors for $a = 3$	$\langle x_1, y \rangle$	$\langle x_2, y \rangle$	$\langle x_3, y \rangle$
$(1, 0, 0; 0, 0, 0, 0, 1, 0, 0, 1, 0)$	-1	0	0
$(1, 0, 0; 0, 0, 0, 1, 0, 0, 0, 0, 1)$	0	0	0
$(1, 0, 0; 0, 0, 1, 0, 0, 0, 1, 0, 0)$	0	0	0
$(1, 0, 0; 0, 1, 0, 0, 0, 0, 0, 1, 0)$	0	-1	0
$(1, 0, 0; 0, 1, 0, 0, 1, 0, 0, 0, 0)$	0	0	-1
$(1, 0, 0; 1, 0, 0, 0, 0, 1, 0, 0, 0)$	0	0	0

Table 4.2.12: Admissible sets $\{x_1, x_2, x_3, y_i\}$ for $\sigma_F = P_2$

	y_2	y_3	y_4	y_5	y_6	y_7	y_8
y_1	-1	-1	-1	-1	-1	0	0
y_2		-1	-1	-1	-1	0	0
y_3			-1	-1	-1	0	0
y_4				-1	-1	0	0
y_5					-1	0	0
y_6						0	0

Table 4.2.13: Lorentzian products $\langle y_i, y_j \rangle$

For $a = 3$, we find six vectors y listed in Table 4.2.12. Again, none of the admissible sets $\{x_1, x_2, x_3, y\}$ leads to a polyhedron of finite volume. Furthermore, there is no admissible set of cardinality > 4 .

(ii) Assume that $\sigma_\infty = \tilde{G}_2 \cup \tilde{G}_2 \cup \tilde{G}_2 \cup \tilde{G}_2 \cup \tilde{G}_2$ and that $F = P_\star$.

For $a_1, a_2, a_3 \in \{\sqrt{3}, 3\}$, write

$$\begin{aligned} x_1 &\leftrightarrow (0, 0, a_1; 0, 0, \sqrt{3}; 0, 0, \sqrt{3}; 0, 0, \sqrt{3}; 0, 0, \sqrt{3}) , \\ x_2 &\leftrightarrow (0, 0, a_2; 1, 0, 0; 1, 0, 0; 1, 0, 0; 1, 0, 0) . \end{aligned}$$

As $\{x_1, x_2\}$ should be an admissible pair, this forces a_2 to be equal to $\sqrt{3}a_1$, that is, $a_1 = \sqrt{3}$ and $a_2 = 3$. We obtain $\langle x_1, x_2 \rangle = 0$. However, these data do not yield a finite-volume polyhedron.

Next, we find the following vectors y_1, \dots, y_4 such that the pairs $\{x_1, y_i\}$ and $\{x_2, y_i\}$ are admissible.

$$\begin{aligned} y_1 &\leftrightarrow (1, 0, 0; 0, 0, 3; 1, 0, 0; 1, 0, 0; 1, 0, 0), \\ y_2 &\leftrightarrow (1, 0, 0; 1, 0, 0; 0, 0, 3; 1, 0, 0; 1, 0, 0), \\ y_3 &\leftrightarrow (1, 0, 0; 1, 0, 0; 1, 0, 0; 0, 0, 3; 1, 0, 0), \\ y_4 &\leftrightarrow (1, 0, 0; 1, 0, 0; 1, 0, 0; 1, 0, 0; 0, 0, 3) . \end{aligned}$$

They all are orthogonal to both x_1 and x_2 , and they are pairwise admissible. However, there is no admissible set giving rise to a finite-volume polyhedron.

Assume that $12 \leq n \leq 18$

There is nothing to check in dimension $n = 12$ as there is neither an ADE-polyhedron nor an ADEG-polyhedron in \mathbb{H}^{10} serving as a G_2 -face F .

For dimension $n = 13$, there are two possibilities for the face F . Either F is an ADE-pyramid or an ADEG-pyramid. The strings are listed in Table 4.2.14. If $\sigma_\infty = \tilde{G}_2 \cup \tilde{A}_2 \cup \tilde{E}_8$, we find no admissible pair, and in the case $\sigma_\infty = \tilde{G}_2 \cup \tilde{G}_2 \cup \tilde{E}_8$, the admissible pairs are listed in Appendix B, Table 2.0.26. None of them yields a finite-volume polyhedron.

For dimension $n = 14$, F has to be the (unique) ADE-pyramid in \mathbb{H}^{12} . The corresponding string is given in Table 4.2.14, and we find no admissible pairs. Hence, there is no ADEG-polyhedron.

For dimension $n = 15$, F has to be the (unique) ADE-pyramid in \mathbb{H}^{13} . The corresponding string is given in Table 4.2.14, and again, we find no admissible pairs and therefore no ADEG-polyhedron.

For dimensions $n = 16, 17$ and 18 , there is neither an ADE-polyhedron nor an ADEG-polyhedron in \mathbb{H}^{n-2} serving as a G_2 -face F .

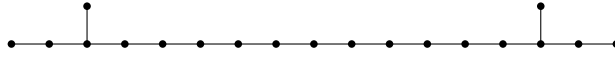
This finishes the proof for $n \leq 18$.

n	σ_∞	String for x
13	$\tilde{G}_2 \cup \tilde{A}_2 \cup \tilde{E}_8$	$(0, 0, a; 1, 0, 0; 0, 0, 0, 0, 0, 0, 0, 1)$
	$\tilde{G}_2 \cup \tilde{G}_2 \cup \tilde{E}_8$	$(0, 0, a; 0, 0, \sqrt{3}; 0, 0, 0, 0, 0, 0, 0, 1)$
14	$\tilde{G}_2 \cup \tilde{A}_3 \cup \tilde{E}_8$	$(0, 0, a; 1, 0, 0, 0; 0, 0, 0, 0, 0, 0, 0, 1)$
15	$\tilde{G}_2 \cup \tilde{D}_4 \cup \tilde{E}_8$	$(0, 0, a; 1, 0, 0, 0, 0; 0, 0, 0, 0, 0, 0, 0, 1)$

Table 4.2.14: Strings for dimensions $12 \leq n \leq 18$

Assume that $n \geq 19$

Let $n = 19$. The single possibility for the G_2 -face $F \subset \mathbb{H}^{17}$ is given by the ADE-pyramid depicted below.



We have $\sigma_\infty = \tilde{G}_2 \cup \tilde{E}_8 \cup \tilde{E}_8$, and we write

$$x \leftrightarrow (0, 0, a; 0, 0, 0, 0, 0, 0, 0, 0, 1; 0, 0, 0, 0, 0, 0, 0, 1) , a \in \{\sqrt{3}, 3\} .$$

For $a = 3$, there is a unique admissible pair which, however, does not yield a finite-volume polyhedron; see Table 2.0.27 in Appendix B.

For $a = \sqrt{3}$, we find 26 vectors y such that $\{x, y\}$ is an admissible pair. They are all listed in Table 2.0.27. Apart from a few exceptions, each admissible set gives rise to a spherical subdiagram of rank > 19 . For the few exceptions left, we do not find any finite-volume polyhedron.

Finally, when $n = 20$, the inductive procedure stops, since there are no ADEG-polyhedron in dimensions 18 and 19.

This finishes the proof of Theorem 4.0.2.

□

3 Further results and comments

3.1 Properties of the polyhedron P_\star

The ADEG-polyhedron $P_\star \subset \mathbb{H}^9$ depicted in Figure 4.0.2 and its associated Coxeter group $\Gamma_\star = \Gamma(P_\star)$ have some interesting properties which we shall develop in what follows.

Let us start with a rough combinatorial information about P_\star provided by the software CoxIter [30, 31]. The f -vector of P_\star is given by

$$f = (134, 671, 1480, 1909, 1606, 917, 356, 91, 14) ,$$

where among the 134 vertices of P_\star , six of them are ideal; see Figure 4.3.3.

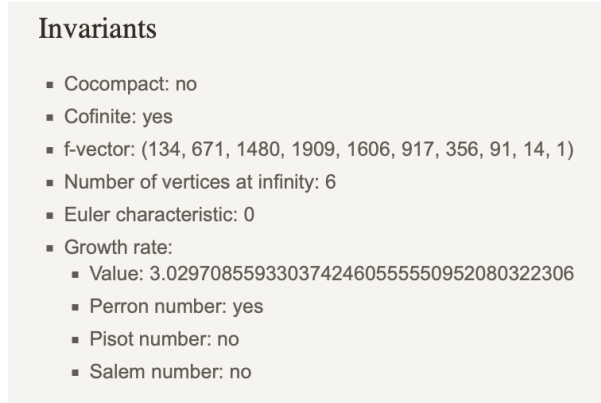


Figure 4.3.3: CoxIter's output for P_\star

As a supplementary information, the growth rate $\tau_\star \approx 3.029708$ of Γ_\star is a Perron number whose minimal polynomial has degree 51 and integral coefficients in the interval $[-217, 283]$. We will come back to growth rates and Perron numbers in Part III.

As for the volume of P_\star , we can derive that

$$\text{vol}(P_\star) \in \mathbb{Q} \cdot \zeta(5) , \quad (4.15)$$

where $\zeta(5)$ denotes Riemann's zeta function evaluated at 5. In fact, the non-cocompact group Γ_\star is arithmetic (over \mathbb{Q}) by the criterion stated in Theorem 1.3.20, and Γ_\star acts on hyperbolic space of odd dimension ≥ 5 . The property (4.15) is now an immediate consequence of Emery's Proposition 2.1 [19], in view of the quadratic form q_\star associated to P_\star ; see the proof of Proposition 4.3.1 below.

More precisely, we shall see that

$$\text{vol}(P_\star) = q \cdot \frac{\zeta(5)}{22, 295, 347, 200} \quad \text{with } q \in \mathbb{Q}_{>1} . \quad (4.16)$$

To this end, consider the Coxeter simplex $\Delta_9 \subset \mathbb{H}^9$ given by the Coxeter diagram depicted in Figure 4.17.

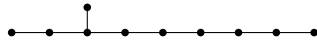


Figure 4.3.4: The Coxeter simplex $\Delta_9 \subset \mathbb{H}^9$

Alike Γ_\star , the Coxeter group $\Gamma_9 = \Gamma(\Delta_9)$ is arithmetic (over \mathbb{Q}), and it is distinguished by the property that among *all* cusped hyperbolic 9-orbifolds, the space \mathbb{H}^9/Γ_9 has minimal volume and is as such unique; see [35]. Moreover, the volume of \mathbb{H}^9/Γ_9 is given by the volume of Δ_9 and has been computed in [40] according to

$$\text{vol}(\Delta_9) = \frac{\zeta(5)}{22,295,347,200} . \quad (4.17)$$

As a consequence, the identity (4.16) is verified.

Recall from Chapter 1 the concept of (widely) commensurable groups of hyperbolic isometries. Moreover, commensurability is an equivalence relation which preserves properties such as arithmeticity, cocompactness and cofiniteness.

Our aim is to show that Γ_\star and Γ_9 are commensurable. We will prove even more by looking also at the group $\Gamma(P_2)$ associated with the ADE-polyhedron P_2 of Prokhorov in \mathbb{H}^9 , depicted in Figure 3.2.8.

The group $\Gamma(P_2)$ is also arithmetic (over \mathbb{Q}), and hence, we obtain

$$\text{vol}(P_2) = q' \cdot \text{vol}(\Delta_9) \text{ with } q' \in \mathbb{Q}_{>1} . \quad (4.18)$$

A natural question is whether *all* three groups Γ_\star , $\Gamma(P_2)$ and Γ_9 are commensurable. In fact, this question can be answered positively as follows.

Proposition 4.3.1. *The Coxeter groups Γ_\star , $\Gamma(P_2)$ and Γ_9 are pairwise commensurable.*

Proof. By Maclachlan's work [57], there is a *complete* set of commensurability invariants for arithmetic groups of hyperbolic isometries. His work has been exploited by Guglielmetti, Jacquemet and Kellerhals [33] who established these invariants in many cases and also for the group Γ_9 . Hence, it is sufficient to show that the sets of invariants for Γ_\star and $\Gamma(P_2)$ coincide with the one of Γ_9 .

Since we are in dimension 9, which is odd, and since all three groups under consideration are defined over \mathbb{Q} , the set of commensurability invariants according to Maclachlan can be described briefly as follows. First, one establishes the Gram matrix G and the different cycle coefficients for each

Coxeter polyhedron in terms of its normal vectors and passes then to the Vinberg form q associated to G ; see Definition 1.3.19 and Appendix C.

Then, one computes the signed determinant $\delta = -\det(q)$ of q in \mathbb{Q}/\mathbb{Q}^2 . The next step is to determine the Hasse invariant $s(q)$ and the Witt invariant $c(q)$ of q . More precisely, by expressing $q = \langle a_1, a_2, \dots, a_{10} \rangle$ in diagonal form, one has

$$s(q) = \bigotimes_{1 \leq i < j \leq 10} (a_i, a_j)$$

in terms of the different quaternion algebras (a_i, a_j) . In our case, $s(q)$ and $c(q)$ coincide. Choose a quaternion algebra B representing $c(q)$, and finally establish the ramification set $\text{Ram}_q(B)$ resp. $\text{Ram}_q(B \otimes_{\mathbb{Q}} \mathbb{Q}(\sqrt{\delta}))$ according to whether δ is a square in \mathbb{Q} or not.

The complete set of commensurability invariants is then given by

$$\begin{aligned} & \{\mathbb{Q}, \delta, \text{Ram}_q(B)\} \text{ if } \delta \text{ is a square in } \mathbb{Q} ; \\ & \{\mathbb{Q}, \delta, \text{Ram}_q(B \otimes_{\mathbb{Q}} \mathbb{Q}(\sqrt{\delta}))\} \text{ if } \delta \text{ is not a square in } \mathbb{Q} . \end{aligned}$$

- ◇ For the group Γ_9 , the invariant set is known and equals to $\{\mathbb{Q}, 1, \emptyset\}$.
- ◇ For the group Γ_* , the Vinberg form is given by

$$q_* = \langle 1, 1, 2, 3, 3, 6, 6, 10, 10, -2 \rangle ;$$

see Appendix C for its computation. Therefore, the signed determinant of q_* equals 1 in \mathbb{Q}/\mathbb{Q}^2 .

By the properties of quaternion algebras, the Hasse invariant $s(q_*)$ given by $(2, -2) \cdot (3, 3) \cdot (6, 6) \cdot (10, 10)$ can be identified with $(5, -1)$.

We derive that the ramification set of $(5, -1)$ is empty, and that the complete set of invariants for Γ_* is given by $\{\mathbb{Q}, 1, \emptyset\}$.

- ◇ For the group $\Gamma(P_2)$ we proceed in a similar way. The Vinberg form, established in Appendix C, is given by

$$q_2 = \langle 1, 1, 3, 6, 7, 10, 10, 15, 21, -10 \rangle ,$$

which yields 1 for the signed determinant of q_2 . Again, we obtain $c(q_2) = (5, -1)$, whose ramification set is empty. Therefore, the set of invariants for $\Gamma(P_2)$ is given by $\{\mathbb{Q}, 1, \emptyset\}$ as well.

We conclude that all three groups Γ_9 , Γ_* and Γ_{P_2} are pairwise commensurable. □

Remark 4.3.2. By [33, 41] and Proposition 4.3.1, it follows that the commensurability class of $\Gamma_\star = \Gamma(P_\star)$ contains all Coxeter simplex groups and all Coxeter pyramid groups in $\text{Isom}\mathbb{H}^9$.

3.2 An angular obstruction

In this section, we present an angular obstruction to the existence of hyperbolic Coxeter polyhedra with mutually intersecting facets.

The following result provides a universal bound from below for dihedral angles of Coxeter polyhedra with mutually intersecting facets in dimensions beyond 6.

Proposition 4.3.3. *Let $n \geq 7$, and let $P \subset \mathbb{H}^n$ be a Coxeter polyhedron with mutually intersecting facets. Then, any dihedral angle of P is of the form $\frac{\pi}{m}$ with $m \leq 6$.*

Proof. Let $n \geq 7$, and assume that all facets of Coxeter polyhedron $P \subset \mathbb{H}^n$ are mutually intersecting. Let Σ be the Coxeter diagram of P , and denote by $\sigma_m = [m]$ a subdiagram of type $G_2^{(m)}$ in Σ . Suppose that P has a dihedral angle $\frac{\pi}{m}$ for $m \geq 7$.

As in the proof of Lemma 4.2.1 and by means of Theorem 1.3.9, we deduce that the $G_2^{(m)}$ -face $F = F(\sigma_m)$ of P is an $(n - 2)$ -Coxeter polyhedron with mutually intersecting facets.

As $n - 2 \geq 5$, the face F is a non-compact Coxeter polyhedron; see Theorem 3.2.2 and Theorem 3.2.3. Therefore, its Coxeter diagram σ_F contains an affine subdiagram σ_F^∞ of rank $n - 3$, which is a component of an affine subdiagram of rank $n - 1$ in Σ . As $\Sigma \setminus \sigma_F^\infty$ contains σ_m , which cannot be extended to yield an affine component, we get a contradiction. □

Final comments. The method we developed in order to classify all ADEG-polyhedra is general and can be applied to Coxeter polyhedra with mutually intersecting facets whose dihedral angles are prescribed.

By Proposition 4.3.3, for dimensions ≥ 7 , all dihedral angles of such polyhedra are uniformly bounded from below by $\frac{\pi}{6}$. Therefore, it is realistic to obtain a complete classification of all Coxeter polyhedra with mutually intersecting facets and for all dimensions in finite time. Observe, however, that the presence of a dihedral angle $\frac{\pi}{4}$ makes the classification task much more voluminous.

PART III:

ON THE GROWTH RATES OF HYPERBOLIC COXETER GROUPS

My work is a game, a very serious game.

M.C. ESCHER

CHAPTER 5

THE GROWTH RATES OF COXETER GROUPS

In this chapter, we provide the necessary background for the study of growth rates of Coxeter groups. We start with basic definitions about the growth series and growth rates of Coxeter groups. Then we present the tools for comparing growth rates of Coxeter groups that will be fundamental for the next chapter about growth minimality. Main references for this chapter are [17, 37, 60, 76].

1 Growth series and growth rates

Let $\Gamma = (W, S)$ be an abstract Coxeter group of rank N generated by S , presented as in (1.9).

Denote by l_S the *length function* of Γ with respect to S , that is, for $w \in W$,

$$l_S(w) = \min\{k \in \mathbb{Z}_{>0} \mid \exists s_1, \dots, s_k \in S, w = s_1 \cdots s_k\}, \quad l_S(1) = 0. \quad (5.1)$$

Define $a_k \in \mathbb{N}$ to be the number of elements $w \in W$ with S -length k , that is,

$$a_k = \#\{w \in W \mid l_S(w) = k\} \in \mathbb{Z}[t]. \quad (5.2)$$

Definition 5.1.1. The *growth series* $f_S(t)$ of $\Gamma = (W, S)$ is the power series defined by

$$f_S(t) = 1 + \sum_{k \geq 1} a_k t^k. \quad (5.3)$$

Notice that if $\Gamma = (W, S)$ is *finite*, then $f_S(t)$ is a polynomial. More specifically, by a classical result of Solomon [74], the growth polynomial $f_S(t)$ can be expressed by means of its *exponents* $\{m_1, m_2, \dots, m_n\}$ according to the formula

$$f_S(t) = \prod_{i=1}^p [m_i + 1], \quad (5.4)$$

where $[m] = 1 + t + \dots + t^{m-1}$ and $[m_1, \dots, m_r] := [m_1] \cdots [m_r]$. The exponents of all irreducible spherical Coxeter groups are listed in Table 5.1.1.

Group	Exponents	Group	Exponents
A_n	$1, 2, \dots, n$	E_6	$1, 4, 5, 7, 8, 11$
B_n	$1, 3, \dots, 2n - 1$	E_7	$1, 5, 7, 9, 11, 13, 17$
D_n	$1, 3, \dots, 2n - 3, n - 1$	E_8	$1, 7, 11, 13, 17, 19, 23, 29$
H_3	$1, 5, 9$	$G_2^{(m)}$	$1, n - 1$
H_4	$1, 11, 19, 29$	F_4	$1, 5, 7, 11$

Table 5.1.1: Exponents of the irreducible spherical Coxeter groups

The following well-known formula due to Steinberg [75] allows one to express the growth series $f_S(t)$ of an arbitrary Coxeter group (W, S) in terms of its finite parabolic subgroups.

Theorem 5.1.2 (Steinberg's formula).

$$\frac{1}{f_S(t^{-1})} = \sum_{\substack{W_T < W \\ |W_T| < \infty}} \frac{(-1)^{|T|}}{f_T(t)}, \quad (5.5)$$

where $W_\emptyset = \{1\}$.

As a consequence, in its disk of convergence, the growth series $f_S(t)$ is a rational function, which can be expressed as the quotient of two coprime monic polynomials $p(t), q(t) \in \mathbb{Z}[t]$ of the same degree.

Definition 5.1.3. The *growth rate* $\tau_\Gamma = \tau_W := \tau_{(W,S)}$ is defined as the inverse of the radius of convergence of the growth series $f_S(t)$ of (W, S) .

By Hadamard's formula, we have

$$\tau_\Gamma = \limsup_{k \rightarrow \infty} a_k^{1/k} . \tag{5.6}$$

Furthermore, the growth rate τ_Γ can be identified with the inverse of the smallest positive real pole of $f_S(t)$. Hence, τ_Γ is an algebraic integer.

For a *reducible* group, the growth series $f_S(t)$ satisfies the following product formula.

Proposition 5.1.4. *The growth series of a reducible Coxeter group (W, S) with factor groups $(W_1, S_1), (W_2, S_2)$ such that $S = (S_1 \times \{1_{W_2}\}) \cup (\{1_{W_1}\} \times S_2)$ satisfies*

$$f_S(t) = f_{S_1}(t) \cdot f_{S_2}(t) .$$

In particular, $\tau_W = \max_{i=1,2} \tau_{W_i}$.

Let $\Gamma \subset \text{Isom}\mathbb{X}^n$ be a (cofinite) geometric Coxeter group, as usually with its canonical system S of generating reflections; see (1.9). If $\mathbb{X}^n = \mathbb{S}^n$, then $\tau_\Gamma = 0$, while for $\mathbb{X}^n = \mathbb{E}^n$, $\tau_\Gamma = 1$. In both cases, Γ is of *polynomial* growth. For the case $\mathbb{X}^n = \mathbb{H}^n$, results of Milnor [63] and de la Harpe [17] imply that Γ has *exponential* growth, that is, $\tau_\Gamma > 1$. More precisely, it was proven by Terragni [76, 77] that for any hyperbolic Coxeter group Γ ,

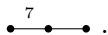
$$\tau_\Gamma \geq \tau_{\Gamma_9} \approx 1.138078 , \tag{5.7}$$

where Γ_9 is the Coxeter 9-simplex group depicted in Figure 5.1.1; see also Chapter 4.



Figure 5.1.1: The Coxeter simplex group $\Gamma_9 \subset \text{Isom}\mathbb{H}^9$

Example 5.1.5. Let $\Gamma = [7, 3]$ be the cocompact hyperbolic triangle group with Coxeter diagram



Recall that the group Γ has smallest co-area among all discrete groups in $\text{Isom}\mathbb{H}^2$; see Chapter 3.

As easily read from the Coxeter diagram above, Γ contains six finite parabolic subgroups. Namely, it contains the three dihedral subgroups $A_1 \times A_1, A_2$ and

$G_2^{(7)}$, each with multiplicity 1, and the subgroup A_1 with multiplicity 3. By means of Steinberg's formula (5.5) and Table 5.1.1, we derive

$$\frac{1}{f_S(t^{-1})} = 1 - \frac{3}{[2]} + \frac{1}{[2, 2]} + \frac{1}{[2, 3]} + \frac{1}{[2, 7]} .$$

It follows that

$$f_S(t) = \frac{C(t)}{L(t)} = \frac{C(t)}{1 + t - t^3 - t^4 - t^5 - t^6 - t^7 + t^9 + t^{10}} \quad (5.8)$$

where $C(t)$ is a certain product of cyclotomic polynomials, and where $L(t)$ is *Lehmer's polynomial*. It is the minimal polynomial of the *Lehmer number* $\alpha_L \approx 1.17628$, which is the smallest known Salem number; see Section 2. As a result of (5.8), we derive $\tau_{[7,3]} = \alpha_L$.

For dimensions $n = 2$ and 3, there are closed formulas for the growth series of cofinite hyperbolic Coxeter groups as follows.

Let us first discuss the 2-dimensional cocompact case.

Theorem 5.1.6 (Floyd, Plotnick [28]). *Let $P \subset \mathbb{H}^2$ be a compact Coxeter N -gon with interior angles $\frac{\pi}{k_1}, \dots, \frac{\pi}{k_N}$. Let Γ be the planar hyperbolic Coxeter group associated with P . Then, the growth series of Γ is given by*

$$f_S(t) = \frac{[2, k_1, \dots, k_N]}{(t - N + 1)[k_1, \dots, k_N] + \sum_{i=1}^N [k_1, \dots, k_{i-1}][k_{i+1}, \dots, k_N]} .$$

As for a formula in dimension 3, let us recall that compact Coxeter polyhedra are simple. Therefore, given a compact Coxeter polyhedron P in \mathbb{H}^3 , each vertex v of P is the intersection of precisely three hyperplanes, giving rise to the stabilizer Γ_v which is a spherical Coxeter subgroup of rank 3 in Γ . Denote by $m_1 = 1, m_2$ and m_3 the exponents of Γ_v according to Table 5.1.1.

Theorem 5.1.7 (Parry [67]). *Let $P \subset \mathbb{H}^3$ be a compact Coxeter polyhedron with associated Coxeter group Γ . Then, the growth series of Γ can be expressed as*

$$f_S(t) = \frac{t-1}{t+1} - \frac{1}{2}t(t-1) \sum_{v \in P} \frac{(t^{m_1} - 1)(t^{m_2} - 1)(t^{m_3} - 1)}{(t^{m_1+1} - 1)(t^{m_2+1} - 1)(t^{m_3+1} - 1)} .$$

In the non-cocompact cofinite case, similar results for dimensions $n = 2$ and 3 are available and due to Floyd [29] and Kellerhals [46].

For a non-compact polyhedron $P \subset \mathbb{H}^n$, denote by $f_0 = f_0^o + f_0^\infty$ the number of vertices of P , where f_0^o is the number of ordinary vertices, and f_0^∞ is the number of ideal vertices of P . When $n \geq 3$, ideal vertices may be non-simple. Again, the stabilizer of an ordinary vertex v of P is a finite subgroup Γ_v of Γ , generated by the reflections in the hyperplanes passing through v .

For the 2-dimensional case, there is the following result.

Theorem 5.1.8 (Floyd [29]). *Let $P \subset \mathbb{H}^2$ be a non-compact Coxeter polygon of finite volume with $f_0 = f_0^o + f_0^\infty$ vertices. Let Γ be the hyperbolic Coxeter group associated with P . Then, the growth series of Γ satisfies*

$$\frac{1}{f_S(t)} = 1 - \frac{t}{[2]} (f_0^\infty + \sum_{v \text{ ordinary}} \frac{[k_v - 1]}{[k_v]}),$$

where $2k_v$ is the order of the dihedral stabilizer group Γ_v of the ordinary vertex v of P .

As for the 3-dimensional case, some preparation is necessary.

Let $P \subset \mathbb{H}^3$ be a non-compact Coxeter polyhedron with associated Coxeter group Γ and Coxeter diagram Σ . If P has an ordinary vertex v , its stabilizer Γ_v in Γ is a spherical Coxeter group with exponents $m_1 = 1, m_2$ and m_3 as above. As for the ideal vertices of P , they can be either simple or non-simple. Suppose that P has a non-simple vertex v_∞ . Then, its subdiagram σ_∞ in Σ is of type $\widetilde{A}_1 \times \widetilde{A}_1$. Now, the polyhedron P can be obtained by a deformation process from a sequence of Coxeter polyhedra $P_k \subset \mathbb{H}^3$ which all have the same combinatorial structure as P , apart from a finite edge with vertices both of type $A_1 \times A_1 \times G_2^{(k)}$ that collapses to yield the vertex v_∞ when $k \rightarrow \infty$. As for the corresponding growth functions $f(t)$ of Γ and $f_k(t)$ of $\Gamma(P_k)$, a result of Kolpakov [50] shows that

$$\frac{1}{f(t)} = \frac{1}{f_k(t)} + \frac{t^k}{t^k - 1} \left(\frac{t - 1}{t + 1} \right)^2 \quad \text{for all } k.$$

As a consequence, it is primarily of interest to have a closed formula for the growth series of a non-compact hyperbolic Coxeter polyhedron with *simple* vertices, only.

Theorem 5.1.9 (Kellerhals [46]). *Let $P \subset \mathbb{H}^3$ be a non-compact simple Coxeter polyhedron of finite volume with associated Coxeter group Γ . Then,*

the growth series of Γ satisfies

$$\frac{1}{f_S(t)} = \frac{1-t}{1+t} \left\{ 1 - \frac{t}{2} \left(\sum_{v \text{ ordinary}} \frac{[m_2, m_3]}{[m_2 + 1, m_3 + 1]} + \sum_{w \text{ ideal}} \frac{[n_w - 1] + t^{n_w - 2}}{[n_w]} \right) \right\}$$

where

$$n_w = \max(n_1^w, n_2^w, n_3^w) = \begin{cases} 3 & \text{if } \Gamma_w = \tilde{A}_2 \\ 4 & \text{if } \Gamma_w = \tilde{B}_2 \\ 6 & \text{if } \Gamma_w = \tilde{G}_2 \end{cases}$$

is defined in terms of the dihedral angles π/n_i^w at the three edges giving rise to the simple ideal vertex w , and where Γ_w is the stabilizer of w .

Let us point out that one does *not* dispose up to now of similar closed formulas for growth series of Coxeter groups $\Gamma \subset \text{Isom}\mathbb{H}^n$ for $n \geq 4$, except for the case related to right-angled compact Coxeter polyhedra; see the work of Kellerhals and Perren [45].

2 About the arithmetic nature of growth rates

In this section we discuss the arithmetic nature of the growth rate of a (cofinite) hyperbolic Coxeter group $\Gamma = (W, S)$. Recall that the growth rate τ_Γ is an algebraic integer which can be identified with the inverse of the smallest positive real pole of the growth series $f_S(t)$.

Definition 5.2.1. The growth series $f_S(t)$ is said to be *reciprocal* if it satisfies $f_S(t^{-1}) = f_S(t)$. It is called *anti-reciprocal* if $f_S(t^{-1}) = -f_S(t)$.

In the cocompact case, it is known by works of Charney and Davis [14] that the growth series is reciprocal in even dimensions, and anti-reciprocal in odd dimensions. However, this property does not hold in the non-cocompact case anymore.

Let us now consider growth rates of hyperbolic Coxeter groups. In low dimensions, they appear to be Salem numbers, Pisot numbers (or Pisot-Vijayaraghavan numbers), or Perron numbers. These algebraic integers are defined as follows.

Definition 5.2.2. An algebraic integer $\tau > 1$ is a *Salem number* if it is either a quadratic unit, or its inverse τ^{-1} is a Galois conjugate of τ and the other Galois conjugates lie on the unit circle.

Definition 5.2.3. An algebraic integer $\tau > 1$ is a *Pisot number* if τ is either an integer, or if all of its other Galois conjugates are contained in the unit open disk.

Definition 5.2.4. An algebraic integer $\tau > 1$ is a *Perron number* if τ is either an integer, or if all of its other Galois conjugates are strictly less than τ in absolute value.

In particular, Salem numbers and Pisot numbers are Perron numbers.

Let us turn back to hyperbolic Coxeter groups.

In [67], Parry proved that the growth rate of any cocompact hyperbolic Coxeter group in $\text{Isom}\mathbb{H}^n$ is a Salem number when $n = 2$ or 3 .

The smallest known Salem number is the Lehmer number α_L which is also the growth rate of the Coxeter triangle group [7, 3]; see Example 5.1.5. However, by a result of Kellerhals and Liechti [44], not every Salem number appears as the growth rate of a cocompact hyperbolic Coxeter group.

In the non-cocompact case, Floyd [29] proved that the growth rates of cofinite hyperbolic Coxeter groups in $\text{Isom}\mathbb{H}^2$ are Pisot numbers. However, the analogous result does not hold anymore in $\text{Isom}\mathbb{H}^3$; see [46] for instance.

Nevertheless, the growth rate of any cofinite hyperbolic Coxeter group in $\text{Isom}\mathbb{H}^3$ is a Perron number. This result was proven in the special case of ideal Coxeter polyhedra by Komori and Yukita [52], as well as by Nonaka and Kellerhals [66]. Soon later, it was proven by Yukita [86] in full generality.

Remark 5.2.5. Related is our joint work with Yukita [9], wherein we extended the results of Parry [67] and Floyd [29] to *abstract* Coxeter groups having 2-dimensional Davis complexes. Namely, we proved that if the Euler characteristic χ of the nerve of a Coxeter group is zero, then its growth rate is a Salem number. If χ is positive, then its growth rate is a Pisot number. For negative Euler characteristic, we provided infinitely many families of Coxeter groups of index of inertia > 1 whose growth rates are Perron numbers. These families contain so-called ∞ -spanned Coxeter groups whose growth rates have already been identified with Perron numbers by Kolpakov and Talambutsa [51].

However, in higher dimensions, only some partial results are available but several questions arise.

The growth rates of cocompact Coxeter groups in $\text{Isom}\mathbb{H}^4$ of rank at most 6 are Perron numbers, as shown by Kellerhals and Perren [45]. The following problem extends their conjecture in the cocompact case to the cofinite setting in a natural way.

Conjecture. *Let $\Gamma \subset \text{Isom}\mathbb{H}^n$ be a cofinite Coxeter group. Then the growth rate τ_Γ with respect to the natural set of generating reflections of Γ is a Perron number.*

A proof of this Conjecture seems to be hard. One reason is the lack of explicit formulas for the growth series for $n > 3$. Other reasons are the number-theoretical difficulties concerning the irreducibility of integer polynomials. Nevertheless, for any *known* Coxeter group $\Gamma \subset \text{Isom}\mathbb{H}^n$, the software Mathematica [85] or the program CoxIter of Guglielmetti [30, 31] allows one to test whether the growth rate τ_Γ is a Perron number.

Example 5.2.6. Consider the Coxeter group $\Gamma_\star = \Gamma(P_\star)$ in $\text{Isom}\mathbb{H}^9$. By the software CoxIter, the minimal polynomial of the growth rate $\tau_\star \approx 3.029708$ of Γ_\star has degree 51. The program shows that τ_\star is neither a Salem number nor a Pisot number, but it is a Perron number; see Figure 4.3.3.

3 Comparing growth rates

In this section, our goal is to compare growth series and growth rates of abstract Coxeter groups. This will be essential when studying minimality aspects of growth rates of cofinite hyperbolic Coxeter groups.

3.1 Partial order and growth monotonicity

In [60], McMullen introduced the following partial order on the set of Coxeter groups.

Let (W, S) and (W', S') be two Coxeter groups. Define $(W, S) \leq (W', S')$ if there exists an injective map $\iota : S \rightarrow S'$ such that

$$m_{st} \leq m'_{\iota(s)\iota(t)} \text{ for all } s, t \in S.$$

As $m_{st} \in \{2, 3, \dots, \infty\}$ for all distinct $s, t \in S$, this partial order satisfies the descending chain condition. Therefore, any strictly decreasing sequence of Coxeter groups is finite.

In addition, one defines $(W, S) < (W', S')$ if $(W, S) \leq (W', S')$ and ι cannot be extended to an isomorphism. In other words, one has $(W, S) < (W', S')$ if $|S| < |S'|$, or if $m_{st} < m'_{\iota(s)\iota(t)}$ for some $s, t \in S$, $s \neq t$.

The following result, established by Terragni [76, 77], is of major importance for the subsequent study of minimal growth rates.

Theorem 5.3.1. *If $(W, S) \leq (W', S')$, then $\tau_{(W,S)} \leq \tau_{(W',S')}$.*

In particular, the growth rate of any parabolic subgroup (W_T, T) of (W, S) satisfies $\tau_{(W_T,T)} \leq \tau_{(W,S)}$.

Remark 5.3.2. Terragni's growth monotonicity result stated in Theorem 5.3.1 is really convenient for the comparison of growth rates. However, this monotonicity property is not proven in its *strict* sense. Indeed, Terragni's proof is based on Hadamard's limit formula (5.6) for the coefficients in the respective growth series which does not allow one to deduce the *strict* monotone behaviour as we observed in practice. Motivated by this, we formulate the following conjecture.

Conjecture. *Let $(W, S), (W', S')$ be two non-spherical, non-affine irreducible Coxeter groups such that $(W, S) < (W', S')$. Then,*

$$\tau_{(W,S)} < \tau_{(W',S')} . \tag{5.9}$$

Remark 5.3.3. The conjectured strict monotonicity property (5.9) for the growth rate of a Coxeter group $\Gamma \subset \text{Isom}\mathbb{H}^n$ comes from the comparison with the strict monotonicity of the volume, with respect to the dihedral angles, of the Coxeter polyhedron associated with Γ ; see Remark 1.2.5.

As a preparation for the subsequent investigations, let us introduce the notion of *extension* of a Coxeter diagram.

Definition 5.3.4. Let Σ be a Coxeter diagram. An *extension* of Σ is a Coxeter diagram Σ' obtained by adding one node linked with a (labelled) edge e to Σ . The extension Σ' is said to be *simple* if the edge e has no label.

Let W be a Coxeter group with Coxeter diagram Σ . By definition, any extension Σ' of Σ encodes a Coxeter group W' such that $W < W'$. Hence, by Theorem 5.3.1, we get $\tau_W \leq \tau_{W'}$.

Furthermore, if Σ'_0 is a simple extension of Σ by an edge e , the extension Σ' of Σ obtained by adding a label on the edge e of Σ'_0 yields the following inequality.

$$\tau_\Sigma \leq \tau_{\Sigma'_0} \leq \tau_{\Sigma'} ,$$

where, by abuse of notation, the growth rate of Σ equals the growth rate of its Coxeter group W .

Next, we reproduce the statements concerning the simple extensions of *affine* Coxeter diagrams of small ranks stated in [8].

Example 5.3.5. Consider a connected affine Coxeter diagram Σ of rank n ; see Table 1.3.2. Then, one verifies that any extension Σ' of Σ corresponds to a non-cocompact Coxeter simplex group in $\text{Isom}\mathbb{H}^{n+1}$. However, notice that the resulting group might not be cofinite.

Nevertheless, we observe that for rank $n \leq 3$, the resulting Coxeter simplex groups in $\text{Isom}\mathbb{H}^{n+1}$ are always cofinite; see Theorem 3.1.1 and Table 3.2.1.

If $\Sigma = [\infty]$ is of rank 1, there is a unique simple extension, up to symmetry, and it corresponds to the Coxeter triangle group $[\infty, 3]$. For ranks 2 and 3, all resulting simple extensions are depicted in Figure 5.3.2 and Figure 5.3.3.

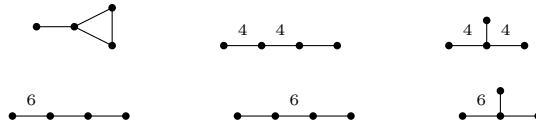


Figure 5.3.2: The simple extensions of \tilde{A}_2 , \tilde{C}_2 and \tilde{G}_2

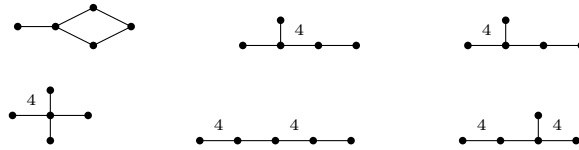


Figure 5.3.3: The simple extensions of \tilde{A}_3 , \tilde{B}_3 and \tilde{C}_3

In the case where Σ is affine of rank $n \geq 4$, *some* simple extensions of Σ yield hyperbolic groups of infinite covolume. Note that for ranks ≥ 9 , *any* extension gives rise to a group of infinite covolume.



Figure 5.3.4: The Coxeter groups $\Delta_1, \dots, \Delta_4$ of infinite covolume

For rank 4, there are fifteen simple extensions of connected affine Coxeter diagrams. There are exactly eleven simple extensions each giving rise to a cofinite Coxeter simplex group in $\text{Isom}\mathbb{H}^5$, and there are four more extensions corresponding to simplex groups Δ_i , $1 \leq i \leq 4$, of infinite covolume depicted in Figure 5.3.4.

3.2 A useful lemma

Let $\Gamma = (W, S)$ and $\Gamma' = (W', S')$ be two abstract Coxeter groups. By means of Steinberg's formula (5.5), one can express their growth series in an effective way allowing one to derive the following lemma which provides a tool to compare the growth rates of Γ and Γ' .

Lemma 5.3.6. *Assume that for all $t > 0$, one has*

$$\frac{1}{f_S(t^{-1})} - \frac{1}{f_{S'}(t^{-1})} > 0 . \quad (5.10)$$

Then, $\tau_\Gamma < \tau_{\Gamma'}$.

Proof. The inequality (5.10) implies that for all $x = t^{-1} \in (0, 1)$, the smallest zero of the function $g(x) := \frac{1}{f_S(t^{-1})}$ is strictly bigger than the smallest zero of $g'(x) := \frac{1}{f_{S'}(t^{-1})}$. As these two zeros correspond to the radii of convergence of the growth series $f_S(t)$ and $f_{S'}(t)$, when passing from x to t , we immediately deduce that their growth rates satisfy $\tau_\Gamma < \tau_{\Gamma'}$. □

We now reproduce in Examples 5.3.7 and 5.3.8 two applications of Lemma 5.3.6 taken from the articles [7, 8].

Example 5.3.7. Consider the Coxeter groups (W_1, S_1) , (W_2, S_2) and (W_3, S_3) given by simple extensions of $[\infty, 3]$ as follows.

$$W_1 \quad \overset{\infty}{\bullet} \text{---} \bullet \text{---} \bullet \quad W_2 \quad \bullet \text{---} \overset{\infty}{\bullet} \text{---} \bullet \quad W_3 \quad \bullet \text{---} \overset{\infty}{\bullet} \text{---} \overset{\bullet}{\bullet}$$

By Steinberg's formula (5.5), we compute

$$\begin{aligned} \frac{1}{f_{S_1}(t^{-1})} &= 1 - \frac{4}{[2]} + \frac{3}{[2, 2]} + \frac{2}{[2, 3]} - \frac{1}{[2, 2, 3]} - \frac{1}{[2, 3, 4]} , \\ \frac{1}{f_{S_2}(t^{-1})} &= 1 - \frac{4}{[2]} + \frac{3}{[2, 2]} + \frac{2}{[2, 3]} - \frac{2}{[2, 2, 3]} , \\ \frac{1}{f_{S_3}(t^{-1})} &= 1 - \frac{4}{[2]} + \frac{3}{[2, 2]} + \frac{2}{[2, 3]} - \frac{1}{[2, 2, 2]} - \frac{1}{[2, 3, 4]} . \end{aligned}$$

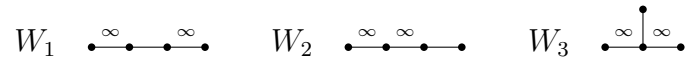
We get positive difference functions for all $t > 0$, according to

$$\frac{1}{f_{S_1}(t^{-1})} - \frac{1}{f_{S_2}(t^{-1})} = \frac{1}{[2, 2, 3]} - \frac{1}{[2, 3, 4]} = \frac{t^2 + t^3}{[2, 2, 3, 4]} ,$$

$$\frac{1}{f_{S_1}(t^{-1})} - \frac{1}{f_{S_3}(t^{-1})} = \frac{1}{[2, 2, 2]} - \frac{1}{[2, 2, 3]} = \frac{t^2}{[2, 2, 2, 3]} .$$

By Lemma 5.3.6, we deduce that $\tau_{W_1} < \tau_{W_2}$ and $\tau_{W_1} < \tau_{W_3}$.

Example 5.3.8. Consider the Coxeter groups (W_1, S_1) , (W_2, S_2) and (W_3, S_3) given by (∞ -labelled) extensions of $[\infty, 3]$.



By means of Steinberg's formula (5.5), we have

$$\begin{aligned} \frac{1}{f_{S_1}(t^{-1})} &= 1 - \frac{4}{[2]} + \frac{3}{[2, 2]} + \frac{1}{[2, 3]} , \\ \frac{1}{f_{S_2}(t^{-1})} &= \frac{1}{f_{S_1}(t^{-1})} - \frac{1}{[2, 2, 3]} , \\ \frac{1}{f_{S_3}(t^{-1})} &= \frac{1}{f_{S_1}(t^{-1})} - \frac{1}{[2, 2, 2]} . \end{aligned}$$

As above, Lemma 5.3.6 implies that $\tau_{W_1} < \tau_{W_2}$ and $\tau_{W_1} < \tau_{W_3}$.

CHAPTER 6

MINIMAL GROWTH RATES FOR HYPERBOLIC COXETER GROUPS

Let $\Gamma \subset \text{Isom}\mathbb{H}^n$ be a cofinite Coxeter group. Let τ_Γ be its growth rate with respect to the canonical system S of generators for Γ ; see (1.9) and Chapter 5. Then, τ_Γ is always bounded from below by the growth rate $\tau_{\Gamma_9} \approx 1.138078$ of the simplex group Γ_9 ; see Figure 5.1.1 and (5.7).

In this chapter, we are interested in providing a sharp lower bound, for fixed dimension n , for the growth rate of a hyperbolic Coxeter group in $\text{Isom}\mathbb{H}^n$.

First, we discuss the low dimensional cases where we dispose of results due to Hironaka [36] and Kellerhals–Kolpakov [43] in the cocompact case, and due to Floyd [29] and Kellerhals [46] in the non-cocompact case. An important observation, motivating our work in higher dimensions, is the following one. In all known cases, the group achieving minimal growth rate is a Coxeter simplex group, and it is distinguished by the fact of being closely related to the fundamental group of minimal covolume when considering (compact, respectively cusped) hyperbolic orbifolds.

The next section is devoted to the study of minimal growth rates in higher dimensions, where we reproduce our results in the joint work with Kellerhals [7] in the cocompact case, and in our work [8] in the non-cocompact case.

1 In low dimensions

It is well known by Siegel's work [73] that the group of minimal co-area among all discrete groups in $\text{Isom}\mathbb{H}^2$ is the planar Coxeter group $\Gamma_2^c = [7, 3]$. In the non-cocompact case, the smallest co-area is achieved by the Coxeter triangle group $\Gamma_2 = [\infty, 3]$ intimately related to the modular group $\text{SL}_2(\mathbb{Z})$. In dimension 3, it was proven by Martin and his collaborators that the \mathbb{Z}_2 -extension of the Coxeter group $\Gamma_3^c = [3, 5, 3]$ gives rise to the smallest volume compact hyperbolic orbifold; see [59] for example. For cusped 3-orbifolds, Meyerhoff [62] showed that the smallest volume is achieved by the orbifold \mathbb{H}^3/Γ_3 , where Γ_3 is the Coxeter group with Coxeter symbol $[6, 3, 3]$.

These Coxeter simplex groups are also distinguished by the fact of having minimal growth rates among all Coxeter groups acting on hyperbolic space. In the cocompact case, this is due to Hironaka [36] for dimension 2, and to Kellerhals and Kolpakov [43] for dimension 3. More precisely, their results are as follows.

Theorem 6.1.1. *Let $n = 2$ or 3 . Among all cocompact Coxeter groups in $\text{Isom}\mathbb{H}^n$, the Coxeter simplex group Γ_n^c depicted in Figure 6.1.1 has minimal growth rate, and as such it is unique.*



Figure 6.1.1: The cocompact Coxeter simplex groups Γ_2^c and Γ_3^c

In the non-cocompact case, a similar result is due to Floyd [29] in dimension 2, and to Kellerhals [46] in dimension 3.

Theorem 6.1.2. *Let $n = 2$ or 3 . Among all non-cocompact cofinite Coxeter groups in $\text{Isom}\mathbb{H}^n$, the Coxeter simplex group Γ_n depicted in Figure 6.1.2 has minimal growth rate, and as such it is unique.*



Figure 6.1.2: The non-cocompact Coxeter simplex groups Γ_2 and Γ_3

The results stated in the previous theorems rely upon explicit formulas for the growth series in dimension 2 and 3, as described in Theorems 5.1.6, 5.1.7, 5.1.8 and 5.1.9. Since in higher dimensions, no such formulas exist, up to now, one needs to develop another, new, strategy to identify minimal growth rate.

2 In higher dimensions

Motivated by Theorems 6.1.1 and 6.1.2, and in view of Remarks 1.2.5 and (5.9), it is guessed that small covolume and small growth rate are intimately related.

In this context, let us mention that in general compact hyperbolic n -orbifolds of minimal volume are not known for dimensions $n \geq 4$. However, by restricting to *arithmetically* defined (orientable) hyperbolic n -orbifolds, minimizers for the volume have been detected, for instance, for $n = 4$ and 5, by exploiting Prasad's formula. These results are due to Belolipetsky [3, 4] and to Emery and Kellerhals [18]; see also [47, 48].

More precisely, among all arithmetic compact hyperbolic 4-orbifolds, the fundamental group of minimal covolume is given by the Coxeter simplex group $\Gamma_4^c = [5, 3, 3, 3]$. In dimension 5, the minimizing group is the Coxeter prism group $\Gamma_5^c = [5, 3, 3, 3, 3, \infty]$. Here, the component ∞ in the Coxeter symbol of Γ_5^c symbolizes the presence of a pair of ultraparallel facets in the underlying Coxeter prism.

In the non-compact case, cusped hyperbolic orbifolds of minimal volume are known up to dimension 9. This result was established by Hild and Kellerhals [34] in dimension 4, and by Hild [35] for dimensions up to 9. They showed that the cusped n -orbifolds of minimal volume are related to the Coxeter simplex groups $\Gamma_n \subset \text{Isom}\mathbb{H}^n$ (up to a \mathbb{Z}_2 -extension for $n = 7$) given in Figure 6.2.3.

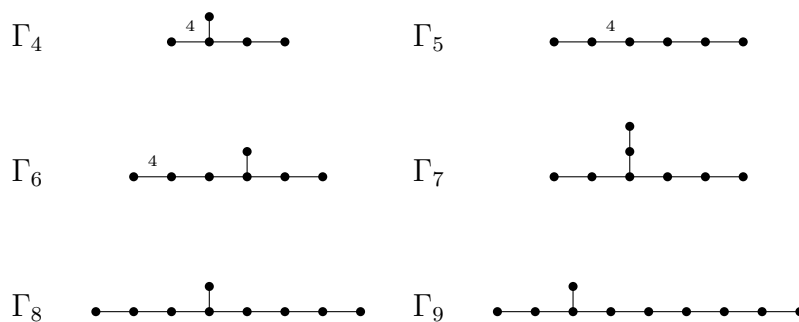


Figure 6.2.3: The non-cocompact Coxeter n -simplex groups $\Gamma_n \subset \text{Isom}\mathbb{H}^n$

Let us now announce our two main results, proved in [7, 8], concerning min-

imal growth rate for cofinite Coxeter groups in $\text{Isom}\mathbb{H}^n$ for $n \geq 4$, which complement the volume minimality results described above.

In a joint work with Kellerhals [7], we established the following result in the cocompact case.

Theorem 6.2.1 (Bredon, Kellerhals [7]). *Let $n = 4$ or 5 . Among all cocompact Coxeter groups in $\text{Isom}\mathbb{H}^n$, the Coxeter group Γ_n^c given in Figure 6.2.4 has minimal growth rate, and as such the group is unique.*

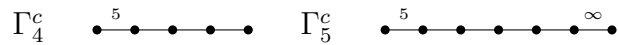


Figure 6.2.4: The cocompact Coxeter groups Γ_4^c and Γ_5^c

In the non-cocompact case, we were able to extend the tools developed for the proof of Theorem 6.2.1 in a suitable way in order to derive the following result.

Theorem 6.2.2 (Bredon [8]). *Let $4 \leq n \leq 9$. Among all non-cocompact Coxeter groups of finite covolume in $\text{Isom}\mathbb{H}^n$, the Coxeter simplex group Γ_n given in Figure 6.2.3 has minimal growth rate, and as such the group is unique.*

3 Proofs of the two main results

In this section, we describe the keys arguments for the proofs of Theorem 6.2.1 and Theorem 6.2.2. In Appendix D, the original articles [7] and [8] are attached.

Let $n \geq 4$, and let $\Gamma \subset \text{Isom}\mathbb{H}^n$ be a cofinite hyperbolic Coxeter group. Denote by $P \subset \mathbb{H}^n$ the associated Coxeter polyhedron and by Σ the Coxeter diagram of Γ and P .

If P is simple, which is always the case when P is compact, we dispose of some explicit results of Felikson and Tumarkin about the combinatorial structure of P ; see Section 2.2 in Chapter 3. The presence of a pair of disjoint facets yields a subdiagram $[\infty]$ in Σ whose simple extensions will play an important role.

If P is non-simple, then P has at least one non-simple ideal vertex which comes with a disconnected affine subdiagram of Σ . In this case, we consider simple extensions of its components of small rank.

In both situations, these extension diagrams with their growth rates, when combined with Terragni's monotonicity result, allow us to complete the proofs of Theorem 6.2.1 and Theorem 6.2.2.

3.1 The cocompact case

By Theorem 3.2.2 of Felikson and Tumarkin, there are only finitely many compact Coxeter polyhedra $P \subset \mathbb{H}^n$, $n \geq 4$, that do not contain any pair of disjoint facets. In fact, they exist only for $n = 4$ and consist of the five compact simplices and the seven Esselmann polyhedra; see Figure 3.2.4 and Figure 3.2.5 for their diagrams.

It is known that the growth rate of Γ_4^c is minimal among all Coxeter simplices; see [45], for example.

For the Esselmann groups E_1, \dots, E_7 , we observe that they all contain a cocompact hyperbolic triangle subgroup with Coxeter symbol $[8, 3]$, $[10, 3]$, $[5, 4]$, $[5, 5]$ or given by a cyclic Coxeter diagram of order 3 with label set $\{4, 3, 3\}$ or $\{5, 3, 3\}$, respectively. It is easy to verify that the group $[8, 3]$ has minimal growth rate among all of them, and that it satisfies

$$\tau_{\Gamma_4^c} < \tau_{[8,3]} . \tag{6.1}$$

By Theorem 5.3.1 of Terragni, and by inequality (6.1), we derive that

$$\tau_{\Gamma_4^c} < \tau_{[8,3]} \leq \tau_{E_i}$$

for all $i = 1, \dots, 7$.

Assume now that $P \subset \mathbb{H}^n$ has at least one pair of ultraparallel facets, and suppose that its Coxeter group Γ is not equal to Γ_4^c . It follows that the Coxeter diagram Σ of P necessarily contains a subdiagram σ of the form



where $p > 2$ and $q \in \{2, 3, \dots, \infty\}$. As $[8, 3] \leq [\infty, 3] \leq \sigma \leq \Gamma$ by the partial ordering of Coxeter groups, we derive by the same argument as above that

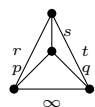
$$\tau_{\Gamma_4^c} < \tau_{[3,8]} \leq \tau_{[3,\infty]} \leq \tau_\sigma \leq \tau_\Gamma .$$

This proves the first part of Theorem 6.2.1 about the group Γ_4^c .

For the second part about $n = 5$, observe that $P \subset \mathbb{H}^5$ has at least 7 facets, and P is either one of the two simplicial prisms K_1, K_2 found by Kaplinskaya, or P has at least 8 facets; see Chapter 3. A direct computation shows that $\tau_{\Gamma_5^c} < \tau_{K_i}$ for $i = 1, 2$.

In the case where P has at least 8 facets, Theorem 3.2.1 of Felikson and Tumarkin implies that P has at least two pairs of disjoint facets.

Hence, we deduce that Σ necessarily contains a subdiagram σ of the form



where $p, q, r, s, t \in \{2, 3, \dots, \infty\}$, and where at least one of them is greater than 2 and at least one of them equals ∞ .

For comparison, consider the diagram $[\infty, 3, \infty]$, which satisfies the inequality $\tau_{\Gamma_5^c} < \tau_{[\infty, 3, \infty]}$. This can be seen by a direct computation.

By means of Theorem 5.3.1 and Example 5.3.8, we derive that

$$\tau_{\Gamma_5^c} < \tau_{[\infty, 3, \infty]} \leq \tau_\sigma \leq \tau_\Gamma ,$$

and the proof of Theorem 6.2.1 is complete. □

3.2 The non-cocompact case

In the non-compact case, if $P \subset \mathbb{H}^n$ is *simple*, Theorem 3.2.3 implies that P is either a simplex, isometric to $P_0 \subset \mathbb{H}^4$ depicted in Figure 3.2.6, or it contains a pair of disjoint facets in \mathbb{H}^n .

Let $4 \leq n \leq 9$. By results of Terragni [77], we know that Γ_n has minimal growth rate among all non-cocompact Coxeter n -simplex groups. Furthermore, we notice that the growth rates of the Coxeter groups Γ_n satisfy the strictly decreasing sequence

$$\tau_{\Gamma_9} < \tau_{\Gamma_8} < \dots < \tau_{\Gamma_5} < \tau_{\Gamma_4} . \tag{6.2}$$

Next, we compute the growth rate τ_0 of the Coxeter group associated with $P_0 \subset \mathbb{H}^4$, and we see that $\tau_{\Gamma_4} < \tau_0$.

Assume now that P is neither a simplex nor isometric to the polyhedron P_0 . As already said, if P is simple, then we know that it admits at least one pair of disjoint facets. In this case, we find that the Coxeter diagram Σ of P contains a subdiagram of type W_i , $1 \leq i \leq 3$, as depicted in Example 5.3.7.

By use of Lemma 5.3.6, we verify that $\tau_{\Gamma_4} < \tau_{W_1}$. From Example 5.3.7, and (6.2), we derive that

$$\tau_{\Gamma_n} < \tau_{W_1} \leq \tau_{\Gamma} .$$

Assume now that P is non-simple. If P contains a pair of disjoint facets in $\overline{\mathbb{H}^n}$, we conclude as before. In particular, this finishes the proof for $n = 4$, as we showed in the proof of Corollary 3.2.4 that non-simple Coxeter polyhedra in \mathbb{H}^4 always admit a pair of parallel facets.

From now on, we assume that $n \geq 5$ and that P does not contain any pair of disjoint facets. Observe the following important inequality refining (6.2)

$$\tau_{\Gamma_5} < \tau_{\Gamma_3} < \tau_{\Gamma_4} , \tag{6.3}$$

where $\Gamma_3 = [6, 3, 3]$.

As P is non-simple, Σ contains an affine subdiagram of rank $n - 1 \geq 4$ which is made of at least two affine components; see Theorem 1.3.8. By assumption, each of these affine components differs from $\tilde{A}_1 = [\infty]$. By (3.1), one verifies that Σ contains at least one connected affine subdiagram of rank 2, 3 or 4. Therefore, as Σ is connected, it contains at least one (possibly non-simple) extension σ of such a diagram.

In Example 5.3.5, we have seen that any *simple* extension of a connected affine diagram of rank 2 or 3 encodes a cofinite Coxeter simplex group in $\text{Isom}\mathbb{H}^3$ or $\text{Isom}\mathbb{H}^4$, whose growth rate is bounded from below by τ_{Γ_3} or τ_{Γ_4} . Therefore, whenever Σ contains an affine diagram of rank $r = 2$ or 3 , we derive from (6.3) that

$$\tau_{\Gamma_n} < \tau_{\Gamma_{r+1}} \leq \tau_{\sigma} \leq \tau_{\Gamma} .$$

Assume that the smallest rank for a connected affine diagram in Σ is 4. By means of (3.1), it follows that $n \geq 7$. Recall that any simple extension of an affine Coxeter diagram of rank 4, up to the four exceptions $\Delta_1, \dots, \Delta_4$, gives rise to cofinite Coxeter simplex group in $\text{Isom}\mathbb{H}^5$ whose growth rate is bounded from below by τ_{Γ_5} ; see Example 5.3.5. A straightforward computation shows that $\tau_{\Gamma_5} < \tau_{\Delta_i}$ for $i = 1, \dots, 4$. Finally, by Terragni's Theorem 5.3.1 and by (6.2), we deduce that

$$\tau_{\Gamma_n} < \tau_{\Gamma_5} \leq \tau_{\sigma} \leq \tau_{\Gamma} .$$

This finishes the proof of Theorem 6.2.2.

□

Final comments. For the proof of Theorem 6.2.1 and Theorem 6.2.2, we developed a new strategy to identify Coxeter groups of minimal growth rate in $\text{Isom}\mathbb{H}^n$ for $4 \leq n \leq 9$. These methods differ completely from the ones exploited for dimensions 2 and 3, and they are applicable to abstract Coxeter groups of arbitrarily large rank as well.

However, in the hyperbolic case, as the potential candidates for minimal growth rate in large dimensions are not simplex groups anymore and have a comparatively big growth rate value, the finding of suitable comparison diagrams causes high computational cost.

In the work of Hild [35], a similar phenomenon showed up in the context of minimal volume cusped hyperbolic n -orbifolds. He developed a general method to identify the minimizers, however, he exploited it for dimensions $n \leq 9$, only. The reason there was that the minimizer orbifolds turned out to be quotients related to the Coxeter simplex groups Γ_n whose properties are most beautiful in various ways.

PART IV:
APPENDICES

Only those who attempt the absurd...
will achieve the impossible.

M.C. ESCHER

APPENDIX A

DATA FOR PROKHOROV'S FORMULA

In this appendix, we provide the quantities involved in Prokhorov's formula for affine components of type \tilde{A} , \tilde{D} or \tilde{E} . For a component of type \tilde{G}_2 , they are computed in Example 5.3.8.

In the sequel, we use the representation $s_{ij}^n = s_i^n s_j^n$ for a specific root system R_n which is justified by the following fact. In (4.9), the scalars s_{ij}^n are expressed in terms of the fundamental weights w_i^n, w_j^n and the coefficients c_i^n, c_j^n of R_n , however they were originally defined as products $\langle s_i^n, s_j^n \rangle$ of specific vectors s_i^n, s_j^n displayed in explicit form in [70]. In order to simplify notations, we write s_{ij} instead of s_{ij}^n for a fixed root system $R = R_n$.

◇ For a component of type \tilde{A}_n

$$s_{ij} = s_i s_j = \frac{(j-i)(n+1-(j-i))}{2(n+1)}.$$

Note that for the proof of Theorem 4.0.2, we need these quantities for \tilde{A}_n for $n \leq 8$, only.

◇ For a component of type \tilde{D}_n

$$\begin{cases} s_i s_j = \frac{j-i}{2} & \text{for } 2 \leq i \leq j \leq n-2 \\ s_{n+1} s_j = s_1 s_j = \frac{j}{4} & \text{for } j \leq n-2 \\ s_1 s_{n-1} = s_1 s_n = s_{n-1} s_{n+1} = s_n s_{n+1} = \frac{n}{8} \\ s_{n-1} s_n = s_1 s_{n+1} = \frac{1}{2}; s_j s_{n-1} = s_j s_n = \frac{n-j}{4} & \text{for } j \leq n-2 \end{cases}$$

Note that for the proof of Theorem 4.0.2, we need these quantities for \tilde{D}_n for $n \leq 6$.

◇ For a component of type \tilde{E}_6, \tilde{E}_7 or \tilde{E}_8

The quantities $(s_i s_j)_{i,j}$ for the components of type \tilde{E}_6, \tilde{E}_7 and \tilde{E}_8 are given in the following tables.

$$\tilde{E}_6$$

	s_2	s_3	s_4	s_5	s_6	s_7
s_1	$5/6$	$1/2$	1	$5/6$	$2/3$	$2/3$
s_2		$2/3$	$1/2$	$2/3$	$5/6$	$1/2$
s_3			$1/2$	$2/3$	$5/6$	$5/6$
s_4				$1/2$	1	1
s_5					$1/2$	$5/6$
s_6						$1/3$

$$\tilde{E}_7$$

	s_2	s_3	s_4	s_5	s_6	s_7	s_8
s_1	$3/4$	$1/2$	1	1	1	1	$1/2$
s_2		$5/8$	$1/2$	$5/8$	$3/4$	$7/8$	$7/8$
s_3			$1/3$	$3/4$	1	$5/4$	1
s_4				$1/2$	1	$3/2$	$3/2$
s_5					$1/2$	1	$5/4$
s_6						$1/2$	1
s_7							$3/4$

$$\tilde{E}_8$$

	s_2	s_3	s_4	s_5	s_6	s_7	s_8	s_9
s_1	$2/3$	$1/2$	1	1	1	1	1	1
s_2		$7/12$	$1/2$	$2/3$	$5/6$	1	$7/6$	$4/3$
s_3			$1/2$	$3/4$	1	$5/4$	$3/2$	$7/4$
s_4				$1/2$	1	$3/2$	2	$5/2$
s_5					$1/2$	1	$3/2$	2
s_6						$1/2$	1	$3/2$
s_7							$1/2$	1
s_8								$1/2$

APPENDIX B

ADMISSIBLE PAIRS

In this appendix, we provide all admissible pairs for the cases of the proof of Theorem 4.0.2 that are not detailed in Chapter 4. Every table contains admissible pairs of the form $\{x, y_i\}$ and indicates the value $\langle x, y_i \rangle$. Furthermore, when relevant, we provide the Lorentzian products $\langle y_i, y_j \rangle$ if $\{y_i, y_j\}$ is an admissible pair.

x	y_i	$\langle x, y_i \rangle$				
$(0, 0, \sqrt{3}; 1, 0, 0, 0, 0, 0, 0)$	$y_1 \leftrightarrow (0, \sqrt{3}, \sqrt{3}; 1, 1, 0, 0, 0, 0, 1)$	0				
	$y_2 \leftrightarrow (1, 3, 3; \sqrt{3}, 0, 0, \sqrt{3}, 0, \sqrt{3}, \sqrt{3})$	0				
	$y_3 \leftrightarrow (1, 3, 3; \sqrt{3}, \sqrt{3}, \sqrt{3}, 0, \sqrt{3}, 0, 0)$	0				
	$y_4 \leftrightarrow (\sqrt{3}, \sqrt{3}, 0; 1, 1, 1, 0, 0, 1, 1)$	0				
	$y_5 \leftrightarrow (0, \sqrt{3}, \sqrt{3}; 0, 0, 0, 1, 0, 1, 1)$	-1				
	$y_6 \leftrightarrow (0, \sqrt{3}, \sqrt{3}; 0, 1, 1, 0, 1, 0, 0)$	-1				
The Lorentzian products $\langle y_i, y_j \rangle$						
	y_2	y_3	y_4	y_5	y_6	
y_1	0	0		0	0	
y_2		0			$-\sqrt{3}$	
y_3			0	$-\sqrt{3}$		
y_4				0	0	
y_5					0	

Table 2.0.1: Admissible pairs $\{x, y_i\}$ for $\sigma_\infty = \tilde{G}_2 \cup \tilde{A}_6$

x	y_i	$\langle x, y_i \rangle$			
$(0, 0, \sqrt{3}; 1, 0, 0, 0, 0, 0, 0)$	$y_1 \leftrightarrow (0, \sqrt{3}, \sqrt{3}; 1, 1, 0, 0, 0, 0, 0)$	0			
	$y_2 \leftrightarrow (1, 3, 3; \sqrt{3}, 0, 0, 0, \sqrt{3}, \sqrt{3}, \sqrt{3})$	0			
	$y_3 \leftrightarrow (\sqrt{3}, \sqrt{3}, \sqrt{3}; 0, 0, 1, 1, 1, 1, 0)$	0			
	$y_4 \leftrightarrow (0, \sqrt{3}, \sqrt{3}; 0, 0, 0, 0, 1, 1, 1)$	-1			
The Lorentzian products $\langle y_i, y_j \rangle$					
		y_2	y_3	y_4	
	y_1	0		0	
	y_2		$-\sqrt{3}$		
	y_3			0	

Table 2.0.2: Admissible pairs $\{x, y_i\}$ for $\sigma_\infty = \tilde{G}_2 \cup \tilde{D}_6$

x	y_i	$\langle x, y_i \rangle$			
$(0, 0, \sqrt{3}; 1, 0, 0, 0, 0, 0, 0)$	$y_1 \leftrightarrow (0, \sqrt{3}, \sqrt{3}; 1, 0, 1, 0, 0, 0, 0)$	0			
	$y_2 \leftrightarrow (1, 3, 3; \sqrt{3}, 0, 0, 0, \sqrt{3}, \sqrt{3}, 0)$	0			
	$y_3 \leftrightarrow (1, 3, 3; \sqrt{3}, \sqrt{3}, 0, 0, 0, 0, \sqrt{3})$	0			
	$y_4 \leftrightarrow (0, \sqrt{3}, \sqrt{3}; 0, 0, 0, 0, 1, 1, 0)$	-1			
	$y_5 \leftrightarrow (0, \sqrt{3}, \sqrt{3}; 0, 1, 0, 0, 0, 0, 1)$	-1			
The Lorentzian products $\langle y_i, y_j \rangle$					
		y_2	y_3	y_4	y_5
	y_1	0	0	0	0

Table 2.0.3: Admissible pairs $\{x, y_i\}$ for $\sigma_\infty = \tilde{G}_2 \cup \tilde{E}_6$

Appendix B. Admissible pairs

x	y_i	$\langle x, y_i \rangle$		
$(0, 0, \sqrt{3}; 0, 0, \sqrt{3}; 0, 0, \sqrt{3}; 0, 0, \sqrt{3})$	$(1, 0, 0; 1, 0, 0; 1, 0, 0; 1, 0, 0)$	0		
$(0, 0, 3; 0, 0, \sqrt{3}; 0, 0, \sqrt{3}; 0, 0, \sqrt{3})$	$y_1 \leftrightarrow (\sqrt{3}, 0, 0; 0, 0, 3; 0, 0, 3; 1, 0, 0)$	0		
	$y_2 \leftrightarrow (\sqrt{3}, 0, 0; 0, 0, 3; 1, 0, 0; 0, 0, 3)$	0		
	$y_3 \leftrightarrow (\sqrt{3}, 0, 0; 1, 0, 0; 0, 0, 3; 0, 0, 3)$	0		
The Lorentzian products $\langle y_i, y_j \rangle$				
		y_2	y_3	
	y_1	0	0	
	y_2		0	

Table 2.0.4: Admissible pairs $\{x, y_i\}$ for $\sigma_\infty = \tilde{G}_2 \cup \tilde{G}_2 \cup \tilde{G}_2 \cup \tilde{G}_2$

x	y_i	$\langle x, y_i \rangle$		
$(0, 0, \sqrt{3}; 0, 0, \sqrt{3}; 0, 0, \sqrt{3}; 1, 0, 0)$	$(1, 0, 0; 1, 0, 0; 1, 0, 0; 0, 0, \sqrt{3})$	0		
	$(1, 0, 0; 1, 0, 0; 1, 0, 0; 0, \sqrt{3}, 0)$	0		
	$(\sqrt{3}, 0, 0; \sqrt{3}, 0, 0; \sqrt{3}, 0, 0; 1, 1, 1)$	0		
$(0, 0, 3; 0, 0, \sqrt{3}; 0, 0, \sqrt{3}; 1, 0, 0)$	$y_1 \leftrightarrow (\sqrt{3}, 0, 0; 0, 0, 3; 0, 0, 3; 0, 0, \sqrt{3})$	0		
	$y_2 \leftrightarrow (\sqrt{3}, 0, 0; 0, 0, 3; 0, 0, 3; 0, \sqrt{3}, 0)$	0		
	$y_3 \leftrightarrow (\sqrt{3}, 0, 0; 0, 0, 3; 1, 0, 0; \sqrt{3}, 0, 0)$	0		
	$y_4 \leftrightarrow (\sqrt{3}, 0, 0; 1, 0, 0; 0, 0, 3; \sqrt{3}, 0, 0)$	0		
The Lorentzian products $\langle y_i, y_j \rangle$				
		y_3	y_4	
	y_1	0	0	
	y_2	0	0	
	y_3		0	

Table 2.0.5: Admissible pairs $\{x, y_i\}$ for $\sigma_\infty = \tilde{G}_2 \cup \tilde{G}_2 \cup \tilde{G}_2 \cup \tilde{A}_2$

x	y_i	$\langle x, y_i \rangle$																																			
$(0, 0, \sqrt{3}; 0, 0, \sqrt{3}; 1, 0, 0; 1, 0, 0)$	$y_1 \leftrightarrow (1, 0, 0; 1, 0, 0; 0, 0, \sqrt{3}; 0, 0, \sqrt{3})$	0																																			
	$y_2 \leftrightarrow (1, 0, 0; 1, 0, 0; 0, 0, \sqrt{3}; 0, \sqrt{3}, 0)$	0																																			
	$y_3 \leftrightarrow (1, 0, 0; 1, 0, 0; 0, \sqrt{3}, 0; 0, 0, \sqrt{3})$	0																																			
	$y_4 \leftrightarrow (1, 0, 0; 1, 0, 0; 0, \sqrt{3}, 0; 0, \sqrt{3}, 0)$	0																																			
x	z_i	$\langle x, z_i \rangle$																																			
$(0, 0, 3; 0, 0, \sqrt{3}; 1, 0, 0; 1, 0, 0)$	$y_1 \leftrightarrow (\sqrt{3}, 0, 0; 0, 0, 3; 0, 0, \sqrt{3}; \sqrt{3}, 0, 0)$	0																																			
	$y_2 \leftrightarrow (\sqrt{3}, 0, 0; 0, 0, 3; 0, \sqrt{3}, 0; \sqrt{3}, 0, 0)$	0																																			
	$y_3 \leftrightarrow (\sqrt{3}, 0, 0; 0, 0, 3; \sqrt{3}, 0, 0; 0, 0, \sqrt{3})$	0																																			
	$y_4 \leftrightarrow (\sqrt{3}, 0, 0; 0, 0, 3; \sqrt{3}, 0, 0; 0, \sqrt{3}, 0)$	0																																			
	$y_5 \leftrightarrow (\sqrt{3}, 0, 0; 1, 0, 0; \sqrt{3}, 0, 0; \sqrt{3}, 0, 0)$	0																																			
The Lorentzian products $\langle y_i, y_j \rangle$ and $\langle z_i, z_j \rangle$																																					
<table border="1" style="margin-left: auto; margin-right: auto;"> <tr> <td></td> <td>y_3</td> <td>y_4</td> <td></td> <td>z_3</td> <td>z_4</td> <td>z_5</td> </tr> <tr> <td></td> <td></td> <td></td> <td></td> <td>z_1</td> <td>0</td> <td>0</td> </tr> <tr> <td>y_1</td> <td></td> <td>0</td> <td></td> <td>z_2</td> <td>0</td> <td>0</td> </tr> <tr> <td>y_2</td> <td>0</td> <td></td> <td></td> <td>z_3</td> <td></td> <td>0</td> </tr> <tr> <td></td> <td></td> <td></td> <td></td> <td>z_4</td> <td></td> <td>0</td> </tr> </table>				y_3	y_4		z_3	z_4	z_5					z_1	0	0	y_1		0		z_2	0	0	y_2	0			z_3		0					z_4		0
	y_3	y_4		z_3	z_4	z_5																															
				z_1	0	0																															
y_1		0		z_2	0	0																															
y_2	0			z_3		0																															
				z_4		0																															

Table 2.0.6: Admissible pairs for $\sigma_\infty = \tilde{G}_2 \cup \tilde{G}_2 \cup \tilde{A}_2 \cup \tilde{A}_2$

Appendix B. Admissible pairs

x	y_i	$\langle x, y_i \rangle$										
$(0, 0, \sqrt{3}; 1, 0, 0; 1, 0, 0; 1, 0, 0)$	$y_1 \leftrightarrow (1, 0, 0; 0, 0, \sqrt{3}; 0, 0, \sqrt{3}; 0, 0, \sqrt{3})$	0										
	$y_2 = (1, 0, 0; 0, 0, \sqrt{3}; 0, 0, \sqrt{3}; 0, \sqrt{3}, 0)$	0										
	$y_3 = (1, 0, 0; 0, 0, \sqrt{3}; 0, \sqrt{3}, 0; 0, 0, \sqrt{3})$	0										
	$y_4 \leftrightarrow (1, 0, 0; 0, 0, \sqrt{3}; 0, \sqrt{3}, 0; 0, \sqrt{3}, 0)$	0										
	$y_5 \leftrightarrow (1, 0, 0; 0, \sqrt{3}, 0; 0, 0, \sqrt{3}; 0, 0, \sqrt{3})$	0										
	$y_6 \leftrightarrow (1, 0, 0; 0, \sqrt{3}, 0; 0, 0, \sqrt{3}; 0, \sqrt{3}, 0)$	0										
	$y_7 \leftrightarrow (1, 0, 0; 0, \sqrt{3}, 0; 0, \sqrt{3}, 0; 0, 0, \sqrt{3})$	0										
	$y_8 \leftrightarrow (1, 0, 0; 0, \sqrt{3}, 0; 0, \sqrt{3}, 0; 0, \sqrt{3}, 0)$	0										
x	z_i	$\langle x, z_i \rangle$										
$(0, 0, 3, 1, 0, 0, 1, 0, 0, 1, 0, 0)$	$z_1 \leftrightarrow (1, 0, 0; 0, 0, 1; 0, 0, 1; 0, 0, 1)$	0										
	$z_2 \leftrightarrow (1, 0, 0; 0, 0, 1; 0, 0, 1; 0, 1, 0)$	0										
	$z_3 \leftrightarrow (1, 0, 0; 0, 0, 1; 0, 1, 0; 0, 0, 1)$	0										
	$z_4 \leftrightarrow (1, 0, 0; 0, 0, 1; 0, 1, 0; 0, 1, 0)$	0										
	$z_5 \leftrightarrow (1, 0, 0; 0, 1, 0; 0, 0, 1; 0, 0, 1)$	0										
	$z_6 \leftrightarrow (1, 0, 0; 0, 1, 0; 0, 0, 1; 0, 1, 0)$	0										
	$z_7 \leftrightarrow (1, 0, 0; 0, 1, 0; 0, 1, 0; 0, 0, 1)$	0										
	$z_8 \leftrightarrow (1, 0, 0; 0, 1, 0; 0, 1, 0; 0, 1, 0)$	0										
	$z_9 \leftrightarrow (\sqrt{3}, 0, 0; 0, 0, \sqrt{3}; \sqrt{3}, 0, 0; \sqrt{3}, 0, 0)$	0										
	$z_{10} \leftrightarrow (\sqrt{3}, 0, 0; 0, \sqrt{3}, 0; \sqrt{3}, 0, 0; \sqrt{3}, 0, 0)$	0										
	$z_{11} \leftrightarrow (\sqrt{3}, 0, 0; \sqrt{3}, 0, 0; 0, 0, \sqrt{3}; \sqrt{3}, 0, 0)$	0										
	$z_{12} \leftrightarrow (\sqrt{3}, 0, 0; \sqrt{3}, 0, 0; 0, \sqrt{3}, 0; \sqrt{3}, 0, 0)$	0										
	$z_{13} \leftrightarrow (\sqrt{3}, 0, 0; \sqrt{3}, 0, 0; \sqrt{3}, 0, 0; 0, 0, \sqrt{3})$	0										
	$z_{14} \leftrightarrow (\sqrt{3}, 0, 0; \sqrt{3}, 0, 0; \sqrt{3}, 0, 0; 0, \sqrt{3}, 0)$	0										
The Lorentzian products $\langle y_i, y_j \rangle$ and $\langle z_i, z_j \rangle$												
y_1	y_2	y_3	y_4	y_5	y_6	y_7	y_8	z_{10}	z_{11}	z_{12}	z_{13}	z_{14}
y_2	0	0	0	-1	0	-1	0	z_9	0	0	0	0
y_3	0	0	0	-1	0	0	0	z_{10}	0	0	0	0
y_4	0	0	0	-1	0	0	0	z_{11}	0	0	0	0
y_5	0	0	0	0	0	0	0	z_{12}	0	0	0	0
y_6	0	0	0	0	0	0	0	z_{13}	0	0	0	0
y_7	0	0	0	0	0	0	0	z_{14}	0	0	0	0
y_8	0	0	0	0	0	0	0	z_{10}	0	0	0	0

Table 2.0.7: Admissible pairs for $\sigma_\infty = \tilde{G}_2 \cup \tilde{A}_2 \cup \tilde{A}_2 \cup \tilde{A}_2$

x	y	$\langle x, y \rangle$
$(0, 0, \sqrt{3}; 0, 0, \sqrt{3}; 1, 0, 0, 0, 0)$	$(0, \sqrt{3}, \sqrt{3}; \sqrt{3}, 0, 0; 1, 1, 0, 0, 1)$	-1
	$(\sqrt{3}, 0, 0; 0, \sqrt{3}, \sqrt{3}; 1, 1, 0, 0, 1)$	-1
$(0, 0, 3; 0, 0, \sqrt{3}; 1, 0, 0, 0, 0)$	$(\sqrt{3}, 0, 0; 1, 0, 0; \sqrt{3}, 0, 0, 0, 0)$	0

Table 2.0.8: Admissible pairs $\{x, y\}$ for $\sigma_\infty = \tilde{G}_2 \cup \tilde{G}_2 \cup \tilde{A}_4$

x	y	$\langle x, y \rangle$
$(0, 0, 3; 1, 0, 0; 1, 0, 0, 0)$	$(\sqrt{3}, 0, 0; 0, 0, \sqrt{3}; \sqrt{3}, 0, 0, 0, 0)$	0
	$(\sqrt{3}, 0, 0; 0, \sqrt{3}, 0; \sqrt{3}, 0, 0, 0, 0)$	0

Table 2.0.9: Admissible pairs $\{x, y\}$ for $\sigma_\infty = \tilde{G}_2 \cup \tilde{A}_2 \cup \tilde{A}_4$

x	y	$\langle x, y \rangle$
$(0, 0, \sqrt{3}; 1, 0, 0; 1, 0, 0, 0)$	$y \leftrightarrow (0, 0, \sqrt{3}; 1, 1, 1; 0, 0, 1, 1, 1)$	0
$(0, 0, 3; 1, 0, 0; 1, 0, 0, 0)$	$(\sqrt{3}, 0, 0, 0, 0, \sqrt{3}, \sqrt{3}, 0, 0, 0, 0)$	0
	$(\sqrt{3}, 0, 0, 0, \sqrt{3}, 0, \sqrt{3}, 0, 0, 0, 0)$	0

Table 2.0.10: Admissible pairs $\{x, y\}$ for $\sigma_\infty = \tilde{G}_2 \cup \tilde{A}_2 \cup \tilde{D}_4$

x	y	$\langle x, y \rangle$
$(0, 0, \sqrt{3}, 0, 0, \sqrt{3}, 1, 0, 0, 0, 0)$	$(0, \sqrt{3}, \sqrt{3}, \sqrt{3}, 0, 0, 1, 1, 0, 0, 0)$	0
	$(\sqrt{3}, 0, 0, 0, \sqrt{3}, \sqrt{3}, 1, 1, 0, 0, 0)$	0
$(0, 0, 3, 0, 0, \sqrt{3}, 1, 0, 0, 0, 0)$	$(\sqrt{3}, 0, 0; 1, 0, 0; \sqrt{3}, 0, 0, 0, 0)$	0

Table 2.0.11: Admissible pairs $\{x, y\}$ for $\sigma_\infty = \tilde{G}_2 \cup \tilde{G}_2 \cup \tilde{D}_4$

x	y	$\langle x, y \rangle$
$(0, 0, \sqrt{3}; 1, 0, 0, 0; 1, 0, 0, 0)$	$(1, 0, 0; 0, 0, \sqrt{3}, 0; 0, 0, \sqrt{3}, 0)$	0
$(0, 0, 3; 1, 0, 0, 0; 1, 0, 0, 0)$	$(1, 0, 0; 0, 0, 1, 0; 0, 0, 1, 0)$	0

Table 2.0.12: Admissible pairs $\{x, y\}$ for $\sigma_\infty = \tilde{G}_2 \cup \tilde{A}_3 \cup \tilde{A}_3$

Appendix B. Admissible pairs

x	y_i	$\langle x, y_i \rangle$												
$(0, 0, \sqrt{3}; 1, 0, 0, 0, 0, 0, 0, 0)$	$y_1 \leftrightarrow (0, \sqrt{3}, \sqrt{3}, 1, 1, 0, 0, 0, 0, 0, 1)$	0												
	$y_2 \leftrightarrow (1, 0, 0, 0, 0, 0, 0, \sqrt{3}, 0, 0, 0)$	0												
	$y_3 \leftrightarrow (1, 3, 3, \sqrt{3}, 0, 0, \sqrt{3}, 0, 0, \sqrt{3}, \sqrt{3})$	0												
	$y_4 \leftrightarrow (1, 3, 3, \sqrt{3}, 0, \sqrt{3}, \sqrt{3}, 0, 0, 0, \sqrt{3})$	0												
	$y_5 \leftrightarrow (1, 3, 3, \sqrt{3}, \sqrt{3}, 0, 0, 0, \sqrt{3}, \sqrt{3}, 0)$	0												
	$y_6 \leftrightarrow (1, 3, 3, \sqrt{3}, \sqrt{3}, \sqrt{3}, 0, 0, \sqrt{3}, 0, 0)$	0												
	$y_7 \leftrightarrow (\sqrt{3}, 0, 0, 0, 0, 0, 0, 1, 1, 1, 0, 0)$	0												
	$y_8 \leftrightarrow (\sqrt{3}, \sqrt{3}, 0, 1, 1, 1, 0, 0, 0, 1, 1)$	0												
	$y_9 \leftrightarrow (0, \sqrt{3}, \sqrt{3}, 0, 0, 0, 1, 0, 0, 1, 1)$	-1												
	$y_{10} \leftrightarrow (0, \sqrt{3}, \sqrt{3}, 0, 0, 1, 1, 0, 0, 0, 1)$	-1												
	$y_{11} \leftrightarrow (0, \sqrt{3}, \sqrt{3}, 0, 1, 0, 0, 0, 1, 1, 0)$	-1												
	$y_{12} \leftrightarrow (0, \sqrt{3}, \sqrt{3}, 0, 1, 1, 0, 0, 1, 0, 0)$	-1												
	$y_{13} \leftrightarrow (1, 3, 3, 0, 0, 0, \sqrt{3}, \sqrt{3}, 0, \sqrt{3}, \sqrt{3})$	$-\sqrt{3}$												
	$y_{14} \leftrightarrow (1, 3, 3, 0, 0, \sqrt{3}, \sqrt{3}, \sqrt{3}, 0, 0, \sqrt{3})$	$-\sqrt{3}$												
	$y_{15} \leftrightarrow (1, 3, 3, 0, \sqrt{3}, 0, 0, \sqrt{3}, \sqrt{3}, \sqrt{3}, 0)$	$-\sqrt{3}$												
	$y_{16} \leftrightarrow (1, 3, 3, 0, \sqrt{3}, \sqrt{3}, 0, \sqrt{3}, \sqrt{3}, 0, 0)$	$-\sqrt{3}$												
$(0, 0, 3; 1, 0, 0, 0, 0, 0, 0, 0)$	$(1, 0, 0; 0, 0, 0, 0, 1, 0, 0, 0)$	0												
The Lorentzian products $\langle y_i, y_j \rangle$														
	y_3	y_4	y_5	y_6	y_8	y_9	y_{10}	y_{11}	y_{12}	y_{13}	y_{14}	y_{15}	y_{16}	
y_1	0	0	0	0		0	0	0	0					
y_2							$-\sqrt{3}$	$-\sqrt{3}$	$-\sqrt{3}$	$-\sqrt{3}$	-1	-1	-1	-1
y_3		-1	-1		0		0	0	$-\sqrt{3}$	1				
y_4				-1	0	0		$-\sqrt{3}$	0		1			
y_5				-1	0	0	$-\sqrt{3}$		0			1		
y_6					0	$-\sqrt{3}$	0	0					1	
y_8						0	0	0	0					
y_9									0		0	0	$-\sqrt{3}$	
y_{10}								0		0		$-\sqrt{3}$	0	
y_{11}										0	$-\sqrt{3}$		0	
y_{12}										$-\sqrt{3}$	0	0		
y_{13}											-1	-1		
y_{14}													-1	
y_{15}													-1	

Table 2.0.13: Admissible pairs $\{x, y_i\}$ for $\sigma_\infty = \tilde{G}_2 \cup \tilde{A}_7$

x	y_i	$\langle x, y_i \rangle$				
$(0, 0, \sqrt{3}; 1, 0, 0, 0, 0, 0, 0, 0)$	$y_1 \leftrightarrow (0, \sqrt{3}, \sqrt{3}; 1, 1, 0, 0, 0, 0, 0, 0)$	0				
	$y_2 \leftrightarrow (1, 3, 3; \sqrt{3}, 0, 0, 0, \sqrt{3}, 0, 0, \sqrt{3})$	0				
	$y_3 \leftrightarrow (\sqrt{3}, \sqrt{3}, \sqrt{3}; 0, 0, 1, 1, 1, 0, 0, 0)$	0				
	$y_4 \leftrightarrow (0, \sqrt{3}, \sqrt{3}; 0, 0, 0, 0, 1, 0, 0, 1)$	-1				
	$y_5 \leftrightarrow (\sqrt{3}, \sqrt{3}, 0; 0, 0, 1, 0, 0, 1, 1, 1)$	-1				
The Lorentzian products $\langle y_i, y_j \rangle$						
		y_2	y_3	y_4	y_5	
	y_1				-1	
	y_2		$\sqrt{3}$		0	
	y_3			0	0	

Table 2.0.14: Admissible pairs $\{x, y_i\}$ for $\sigma_\infty = \tilde{G}_2 \cup \tilde{D}_7$

x	y_i	$\langle x, y_i \rangle$				
$(0, 0, \sqrt{3}; 0, 0, 0, 0, 0, 0, 0, 1)$	$y_1 \leftrightarrow (0, \sqrt{3}, \sqrt{3}; 1, 0, 0, 0, 0, 0, 0, 1)$	0				
	$y_2 \leftrightarrow (1, 3, 3; 0, \sqrt{3}, 0, 0, 0, 0, \sqrt{3}, \sqrt{3})$	0				
	$y_3 \leftrightarrow (\sqrt{3}, \sqrt{3}, 0; 1, 0, 0, 0, 0, 1, 0, 1)$	0				
	$y_4 \leftrightarrow (\sqrt{3}, \sqrt{3}, \sqrt{3}; 0, 0, 0, 0, 1, 1, 1, 0)$	0				
	$y_5 \leftrightarrow (0, \sqrt{3}, \sqrt{3}; 0, 1, 0, 0, 0, 0, 1, 0)$	-1				
	$y_6 \leftrightarrow (\sqrt{3}, \sqrt{3}, 0; 0, 1, 0, 0, 1, 0, 0, 0)$	-1				
The Lorentzian products $\langle y_i, y_j \rangle$						
		y_2	y_3	y_4	y_5	y_6
	y_1	0			0	1
	y_2		0	$-\sqrt{3}$		0
	y_3			-1	0	0
	y_4				0	0

Table 2.0.15: Admissible pairs $\{x, y_i\}$ for $\sigma_\infty = \tilde{G}_2 \cup \tilde{E}_7$

Appendix B. Admissible pairs

x	y	$\langle x, y \rangle$
$(0, 0, \sqrt{3}; 0, 0, \sqrt{3}; 1, 0, 0, 0, 0, 0)$	$(0, \sqrt{3}, \sqrt{3}; \sqrt{3}, 0, 0; 1, 1, 0, 0, 0, 0)$	-1
	$(\sqrt{3}, 0, 0; 0, \sqrt{3}, \sqrt{3}; 1, 1, 0, 0, 0, 0)$	-1
$(0, 0, 3; 0, 0, \sqrt{3}; 1, 0, 0, 0, 0, 0)$	$(\sqrt{3}, 0, 0; 1, 0, 0; \sqrt{3}, 0, 0, 0, 0, 0)$	0

Table 2.0.16: Admissible pairs $\{x, y\}$ for $\sigma_\infty = \tilde{G}_2 \cup \tilde{G}_2 \cup \tilde{D}_5$

x	y	$\langle x, y \rangle$
$(0, 0, \sqrt{3}; 1, 0, 0; 1, 0, 0, 0, 0, 0)$	$(0, \sqrt{3}, \sqrt{3}; 1, 1, 1; 0, 0, 1, 0, 0, 1)$	-1
$(0, 0, 3; 1, 0, 0; 1, 0, 0, 0, 0, 0)$	$(\sqrt{3}, 0, 0; 0, 0, \sqrt{3}; \sqrt{3}, 0, 0, 0, 0, 0)$	0
	$(\sqrt{3}, 0, 0; 0, \sqrt{3}, 0; \sqrt{3}, 0, 0, 0, 0, 0)$	0

Table 2.0.17: Admissible pairs $\{x, y\}$ for $\sigma_\infty = \tilde{G}_2 \cup \tilde{A}_2 \cup \tilde{D}_5$

x	y_i	$\langle x, y_i \rangle$					
$(0, 0, \sqrt{3}; 1, 0, 0, 0; 1, 0, 0, 0, 0)$	$y_1 \leftrightarrow (0, \sqrt{3}, \sqrt{3}; 0, 1, 1, 1; 1, 0, 0, 1, 1)$	-1					
	$y_2 \leftrightarrow (0, \sqrt{3}, \sqrt{3}; 0, 1, 1, 1; 1, 0, 1, 0, 1)$	-1					
	$y_3 \leftrightarrow (0, \sqrt{3}, \sqrt{3}; 0, 1, 1, 1; 1, 0, 1, 1, 0)$	-1					
	$y_4 \leftrightarrow (0, \sqrt{3}, \sqrt{3}; 1, 1, 0, 1; 0, 0, 1, 1, 1)$	-1					
	$y_5 \leftrightarrow (1, 0, 0; 0, 0, \sqrt{3}, 0; 0, 0, 0, 0, \sqrt{3})$	0					
	$y_6 \leftrightarrow (1, 0, 0; 0, 0, \sqrt{3}, 0; 0, 0, 0, \sqrt{3}, 0)$	0					
	$y_7 \leftrightarrow (1, 0, 0; 0, 0, \sqrt{3}, 0; 0, 0, \sqrt{3}, 0, 0)$	0					
$(0, 0, 3; 1, 0, 0, 0; 1, 0, 0, 0, 0)$	$(1, 0, 0; 0, 0, 1, 0; 0, 0, 0, 0, 1)$	0					
	$(1, 0, 0; 0, 0, 1, 0; 0, 0, 0, 1, 0)$	0					
	$(1, 0, 0; 0, 0, 1, 0; 0, 0, 1, 0, 0)$	0					
The Lorentzian products $\langle y_i, y_j \rangle$							
	y_2	y_3	y_4	y_5	y_6	y_7	
	y_1					$-\sqrt{3}$	
	y_2				$-\sqrt{3}$		
	y_3			$-\sqrt{3}$			
	y_4			$-\sqrt{3}$	$-\sqrt{3}$	$-\sqrt{3}$	

Table 2.0.18: Admissible pairs $\{x, y_i\}$ for $\sigma_\infty = \tilde{G}_2 \cup \tilde{A}_3 \cup \tilde{D}_4$

x	y_i	$\langle x, y_i \rangle$
$(0, 0\sqrt{3}; 1, 0, 0, 0, 0, 0, 0, 0, 0)$	$y_1 \leftrightarrow (0, \sqrt{3}, \sqrt{3}; 1, 1, 0, 0, 0, 0, 0, 0)$	0
	$y_2 \leftrightarrow (1, 0, 0; 0, 0, 0, 0, 0, 0, 0, \sqrt{3}, 0)$	0
	$y_3 \leftrightarrow (1, 0, 0; 0, 0, 0, 0, 0, 0, \sqrt{3}, 0, 0)$	0
	$y_4 \leftrightarrow (1, 3, 3; 0, 0, 0, 0, \sqrt{3}, 0, 0, \sqrt{3}, \sqrt{3})$	$-\sqrt{3}$
	$y_5 \leftrightarrow (1, 3, 3; 0, 0, 0, 0, \sqrt{3}, 0, \sqrt{3}, 0, \sqrt{3})$	$-\sqrt{3}$
	$y_6 \leftrightarrow (1, 3, 3; 0, 0, \sqrt{3}, 0, 0, 0, \sqrt{3}, \sqrt{3}, 0)$	$-\sqrt{3}$
	$y_7 \leftrightarrow (1, 3, 3; \sqrt{3}, 0, 0, 0, \sqrt{3}, 0, 0, 0, \sqrt{3})$	0
	$y_8 \leftrightarrow (1, 3, 3; \sqrt{3}, 0, \sqrt{3}, 0, 0, 0, 0, \sqrt{3}, 0)$	0
	$y_9 \leftrightarrow (1, 3, 3; \sqrt{3}, 0, \sqrt{3}, 0, 0, 0, \sqrt{3}, 0, 0)$	0
	$y_{10} \leftrightarrow (\sqrt{3}, 0, 0; 0, 0, 0, 0, 0, 1, 0, 1, 0)$	0
	$y_{11} \leftrightarrow (\sqrt{3}, 0, 0; 0, 0, 0, 0, 0, 1, 1, 0, 0)$	0
	$y_{12} \leftrightarrow (\sqrt{3}, \sqrt{3}, 0; 1, 1, 0, 0, 0, 0, 0, 1, 1)$	0
	$y_{13} \leftrightarrow (\sqrt{3}, \sqrt{3}, 0; 1, 1, 0, 0, 0, 0, 1, 0, 1)$	0
	$y_{14} \leftrightarrow (\sqrt{3}, \sqrt{3}, 0; 1, 1, 0, 1, 0, 0, 0, 0, 0)$	0
	$y_{15} \leftrightarrow (\sqrt{3}, \sqrt{3}, \sqrt{3}; 0, 0, 1, 0, 0, 1, 0, 1, 1)$	0
	$y_{16} \leftrightarrow (\sqrt{3}, \sqrt{3}, \sqrt{3}; 0, 0, 1, 0, 0, 1, 1, 0, 1)$	0
	$y_{17} \leftrightarrow (\sqrt{3}, \sqrt{3}, \sqrt{3}; 0, 0, 1, 1, 1, 0, 0, 0, 0)$	0
	$y_{18} \leftrightarrow (\sqrt{3}, \sqrt{3}, \sqrt{3}; 0, 1, 0, 0, 1, 0, 1, 1, 0)$	0
$(0, 0, 3; 1, 0, 0, 0, 0, 0, 0, 0, 0)$	$(1, 0, 0; 0, 0, 0, 0, 0, 0, 0, 1, 0)$	0
	$(1, 0, 0; 0, 0, 0, 0, 0, 0, 1, 0, 0)$	0

The Lorentzian products $\langle y_i, y_j \rangle$

	y_4	y_5	y_6	y_7	y_8	y_9	y_{14}	y_{15}	y_{16}	y_{17}	y_{18}
y_1				0	0	0					
y_2	-1		-1					0		$-\sqrt{3}$	0
y_3		-1	-1						0	$-\sqrt{3}$	0
y_4			-1	-1			0			$-\sqrt{3}$	0
y_5			-1	-1					0	$-\sqrt{3}$	0
y_6					-1	-1		0	0	$-\sqrt{3}$	0
y_7					-1					$-\sqrt{3}$	$-\sqrt{3}$
y_9										$-\sqrt{3}$	$-\sqrt{3}$
y_{10}								-1			-1
y_{11}									-1		-1
y_{14}										-1	
y_{15}										0	
y_{16}										0	
y_{17}											0

Appendix B. Admissible pairs

x	y_i	$\langle x, y_i \rangle$				
$(0, 0, \sqrt{3}; 0, 0, 0, 0, 0, 0, 0, 0, 1)$	$y_1 \leftrightarrow (0, \sqrt{3}, \sqrt{3}; 0, 0, 0, 0, 0, 0, 0, 1, 1)$,	0				
	$y_2 \leftrightarrow (0, \sqrt{3}, \sqrt{3}; 0, 1, 0, 0, 0, 0, 0, 0, 0)$,	-1				
	$y_3 \leftrightarrow (1, 3, 3; 0, \sqrt{3}, 0, 0, 0, 0, 0, 0, \sqrt{3})$,	0				
	$y_4 \leftrightarrow (\sqrt{3}, \sqrt{3}, 0; 0, 0, 0, 0, 1, 0, 0, 0, 0)$	-1				
	$y_5 \leftrightarrow (\sqrt{3}, \sqrt{3}, 0; 1, 0, 0, 0, 0, 0, 0, 1, 1)$	0				
	$y_6 \leftrightarrow (\sqrt{3}, \sqrt{3}, \sqrt{3}; 1, 0, 1, 0, 0, 0, 0, 0, 0)$	0				
The Lorentzian products $\langle y_i, y_j \rangle$						
	y_2	y_3	y_4	y_5	y_6	
y_1	0	0	-1			
y_2				0	0	
y_3			0	0	$-\sqrt{3}$	
y_4				0	0	
y_5					-1	

Table 2.0.20: Admissible pairs $\{x, y_i\}$ for $\sigma_\infty = \tilde{G}_2 \cup \tilde{E}_8$

x	y	$\langle x, y \rangle$
$(0, 0, 3; 1, 0, 0, 0, 0; 1, 0, 0, 0, 0)$	$(1, 0, 0; 0, 0, 0, 0, 1; 0, 0, 0, 0, 1)$	0
	$(1, 0, 0; 0, 0, 0, 0, 1; 0, 0, 0, 1, 0)$	0
	$(1, 0, 0; 0, 0, 0, 0, 1; 0, 0, 1, 0, 0)$	0
	$(1, 0, 0; 0, 0, 0, 1, 0; 0, 0, 0, 0, 1)$	0
	$(1, 0, 0; 0, 0, 0, 1, 0; 0, 0, 0, 1, 0)$	0
	$(1, 0, 0; 0, 0, 0, 1, 0; 0, 0, 1, 0, 0)$	0
	$(1, 0, 0; 0, 0, 1, 0, 0; 0, 0, 0, 0, 1)$	0
	$(1, 0, 0; 0, 0, 1, 0, 0; 0, 0, 0, 1, 0)$	0
	$(1, 0, 0; 0, 0, 1, 0, 0; 0, 0, 1, 0, 0)$	0

Table 2.0.21: Admissible pairs $\{x, y\}$ for $\sigma_\infty = \tilde{G}_2 \cup \tilde{D}_4 \cup \tilde{D}_4$

x	y	$\langle x, y \rangle$
$(0, 0, \sqrt{3}; 1, 0, 0, 0, 0; 1, 0, 0, 0, 0)$	$y_1 \leftrightarrow (1, 0, 0; 0, 0, 0, 0, \sqrt{3}; 0, 0, 0, 0, \sqrt{3})$	0
	$y_2 \leftrightarrow (1, 0, 0; 0, 0, 0, 0, \sqrt{3}; 0, 0, 0, \sqrt{3}, 0)$	0
	$y_3 \leftrightarrow (1, 0, 0; 0, 0, 0, 0, \sqrt{3}; 0, 0, \sqrt{3}, 0, 0)$	0
	$y_4 \leftrightarrow (1, 0, 0; 0, 0, 0, \sqrt{3}, 0; 0, 0, 0, 0, \sqrt{3})$	0
	$y_5 \leftrightarrow (1, 0, 0; 0, 0, 0, \sqrt{3}, 0; 0, 0, 0, \sqrt{3}, 0)$	0
	$y_6 \leftrightarrow (1, 0, 0; 0, 0, 0, \sqrt{3}, 0; 0, 0, \sqrt{3}, 0, 0)$	0
	$y_7 \leftrightarrow (1, 0, 0; 0, 0, \sqrt{3}, 0, 0; 0, 0, 0, 0, \sqrt{3})$	0
	$y_8 \leftrightarrow (1, 0, 0; 0, 0, \sqrt{3}, 0, 0; 0, 0, 0, \sqrt{3}, 0)$	0
	$y_9 \leftrightarrow (1, 0, 0; 0, 0, \sqrt{3}, 0, 0; 0, 0, \sqrt{3}, 0, 0)$	0
	$y_{10} \leftrightarrow (0, \sqrt{3}, \sqrt{3}; 0, 0, 1, 1, 1; 1, 1, 0, 0, 0)$	-1
	$y_{11} \leftrightarrow (0, \sqrt{3}, \sqrt{3}; 0, 1, 0, 0, 1; 1, 0, 0, 1, 1)$	-1
	$y_{12} \leftrightarrow (0, \sqrt{3}, \sqrt{3}; 0, 1, 0, 0, 1; 1, 0, 1, 0, 1)$	-1
	$y_{13} \leftrightarrow (0, \sqrt{3}, \sqrt{3}; 0, 1, 0, 0, 1; 1, 0, 1, 1, 0)$	-1
	$y_{14} \leftrightarrow (0, \sqrt{3}, \sqrt{3}; 0, 1, 0, 1, 0; 1, 0, 0, 1, 1)$	-1
	$y_{15} \leftrightarrow (0, \sqrt{3}, \sqrt{3}; 0, 1, 0, 1, 0; 1, 0, 1, 0, 1)$	-1
	$y_{16} \leftrightarrow (0, \sqrt{3}, \sqrt{3}; 0, 1, 0, 1, 0; 1, 0, 1, 1, 0)$	-1
	$y_{17} \leftrightarrow (0, \sqrt{3}, \sqrt{3}; 0, 1, 1, 0, 0; 1, 0, 0, 1, 1)$	-1
	$y_{18} \leftrightarrow (0, \sqrt{3}, \sqrt{3}; 0, 1, 1, 0, 0; 1, 0, 1, 0, 1)$	-1
	$y_{19} \leftrightarrow (0, \sqrt{3}, \sqrt{3}; 0, 1, 1, 0, 0; 1, 0, 1, 1, 0)$	-1
	$y_{20} \leftrightarrow (0, \sqrt{3}, \sqrt{3}; 1, 0, 0, 1, 1; 0, 1, 0, 0, 1)$	-1
	$y_{21} \leftrightarrow (0, \sqrt{3}, \sqrt{3}; 1, 0, 0, 1, 1; 0, 1, 0, 1, 0)$	-1
	$y_{22} \leftrightarrow (0, \sqrt{3}, \sqrt{3}; 1, 0, 0, 1, 1; 0, 1, 1, 0, 0)$	-1
	$y_{23} \leftrightarrow (0, \sqrt{3}, \sqrt{3}; 1, 0, 1, 0, 1; 0, 1, 0, 0, 1)$	-1
	$y_{24} \leftrightarrow (0, \sqrt{3}, \sqrt{3}; 1, 0, 1, 0, 1; 0, 1, 0, 1, 0)$	-1
	$y_{25} \leftrightarrow (0, \sqrt{3}, \sqrt{3}; 1, 0, 1, 0, 1; 0, 1, 1, 0, 0)$	-1
	$y_{26} \leftrightarrow (0, \sqrt{3}, \sqrt{3}; 1, 0, 1, 1, 0; 0, 1, 0, 0, 1)$	-1
	$y_{27} \leftrightarrow (0, \sqrt{3}, \sqrt{3}; 1, 0, 1, 1, 0; 0, 1, 0, 1, 0)$	-1
	$y_{28} \leftrightarrow (0, \sqrt{3}, \sqrt{3}; 1, 0, 1, 1, 0; 0, 1, 1, 0, 0)$	-1
	$y_{29} \leftrightarrow (0, \sqrt{3}, \sqrt{3}; 1, 1, 0, 0, 0; 0, 0, 1, 1, 1)$	-1

Table 2.0.22: Admissible pairs $\{x, y_i\}$ for $\sigma_\infty = \tilde{G}_2 \cup \tilde{D}_4 \cup \tilde{D}_4$ (continued)

Appendix B. Admissible pairs

The Lorentzian products $\langle y_i, y_j \rangle$														
	y_4	y_5	y_6	y_7	y_8	y_9	y_{10}	y_{11}	y_{12}	y_{13}	y_{14}	y_{15}	y_{16}	y_{17}
y_1		1	1		1	1	$-\sqrt{3}$			$-\sqrt{3}$	$-\sqrt{3}$	$-\sqrt{3}$		$-\sqrt{3}$
y_2	1		1	1		1	$-\sqrt{3}$		$-\sqrt{3}$		$-\sqrt{3}$		$-\sqrt{3}$	$-\sqrt{3}$
y_3	1	1		1	1		$-\sqrt{3}$	$-\sqrt{3}$				$-\sqrt{3}$	$-\sqrt{3}$	
y_4					1	1	$-\sqrt{3}$	$-\sqrt{3}$	$-\sqrt{3}$				$-\sqrt{3}$	
y_5				1		1	$-\sqrt{3}$	$-\sqrt{3}$		$-\sqrt{3}$		$-\sqrt{3}$		$-\sqrt{3}$
y_6				1	1		$-\sqrt{3}$		$-\sqrt{3}$	$-\sqrt{3}$	$-\sqrt{3}$			
y_7							$-\sqrt{3}$	$-\sqrt{3}$	$-\sqrt{3}$		$-\sqrt{3}$	$-\sqrt{3}$		
y_8							$-\sqrt{3}$	$-\sqrt{3}$		$-\sqrt{3}$	$-\sqrt{3}$		$-\sqrt{3}$	
y_9							$-\sqrt{3}$		$-\sqrt{3}$	$-\sqrt{3}$		$-\sqrt{3}$	$-\sqrt{3}$	$-\sqrt{3}$

	y_{18}	y_{19}	y_{20}	y_{21}	y_{22}	y_{23}	y_{24}	y_{25}	y_{26}	y_{27}	y_{28}	y_{29}
y_1	$-\sqrt{3}$			$-\sqrt{3}$	$-\sqrt{3}$		$-\sqrt{3}$	$-\sqrt{3}$	$-\sqrt{3}$			$-\sqrt{3}$
y_2		$-\sqrt{3}$	$-\sqrt{3}$		$-\sqrt{3}$	$-\sqrt{3}$		$-\sqrt{3}$		$-\sqrt{3}$		$-\sqrt{3}$
y_3	$-\sqrt{3}$	$-\sqrt{3}$	$-\sqrt{3}$	$-\sqrt{3}$		$-\sqrt{3}$	$-\sqrt{3}$				$-\sqrt{3}$	$-\sqrt{3}$
y_4	$-\sqrt{3}$			$-\sqrt{3}$	$-\sqrt{3}$	$-\sqrt{3}$				$-\sqrt{3}$	$-\sqrt{3}$	$-\sqrt{3}$
y_5		$-\sqrt{3}$	$-\sqrt{3}$		$-\sqrt{3}$		$-\sqrt{3}$		$-\sqrt{3}$		$-\sqrt{3}$	$-\sqrt{3}$
y_6	$-\sqrt{3}$	$-\sqrt{3}$	$-\sqrt{3}$	$-\sqrt{3}$				$-\sqrt{3}$	$-\sqrt{3}$	$-\sqrt{3}$		$-\sqrt{3}$
y_7		$-\sqrt{3}$	$-\sqrt{3}$				$-\sqrt{3}$	$-\sqrt{3}$		$-\sqrt{3}$	$-\sqrt{3}$	$-\sqrt{3}$
y_8	$-\sqrt{3}$			$-\sqrt{3}$		$-\sqrt{3}$		$-\sqrt{3}$	$-\sqrt{3}$		$-\sqrt{3}$	$-\sqrt{3}$
y_9					$-\sqrt{3}$	$-\sqrt{3}$	$-\sqrt{3}$		$-\sqrt{3}$	$-\sqrt{3}$		$-\sqrt{3}$

	y_{20}	y_{21}	y_{22}	y_{23}	y_{24}	y_{25}	y_{26}	y_{27}	y_{28}	y_{29}
y_{10}										0
y_{11}									0	
y_{12}								0		
y_{13}							0			
y_{14}						0				
y_{15}					0					
y_{16}			0							
y_{17}			0							
y_{18}		0								
y_{19}	0									

Table 2.0.23: Lorentzian products $\langle y_i, y_j \rangle$ for $\sigma_\infty = \tilde{G}_2 \cup \tilde{D}_4 \cup \tilde{D}_4$

x	y_i	$\langle x, y_i \rangle$																																				
$(0, 0\sqrt{3}; 1, 0, 0; 1, 0, 0, 0, 0, 0, 0)$	$y_1 \leftrightarrow (1, 0, 0; 0, 0, \sqrt{3}; 0, 0, 0, 0, 0, 0, \sqrt{3})$ $y_2 = (1, 0, 0; 0, 0, \sqrt{3}; 0, 0, 0, 0, 0, 0, \sqrt{3}, 0)$ $y_3 = (1, 0, 0; 0, \sqrt{3}, 0; 0, 0, 0, 0, 0, 0, \sqrt{3})$ $y_4 = (1, 0, 0; 0, \sqrt{3}, 0; 0, 0, 0, 0, 0, 0, \sqrt{3}, 0)$ $y_5 = (0, \sqrt{3}, \sqrt{3}; 1, 1, 1; 0, 0, 0, 1, 0, 0, 0)$ $y_6 = (0, 3, 3; \sqrt{3}, \sqrt{3}, \sqrt{3}; \sqrt{3}, 0, 0, 0, 0, \sqrt{3}, \sqrt{3})$																																					
$(0, 0, 3; 1, 0, 0; 1, 0, 0, 0, 0, 0, 0)$	$(1, 0, 0; 0, 0, 1; 0, 0, 0, 0, 0, 0, 1)$ $(1, 0, 0; 0, 0, 1; 0, 0, 0, 0, 0, 1, 0)$ $(1, 0, 0; 0, 1, 0; 0, 0, 0, 0, 0, 0, 1)$ $(1, 0, 0; 0, 1, 0; 0, 0, 0, 0, 0, 1, 0)$ $(\sqrt{3}, 0, 0; 0, 0, \sqrt{3}; \sqrt{3}, 0, 0, 0, 0, 0, 0)$ $(\sqrt{3}, 0, 0; 0, \sqrt{3}, 0; \sqrt{3}, 0, 0, 0, 0, 0, 0)$																																					
The Lorentzian products $\langle y_i, y_j \rangle$																																						
	<table border="1" style="margin-left: auto; margin-right: auto;"> <thead> <tr> <th></th> <th>y_2</th> <th>y_3</th> <th>y_4</th> <th>y_5</th> <th>y_6</th> </tr> </thead> <tbody> <tr> <th>y_1</th> <td></td> <td></td> <td>0</td> <td>$-\sqrt{3}$</td> <td></td> </tr> <tr> <th>y_2</th> <td></td> <td>0</td> <td></td> <td>$-\sqrt{3}$</td> <td></td> </tr> <tr> <th>y_3</th> <td></td> <td></td> <td></td> <td>$-\sqrt{3}$</td> <td></td> </tr> <tr> <th>y_4</th> <td></td> <td></td> <td></td> <td>$-\sqrt{3}$</td> <td></td> </tr> <tr> <th>y_5</th> <td></td> <td></td> <td></td> <td></td> <td>0</td> </tr> </tbody> </table>		y_2	y_3	y_4	y_5	y_6	y_1			0	$-\sqrt{3}$		y_2		0		$-\sqrt{3}$		y_3				$-\sqrt{3}$		y_4				$-\sqrt{3}$		y_5					0	
	y_2	y_3	y_4	y_5	y_6																																	
y_1			0	$-\sqrt{3}$																																		
y_2		0		$-\sqrt{3}$																																		
y_3				$-\sqrt{3}$																																		
y_4				$-\sqrt{3}$																																		
y_5					0																																	

Table 2.0.24: Admissible pairs $\{x, y_i\}$ for $\sigma_\infty = \tilde{G}_2 \cup \tilde{A}_2 \cup \tilde{E}_6$

Appendix B. Admissible pairs

x	y_i	$\langle x, y \rangle$					
$(0, 0, \sqrt{3}; 0, 0, \sqrt{3}; 1, 0, 0, 0, 0, 0, 0)$	$y_1 \leftrightarrow (1, 0, 0; 1, 0, 0; 0, 0, 0, 0, 0, \sqrt{3})$	0					
	$y_2 \leftrightarrow (1, 0, 0; 1, 0, 0; 0, 0, 0, 0, 0, \sqrt{3}, 0)$	0					
	$y_3 \leftrightarrow (\sqrt{3}, 0, 0; \sqrt{3}, 0, 0; 0, 0, 0, 0, 1, 1, 0)$	0					
	$y_4 \leftrightarrow (\sqrt{3}, 0, 0; \sqrt{3}, 0, 0; 0, 1, 0, 0, 0, 0, 1)$	0					
	$y_5 \leftrightarrow (0, \sqrt{3}, \sqrt{3}; \sqrt{3}, 0, 0; 1, 0, 1, 0, 0, 0, 0)$	-1					
	$y_6 \leftrightarrow (\sqrt{3}, 0, 0; 0, \sqrt{3}, \sqrt{3}; 1, 0, 1, 0, 0, 0, 0)$	-1					
$(0, 0, 3; 0, 0, \sqrt{3}; 1, 0, 0, 0, 0, 0, 0)$	$(\sqrt{3}, 0, 0; 1, 0, 0; \sqrt{3}, 0, 0, 0, 0, 0, 0)$	0					
The Lorentzian products $\langle y_i, y_j \rangle$							
		y_2	y_3	y_4	y_5	y_6	
	y_1				$\sqrt{3}$	$\sqrt{3}$	
	y_2				$\sqrt{3}$	$\sqrt{3}$	

Table 2.0.25: Admissible pairs $\{x, y_i\}$ for $\sigma_\infty = \tilde{G}_2 \cup \tilde{G}_2 \cup \tilde{E}_6$

x	y	$\langle x, y \rangle$
$(0, 0, \sqrt{3}; 0, 0, \sqrt{3}; 0, 0, 0, 0, 0, 0, 0, 0, 1)$	$(\sqrt{3}, 0, 0; \sqrt{3}, 0, 0; 0, 1, 0, 0, 0, 0, 0, 0, 0)$	0
	$(0, \sqrt{3}, \sqrt{3}; \sqrt{3}, 0, 0; 0, 0, 0, 0, 0, 0, 0, 1, 1)$	-1
	$(\sqrt{3}, 0, 0; 0, \sqrt{3}, \sqrt{3}; 0, 0, 0, 0, 0, 0, 0, 1, 1)$	-1
$(0, 0, 3; 0, 0, \sqrt{3}; 0, 0, 0, 0, 0, 0, 0, 0, 1)$	$(\sqrt{3}, 0, 0; 1, 0, 0; 0, 0, 0, 0, 0, 0, 0, 0, \sqrt{3})$	0

Table 2.0.26: Admissible pairs $\{x, y\}$ for $\sigma_\infty = \tilde{G}_2 \cup \tilde{G}_2 \cup \tilde{E}_8$

x	y_i	$\langle x, y_i \rangle$	
$a = \sqrt{3}$	$y_1 \leftrightarrow (1, 0, 3; \sqrt{3}, 0, 0, 0, 0, 0, 0, 0, 0; \sqrt{3}, 0, 0, 0, 0, 0, 0, 0, 0)$	0	
	$y_2 \leftrightarrow (\sqrt{3}, 0, 0; 0, 0, 0, 0, 0, 0, 1, 0, 0; 0, 1, 0, 0, 0, 0, 0, 0, 0)$	0	
	$y_3 \leftrightarrow (\sqrt{3}, 0, 0; 0, 1, 0, 0, 0, 0, 0, 0, 0; 0, 0, 0, 0, 0, 0, 1, 0, 0)$	0	
	$y_4 \leftrightarrow (\sqrt{3}, 0, \sqrt{3}; 0, 0, 1, 0, 0, 0, 0, 0, 0; 0, 0, 1, 0, 0, 0, 0, 0, 0)$	0	
	$(\sqrt{3}, \sqrt{3}, \sqrt{3}; 0, 0, 0, 0, 0, 0, 1, 1, 1; 1, 0, 0, 0, 0, 0, 1, 0, 1)$	0	
	$(\sqrt{3}, \sqrt{3}, \sqrt{3}; 0, 1, 0, 0, 0, 0, 0, 1, 1; 0, 1, 0, 0, 0, 0, 0, 0, 1, 1)$	0	
	$(\sqrt{3}, \sqrt{3}, \sqrt{3}; 1, 0, 0, 0, 0, 0, 1, 0, 1; 0, 0, 0, 0, 0, 0, 1, 1, 1)$	0	
	$(0, \sqrt{3}, \sqrt{3}; 0, 0, 0, 0, 0, 0, 0, 1, 1; 0, 0, 0, 0, 0, 0, 1, 0, 0)$	-1	
	$(0, \sqrt{3}, \sqrt{3}; 0, 0, 0, 0, 0, 0, 1, 0, 0; 0, 0, 0, 0, 0, 0, 0, 0, 1, 1)$	-1	
	$(0, \sqrt{3}, \sqrt{3}; 1, 0, 0, 0, 0, 0, 0, 0, 1; 1, 0, 0, 0, 0, 0, 0, 0, 0, 1)$	-1	
	$(\sqrt{3}, \sqrt{3}, 0; 1, 0, 0, 0, 0, 0, 0, 1, 1; 1, 0, 0, 0, 0, 0, 0, 0, 1, 1)$	-1	
	$(\sqrt{3}, \sqrt{3}, \sqrt{3}; 0, 0, 0, 0, 0, 0, 1, 1, 1; 0, 0, 0, 1, 0, 0, 0, 0, 0, 0)$	-1	
	$(\sqrt{3}, \sqrt{3}, \sqrt{3}; 0, 0, 0, 0, 0, 0, 1, 0, 1, 0; 0, 0, 0, 0, 0, 0, 1, 0, 1, 0)$	-1	
	$(\sqrt{3}, \sqrt{3}, \sqrt{3}; 0, 0, 0, 0, 0, 0, 1, 0, 1, 0; 1, 1, 0, 0, 0, 0, 0, 0, 0, 1)$	-1	
	$(\sqrt{3}, \sqrt{3}, \sqrt{3}; 0, 0, 0, 0, 1, 0, 0, 0, 0, 1; 0, 0, 1, 0, 0, 0, 0, 0, 1, 0)$	-1	
	$(\sqrt{3}, \sqrt{3}, \sqrt{3}; 0, 0, 0, 1, 0, 0, 0, 0, 0, 0; 0, 0, 0, 0, 0, 0, 0, 1, 1, 1)$	-1	
	$(\sqrt{3}, \sqrt{3}, \sqrt{3}; 0, 0, 1, 0, 0, 0, 0, 1, 0; 0, 0, 0, 0, 0, 1, 0, 0, 0, 0, 1)$	-1	
	$(\sqrt{3}, \sqrt{3}, \sqrt{3}; 0, 1, 0, 0, 0, 0, 0, 1, 1; 1, 0, 0, 0, 0, 0, 1, 0, 0, 0, 0)$	-1	
	$(\sqrt{3}, \sqrt{3}, \sqrt{3}; 0, 1, 0, 0, 0, 0, 0, 1, 0, 0; 1, 0, 0, 0, 0, 0, 0, 1, 0, 0, 1)$	-1	
	$(\sqrt{3}, \sqrt{3}, \sqrt{3}; 1, 0, 0, 0, 0, 0, 0, 1, 0, 1; 0, 1, 0, 0, 0, 0, 0, 1, 0, 0, 0)$	-1	
	$(\sqrt{3}, \sqrt{3}, \sqrt{3}; 1, 0, 0, 0, 0, 0, 1, 0, 0, 0; 0, 1, 0, 0, 0, 0, 0, 0, 1, 1, 1)$	-1	
	$(\sqrt{3}, \sqrt{3}, \sqrt{3}; 1, 1, 0, 0, 0, 0, 0, 0, 0, 1; 0, 0, 0, 0, 0, 0, 1, 0, 1, 0, 0)$	-1	
	$(\sqrt{3}, \sqrt{3}, \sqrt{3}; 1, 1, 0, 0, 0, 0, 0, 0, 0, 1; 1, 1, 0, 0, 0, 0, 0, 0, 0, 0, 1)$	-1	
	$(1, 3, 3; 0, 0, 0, 0, 0, 0, \sqrt{3}, 0, \sqrt{3}; \sqrt{3}, 0, 0, 0, 0, 0, 0, 0, \sqrt{3}, 0)$	$-\sqrt{3}$	
$(1, 3, 3; 0, \sqrt{3}, 0, 0, 0, 0, 0, 0, \sqrt{3}; 0, \sqrt{3}, 0, 0, 0, 0, 0, 0, 0, \sqrt{3})$	$-\sqrt{3}$		
$(1, 3, 3; \sqrt{3}, 0, 0, 0, 0, 0, 0, \sqrt{3}, 0; 0, 0, 0, 0, 0, 0, \sqrt{3}, 0, \sqrt{3})$	$-\sqrt{3}$		
$a = 3$	$(1, 0, 3; 1, 0, 0, 0, 0, 0, 0, 0, 0; 1, 0, 0, 0, 0, 0, 0, 0, 0)$	0	
The Lorentzian products $\langle y_i, y_j \rangle$			
	y_2	y_3	y_4
y_1	$-\sqrt{3}$	$-\sqrt{3}$	0
y_2		0	0
y_3			0

Table 2.0.27: Admissible pairs $\{x, y_i\}$ for $\sigma_\infty = \tilde{G}_2 \cup \tilde{E}_8 \cup \tilde{E}_8$ and where $x \leftrightarrow (0, 0, a; 0, 0, 0, 0, 0, 0, 0, 0, 0, 1; 0, 0, 0, 0, 0, 0, 0, 0, 0, 1)$

APPENDIX C

NORMAL VECTORS AND VINBERG FORM

In this appendix, we provide the normal vectors of the ADEG-polyhedron P_\star and the ADE-polyhedron P_2 in \mathbb{H}^9 . For the proof of Corollary 4.3.1, we construct the Vinberg forms of their associated Coxeter groups. Very useful in this context is the material with the worked examples as presented in [32, 33]. We start by a short description of the procedure.

◇ Establishing the Vinberg form

Let $\Gamma(P)$ be a hyperbolic Coxeter group of rank N .

Let e_1, \dots, e_N be the unit outer normal vectors of its Coxeter polyhedron $P \subset \mathbb{H}^n$. For $G = (g_{ij})_{i,j}$ its Gram matrix, consider all cycles of $2G$, that is,

$$c_{i_1 i_2 \dots i_k} = 2^k g_{i_1 i_2} \cdots g_{i_{k-1} i_k} g_{i_k i_1} \quad \text{for } i_1, \dots, i_k \in \{1, \dots, N\}, \quad k \geq 2;$$

see Definition 1.3.19. The field of definition K of Γ is the field $\mathbb{Q}(\{c_{i_1 i_2 \dots i_k}\})$ of all cycles of $2G$.

Define the vectors

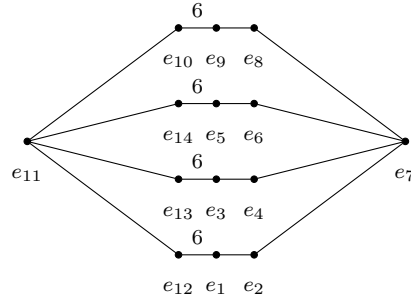
$$v_1 := 2e_1 \quad \text{and} \quad v_{i_1 i_2 \dots i_k} := 2^k g_{i_1 i_2} \cdots g_{i_{k-1} i_k} e_{i_k} \tag{C.1}$$

by multiplication of the vectors e_1, \dots, e_N with partial cycles. Then, the K -vector space V spanned by the vectors $v_{i_1 i_2 \dots i_k}$ has dimension $n + 1$, and the restriction of the Lorentzian product on V yields a quadratic form q of signature $(n, 1)$, called the *Vinberg form* of Γ .

Next, we apply this procedure for the arithmetic groups Γ_\star and $\Gamma(P_2)$, where the field $K = \mathbb{Q}$; see Theorem 1.3.20.

◇ For the Coxeter polyhedron P_\star

We give below the Coxeter diagram of $P_\star \subset \mathbb{H}^9$ where the nodes are indexed by its unit outer normal vectors.



The vectors $e_1, \dots, e_{14} \in \mathbb{R}^{10}$ and their Gram matrix G_\star are given as follows.

$$\begin{aligned}
e_1 &= (1, 0, 0, 0, 0, 0, 0, 0, 0, 0) \\
e_2 &= \left(-\frac{1}{2}, \frac{\sqrt{3}}{2}, 0, 0, 0, 0, 0, 0, 0, 0\right) \\
e_3 &= (0, 0, 1, 0, 0, 0, 0, 0, 0, 0) \\
e_4 &= \left(0, 0, -\frac{1}{2}, \frac{\sqrt{3}}{2}, 0, 0, 0, 0, 0, 0\right) \\
e_5 &= (0, 0, 0, 0, 1, 0, 0, 0, 0, 0) \\
e_6 &= \left(0, 0, 0, 0, -\frac{1}{2}, \frac{\sqrt{3}}{2}, 0, 0, 0, 0\right) \\
e_7 &= \left(0, -\frac{1}{\sqrt{3}}, 0, -\frac{1}{\sqrt{3}}, 0, -\frac{1}{\sqrt{3}}, 0, 0, -1, 1\right) \\
e_8 &= \left(0, 0, 0, 0, 0, 0, \frac{1}{2}, 0, 1, -\frac{1}{2}\right) \\
e_9 &= (0, 0, 0, 0, 0, 0, 0, -1, -1, 1) \\
e_{10} &= \left(0, 0, 0, 0, 0, -\frac{1}{2}, \frac{\sqrt{3}}{2}, \frac{1}{2}, -\frac{1}{2}\right) \\
e_{11} &= (0, 0, 0, 0, 0, 0, 1, 0, -1, 1) \\
e_{12} &= \left(-\frac{\sqrt{3}}{2}, -\frac{1}{2}, 0, 0, 0, 0, \frac{-3+\sqrt{3}}{6}, -\frac{1}{2\sqrt{3}}, \frac{3-2\sqrt{3}}{6}, \frac{-1+\sqrt{3}}{2}\right) \\
e_{13} &= \left(0, 0, -\frac{\sqrt{3}}{2}, -\frac{1}{2}, 0, 0, \frac{-3+\sqrt{3}}{6}, -\frac{1}{2\sqrt{3}}, \frac{3-2\sqrt{3}}{6}, \frac{-1+\sqrt{3}}{2}\right) \\
e_{14} &= \left(0, 0, 0, 0, -\frac{\sqrt{3}}{2}, -\frac{1}{2}, \frac{-3+\sqrt{3}}{6}, -\frac{1}{2\sqrt{3}}, \frac{3-2\sqrt{3}}{6}, \frac{-1+\sqrt{3}}{2}\right)
\end{aligned}$$

$$\begin{bmatrix}
1 & -1/2 & 0 & 0 & 0 & 0 & 0 & 0 & 0 & 0 & 0 & -\sqrt{3}/2 & 0 & 0 \\
-1/2 & 1 & 0 & 0 & 0 & 0 & -1/2 & 0 & 0 & 0 & 0 & 0 & 0 & 0 \\
0 & 0 & 1 & -1/2 & 0 & 0 & 0 & 0 & 0 & 0 & 0 & 0 & -\sqrt{3}/2 & 0 \\
0 & 0 & -1/2 & 1 & 0 & 0 & -1/2 & 0 & 0 & 0 & 0 & 0 & 0 & 0 \\
0 & 0 & 0 & 0 & 1 & -1/2 & 0 & 0 & 0 & 0 & 0 & 0 & 0 & -\sqrt{3}/2 \\
0 & 0 & 0 & 0 & -1/2 & 1 & -1/2 & 0 & 0 & 0 & 0 & 0 & 0 & 0 \\
0 & -1/2 & 0 & -1/2 & 0 & -1/2 & 1 & -1/2 & 0 & 0 & 0 & 0 & 0 & 0 \\
0 & 0 & 0 & 0 & 0 & 0 & -1/2 & 1 & -1/2 & 0 & 0 & 0 & 0 & 0 \\
0 & 0 & 0 & 0 & 0 & 0 & 0 & -1/2 & 1 & -\sqrt{3}/2 & 0 & 0 & 0 & 0 \\
0 & 0 & 0 & 0 & 0 & 0 & 0 & 0 & -\sqrt{3}/2 & 1 & -1/2 & 0 & 0 & 0 \\
0 & 0 & 0 & 0 & 0 & 0 & 0 & 0 & 0 & -1/2 & 1 & -1/2 & -1/2 & -1/2 \\
-\sqrt{3}/2 & 0 & 0 & 0 & 0 & 0 & 0 & 0 & 0 & 0 & -1/2 & 1 & 0 & 0 \\
0 & 0 & -\sqrt{3}/2 & 0 & 0 & 0 & 0 & 0 & 0 & 0 & -1/2 & 0 & 1 & 0 \\
0 & 0 & 0 & 0 & -\sqrt{3}/2 & 0 & 0 & 0 & 0 & 0 & -1/2 & 0 & 0 & 1
\end{bmatrix}$$

Appendix C. Normal vectors and Vinberg form

Let $V(\Gamma_\star)$ be the \mathbb{Q} -vector space of dimension 10 spanned by the vectors as given by (C.1). The following vectors form a basis of $V(\Gamma_\star)$.

$$\begin{aligned}
v_1 &= 2 \cdot e_1 = (2, 0, 0, 0, 0, 0, 0, 0, 0, 0) \\
v_2 &= 2^2 g_{11} g_{12} \cdot e_2 = (1, -\sqrt{3}, 0, 0, 0, 0, 0, 0, 0, 0) \\
v_3 &= 2^3 g_{11} g_{12} g_{27} \cdot e_7 = (0, -\frac{2}{\sqrt{3}}, 0, -\frac{2}{\sqrt{3}}, 0, -\frac{2}{\sqrt{3}}, 0, 0, -2, 2) \\
v_4 &= 2^4 g_{11} g_{12} g_{27} g_{74} \cdot e_4 = (0, 0, 1, -\sqrt{3}, 0, 0, 0, 0, 0, 0) \\
v_5 &= 2^6 g_{11} g_{12} g_{27} g_{74} g_{43} g_{3,13} \cdot e_{13} = (0, 0, 3, \sqrt{3}, 0, 0, \frac{3-\sqrt{3}}{\sqrt{3}}, 1, \frac{-3+2\sqrt{3}}{\sqrt{3}}, \sqrt{3}-3) \\
v_6 &= 2^7 g_{11} g_{12} g_{27} g_{74} g_{43} g_{3,13} g_{13,11} \cdot e_{11} = (0, 0, 0, 0, 0, 0, 2\sqrt{3}, 0, -2\sqrt{3}, 2\sqrt{3}) \\
v_7 &= 2^8 g_{11} g_{12} g_{27} g_{74} g_{43} g_{3,13} g_{13,11} g_{11,12} \cdot e_{12} = (0, 0, 0, 0, 0, 0, -1, 0, -2, 1) \\
v_8 &= 2^4 g_{11} g_{12} g_{27} g_{78} \cdot e_8 = (0, 0, 0, 0, 1, -\sqrt{3}, 0, 0, 0, 0) \\
v_9 &= 2^5 g_{11} g_{12} g_{27} g_{78} g_{89} \cdot e_9 = (0, 0, 0, 0, 0, 0, -2, -2, 2, 2) \\
v_{10} &= 2^4 g_{11} g_{12} g_{27} g_{76} \cdot e_6 = (3, \sqrt{3}, 0, 0, 0, 0, \frac{3-\sqrt{3}}{\sqrt{3}}, 1, \frac{3-2\sqrt{3}}{\sqrt{3}}, -3+\sqrt{3})
\end{aligned}$$

Therefore, the matrix representing the Vinberg form q_\star of Γ_\star is as follows.

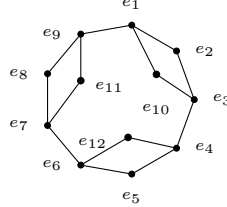
$$\langle \langle v_i, v_j \rangle \rangle_{ij} = \begin{bmatrix} 4 & 2 & 0 & 0 & 0 & 0 & 0 & 0 & 0 & 6 \\ 2 & 4 & 2 & 0 & 0 & 0 & 0 & 0 & 0 & 0 \\ 0 & 2 & 4 & 2 & 0 & 0 & 2 & 2 & 0 & 0 \\ 0 & 0 & 2 & 4 & 0 & 0 & 0 & 0 & 0 & 0 \\ 0 & 0 & 0 & 0 & 12 & 6 & 0 & 0 & 0 & 0 \\ 0 & 0 & 0 & 0 & 6 & 12 & 0 & 0 & 0 & 6 \\ 0 & 0 & 2 & 0 & 0 & 0 & 4 & 0 & 2 & 0 \\ 0 & 0 & 2 & 0 & 0 & 0 & 0 & 4 & 0 & 0 \\ 0 & 0 & 0 & 0 & 0 & 0 & 2 & 0 & 4 & 0 \\ 6 & 0 & 0 & 0 & 0 & 6 & 0 & 0 & 0 & 12 \end{bmatrix}$$

With the help of Mathematica [85], we derive that the diagonal form of q_\star is given by

$$\langle 1, 1, 2, 3, 3, 6, 6, 10, 10, -2 \rangle .$$

◇ For the Coxeter polyhedron P_2

We give below the Coxeter diagram of $P_2 \subset \mathbb{H}^9$ where the nodes are indexed by its outer normal vectors.



The vectors $e_1, \dots, e_{12} \in \mathbb{R}^{10}$ and their Gram matrix are given as follows.

$$\begin{aligned}
e_1 &= (1, 0, 0, 0, 0, 0, 0, 0, 0, 0) \\
e_2 &= \left(-\frac{1}{2}, \frac{\sqrt{3}}{2}, 0, 0, 0, 0, 0, 0, 0, 0\right) \\
e_3 &= \left(0, -\frac{1}{\sqrt{3}}, 0, 0, 0, 0, 0, 0, -\frac{\sqrt{2}}{\sqrt{3}}, 0\right) \\
e_4 &= \left(0, 0, 0, 0, 0, 0, 0, -\frac{\sqrt{5}}{2\sqrt{2}}, \frac{\sqrt{3}}{2\sqrt{2}}, 0\right) \\
e_5 &= \left(0, 0, 1, 0, 0, 0, -\frac{\sqrt{3}}{\sqrt{5}}, \frac{\sqrt{2}}{\sqrt{5}}, 0, 1\right) \\
e_6 &= \left(0, 0, 1, 0, 0, -\frac{\sqrt{7}}{2\sqrt{3}}, \frac{\sqrt{5}}{2\sqrt{3}}, 0, 0, 1\right) \\
e_7 &= \left(0, 0, 1, 0, -\frac{2}{\sqrt{7}}, \frac{\sqrt{3}}{\sqrt{7}}, 0, 0, 0, 1\right) \\
e_8 &= \left(0, 0, 0, -\frac{3}{4}, \frac{\sqrt{7}}{4}, 0, 0, 0, 0, 0\right) \\
e_9 &= \left(-\frac{1}{2}, -\frac{1}{2\sqrt{3}}, 0, \frac{3}{4}, \frac{1}{4\sqrt{7}}, \frac{1}{2\sqrt{21}}, \frac{1}{2\sqrt{15}}, \frac{1}{2\sqrt{10}}, \frac{1}{2\sqrt{6}}, 0\right) \\
e_{10} &= \left(-\frac{1}{2}, -\frac{1}{2\sqrt{3}}, \frac{16}{6}, -\frac{2}{3}, -\frac{2}{\sqrt{7}}, -\frac{5}{3\sqrt{21}}, \frac{1}{3\sqrt{15}}, \frac{\sqrt{2}}{\sqrt{5}}, \frac{\sqrt{2}}{\sqrt{3}}, \frac{5}{2}\right) \\
e_{11} &= \left(0, 0, -\frac{5}{6}, -\frac{1}{6}, -\frac{1}{2\sqrt{7}}, \frac{4}{3\sqrt{21}}, \frac{1}{3\sqrt{15}}, \frac{\sqrt{2}}{\sqrt{5}}, 0, -\frac{1}{2}\right) \\
e_{12} &= \left(0, 0, \frac{1}{6}, -\frac{5}{12}, -\frac{5}{4\sqrt{7}}, -\frac{11}{3\sqrt{21}}, -\frac{\sqrt{5}}{3\sqrt{3}}, 0, 0, \frac{1}{2}\right)
\end{aligned}$$

$$\begin{bmatrix}
1 & -1/2 & 0 & 0 & 0 & 0 & 0 & 0 & -1/2 & -1/2 & 0 & 0 \\
-1/2 & 1 & -1/2 & 0 & 0 & 0 & 0 & 0 & 0 & 0 & 0 & 0 \\
0 & -1/2 & 1 & -1/2 & 0 & 0 & 0 & 0 & 0 & -1/2 & 0 & 0 \\
0 & 0 & -1/2 & 1 & -1/2 & 0 & 0 & 0 & 0 & 0 & -1/2 & 0 \\
0 & 0 & 0 & -1/2 & 1 & -1/2 & 0 & 0 & 0 & 0 & 0 & 0 \\
0 & 0 & 0 & 0 & -1/2 & 1 & -1/2 & 0 & 0 & 0 & -1/2 & 0 \\
0 & 0 & 0 & 0 & 0 & -1/2 & 1 & -1/2 & 0 & 0 & 0 & -1/2 \\
0 & 0 & 0 & 0 & 0 & 0 & -1/2 & 1 & -1/2 & 0 & 0 & 0 \\
-1/2 & 0 & 0 & 0 & 0 & 0 & 0 & -1/2 & 1 & 0 & 0 & -1/2 \\
-1/2 & 0 & -1/2 & 0 & 0 & 0 & 0 & 0 & 0 & 1 & 0 & 0 \\
0 & 0 & 0 & -1/2 & 0 & -1/2 & 0 & 0 & 0 & 0 & 1 & 0 \\
0 & 0 & 0 & 0 & 0 & 0 & -1/2 & 0 & -1/2 & 0 & 0 & 1
\end{bmatrix}$$

Appendix C. Normal vectors and Vinberg form

Let $V(\Gamma(P_2))$ be the \mathbb{Q} -vector space of dimension 10 spanned by the vectors as given by (C.1). The following vectors form a basis of $V(\Gamma(P_2))$.

$$\begin{aligned}
 v_1 &= (2, 0, 0, 0, 0, 0, 0, 0, 0, 0) \\
 v_2 &= (1, -\sqrt{3}, 0, 0, 0, 0, 0, 0, 0, 0) \\
 v_3 &= (0, -\frac{2}{\sqrt{3}}, 0, 0, 0, 0, 0, 0, -2\frac{\sqrt{2}}{\sqrt{3}}, 0) \\
 v_4 &= (0, 0, 0, 0, 0, 0, \frac{\sqrt{5}}{\sqrt{2}}, -\frac{\sqrt{3}}{\sqrt{2}}, 0) \\
 v_5 &= (0, 0, 2, 0, 0, 0, -2\frac{\sqrt{3}}{\sqrt{5}}, \frac{2\sqrt{2}}{\sqrt{5}}, 0, 2) \\
 v_6 &= (0, 0, -2, 0, 0, \frac{\sqrt{7}}{\sqrt{3}}, -\frac{\sqrt{5}}{\sqrt{3}}, 0, 0, -2) \\
 v_7 &= (0, 0, 2, 0, -\frac{4}{\sqrt{3}}, 2\frac{\sqrt{3}}{\sqrt{7}}, 0, 0, 0, 2) \\
 v_8 &= (0, 0, 0, \frac{3}{2}, -\frac{7}{2}, 0, 0, 0, 0, 0) \\
 v_9 &= (1, \frac{1}{\sqrt{3}}, -\frac{13}{3}, \frac{4}{3}, \frac{4}{\sqrt{7}}, \frac{10}{3\sqrt{21}}, -\frac{2}{3\sqrt{15}}, -2\frac{\sqrt{2}}{\sqrt{5}}, -2\frac{\sqrt{2}}{\sqrt{3}}, -5) \\
 v_{10} &= (-1, -\frac{1}{\sqrt{3}}, 0, \frac{3}{2}, \frac{1}{2\sqrt{7}}, \frac{1}{\sqrt{21}}, \frac{1}{\sqrt{15}}, \frac{1}{\sqrt{10}}, \frac{1}{\sqrt{6}}, 0)
 \end{aligned}$$

The matrix representing the Vinberg form q_2 of $\Gamma(P_2)$ is given below.

$$(\langle v_i, v_j \rangle)_{ij} = \begin{bmatrix} 4 & 2 & 0 & 0 & 0 & 0 & 0 & 0 & 2 & -2 \\ 2 & 4 & 2 & 0 & 0 & 0 & 0 & 0 & 0 & 0 \\ 0 & 2 & 4 & 2 & 0 & 0 & 0 & 0 & 2 & 0 \\ 0 & 0 & 2 & 4 & 2 & 0 & 0 & 0 & 0 & 0 \\ 0 & 0 & 0 & 2 & 4 & 2 & 0 & 0 & 0 & 0 \\ 0 & 0 & 0 & 0 & 2 & 4 & 2 & 0 & 0 & 0 \\ 0 & 0 & 0 & 0 & 0 & 2 & 4 & 2 & 0 & 0 \\ 0 & 0 & 0 & 0 & 0 & 0 & 2 & 4 & 0 & 2 \\ 2 & 0 & 2 & 0 & 0 & 0 & 0 & 0 & 4 & 0 \\ -2 & 0 & 0 & 0 & 0 & 6 & 0 & 2 & 0 & 4 \end{bmatrix}$$

With the help of Mathematica [85], we derive that the diagonal form of q_2 is given by

$$\langle 1, 1, 3, 6, 7, 10, 10, 15, 21, -10 \rangle .$$

APPENDIX D

THE TWO REPRINTS

This appendix consists of reprints of the following two articles.

- N. Bredon, R. Kellerhals, *Hyperbolic Coxeter groups and minimal growth rates in dimensions four and five*, Groups Geom. Dyn. 16 (2022), 725–741.
- N. Bredon, *Hyperbolic Coxeter groups of minimal growth rates in higher dimensions*, Canad. Math. Bull. 66 (2023), 232–242.

Hyperbolic Coxeter groups and minimal growth rates in dimensions four and five

Naomi Bredon and Ruth Kellerhals

Abstract. For small n , the known compact hyperbolic n -orbifolds of minimal volume are intimately related to Coxeter groups of smallest rank. For $n = 2$ and 3 , these Coxeter groups are given by the triangle group $[7, 3]$ and the tetrahedral group $[3, 5, 3]$, and they are also distinguished by the fact that they have minimal growth rate among *all* cocompact hyperbolic Coxeter groups in $\text{Isom } \mathbb{H}^n$, respectively. In this work, we consider the cocompact Coxeter simplex group G_4 with Coxeter symbol $[5, 3, 3, 3]$ in $\text{Isom } \mathbb{H}^4$ and the cocompact Coxeter prism group G_5 based on $[5, 3, 3, 3, 3]$ in $\text{Isom } \mathbb{H}^5$. Both groups are arithmetic and related to the fundamental group of the minimal volume arithmetic compact hyperbolic n -orbifold for $n = 4$ and 5 , respectively. Here, we prove that the group G_n is distinguished by having smallest growth rate among all Coxeter groups acting cocompactly on \mathbb{H}^n for $n = 4$ and 5 , respectively. The proof is based on combinatorial properties of compact hyperbolic Coxeter polyhedra, some partial classification results and certain monotonicity properties of growth rates of the associated Coxeter groups.

In memoriam Ernest B. Vinberg

1. Introduction

Let \mathbb{H}^n denote the real hyperbolic n -space and $\text{Isom } \mathbb{H}^n$ its isometry group. A hyperbolic Coxeter group $G \subset \text{Isom } \mathbb{H}^n$ of rank N is a cofinite discrete group generated by N reflections with respect to hyperplanes in \mathbb{H}^n . Such a group corresponds to a finite volume Coxeter polyhedron $P \subset \mathbb{H}^n$ with N facets, which in turn is a convex polyhedron all of whose dihedral angles are of the form $\frac{\pi}{k}$ for an integer $k \geq 2$. Hyperbolic Coxeter groups are geometric realisations of abstract Coxeter systems (W, S) consisting of a group W with a finite set S of generators satisfying the relations $s^2 = 1$ and $(ss')^{m_{ss'}} = 1$ where $m_{ss'} = m_{s's} \in \{2, 3, \dots, \infty\}$ for $s \neq s'$. For small rank N , the group W is characterised most conveniently by its Coxeter symbol or its Coxeter graph.

Hyperbolic Coxeter groups are not only characterised by a simple presentation but they are also distinguished in other ways. For example, for small n , they appear as fundamental groups of smallest volume orbifolds $O^n = \mathbb{H}^n / \Gamma$ where $\Gamma \subset \text{Isom } \mathbb{H}^n$ is a discrete subgroup; see, e.g., [1, 2, 7, 15, 20, 27]. In particular, for $n = 2$ and 3 , the compact

hyperbolic n -orbifold of minimal volume is the quotient of \mathbb{H}^n by a Coxeter group of smallest rank and given by the triangle group $[7, 3]$ and the \mathbb{Z}_2 -extension of the tetrahedral group $[3, 5, 3]$. For $n = 4$ and 5 , and by restricting to the arithmetic context, the compact hyperbolic n -orbifold of minimal volume is the quotient of \mathbb{H}^n by the 4-simplex group $[5, 3, 3, 3]$ and by the Coxeter 5-prism group based on $[5, 3, 3, 3, 3]$, respectively.

In parallel to volume we are interested in the spectrum of small growth rates of hyperbolic Coxeter groups $G = (W, S)$. In general, the growth series $f_S(t)$ of a Coxeter system (W, S) is given by

$$f_S(t) = 1 + \sum_{k \geq 1} a_k t^k,$$

where $a_k \in \mathbb{Z}$ is the number of elements $w \in W$ with S -length k . The series $f_S(t)$ can be computed by Steinberg's formula

$$\frac{1}{f_S(t^{-1})} = \sum_{\substack{W_T < W \\ |W_T| < \infty}} \frac{(-1)^{|T|}}{f_T(t)},$$

where $W_T, T \subset S$, is a finite Coxeter subgroup of W , and where $W_\emptyset = \{1\}$. In particular, $f_S(t)$ is a rational function that can be expressed as the quotient of coprime monic polynomials $p(t), q(t) \in \mathbb{Z}[t]$ of equal degree. For cocompact hyperbolic Coxeter groups, the series $f_S(t)$ is infinite and has radius of convergence $R < 1$ which can be identified with the real algebraic integer given by the smallest positive root of the denominator polynomial $q(t)$. The growth rate $\tau_G = \tau_{(W,S)}$ is defined by

$$\tau_G = \limsup_{k \rightarrow \infty} \sqrt[k]{a_k},$$

and τ_G coincides with the inverse of the radius of convergence R of $f_S(t)$. In contrast to the finite and affine cases, hyperbolic Coxeter groups are of exponential growth.

In [16] and [21], it is shown that the triangle group $[7, 3]$ and the tetrahedral group $[3, 5, 3]$ have minimal growth rate among *all* cocompact hyperbolic Coxeter groups in $\text{Isom } \mathbb{H}^n$ for $n = 2$ and 3 , respectively. These results have an interesting number theoretical component since the growth rate τ of any Coxeter group acting cocompactly on \mathbb{H}^n for $n = 2$ and 3 is either a quadratic unit or a Salem number, that is, τ is a real algebraic integer $\alpha > 1$ whose inverse is a conjugate of α , and all other conjugates lie on the unit circle. In particular, the growth rate $\tau_{[7,3]}$ equals the smallest known Salem number, and it is given by Lehmer's number $\alpha_L \approx 1.17628$ with minimal polynomial

$$L(t) = t^{10} + t^9 - t^7 - t^6 - t^5 - t^4 - t^3 + t + 1.$$

The constant α_L plays an important role in the strong version of Lehmer's problem about a universal lower bound for Mahler measures of non-zero non-cyclotomic irreducible integer polynomials; see [32].

The proof in [21] of the two results above is based on the fact that for $n = 2$ and 3 the rational function $f_S(t)$ comes with an explicit formula in terms of the exponents of the Coxeter group $G = (W, S) \subset \text{Isom } \mathbb{H}^n$.

For dimensions $n \geq 4$, however, there are only a few structural results, and closed formulas for growth functions do not exist in general. In this work, we establish the following results for $n = 4$ and 5 by developing a new proof strategy.

Theorem A. *Among all Coxeter groups acting cocompactly on \mathbb{H}^4 , the Coxeter simplex group $[5, 3, 3, 3]$ has minimal growth rate, and as such it is unique.*

The cocompact Coxeter prism group based on $[5, 3, 3, 3, 3]$ in $\text{Isom } \mathbb{H}^5$ was first discovered by Makarov [26] and arises as the discrete group generated by the reflections in the compact straight Coxeter prism M with base $[5, 3, 3, 3]$. More concretely, the prism M is the truncation of the (infinite volume) Coxeter 5-simplex $[5, 3, 3, 3, 3]$ by means of the polar hyperplane associated to its ultra-ideal vertex characterised by the vertex simplex $[5, 3, 3, 3]$. Our second result can be stated as follows.

Theorem B. *Among all Coxeter groups acting cocompactly on \mathbb{H}^5 , the Coxeter prism group based on $[5, 3, 3, 3, 3]$ has minimal growth rate, and as such it is unique.*

The work is organised as follows.

In Section 2.1, we provide the necessary background about hyperbolic Coxeter polyhedra, their reflection groups and the characterisation by means of the Vinberg graph and the Gram matrix. We present the relevant classification results for families of Coxeter polyhedra with few facets due to Esselmann, Kaplinskaja and Tumarkin. Of particular importance is the structural result, presented in Theorem 1 and due to Felikson and Tumarkin, about the existence of non-intersecting facets of a compact Coxeter polyhedron.

In Section 2.2, we consider abstract Coxeter systems with their Coxeter graphs and Coxeter symbols and introduce the notions of growth series and growth rates. Another important ingredient is the growth monotonicity result of Terragni as given in Theorem 2.

The proofs of our results are presented in Section 3. The proof of Theorem A is based on a simple growth rate comparison argument and serves as an inspiration how to attack the proof of Theorem B. To this end, we establish Lemma 1 and Lemma 2 about the comparison of growth rates of certain Coxeter groups of rank 4. Then, we consider compact Coxeter polyhedra in \mathbb{H}^5 in terms of the number $N \geq 6$ of their facets. Since compact hyperbolic Coxeter n -simplices exist only for $n \leq 4$, we look at compact Coxeter polyhedra $P \subset \mathbb{H}^5$ with $N = 7$, $N = 8$ and $N \geq 9$ facets, respectively. Certain classification results help us dealing with the cases $N = 7$ and 8 while for $N \geq 9$, we look for particular subgraphs in the Coxeter graph of P and conclude by means of Lemma 1, Lemma 2 and Theorem 2.

2. Hyperbolic Coxeter polyhedra and growth rates

2.1. Hyperbolic Coxeter polyhedra and their reflection groups

Denote by \mathbb{H}^n the standard hyperbolic n -space realised by the upper sheet of the hyperboloid in \mathbb{R}^{n+1} according to

$$\mathbb{H}^n = \{x \in \mathbb{R}^{n+1} \mid q_{n,1}(x) = x_1^2 + \dots + x_n^2 - x_{n+1}^2 = -1, x_{n+1} > 0\}.$$

A hyperbolic hyperplane H is the intersection of a vector subspace of dimension n with \mathbb{H}^n and can be represented as the Lorentz-orthogonal complement $H = e^\perp$ by means of a vector e of (normalised) Lorentzian norm $q_{n,1}(e) = 1$. The isometry group $\text{Isom } \mathbb{H}^n$ of \mathbb{H}^n is given by the group $O^+(n, 1)$ of positive Lorentzian matrices leaving the bilinear form $\langle x, y \rangle_{n,1}$ associated to $q_{n,1}$ and the upper sheet invariant. It is well known that $O^+(n, 1)$ is generated by linear reflections $r = r_H : x \mapsto x - 2 \langle e, x \rangle_{n,1} e$ with respect to hyperplanes $H = e^\perp$; see [3, Section A.2].

A hyperbolic n -polyhedron $P \subset \mathbb{H}^n$ is the non-empty intersection of a finite number $N \geq n + 1$ of half-spaces H_i^- bounded by hyperplanes H_i all of whose normal unit vectors e_i are directed outwards with respect to P , say. A facet of P is the intersection of P with one of the hyperplanes H_i , $1 \leq i \leq N$. A polyhedron is a *Coxeter polyhedron* if all of its dihedral angles are of the form $\frac{\pi}{k}$ for an integer $k \geq 2$.

In this work, we suppose that P is a *compact* hyperbolic Coxeter polyhedron so that P is the convex hull of finitely many points in \mathbb{H}^n . In particular, P is *simple* since all dihedral angles of P are less than or equal to $\frac{\pi}{2}$. As a consequence, each vertex p of P is the intersection of n hyperplanes bounding P and characterised by a vertex neighbourhood which is a cone over a spherical Coxeter $(n - 1)$ -simplex.

The following structural result of A. Felikson and P. Tumarkin [10, Theorem A] will be of importance later in this work. For its statement, the compact Coxeter polyhedra in \mathbb{H}^4 that are products of two simplices of dimensions greater than 1 will play a certain role. There are seven such polyhedra which were discovered by F. Esselmann [8]; see also [9] and Examples 2, 4 and 10 below.

Theorem 1. *Let $P \subset \mathbb{H}^n$ be a compact Coxeter polyhedron. If $n \leq 4$ and all facets of P are mutually intersecting, then P is either a simplex or one of the seven Esselmann polyhedra. If $n > 4$, then P has a pair of non-intersecting facets.*

Fix a compact Coxeter polyhedron $P \subset \mathbb{H}^n$ with its bounding hyperplanes H_1, \dots, H_N as above. Denote by G the group generated by the reflections $r_i = r_{H_i}$, $1 \leq i \leq N$. Then, G is a cocompact discrete subgroup of $\text{Isom } \mathbb{H}^n$ with P equal to the closure of a fundamental domain for G . The group G is called a (*cocompact*) *hyperbolic Coxeter group*. It follows that G is finitely presented with natural generating set $S = \{r_1, \dots, r_N\}$ and relations

$$r_i^2 = 1 \quad \text{and} \quad (r_i r_j)^{m_{ij}} = 1, \tag{1}$$

where $m_{ij} = m_{ji} \in \{2, 3, \dots, \infty\}$ for $i \neq j$. Here, $m_{ij} = \infty$ means that the product $r_i r_j$

is of infinite order which fits into the following geometric picture. Denote by $\text{Gr}(P) = (\langle e_i, e_j \rangle_{n,1}) \in \text{Mat}(N; \mathbb{R})$ the Gram matrix of P . Then, the coefficients of $\text{Gr}(P)$ off its diagonal can be interpreted as follows:

$$-\langle e_i, e_j \rangle_{n,1} = \begin{cases} \cos \frac{\pi}{m_{ij}} & \text{if } \angle(H_i, H_j) = \frac{\pi}{m_{ij}}; \\ \cosh l_{ij} & \text{if } d_{\mathbb{H}}(H_i, H_j) = l_{ij} > 0. \end{cases}$$

The matrix $\text{Gr}(P)$ is of signature $(n, 1)$. Furthermore, it contains important information about P . For example, each vertex of P is characterised by a positive definite $n \times n$ principal submatrix of $\text{Gr}(P)$.

Beside the Gram matrix $\text{Gr}(P)$, the Vinberg graph $\Sigma(P)$ is very useful to describe a Coxeter polyhedron P (and its associated reflection group G) if the number N of its facets is small in comparison with the dimension n . The Vinberg graph $\Sigma(P)$ consists of nodes $v_i, 1 \leq i \leq N$, which correspond to the hyperplanes H_i or their unit normal vectors e_i . The number N of nodes is called the *order* of $\Sigma(P)$. If the hyperplanes H_i and H_j are not orthogonal, the corresponding nodes v_i and v_j are connected by an edge with weight $m_{ij} \geq 3$ if $\angle(H_i, H_j) = \frac{\pi}{m_{ij}}$; they are connected by a dotted edge (sometimes with weight l_{ij}) if H_i and H_j are at distance $l_{ij} > 0$ in \mathbb{H}^n . The weight $m_{ij} = 3$ is omitted since it occurs very frequently.

Since P is compact (and hence of finite volume), the Vinberg graph $\Sigma(P)$ is connected. Furthermore, by deleting a node together with the edges emanating from it so that $\Sigma(P)$ gives rise to two connected components Σ_1 and Σ_2 , at most one of the two subgraphs Σ_1, Σ_2 can have a dotted edge (since otherwise, the signature condition of $\text{Gr}(P)$ is violated).

The subsequent examples summarise the classification results for compact Coxeter n -polyhedra in terms of the number $N = n + k, 1 \leq k \leq 3$, of their facets.

Example 1. The compact hyperbolic Coxeter simplices were classified by Lannér [25] and exist for $n \leq 4$, only. In the case $n = 4$, there are precisely five simplices L_i whose Vinberg graphs $\Sigma_i = \Sigma(L_i), 1 \leq i \leq 5$, are given in Figure 1. The simplex $L = L_1$ described by the top left Vinberg graph (or by its Coxeter symbol [5, 3, 3, 3]; see Section 2.2 and [18]) will be of particular importance.

Example 2. The compact Coxeter polyhedra with $n + 2$ facets in \mathbb{H}^n have been classified. The list consists of the 7 examples of Esselmann and the (gluings of) straight Coxeter prisms due to I. Kaplinskaja; see, e.g., [9, 31]. The examples of Esselmann are products of two simplices of dimensions bigger than 1 and exist in \mathbb{H}^4 , only. The prisms (and their gluings) of Kaplinskaja exist for $n \leq 5$, and the list includes the Makarov prism M based on [5, 3, 3, 3, 3]; see Theorem B. Observe that the Vinberg graphs of all Kaplinskaja examples (including their gluings) contain one dotted edge.

Example 3. The compact hyperbolic Coxeter polyhedra $P \subset \mathbb{H}^n, n \geq 4$, with $n + 3$ facets exist up to $n = 8$ and have been enumerated by Tumarkin [35]. For $n = 5$, his list comprises 16 polyhedra, and they are characterised by Vinberg graphs with exactly three

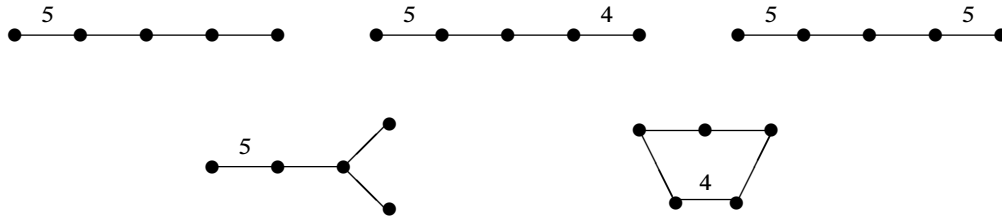


Figure 1. The compact Coxeter simplices in \mathbb{H}^4 .

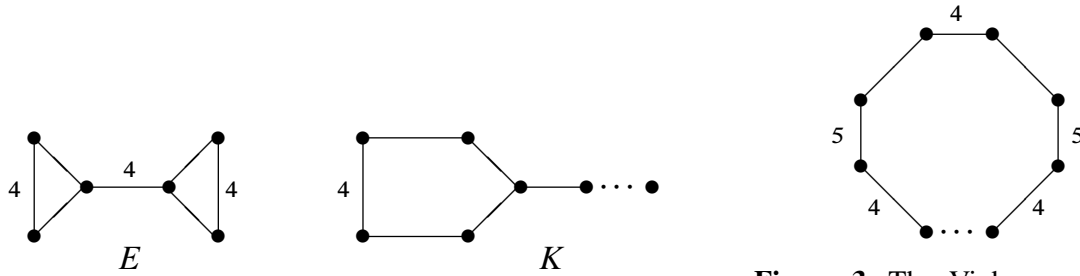


Figure 2. The Vinberg graphs of an Esselmann polyhedron $E \subset \mathbb{H}^4$ and of a Kaplinskaja prism $K \subset \mathbb{H}^5$.

Figure 3. The Vinberg graph of Tumarkin’s polyhedron $T \subset \mathbb{H}^5$ with one pair of disjoint facets.

(consecutive) dotted edges, up to the exceptional case $T \subset \mathbb{H}^5$. The polyhedron T has exactly one pair of non-intersecting facets and is depicted in Figure 3.

Remark 1. By a result of Felikson and Tumarkin [11, Corollary], the Coxeter polyhedra in Examples 1, 2 and 3 contain *all* compact Coxeter polyhedra with exactly one pair of non-intersecting facets. In particular, each compact Coxeter polyhedron $P \subset \mathbb{H}^n$ with $N \geq n + 4$ facets has a Vinberg graph with at least two dotted edges.

Every compact Coxeter polyhedron $P \subset \mathbb{H}^n$ gives rise to a hyperbolic Coxeter group acting cocompactly on \mathbb{H}^n , and each cocompact discrete group $G \subset \text{Isom } \mathbb{H}^n$ generated by finitely many hyperplane reflections has a fundamental domain whose closure is a compact Coxeter polyhedron in \mathbb{H}^n . In the sequel, we often use identical notions and descriptions for both, the polyhedron P and the reflection group G .

For further details and results about hyperbolic Coxeter polyhedra and Coxeter groups, their geometric-combinatorial and arithmetical characterisation as well as general (non-) existence results, we refer to the foundational work of E. Vinberg [36, 37]. An overview about the diverse partial classification results can be found in [9].

2.2. Coxeter groups and growth rates

A hyperbolic Coxeter group $G = (G, S)$ with $S = \{r_1, \dots, r_N\}$ as above is the geometric realisation of an abstract Coxeter system (W, S) of rank N consisting of a group W generated by a subset S of elements s_1, \dots, s_N satisfying the relations as given by (1). In the fundamental work [6] of Coxeter, the irreducible finite (or spherical) and affine Coxeter groups are classified. Abstract Coxeter groups are most conveniently described

by their *Coxeter graphs* or by their *Coxeter symbols*. More precisely, the Coxeter graph $\Sigma = \Sigma(W)$ of a Coxeter system (W, S) has nodes v_1, \dots, v_N corresponding to the generators s_1, \dots, s_N of W , and two nodes v_i and v_j are joined by an edge with weight $m_{ij} \geq 3$. In particular, there will be no edge if $m_{ij} = 2$ and there will be an edge decorated by ∞ if the product element $s_i s_j$ is of infinite order $m_{ij} = \infty$.

In this way, the Vinberg graph of a hyperbolic Coxeter group is a refined version of its Coxeter graph. In this context, observe that the Coxeter graph $\overset{\infty}{\bullet}\text{---}\overset{\infty}{\bullet}$ describes the affine group \tilde{A}_1 and – simultaneously – is underlying the Vinberg graph $\bullet\cdots\bullet$ of a compact hyperbolic Coxeter 1-simplex as given by any geodesic segment. Furthermore, the reflection group in $\text{Isom } \mathbb{H}^2$ associated to the compact Lambert quadrilateral with Vinberg graph $\bullet\cdots\bullet\text{---}\overset{\infty}{\bullet}\text{---}\overset{\infty}{\bullet}$ is given by the Coxeter graph $\overset{\infty}{\bullet}\text{---}\overset{\infty}{\bullet}\text{---}\overset{\infty}{\bullet}$ while the Vinberg graph $\overset{\infty}{\bullet}\text{---}\overset{\infty}{\bullet}$ (coinciding with its Coxeter graph) describes a non-compact hyperbolic triangle of area $\frac{\pi}{6}$.

In the case that the rank N of the Coxeter system (W, S) is small, a description by the Coxeter symbol is more convenient. For example, $[p_1, \dots, p_k]$ with integer labels $p_i \geq 3$ is associated to a linear Coxeter graph with $k + 1$ edges marked by the respective weights. The Coxeter symbol $[(p, q, r)]$ describes a cyclic Coxeter graph with 3 edges of weights p, q and r . We assemble the different symbols into a single one in order to describe the different nature of parts of the Coxeter graph in question; see, e.g., [18, Appendix].

Example 4. The Coxeter symbols of the seven Esselmann polyhedra in \mathbb{H}^4 are characterised by the fact that they contain two disjoint Coxeter symbols associated to compact hyperbolic triangles and called *triangular components* that are separated by at least one edge of (finite) weight $m \geq 3$. Accordingly, the Esselmann polyhedron $E \subset \mathbb{H}^4$ as depicted in Figure 2 is described by the Coxeter symbol $[(3, 4, 3), 4, (3, 4, 3)]$. Notice that none of the triangular components (p, q, r) , given by integers $p, q, r \geq 2$ such that $\frac{1}{p} + \frac{1}{q} + \frac{1}{r} < 1$, of the Coxeter symbols appearing in Esselmann’s list is equal to $(2, 3, 7)$.

For a Coxeter system (W, S) with generating set $S = \{s_1, \dots, s_N\}$, the (spherical) growth series $f_S(t)$ is defined by

$$f_S(t) = 1 + \sum_{k \geq 1} a_k t^k,$$

where $a_k \in \mathbb{Z}$ is the number of words $w \in W$ with S -length k . For references of the subsequent basic properties of $f_S(t)$, see for example [17, 21, 23]. The series $f_S(t)$ can be computed by Steinberg’s formula

$$\frac{1}{f_S(t^{-1})} = \sum_{\substack{W_T < W \\ |W_T| < \infty}} \frac{(-1)^{|T|}}{f_T(t)}, \tag{2}$$

where $W_T, T \subset S$, is a finite Coxeter subgroup of W , and where $W_\emptyset = \{1\}$. By a result of Solomon, the growth polynomials $f_T(t)$ in (2) can be expressed by means of their

Group	Exponents	Growth polynomial $f_S(x)$
A_n	$1, 2, \dots, n - 1, n$	$[2, 3, \dots, n, n + 1]$
B_n	$1, 3, \dots, 2n - 3, 2n - 1$	$[2, 4, \dots, 2n - 2, 2n]$
D_n	$1, 3, \dots, 2n - 5, 2n - 3, n - 1$	$[2, 4, \dots, 2n - 2, n]$
$G_2^{(m)}$	$1, m - 1$	$[2, m]$
F_4	$1, 5, 7, 11$	$[2, 6, 8, 12]$
H_3	$1, 5, 9$	$[2, 6, 10]$
H_4	$1, 11, 19, 29$	$[2, 12, 20, 30]$

Table 1. Exponents and growth polynomials of irreducible finite Coxeter groups.

exponents $m_1 = 1, m_2, \dots, m_p$ according to the formula

$$f_T(t) = \prod_{i=1}^p [m_i + 1].$$

Here we use the standard notation $[k] = 1 + t + \dots + t^{k-1}$ with $[k, l] = [k] \cdot [l]$ and so on. By replacing the variable t by t^{-1} , the function $[k]$ satisfies the property $[k](t) = t^{k-1}[k](t^{-1})$.

Table 1 lists all irreducible finite Coxeter groups together with their growth polynomials up to the exceptional groups E_6, E_7 and E_8 which are irrelevant for this work. Let us add that the growth series of a reducible Coxeter system (W, S) with factor groups (W_1, S_1) and (W_2, S_2) such that $S = (S_1 \times \{1_{W_2}\}) \cup (\{1_{W_1}\} \times S_2)$, satisfies the product formula $f_S(t) = f_{S_1}(t) \cdot f_{S_2}(t)$.

By the above, in its disk of convergence, the growth series $f_S(t)$ is a rational function that can be expressed as the quotient of coprime monic polynomials $p(t), q(t) \in \mathbb{Z}[t]$ of equal degree. The *growth rate* $\tau_W = \tau_{(W,S)}$ is defined by

$$\tau_W = \limsup_{k \rightarrow \infty} \sqrt[k]{a_k},$$

and it coincides with the inverse of the radius of convergence R of $f_S(t)$. Since τ_W equals the biggest real root of the denominator polynomial $q(t)$, it is a real algebraic integer.

Consider a cocompact hyperbolic Coxeter group $G = (G, S)$. Then, the rational function $f_S(t)$ is reciprocal (resp. anti-reciprocal) for n even (resp. n odd); see, e.g., [23]. In particular, for $n = 2$ and 4 , one has $f_S(t^{-1}) = f_S(t)$ for all $t \neq 0$. Furthermore, a result of Milnor [29] implies that the growth rate τ_G is strictly bigger than 1 so that G is of exponential growth. More specifically, for $n = 2$ and 3 , τ_G is either a quadratic unit or a *Salem number*, that is, τ_G is a real algebraic integer $\alpha > 1$ whose inverse is a conjugate of α , and all other conjugates lie on the unit circle; see, e.g., [24]. However, by a result of Cannon [4, 5] (see also [23, Theorem 4.1]), the growth rates of the five Lannér groups acting on \mathbb{H}^4 and shown in Figure 1 are not Salem numbers anymore; they are so-called

Perron numbers, that is, real algebraic integers > 1 all of whose other conjugates are of strictly smaller absolute value.

Example 5. The smallest known Salem number $\alpha_L \approx 1.176281$ with minimal polynomial $L(t) = t^{10} + t^9 - t^7 - t^6 - t^5 - t^4 - t^3 + t + 1$ equals the growth rate $\tau_{[7,3]}$ of the cocompact Coxeter triangle group $G = [7, 3]$ with Coxeter graph $\bullet \overset{7}{\text{---}} \bullet$ which in turn is the smallest growth rate among *all* cocompact planar hyperbolic Coxeter groups; see [16, 21].

The second smallest growth rate among them is realised by the Coxeter triangle group $[8, 3]$ with Coxeter graph $\bullet \overset{8}{\text{---}} \bullet$ and appears as the seventh smallest known Salem number ≈ 1.23039 given by the minimal polynomial $t^{10} - t^7 - t^5 - t^3 + 1$; see [22].

As a consequence, the growth rate of the cocompact Lambert quadrilateral group Q with Vinberg graph $\bullet \cdots \bullet \text{---} \bullet \cdots \bullet$ is strictly bigger than $\tau_{[8,3]}$. More precisely, the growth rate of Q is the Salem number $\tau_Q \approx 1.72208$ with minimal polynomial $t^4 - t^3 - t^2 - t - 1$. Notice also that the Coxeter graph of Q equals $\bullet \overset{\infty}{\text{---}} \bullet \overset{\infty}{\text{---}} \bullet$; see the proof of Theorem B in Section 3.

By applying similar techniques, it was shown in [19] (see also Floyd’s work [12]) that the Coxeter triangle group with Vinberg graph $\bullet \overset{\infty}{\text{---}} \bullet$ has smallest growth rate among all non-cocompact hyperbolic Coxeter groups of finite coarea in $\text{Isom } \mathbb{H}^2$, and as such it is unique. The growth rate $\tau_{[\infty,3]} \approx 1.32471$ has minimal polynomial $t^3 - t - 1$ and equals the smallest Pisot number α_S as shown by C. Smyth; see, e.g., [32] and [19, Section 3.2]. Recall that a *Pisot number* is an algebraic integer $\alpha > 1$ all of whose other conjugates are of absolute value less than 1.

For later purpose, let us emphasize the above comparison result as follows:

$$\tau_{[8,3]} < \tau_{[\infty,3]}. \tag{3}$$

Example 6. Among the cocompact Coxeter tetrahedral groups, the smallest growth rate is about 1.35098 with minimal polynomial $t^{10} - t^9 - t^6 + t^5 - t^4 - t + 1$; it is achieved in a unique way by the group $G = [3, 5, 3]$ with Coxeter graph $\bullet \overset{5}{\text{---}} \bullet$; see [21].

Example 7. Consider the (arithmetic) Lannér group $L = [5, 3, 3, 3]$ with Coxeter graph $\bullet \overset{5}{\text{---}} \bullet \text{---} \bullet \text{---} \bullet$ mentioned in Example 1. By means of Steinberg’s formula (2) and Table 1, the growth function $f_L(t) = f_S(t)$ can be expressed according to

$$\begin{aligned} \frac{1}{f_L(t^{-1})} &= \frac{1}{f_L(t)} = 1 - \frac{5}{[2]} + \frac{6}{[2, 2]} + \frac{3}{[2, 3]} + \frac{1}{[2, 5]} \\ &\quad - \left\{ \frac{1}{[2, 2, 2]} + \frac{4}{[2, 2, 3]} + \frac{2}{[2, 2, 5]} + \frac{2}{[2, 3, 4]} + \frac{1}{[2, 6, 10]} \right\} \\ &\quad + \frac{1}{[2, 2, 3, 4]} + \frac{1}{[2, 2, 3, 5]} + \frac{1}{[2, 2, 6, 10]} + \frac{1}{[2, 3, 4, 5]} + \frac{1}{[2, 12, 20, 30]}. \end{aligned}$$

It follows that

$$f_L(t) = \frac{[2, 12, 20, 30]}{q(t)},$$

where

$$\begin{aligned}
 q(t) = & 1 - t - t^7 + t^8 - t^9 + t^{10} - t^{11} + t^{14} - t^{15} + t^{16} - 2t^{17} + 2t^{18} - t^{19} \\
 & + t^{20} - t^{21} + t^{22} - t^{23} + 2t^{24} - 2t^{25} + 2t^{26} - 2t^{27} + 2t^{28} - t^{29} + t^{30} \\
 & - t^{31} + 2t^{32} - 2t^{33} + 2t^{34} - 2t^{35} + 2t^{36} - t^{37} + t^{38} - t^{39} + t^{40} - t^{41} \\
 & + 2t^{42} - 2t^{43} + t^{44} - t^{45} + t^{46} - t^{49} + t^{50} - t^{51} + t^{52} - t^{53} - t^{59} + t^{60}.
 \end{aligned}$$

The denominator polynomial $q(t)$ of $f_L(t)$ is palindromic and of degree 60. By means of the software PARI/GP [30], one checks that $q(t)$ is irreducible and has – beside non-real roots some of them being of absolute value one – exactly two inversive pairs $\alpha^{\pm 1}, \beta^{\pm 1}$ of real roots such that $\alpha > \beta > 1$. Indeed, by the results in [4, 5], α is not a Salem number anymore. As a consequence, the growth rate $\tau_L = \alpha \approx 1.19988$ of the Lannér group $L = [5, 3, 3, 3]$ is *not* a Salem number. However, $\tau_{[5,3,3,3]}$ is a Perron number. All these properties can be checked by the software CoxIter developed by R. Guglielmetti [13, 14].

Example 8. The Coxeter prism $M \subset \mathbb{H}^5$ found by Makarov is given by the Vinberg graph $\overset{5}{\bullet} \text{---} \bullet \text{---} \bullet \text{---} \bullet \text{---} \overset{l}{\bullet}$ where the hyperbolic distance l between the (unique) pair of non-intersecting facets of M satisfies

$$\cosh l = \frac{1}{2} \sqrt{\frac{7 + \sqrt{5}}{2}} \approx 1.07448.$$

In fact, the computation of l is easy since the determinant of the Gram matrix of M vanishes. As in Example 7, one can exploit Steinberg’s formula (2) and Table 1 in order to establish the growth function $f_M(t)$. The denominator polynomial of $f_M(t)$ splits into the factor $t - 1$ and a certain irreducible palindromic polynomial $q(t)$. As above, the software CoxIter allows us to identify the growth rate of the reflection group $[5, 3, 3, 3, 3]$ associated to M , as given by the largest zero of $q(t)$, with the Perron number $\tau_M \approx 1.64759$. Notice that the factor $t - 1$ is responsible for the vanishing of the Euler characteristic of M ; see, e.g., [21, (2.7)].

Example 9. For the Kaplinskaja prism $K \subset \mathbb{H}^5$ depicted in Figure 2, the denominator polynomial of the growth function $f_K(t)$ splits into the factor $t - 1$ and an irreducible palindromic polynomial $q(t)$ of degree 32. By means of CoxIter, one deduces that the growth rate is a Perron number of value $\tau_K \approx 2.08379$.

In a similar way, one computes the individual growth series and related invariants and properties of any cocompact (or cofinite) hyperbolic Coxeter group with given Vinberg graph.

Growth rates satisfy an important monotonicity property on the partially ordered set of Coxeter systems as follows. For two Coxeter systems (W, S) and (W', S') , one defines $(W, S) \leq (W', S')$ if there is an injective map $\iota : S \rightarrow S'$ such that $m_{st} \leq m'_{\iota(s)\iota(t)}$ for all $s, t \in S$. If ι extends to an isomorphism between W and W' , one writes $(W, S) \simeq (W', S')$, and $(W, S) < (W', S')$ otherwise. This partial order satisfies the descending chain condi-

tion since $m_{st} \in \{2, 3, \dots, \infty\}$ where $s \neq t$. In particular, any strictly decreasing sequence of Coxeter systems is finite; see [28]. In this work, the following result of Terragni [34, Section 3] will play an essential role.

Theorem 2. *If $(W, S) \leq (W', S')$, then $\tau_{(W,S)} \leq \tau_{(W',S')}$.*

Example 10. Consider the seven Esselmann groups $E_i \subset \text{Isom } \mathbb{H}^4$, $1 \leq i \leq 7$, whose Coxeter symbols consist of two triangular components separated by at least one edge of weight $m \geq 3$; see Example 4. Each of their triangular components describes a cocompact Coxeter group in $\text{Isom } \mathbb{H}^2$ of the type $(2, 3, 8)$, $(2, 3, 10)$, $(2, 4, 5)$, $(2, 5, 5)$, $(3, 3, 4)$ or $(3, 3, 5)$. By means of Theorem 2, we conclude that

$$\tau_{[8,3]} \leq \tau_{E_i}, \quad 1 \leq i \leq 7. \tag{4}$$

Notice. In the sequel, we will work with the Coxeter graph instead of the Vinberg graph associated to a hyperbolic Coxeter group (W, S) . Hence, we replace each dotted edge between two nodes v_s and $v_{s'}$ by an edge with weight ∞ , just indicating that the product element $ss' \in W$ is of infinite order.

3. Growth minimality in dimensions four and five

In this section, we prove the following two results as announced in Section 1.

Theorem A. *Among all Coxeter groups acting cocompactly on \mathbb{H}^4 , the Coxeter simplex group $[5, 3, 3, 3]$ has minimal growth rate, and as such it is unique.*

Theorem B. *Among all Coxeter groups acting cocompactly on \mathbb{H}^5 , the Coxeter prism group based on $[5, 3, 3, 3, 3]$ has minimal growth rate, and as such it is unique.*

Proof of Theorem A. Consider a group $G \subset \text{Isom } \mathbb{H}^4$ generated by the set S of reflections r_1, \dots, r_N in the N facet hyperplanes bounding a compact Coxeter polyhedron $P \subset \mathbb{H}^4$. The group $G = (G, S)$ is a cocompact hyperbolic Coxeter group of rank $N \geq 5$. Assume that the group G is not isomorphic to the Coxeter simplex group $L = [5, 3, 3, 3]$. We have to show that $\tau_G > \tau_{[5,3,3,3]} \approx 1.19988$.

In view of Theorem 1, we distinguish between the two cases whether all facets of P are mutually intersecting or not. In the case that all facets of P are mutually intersecting, P is either a Lannér simplex and G is of rank 5, or P is one of the seven Esselmann polyhedra with related Coxeter groups E_i , $1 \leq i \leq 7$, of rank 6.

(1a) The Coxeter graphs of the five Lannér simplices $L = L_1, \dots, L_5$ in \mathbb{H}^4 are given in Figure 1. The associated growth rates have been computed by means of Steinberg’s formula and are well known; see also [4, 31, 33]. The software CoxIter yields the values

$$\begin{aligned} \tau_{[5,3,3,4]} &\approx 1.38868, & \tau_{[5,3,3,5]} &\approx 1.51662, \\ \tau_{[5,3,3^{1.1}]} &\approx 1.44970, & \tau_{[(3^4,4)]} &\approx 1.62282, \end{aligned}$$

implying that the growth rate of $L = [5, 3, 3, 3]$ is strictly smaller than those of L_2, \dots, L_5 .

(1b) Let us investigate the growth rates of the Esselmann groups E_1, \dots, E_7 . By Example 10, (4), we have that

$$\tau_{[8,3]} \leq \tau_{E_i}, \quad 1 \leq i \leq 7.$$

It follows from Example 5 and Example 7 that

$$1.19988 \approx \tau_{[5,3,3,3]} < 1.2 < \tau_{[8,3]} \approx 1.23039,$$

which shows that the growth rate of $L = [5, 3, 3, 3]$ is strictly smaller than those of the Esselmann groups E_1, \dots, E_7 .

(2) Suppose that P has at least one pair of non-intersecting facets. Therefore, the Coxeter graph Σ of P contains at least one edge with weight ∞ . Since P has at least $N \geq 6$ facets, the graph Σ – being connected – contains a proper connected subgraph σ of order 3 with weights $p, q \in \{2, 3, \dots, \infty\}$ of the form as depicted in Figure 4.

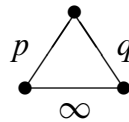


Figure 4. A subgraph σ of Σ .

By construction, the subgraph σ gives rise to a standard Coxeter subgroup (W, T) of rank 3 of (G, S) that satisfies $(W, T) \leq (G, S)$. By Theorem 2, Example 5, (3), and Example 7, we deduce in a similar way as above that

$$\tau_{[5,3,3,3]} < \tau_{[8,3]} < \tau_{[\infty,3]} \leq \tau_\sigma \leq \tau_\Sigma,$$

which finishes the proof of Theorem A. □

Proof of Theorem B. Let $G \subset \text{Isom } \mathbb{H}^5$ be a discrete group generated by the set S of reflections r_1, \dots, r_N in the N facet hyperplanes of a compact Coxeter polyhedron $P \subset \mathbb{H}^5$. The group $G = (G, S)$ is a cocompact hyperbolic Coxeter group of rank $N \geq 6$. Assume that G is not isomorphic to Makarov’s rank 7 prism group based on $[5, 3, 3, 3, 3]$. The associated Coxeter prism M is described and the growth rate τ_M is given in Example 8. We have to show that $\tau_G > \tau_M \approx 1.64759$.

Inspired by the proof of Theorem A, we look for appropriate Coxeter groups of smaller rank such that their growth data can be exploited to derive suitable lower bounds in view of Theorem 2. To this end, consider the following abstract Coxeter groups W_1, W_2 and W_3 with generating subsets S_1, S_2 and S_3 of rank 4 as defined by the Coxeter graphs in Figure 5.

The Coxeter systems (W_i, S_i) can be represented by hyperbolic Coxeter groups G_i for each $1 \leq i \leq 3$, and they will play an important role when comparing growth rates. In fact, the Coxeter graph of W_1 coincides with the Coxeter graph of the cocompact Lambert

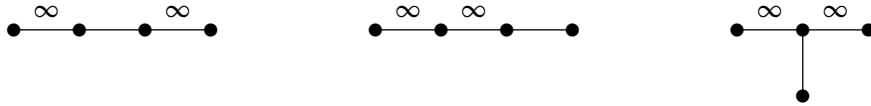


Figure 5. The three abstract Coxeter groups W_1, W_2 and W_3 .

quadrilateral group $Q \subset \text{Isom } \mathbb{H}^2$ with growth rate $\tau_Q \approx 1.72208$; see Example 5. Since, for the Makarov prism M , we have $\tau_M \approx 1.64759$, we deduce the following important fact:

$$\tau_M < \tau_Q = \tau_{G_1}. \tag{5}$$

Each of the remaining Coxeter groups W_2 and W_3 can be represented as a discrete subgroup of $O^+(3, 1)$ generated by reflections in the facets of a Coxeter tetrahedron of infinite volume. Indeed, one easily checks that the associated Tits form is of signature $(3, 1)$ and that some of the simplex vertices are not hyperbolic but ultra-ideal points (of positive Lorentzian norm). More importantly, the following result holds.

Lemma 1. (1) $\tau_{G_1} < \tau_{G_2}$. (2) $\tau_{G_1} < \tau_{G_3}$.

Proof. By means of Steinberg’s formula (2), we identify for each G_i the finite Coxeter subgroups with their growth polynomials according to Table 1 in order to deduce the following expressions for their growth functions $f_i(t)$, $1 \leq i \leq 3$:

$$\frac{1}{f_1(t^{-1})} = h(t), \tag{a}$$

$$\frac{1}{f_2(t^{-1})} = h(t) - \frac{1}{[2, 2, 3]}, \tag{b}$$

$$\frac{1}{f_3(t^{-1})} = h(t) - \frac{1}{[2, 2, 2]}. \tag{c}$$

Here, the help function $h(t)$, $t \neq 0$, is given by

$$h(t) = 1 - \frac{4}{[2]} + \frac{3}{[2, 2]} + \frac{1}{[2, 3]}. \tag{6}$$

By taking the differences between (a) and (b), (c), respectively, one obtains, for all $t > 0$,

$$\frac{1}{f_1(t^{-1})} - \frac{1}{f_2(t^{-1})} = \frac{1}{[2, 2, 3]} > 0, \quad \frac{1}{f_1(t^{-1})} - \frac{1}{f_3(t^{-1})} = \frac{1}{[2, 2, 2]} > 0.$$

For $x = t^{-1} \in (0, 1)$, we deduce that the smallest zero of $1/f_1(x)$ as given by the radius of convergence of the growth series $f_1(x)$ of G_1 is strictly bigger than the one of $1/f_2(x)$ and of $1/f_3(x)$. Hence, we get $\tau_{G_1} < \tau_{G_2}$ and $\tau_{G_1} < \tau_{G_3}$. \square

For later use, we also compare the growth rate of $W_1 = Q$ with the one of the Coxeter group W_4 with generating subset S_4 of rank 4 given by the Coxeter graph according to Figure 6. Again, the group W_4 can be interpreted as a discrete subgroup $G_4 \subset O^+(3, 1)$ generated by the reflections in the facets of a Coxeter tetrahedron of infinite volume.

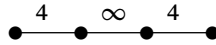


Figure 6. The abstract Coxeter group W_4 .

Lemma 2. $\tau_{G_1} < \tau_{G_4}$.

Proof. We proceed as in the proof of Lemma 1 and establish the growth function $f_4(t)$ by means of Steinberg’s formula. We obtain the following expression:

$$\frac{1}{f_4(t^{-1})} = 1 - \frac{4}{[2]} + \frac{3}{[2, 2]} + \frac{2}{[2, 4]} - \frac{2}{[2, 2, 4]}. \tag{d}$$

By means of (a), (d) and (6), we obtain the difference function

$$\frac{1}{f_1(t^{-1})} - \frac{1}{f_5(t^{-1})} = \frac{1}{[2, 3]} - \frac{2}{[2, 4]} + \frac{2}{[2, 2, 4]} = \frac{t^4 + 1}{[2, 3](t^2 + 1)} > 0, \quad \forall t > 0,$$

and conclude as at the end of the previous proof. □

Let us return and consider a compact Coxeter polyhedron $P \subset \mathbb{H}^5$ with N facets and associated hyperbolic Coxeter group G . By Example 1, we know that there are no compact Coxeter simplices anymore so that $N \geq 7$. Furthermore, by Theorem 1, P has at least one pair of non-intersecting facets. In the sequel, we discuss the cases $N = 7$, $N = 8$ and $N \geq 9$.

For $N = 7$, we are left with the three Kaplinskaja prisms (and their gluings) as given by the Makarov prism $M =: M_3$ based on $[5, 3, 3, 3, 3]$, its closely related Coxeter prism M_4 based on $[5, 3, 3, 3, 4]$ as well as the Coxeter prism K with Vinberg graph depicted in Figure 2 and treated in Example 9. By means of the software CoxIter (or some lengthy computation), one obtains the growth rate inequalities

$$1.64759 \approx \tau_M < \tau_{M_4} < 1.84712 < \tau_K \approx 2.08379,$$

which confirm the assertion of Theorem B in this case.

For $N = 8$, we dispose of Tumarkin’s classification list comprising all compact Coxeter polyhedra with $n + 3$ facets. For $n = 5$, these polyhedra have Vinberg graphs with exactly three (consecutive) dotted edges except for the polyhedron $T \subset \mathbb{H}^5$ depicted in Figure 3.

The Coxeter graph associated to T contains the proper subgraph $\bullet \overset{4}{\text{---}} \bullet \overset{\infty}{\text{---}} \bullet \overset{4}{\text{---}} \bullet$ which is associated to the Coxeter group W_4 studied above; see Figure 6. By means of Theorem 2, Lemma 2 and (5), we deduce that

$$\tau_M < \tau_{G_4} \leq \tau_T.$$

For the Coxeter graph of a polyhedron P with 8 facets in \mathbb{H}^5 that is not isometric to T , we consider its proper order 4 subgraph $\bullet \overset{\infty}{\text{---}} \bullet \overset{\infty}{\text{---}} \bullet \overset{\infty}{\text{---}} \bullet$. In a similar way, by Theorem 2, Lemma 1 and (5), we obtain

$$\tau_M < \tau_Q \leq \tau_P.$$

Let $N \geq 9$. By Remark 1, the Vinberg graph of the polyhedron $P \subset \mathbb{H}^5$ with N facets has at least two dotted edges. However, two dotted edges are separated by an edge in view of the signature condition of the Gram matrix $\text{Gr}(P)$; see Section 2.1.

Consider the Coxeter graph Σ of order N of the hyperbolic Coxeter group G associated to P . By the above, there is a proper connected subgraph σ of order 4 in Σ , depicted in Figure 7, with weights $p, q, r, s, t \in \{2, 3, \dots, \infty\}$ where at least one of them is equal to ∞ .

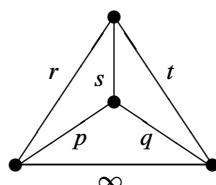


Figure 7. The subgraph $\sigma = \sigma(p, q, r, s, t)$.

In view of Figure 5, describing the three Coxeter groups G_1, G_2 and G_3 , and by means of Theorem 2, the growth rate of Σ , and hence of P , can be estimated from below according to

$$\tau_{G_i} \leq \tau_\sigma \leq \tau_\Sigma \quad \text{for at least one } i \in \{1, 2, 3\}.$$

By Lemma 1 and (5), we finally obtain that

$$\tau_M < \tau_{G_1} \leq \tau_P,$$

as desired. This finishes the proof of Theorem B. \square

Acknowledgements. The authors would like to thank Yohei Komori for helpful comments on an earlier version of the paper.

Funding. Naomi Bredon and Ruth Kellerhals are partially supported by the Swiss National Science Foundation 200021–172583.

References

- [1] M. Belolipetsky, On volumes of arithmetic quotients of $\text{SO}(1, n)$. *Ann. Sc. Norm. Super. Pisa Cl. Sci. (5)* **3** (2004), no. 4, 749–770 Zbl [1170.11307](#) MR [2124587](#)
- [2] M. Belolipetsky, Addendum to: “On volumes of arithmetic quotients of $\text{SO}(1, n)$ ”. *Ann. Sc. Norm. Super. Pisa Cl. Sci. (5)* **6** (2007), no. 2, 263–268 Zbl [1278.11044](#) MR [2352518](#)
- [3] R. Benedetti and C. Petronio, *Lectures on hyperbolic geometry*. Universitext, Springer, Berlin, 1992 Zbl [0768.51018](#) MR [1219310](#)
- [4] J. Cannon, The growth of the closed surface groups and the compact hyperbolic Coxeter groups. Unpublished manuscript

- [5] J. W. Cannon and P. Wagreich, Growth functions of surface groups. *Math. Ann.* **293** (1992), no. 2, 239–257 Zbl [0734.57001](#) MR [1166120](#)
- [6] H. S. M. Coxeter, Discrete groups generated by reflections. *Ann. of Math. (2)* **35** (1934), no. 3, 588–621 Zbl [0010.01101](#) MR [1503182](#)
- [7] V. Emery and R. Kellerhals, The three smallest compact arithmetic hyperbolic 5-orbifolds. *Algebr. Geom. Topol.* **13** (2013), no. 2, 817–829 Zbl [1266.22014](#) MR [3044594](#)
- [8] F. Esselmann, The classification of compact hyperbolic Coxeter d -polytopes with $d + 2$ facets. *Comment. Math. Helv.* **71** (1996), no. 2, 229–242 Zbl [0856.51016](#) MR [1396674](#)
- [9] A. Felikson, Hyperbolic Coxeter polytopes. <http://www.maths.dur.ac.uk/users/anna.felikson/Polytopes/polytopes.html>
- [10] A. Felikson and P. Tumarkin, On hyperbolic Coxeter polytopes with mutually intersecting facets. *J. Combin. Theory Ser. A* **115** (2008), no. 1, 121–146 Zbl [1141.52014](#) MR [2378860](#)
- [11] A. Felikson and P. Tumarkin, Coxeter polytopes with a unique pair of non-intersecting facets. *J. Combin. Theory Ser. A* **116** (2009), no. 4, 875–902 Zbl [1168.52011](#) MR [2513640](#)
- [12] W. J. Floyd, Growth of planar Coxeter groups, P.V. numbers, and Salem numbers. *Math. Ann.* **293** (1992), no. 3, 475–483 Zbl [0735.51016](#) MR [1170521](#)
- [13] R. Guglielmetti, CoxIter—computing invariants of hyperbolic Coxeter groups. *LMS J. Comput. Math.* **18** (2015), no. 1, 754–773 Zbl [1333.20040](#) MR [3434903](#)
- [14] R. Guglielmetti, CoxIterWeb. <https://coxiterweb.rafaelguglielmetti.ch/>
- [15] T. Hild, The cusped hyperbolic orbifolds of minimal volume in dimensions less than ten. *J. Algebra* **313** (2007), no. 1, 208–222 Zbl [1119.52011](#) MR [2326144](#)
- [16] E. Hironaka, The Lehmer polynomial and pretzel links. *Canad. Math. Bull.* **44** (2001), no. 4, 440–451 Zbl [0999.57001](#) MR [1863636](#)
- [17] J. E. Humphreys, *Reflection groups and Coxeter groups*. Camb. Stud. Adv. Math. 29, Cambridge University Press, Cambridge, 1990 Zbl [0725.20028](#) MR [1066460](#)
- [18] N. W. Johnson, J. G. Ratcliffe, R. Kellerhals, and S. T. Tschantz, The size of a hyperbolic Coxeter simplex. *Transform. Groups* **4** (1999), no. 4, 329–353 Zbl [0953.20041](#) MR [1726696](#)
- [19] R. Kellerhals, Cofinite hyperbolic Coxeter groups, minimal growth rate and Pisot numbers. *Algebr. Geom. Topol.* **13** (2013), no. 2, 1001–1025 Zbl [1281.20044](#) MR [3044599](#)
- [20] R. Kellerhals, Hyperbolic orbifolds of minimal volume. *Comput. Methods Funct. Theory* **14** (2014), no. 2-3, 465–481 Zbl [1307.57001](#) MR [3265373](#)
- [21] R. Kellerhals and A. Kolpakov, The minimal growth rate of cocompact Coxeter groups in hyperbolic 3-space. *Canad. J. Math.* **66** (2014), no. 2, 354–372 Zbl [1302.20045](#) MR [3176145](#)
- [22] R. Kellerhals and L. Liechti, Salem numbers, spectral radii and growth rates of hyperbolic Coxeter groups. *Transform. Groups* (2022), DOI [10.1007/s00031-022-09715-x](https://doi.org/10.1007/s00031-022-09715-x)
- [23] R. Kellerhals and G. Perren, On the growth of cocompact hyperbolic Coxeter groups. *European J. Combin.* **32** (2011), no. 8, 1299–1316 Zbl [1242.20049](#) MR [2838016](#)
- [24] Y. Komori, Coxeter garlands in H^4 and 2-Salem numbers. IML Workshop on Growth and Mahler Measures in Geometry and Topology, Institut Mittag-Leffler, Report No. 1, 2013
- [25] F. Lannér, On complexes with transitive groups of automorphisms. *Comm. Sém. Math. Univ. Lund [Medd. Lunds Univ. Mat. Sem.]* **11** (1950), 1–71 MR [42129](#)
- [26] V. S. Makarov, The Fedorov groups of four-dimensional and five-dimensional Lobachevskii space. In *Studies in General Algebra*, No. 1 (Russian), pp. 120–129, Kišinev. Gos. Univ., Kishinev, 1968 MR [0259735](#)

- [27] G. J. Martin, Siegel's problem in three dimensions. *Notices Amer. Math. Soc.* **63** (2016), no. 11, 1244–1247 Zbl [1356.30026](#) MR [3560949](#)
- [28] C. T. McMullen, Coxeter groups, Salem numbers and the Hilbert metric. *Publ. Math. Inst. Hautes Études Sci.* (2002), no. 95, 151–183 Zbl [1148.20305](#) MR [1953192](#)
- [29] J. Milnor, A note on curvature and fundamental group. *J. Differential Geometry* **2** (1968), 1–7 Zbl [0162.25401](#) MR [232311](#)
- [30] The PARI Group, PARI/GP version 2.11.2. Université Bordeaux, 2019, <http://pari.math.u-bordeaux.fr/>
- [31] G. Perren, Growth of cocompact hyperbolic Coxeter groups and their rate. PhD thesis no. 1656, University of Fribourg, 2007
- [32] C. Smyth, Seventy years of Salem numbers. *Bull. Lond. Math. Soc.* **47** (2015), no. 3, 379–395 Zbl [1321.11111](#) MR [3354434](#)
- [33] T. Terragni, On the growth of a Coxeter group (extended version). 2013, arXiv:[1312.3437v2](#)
- [34] T. Terragni, On the growth of a Coxeter group. *Groups Geom. Dyn.* **10** (2016), no. 2, 601–618 Zbl [1356.20023](#) MR [3513110](#)
- [35] P. Tumarkin, Compact hyperbolic Coxeter n -polytopes with $n + 3$ facets. *Electron. J. Combin.* **14** (2007), no. 1, Research Paper 69 Zbl [1168.51311](#) MR [2350459](#)
- [36] È. B. Vinberg, Hyperbolic groups of reflections. *Uspekhi Mat. Nauk* **40** (1985), no. 1, 29–66 MR [783604](#)
- [37] È. B. Vinberg and O. V. Shvartsman, Discrete groups of motions of spaces of constant curvature. In *Geometry, II*, pp. 139–248, Encyclopaedia Math. Sci. 29, Springer, Berlin, 1993 MR [1254933](#)

Received 25 August 2020.

Naomi Bredon

Department of Mathematics, University of Fribourg, 1700 Fribourg, Switzerland;
naomi.bredon@unifr.ch

Ruth Kellerhals

Department of Mathematics, University of Fribourg, 1700 Fribourg, Switzerland;
ruth.kellerhals@unifr.ch



Hyperbolic Coxeter groups of minimal growth rates in higher dimensions

Naomi Bredon

Abstract. The cusped hyperbolic n -orbifolds of minimal volume are well known for $n \leq 9$. Their fundamental groups are related to the Coxeter n -simplex groups Γ_n . In this work, we prove that Γ_n has minimal growth rate among all non-cocompact Coxeter groups of finite covolume in $\text{Isom}\mathbb{H}^n$. In this way, we extend previous results of Floyd for $n = 2$ and of Kellerhals for $n = 3$, respectively. Our proof is a generalization of the methods developed together with Kellerhals for the cocompact case.

1 Introduction

Let \mathbb{H}^n denote the real hyperbolic n -space with its isometry group $\text{Isom}\mathbb{H}^n$.

A *hyperbolic Coxeter polyhedron* $P \subset \mathbb{H}^n$ is a convex polyhedron of finite volume all of whose dihedral angles are integral submultiples of π . Associated to P is the *hyperbolic Coxeter group* $\Gamma \subset \text{Isom}\mathbb{H}^n$ generated by the reflections in the bounding hyperplanes of P . By construction, Γ is a discrete group with associated orbifold $O^n = \mathbb{H}^n/\Gamma$ of finite volume.

We focus on *non-compact* hyperbolic Coxeter polyhedra, having at least one ideal vertex $v_\infty \in \partial\mathbb{H}^n$. Notice that the stabilizer of the vertex v_∞ is isomorphic to an affine Coxeter group. The group Γ is called *non-cocompact*, and its quotient space O^n has at least one cusp.

The hyperbolic Coxeter group Γ is the geometric realization of an abstract Coxeter system (W, S) consisting of a group W with a finite generating set S together with the relations $s^2 = 1$ and $(ss')^{m_{ss'}} = 1$, where $m_{ss'} = m_{s's} \in \{2, 3, \dots, \infty\}$ for all $s, s' \in S$ with $s \neq s'$. The *growth series* $f_S(t)$ of $W = (W, S)$ is given by

$$f_S(t) = 1 + \sum_{k \geq 1} a_k t^k,$$

where $a_k \in \mathbb{Z}$ is the number of elements in W with S -length k . The *growth rate* τ_W of $W = (W, S)$ is defined as the inverse of the radius of convergence of $f_S(t)$.

We are interested in small growth rates of non-cocompact hyperbolic Coxeter groups in $\text{Isom}\mathbb{H}^n$ for $n \geq 2$. For $n = 2$, Floyd [6] showed that the Coxeter group $\Gamma_2 = [3, \infty]$ generated by the reflections in the triangle with angles $\pi/2, \pi/3$, and 0 is the (unique) group of minimal growth rate. For $n = 3$, Kellerhals [13] proved that

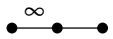
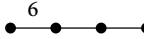
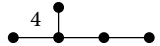
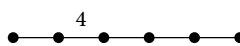




Received by the editors November 17, 2021; revised March 25, 2022; accepted March 25, 2022.

Published online on Cambridge Core April 6, 2022.

AMS subject classification: 20F55, 26A12, 22E40, 11R06.

Keywords: Coxeter group, growth rate, hyperbolic Coxeter polyhedron, affine vertex stabilizer.

Table 1: The hyperbolic Coxeter n -simplex group Γ_n .

Γ_2		Γ_3	
Γ_4		Γ_5	
Γ_6		Γ_7	
Γ_8		Γ_9	

the tetrahedral group Γ_3 generated by the reflections in the Coxeter tetrahedron with symbol $[6, 3, 3]$ realizes minimal growth rate in a unique way.

Consider the hyperbolic Coxeter n -simplices and their reflection groups $\Gamma_n \subset \text{Isom} \mathbb{H}^n$ depicted in Table 1. For their volumes, we refer to [12]. Observe that Γ_n is of minimal covolume among all non-cocompact hyperbolic Coxeter n -simplex groups.

The aim of this work is to prove the following result in the context of growth rates.

Theorem *Let $2 \leq n \leq 9$. Among all non-cocompact hyperbolic Coxeter groups of finite covolume in $\text{Isom} \mathbb{H}^n$, the group Γ_n given in Table 1 has minimal growth rate, and as such the group is unique.*

Our Theorem should be compared with the volume minimality results for cusped hyperbolic n -orbifolds O^n for $2 \leq n \leq 9$. These results are due to Siegel [16] for $n = 2$, Meyerhoff [15] for $n = 3$, Hild and Kellerhals [10] for $n = 4$, and Hild [9] for $n \leq 9$. Indeed, the fundamental group of O^n is related to Γ_n in all these cases.

The work is organized as follows. In Section 2.1, we set the background about hyperbolic Coxeter polyhedra and their associated reflection groups. Furthermore, we present a result of Felikson and Tumarkin about their combinatorics as given by [5, Theorem B], which will play a crucial role in our proof. In fact, we will exploit the (non-)simplicity of the Coxeter polyhedra in a most useful way. In Section 2.2, we discuss growth series and growth rates of Coxeter groups and introduce the notion of extension of a Coxeter graph. We also provide some illustrating examples. The monotonicity result of Terragni [18] for growth rates, presented in Theorem 2.2, will be another major ingredient in our proof. Finally, Section 3 is devoted to the proof of our result. We perform it in two steps by assuming that the Coxeter graph under consideration has an affine component of type \tilde{A}_1 or not.

2 Hyperbolic Coxeter groups and growth rates

2.1 Coxeter polyhedra and their reflection groups

Let \mathbb{X}^n denote one of the geometric n -spaces of constant curvature, the unit n -sphere \mathbb{S}^n , the Euclidean n -space \mathbb{E}^n , or the real hyperbolic n -space \mathbb{H}^n . As usual, we embed \mathbb{X}^n in a suitable quadratic space \mathbb{Y}^{n+1} . In the Euclidean case, we take the affine model and write $\mathbb{E}^n = \{x \in \mathbb{E}^{n+1} \mid x_{n+1} = 0\}$. In the hyperbolic case, we interpret \mathbb{H}^n as the

upper sheet of the hyperboloid in \mathbb{R}^{n+1} , that is,

$$\mathbb{H}^n = \{x \in \mathbb{R}^{n+1} \mid \langle x, x \rangle_{n,1} = -1, x_{n+1} > 0\},$$

where $\langle x, x \rangle_{n,1} = x_1^2 + \dots + x_n^2 - x_{n+1}^2$ is the standard Lorentzian form. Its boundary $\partial\mathbb{H}^n$ can be identified with the set

$$\partial\mathbb{H}^n = \{x \in \mathbb{R}^{n+1} \mid \langle x, x \rangle_{n,1} = 0, \sum_{k=1}^{n+1} x_k^2 = 1, x_{n+1} > 0\}.$$

In this picture, the isometry group of \mathbb{H}^n is isomorphic to the group $O^+(n, 1)$ of positive Lorentzian matrices leaving the bilinear form $\langle \cdot, \cdot \rangle_{n,1}$ and the upper sheet invariant.

It is well known that each isometry of \mathbb{X}^n is a finite composition of reflections in hyperplanes, where a hyperplane $H = H_\nu$ in \mathbb{X}^n is characterized by a normal unit vector $\nu \in \mathbb{Y}^{n+1}$. Associated to H_ν are two closed half-spaces. We denote by H_ν^- the half-space in \mathbb{X}^n with outer normal vector ν .

A (convex) n -polyhedron $P = \cap_{i \in I} H_i^- \subset \mathbb{X}^n$ is the non-empty intersection of a finite number of half-spaces H_i^- bounded by the hyperplanes $H_i = H_{\nu_i}$ for $i \in I$. A facet of P is of the form $F_i = P \cap H_i$ for some $i \in I$. In the sequel, for $\mathbb{X}^n \neq \mathbb{S}^n$, we always assume that P is of finite volume. In the Euclidean case, this implies that P is compact, and in the hyperbolic case, P is the convex hull of finitely many points $\nu_1, \dots, \nu_k \in \mathbb{H}^n \cup \partial\mathbb{H}^n$. If $\nu_i \in \mathbb{H}^n$, then ν_i is an ordinary vertex, and if $\nu_i \in \partial\mathbb{H}^n$, then ν_i is an ideal vertex of P , respectively.

If all dihedral angles $\alpha_{ij} = \sphericalangle(H_i, H_j)$ formed by intersecting hyperplanes H_i, H_j in the boundary of P are either zero or of the form $\frac{\pi}{m_{ij}}$ for an integer $m_{ij} \geq 2$, then P is called a Coxeter polyhedron in \mathbb{X}^n . Observe that the Gram matrix $\text{Gr}(P) = (\langle \nu_i, \nu_j \rangle_{\mathbb{Y}^{n+1}})_{i,j \in I}$ is a real symmetric matrix with 1's on the diagonal and non-positive coefficients off the diagonal. In this way, the theory of Perron–Frobenius applies. For further details and references about Coxeter polyhedra in \mathbb{X}^n , we refer to [4, 19, 20].

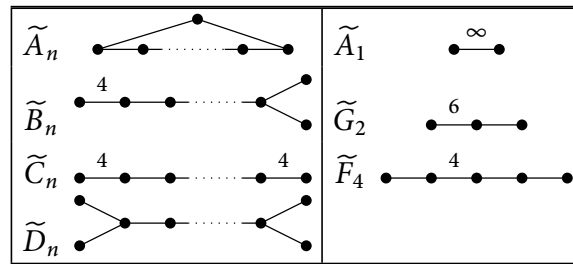
Let $P = \cap_{i=1}^N H_i^- \subset \mathbb{X}^n$ be a Coxeter n -polyhedron. Denote by $r_i = r_{H_i}$ the reflection in the bounding hyperplane H_i of P , and let $G = G_P$ be the group generated by r_1, \dots, r_N . It follows that G is a discrete subgroup of finite covolume in $\text{Isom}\mathbb{X}^n$, called a geometric Coxeter group.

A geometric Coxeter group $G \subset \text{Isom}\mathbb{X}^n$ with generating system $S = \{r_1, \dots, r_N\}$ is the geometric realization of an abstract Coxeter system (W, S) . In fact, we have $r_i^2 = 1$ and $(r_i r_j)^{m_{ij}} = 1$ with $m_{ij} = m_{ji} \in \{2, 3, \dots, \infty\}$ as above. Here, $m_{ij} = \infty$ indicates that $r_i r_j$ is of infinite order.

For $\mathbb{X}^n = \mathbb{S}^n$, G is a spherical Coxeter group and as such finite. For $\mathbb{X}^n = \mathbb{E}^n$, G is a Euclidean or affine Coxeter group and of infinite order. By a result of Coxeter [3], the irreducible spherical and Euclidean Coxeter groups are entirely classified. In contrast to this fact, hyperbolic Coxeter groups are far from being classified. For a survey about partial classification results, we refer to [4].

For the description of abstract and geometric Coxeter groups, one commonly uses the language of weighted graphs and Coxeter symbols. Let (W, S) be an abstract Coxeter system with generating system $S = \{s_1, \dots, s_N\}$ and relations of the form $s_i^2 = 1$ and $s_i s_j^{m_{ij}} = 1$ with $m_{ij} = m_{ji} \in \{2, 3, \dots, \infty\}$. The Coxeter graph of the Coxeter

Table 2: Connected affine Coxeter graphs of order $n + 1$.



system (W, S) is the non-oriented graph Σ whose nodes correspond to the generators s_1, \dots, s_N . If s_i and s_j do not commute, their nodes n_i, n_j are connected by an edge with weight $m_{ij} \geq 3$. We omit the weight $m_{ij} = 3$ since it occurs frequently. The number N of nodes is the *order* of Σ . A subgraph $\sigma \subset \Sigma$ corresponds to a *special* subgroup of (W, S) , that is, a subgroup of the form (W_T, T) for a subset $T \subset S$. Observe that the Coxeter graph Σ is connected if (W, S) is irreducible.

In the case of a geometric Coxeter group $G = (W, S) \subset \text{Isom}\mathbb{X}^n$, we call its Coxeter graph Σ *spherical*, *affine*, or *hyperbolic*, if $\mathbb{X}^n = \mathbb{S}^n, \mathbb{E}^n$, or \mathbb{H}^n , respectively. In Table 2, we reproduce all the connected affine Coxeter graphs, using the classical notation, with the exception of the three groups $\tilde{E}_6, \tilde{E}_7, \tilde{E}_8$ (they will not appear in the following).

An abstract Coxeter group with a simple presentation can conveniently be described by its *Coxeter symbol*. For example, the linear Coxeter graph with edges of successive weights $k_1, \dots, k_N \geq 3$ is abbreviated by the Coxeter symbol $[k_1, \dots, k_N]$. The Y-shaped graph made of one edge with weight p and of two strings of k and l edges emanating from a central vertex of valency 3 is denoted by $[p, 3^{k,l}]$ (see [12]).

Let us specify the context and consider a Coxeter polyhedron $P = \cap_{i=1}^N H_i^- \subset \mathbb{H}^n$. Denote by $\Gamma = G_P \subset \text{Isom}\mathbb{H}^n$ its associated Coxeter group and by Σ its Coxeter graph. Since P is of finite volume, the graph Σ is connected. Furthermore, if P is not compact, then P has at least one ideal vertex.

Let $v \in \mathbb{H}^n$ be an ordinary vertex of P . Then, its *link* L_v is the intersection of P with a small sphere of center v that does not intersect any facet of P not incident to v . It corresponds to a spherical Coxeter polyhedron of \mathbb{S}^{n-1} and therefore to a spherical Coxeter subgraph σ of order n in Σ .

Let $v_\infty \in \partial\mathbb{H}^n$ be an ideal vertex of P . Then, its link, denoted by L_∞ , is given by the intersection of P with a sufficiently small horosphere centered at v_∞ as above. The link L_∞ corresponds to a Euclidean Coxeter polyhedron in \mathbb{E}^{n-1} and is related to an affine Coxeter subgraph σ_∞ of order $\geq n$ in Σ .

More precisely, if v_∞ is a *simple* ideal vertex, that is, v_∞ is the intersection of exactly n among the N bounding hyperplanes of P , the Coxeter graph σ_∞ is connected and of order n . Otherwise, σ_∞ has $n_c(\sigma_\infty) \geq 2$ affine components, and we have the following formula:

$$(1) \quad n - 1 = \text{order}(\sigma_\infty) - n_c(\sigma_\infty).$$

Recall that a polyhedron is *simple* if all of its vertices are simple.

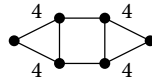


Figure 1: The Coxeter polyhedron $P_0 \subset \mathbb{H}^4$.

As in the spherical and Euclidean cases, hyperbolic Coxeter simplices in \mathbb{H}^n are all known, and they exist for $n \leq 9$ (see [1] or [20]). A list of their Coxeter graphs, Coxeter symbols, and volumes can be found in [12]. Among the related Coxeter n -simplex groups, the group Γ_n , as given in Table 1, is of minimal covolume.

The following structural result for simple hyperbolic Coxeter polyhedra due to Felikson and Tumarkin [5, Theorem B] will be a corner stone for the proof of our Theorem.

Theorem 2.1 *Let $n \leq 9$, and let $P \subset \mathbb{H}^n$ be a non-compact simple Coxeter polyhedron. If all facets of P are mutually intersecting, then P is either a simplex or isometric to the polyhedron P_0 whose Coxeter graph is depicted in Figure 1.*

2.2 Growth rates and their monotonicity

Let (W, S) be a Coxeter system and denote by $a_k \in \mathbb{Z}$ the number of elements $w \in W$ with S -length k . The growth series $f_S(t)$ of (W, S) is defined by

$$f_S(t) = 1 + \sum_{k \geq 1} a_k t^k.$$

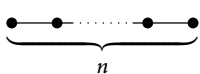
In the following, we list some properties of $f_S(t)$. For references, we refer to [11].

There is a formula due to Steinberg expressing the growth series $f_S(t)$ of a Coxeter system (W, S) in terms of its finite special subgroups W_T for $T \subseteq S$,

$$(2) \quad \frac{1}{f_S(t^{-1})} = \sum_{\substack{W_T \leq W \\ |W_T| < \infty}} \frac{(-1)^{|T|}}{f_T(t)},$$

where $W_\emptyset = \{1\}$. By a result of Solomon, the growth polynomial of each term $f_T(t)$ in (2) can be expressed by means of its exponents $\{m_1, m_2, \dots, m_p\}$ according to the formula

$$(3) \quad f_T(t) = \prod_{i=1}^p [m_i + 1],$$

where $[k] = 1 + t + \dots + t^{k-1}$ and, more generally, $[k_1, \dots, k_r] := [k_1] \cdots [k_r]$. A complete list of the irreducible spherical Coxeter groups together with their exponents can be found in [14]. For example, the exponents of the Coxeter group A_n with Coxeter graph  are $\{1, 2, \dots, n\}$ so that

$$(4) \quad f_{A_n}(t) = [2, \dots, n + 1].$$

Furthermore, the growth series of a reducible Coxeter system (W, S) with factor groups (W_1, S_1) and (W_2, S_2) such that $S = (S_1 \times \{1_{W_2}\}) \cup (\{1_{W_1}\} \times S_2)$ satisfies the product formula

$$f_S(t) = f_{S_1}(t) \cdot f_{S_2}(t).$$

In its disk of convergence, the growth series $f_S(t)$ is a rational function, which can be expressed as the quotient of coprime monic polynomials $p(t), q(t) \in \mathbb{Z}[t]$ of the same degree. The growth rate $\tau_W = \tau_{(W,S)}$ is defined by the inverse of the radius of convergence of $f_S(t)$ and can be expressed by

$$\tau_W = \limsup_{k \rightarrow \infty} a_k^{1/k}.$$

It is the inverse of the smallest positive real pole of $f_S(t)$ and hence an algebraic integer.

Important for the proof of our Theorem is the following result of Terragni [17] about the growth monotonicity.

Theorem 2.2 *Let (W, S) and (W', S') be two Coxeter systems such that there is an injective map $\iota : S \rightarrow S'$ with $m_{st} \leq m'_{\iota(s)\iota(t)}$ for all $s, t \in S$. Then, $\tau_{(W,S)} \leq \tau_{(W',S')}$.*

For $n \geq 2$, consider a Coxeter group $\Gamma \subset \text{Isom}\mathbb{H}^n$ of finite covolume. By results of Milnor and de la Harpe, we know that $\tau_\Gamma > 1$. More precisely, and as shown by Terragni [17], $\tau_\Gamma \geq \tau_{\Gamma_9} \approx 1.1380$, where Γ_9 is the Coxeter simplex group given in Table 1.

Next, we introduce another tool in the proof of our result, the (simple) extension of a Coxeter graph.

Definition 2.1 Let Σ be an abstract Coxeter graph. A (simple) extension of Σ is a Coxeter graph Σ' obtained by adding one node linked with a (simple) edge to the Coxeter graph Σ .

As a direct consequence of Theorem 2.2, if W is a Coxeter group with Coxeter graph Σ , any extension Σ' of Σ encodes a Coxeter group W' such that $\tau_W \leq \tau_{W'}$.

Example 2.3 Consider an irreducible affine Coxeter graph of order 3 as given in Table 2. Up to symmetry, the graph \tilde{A}_2 has a unique extension given by the Coxeter graph at the top left in Figure 2. This graph describes the Coxeter tetrahedron $[3, 3^{[3]}]$ of finite volume. The Coxeter graphs \tilde{C}_2 and \tilde{G}_2 give rise to the remaining five extensions depicted in Figure 2. By a result of Kellerhals [13], these six Coxeter graphs describe Coxeter tetrahedral groups Λ of finite covolume in $\text{Isom}\mathbb{H}^3$ whose growth rates satisfy $\tau_\Lambda \geq \tau_{\Gamma_3}$.

Example 2.4 In a similar way, any extension of an irreducible affine Coxeter graph of order 4 yields a Coxeter simplex group of finite covolume in $\text{Isom}\mathbb{H}^4$. They are given in Figure 3. Notice that $\Gamma_4 = [4, 3^{2,1}]$ is part of them.

Remark 2.5 When considering irreducible affine Coxeter graphs of order greater than or equal to 5, the resulting extensions do not always relate to hyperbolic Coxeter

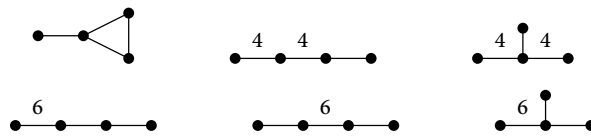


Figure 2: Extensions of \tilde{A}_2 , \tilde{C}_2 , and \tilde{G}_2 .

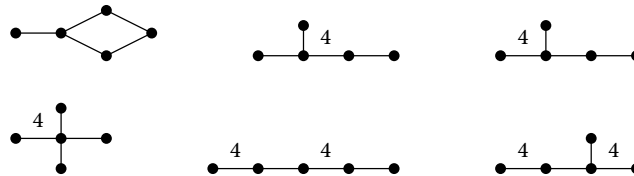


Figure 3: Extensions of \tilde{A}_3 , \tilde{B}_3 , and \tilde{C}_3 .

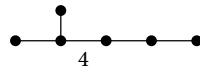


Figure 4: An infinite volume 5-simplex.

n -simplex groups of finite covolume. For example, among the extensions of \tilde{F}_4 , the graph depicted in Figure 4 describes an infinite volume simplex in \mathbb{H}^5 .

3 Proof of the Theorem

Let $2 \leq n \leq 9$, and consider the Coxeter simplex group $\Gamma_n \subset \text{Isom}\mathbb{H}^n$ whose Coxeter graph is depicted in Table 1. In this section, we provide the proof of our main result stated as follows.

Theorem *For any $2 \leq n \leq 9$, the group Γ_n has minimal growth rate among all non-cocompact hyperbolic Coxeter groups of finite covolume in $\text{Isom}\mathbb{H}^n$, and as such the group is unique.*

For $n = 2$ and for $n = 3$, the result has been established by Floyd [6] and Kellerhals [13]. Therefore, it suffices to prove the Theorem for $4 \leq n \leq 9$.

Observe that the growth rates of all Coxeter simplex groups in $\text{Isom}\mathbb{H}^n$ are known. Their list can be found in [17]. In particular, one deduces the following strict inequalities:

$$(5) \quad \tau_{\Gamma_9} \approx 1.1380 < \dots < \tau_{\Gamma_5} \approx 1.2481 < \tau_{\Gamma_4} \approx 1.3717,$$

$$(6) \quad \tau_{\Gamma_5} < \tau_{\Gamma_3} \approx 1.2964.$$

For a fixed dimension n , one also checks that Γ_n has minimal growth rate among (all the finitely many) non-cocompact Coxeter simplex groups $\Lambda \subset \text{Isom}\mathbb{H}^n$.

As a consequence, we focus on hyperbolic Coxeter groups $\Gamma \subset \text{Isom}\mathbb{H}^n$ generated by at least $N \geq n + 2$ reflections in the facets of a non-compact finite volume Coxeter

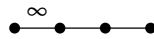


Figure 5: The Coxeter group $W_0 = [\infty, 3, 3]$.



Figure 6: The Coxeter groups $W_1 = [3, \infty, 3]$ and $W_2 = [\infty, 3^{1,1}]$.

polyhedron $P \subset \mathbb{H}^n$. We have to show that $\tau_{\Gamma_n} < \tau_\Gamma$, which yields unicity of the group Γ_n with this property.

Suppose that the Coxeter polyhedron P is simple. By Theorem 2.1, P is either isometric to the polyhedron $P_0 \subset \text{Isom}\mathbb{H}^4$ depicted in Figure 1, or P has a pair of disjoint facets. For the growth rate τ of the Coxeter group associated to P_0 , one easily checks with help of the software CoxIter [7, 8] that $\tau_{\Gamma_4} < \tau \approx 2.8383$. Hence, we can assume that P is not isometric to P_0 . If P has a pair of disjoint facets, then the Coxeter graph Σ of P and its associated group Γ contains a subgraph $\bullet \xrightarrow{\infty} \bullet$.

The property that the Coxeter graph Σ contains such a subgraph of type $\tilde{A}_1 = [\infty]$ allows us to conclude the proof, whether the polyhedron P is simple or not. In the following, we first look at this property and analyze it more closely.

3.1 In the presence of \tilde{A}_1

We start by considering particular Coxeter graphs of order 4 containing \tilde{A}_1 . Their related growth rates will be useful when comparing with the one of Γ . This approach is similar to the one developed in [2].

Let $W_0 = [\infty, 3, 3]$ be the abstract Coxeter group depicted in Figure 5. By means of the software CoxIter, one checks that

$$(7) \quad \tau_{\Gamma_4} < \tau_{W_0} \approx 1.4655.$$

Furthermore, consider the two abstract Coxeter groups $W_1 = [3, \infty, 3]$ and $W_2 = [\infty, 3^{1,1}]$ given in Figure 6.

For their growth rates, we prove the following auxiliary result.

Lemma 3.1 $\tau_{W_0} < \tau_{W_1}$ and $\tau_{W_0} < \tau_{W_2}$.

Proof For $0 \leq i \leq 2$, denote by $f_i := f_{W_i}$ the growth series of W_i and by R_i its radius of convergence. Recall that R_i is the smallest positive pole of f_i , and that $\tau_{W_i} = \frac{1}{R_i}$.

We establish the growth functions f_i according to Steinberg’s formula (2). They are given as follows:

$$\frac{1}{f_0(t^{-1})} = 1 - \frac{4}{[2]} + \frac{3}{[2,2]} + \frac{2}{[2,3]} - \frac{1}{[2,2,3]} - \frac{1}{[2,3,4]},$$

$$\frac{1}{f_1(t^{-1})} = 1 - \frac{4}{[2]} + \frac{3}{[2,2]} + \frac{2}{[2,3]} - \frac{2}{[2,2,3]},$$

$$\frac{1}{f_2(t^{-1})} = 1 - \frac{4}{[2]} + \frac{3}{[2,2]} + \frac{2}{[2,3]} - \frac{1}{[2,2,2]} - \frac{1}{[2,3,4]}.$$

Hence, for any $t > 0$, one has the positive difference functions given by

$$\begin{aligned} \frac{1}{f_0(t^{-1})} - \frac{1}{f_1(t^{-1})} &= \frac{1}{[2,2,3]} - \frac{1}{[2,3,4]} = \frac{t^2+t^3}{[2,2,3,4]} > 0, \\ \frac{1}{f_0(t^{-1})} - \frac{1}{f_2(t^{-1})} &= \frac{1}{[2,2,2]} - \frac{1}{[2,2,3]} = \frac{t^2}{[2,2,2,3]} > 0. \end{aligned}$$

Therefore, for $i = 1, 2$, and for $u = t^{-1} \in (0, 1)$, the smallest positive root R_0 of $\frac{1}{f_0(u)}$ is strictly bigger than the one of $\frac{1}{f_i(u)}$. This finishes the proof.

As a first consequence, combining (5), (7), and Lemma 3.1, one obtains that

$$(8) \quad \tau_{\Gamma_n} < \tau_{W_i},$$

for all $4 \leq n \leq 9$ and $0 \leq i \leq 2$.

Next, suppose that the Coxeter graph Σ of Γ contains a subgraph \tilde{A}_1 . Since Σ is connected of order $N \geq n + 2 \geq 6$, the subgraph \tilde{A}_1 is contained in a connected subgraph σ of order 4 in Σ , which is related to a special subgroup W of Γ . By Theorem 2.2, one has that $\tau_{W_i} \leq \tau_W$ for some $0 \leq i \leq 2$. By combining (8) with these findings, and by Theorem 2.2 and Lemma 3.1, one deduces that

$$(9) \quad \tau_{\Gamma_n} < \tau_{W_0} \leq \tau_W \leq \tau_{\Gamma}.$$

This finishes the proof of the Theorem in the presence of a subgraph \tilde{A}_1 in Σ .

3.2 In the absence of \tilde{A}_1

Suppose that the Coxeter graph Σ with $N \geq n + 2$ nodes does *not* contain a subgraph of type \tilde{A}_1 . In particular, by Theorem 2.1, the corresponding Coxeter polyhedron $P \subset \text{Isom}\mathbb{H}^n$ is not simple, and it follows that $5 \leq n \leq 9$.

Consider a non-simple ideal vertex $v_\infty \in P$. Its link $L_\infty \subset \mathbb{E}^{n-1}$ is described by a reducible affine subgraph σ_∞ with $n_c = n_c(\infty) \geq 2$ components which satisfies $n - 1 = \text{order}(\sigma_\infty) - n_c$ by (1). In Table 3, we list all possible realizations for σ_∞ by using the following notations.

Let $\tilde{\sigma}_k$ be a connected affine Coxeter graph of order $k \geq 3$ as listed in Table 2, and denote by $\bigsqcup_k \tilde{\sigma}_k$ the Coxeter graph consisting of the components of type $\tilde{\sigma}_k$.

Observe that for any graph $\bigsqcup_k \tilde{\sigma}_k$ in Table 3, one has $3 \leq \min_k k \leq 5$, and that the case $\min_k k = 5$ appears only when $n = 9$.

Among the different components of σ_∞ , we consider the ones of smallest order ≥ 3 together with their extensions.

- Assume that the graph σ_∞ of the vertex link L_∞ contains an affine component $\tilde{\sigma}$ of order 3. By Example 2.3, we know that any extension of $\tilde{\sigma}$ encodes a Coxeter tetrahedral group $\Lambda \subset \text{Isom}\mathbb{H}^3$ of finite covolume. The graph Σ itself contains a subgraph σ of order 4 which in turn comprises $\tilde{\sigma}$. The Coxeter graph σ corresponds to a special subgroup W of Γ , and by Theorem 2.2, we deduce that $\tau_\Lambda \leq \tau_W$.

Table 3: Reducible affine Coxeter graphs σ_∞ with $n_c \geq 2$ components $\tilde{\sigma}_k$ of order $k \geq 3$ such that $n = \text{order}(\sigma_\infty) - n_c + 1$.

n	5	6	7	8	9
	$\tilde{\sigma}_3 \sqcup \tilde{\sigma}_3$	$\tilde{\sigma}_3 \sqcup \tilde{\sigma}_4$	$\tilde{\sigma}_3 \sqcup \tilde{\sigma}_5$ $\tilde{\sigma}_4 \sqcup \tilde{\sigma}_4$ $\tilde{\sigma}_3 \sqcup \tilde{\sigma}_3 \sqcup \tilde{\sigma}_3$	$\tilde{\sigma}_3 \sqcup \tilde{\sigma}_6$ $\tilde{\sigma}_4 \sqcup \tilde{\sigma}_5$ $\tilde{\sigma}_3 \sqcup \tilde{\sigma}_3 \sqcup \tilde{\sigma}_4$	$\tilde{\sigma}_3 \sqcup \tilde{\sigma}_7$ $\tilde{\sigma}_4 \sqcup \tilde{\sigma}_6$ $\tilde{\sigma}_5 \sqcup \tilde{\sigma}_5$ $\tilde{\sigma}_3 \sqcup \tilde{\sigma}_4 \sqcup \tilde{\sigma}_4$ $\tilde{\sigma}_3 \sqcup \tilde{\sigma}_3 \sqcup \tilde{\sigma}_3 \sqcup \tilde{\sigma}_3$

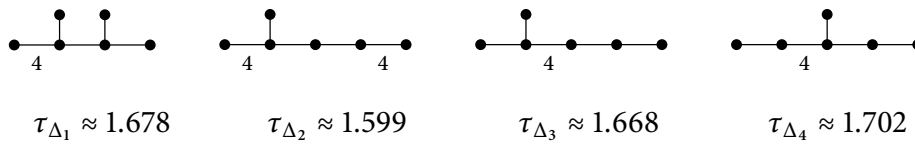


Figure 7: The Coxeter groups $\Delta_i, i = 1, \dots, 4$.

Since $\tau_{\Gamma_3} \leq \tau_\Lambda$, and in view of (5) and (6), Theorem 2.2 yields the desired inequality

$$(10) \quad \tau_{\Gamma_n} < \tau_{\Gamma_3} \leq \tau_\Lambda \leq \tau_W \leq \tau_\Gamma,$$

which finishes the proof in this case, and for $n = 5$ and $n = 6$; see Table 3.

- Assume that the graph σ_∞ contains an affine component $\tilde{\sigma}$ of order 4. We apply the same reasoning as above. By Example 2.4, any extension of $\tilde{\sigma}$ corresponds to a Coxeter 4-simplex group Λ of finite covolume, and $\tau_{\Gamma_4} \leq \tau_\Lambda$. Again, Σ contains a subgraph σ comprising $\tilde{\sigma}$. Hence, there exists a special subgroup W of Γ described by σ so that

$$(11) \quad \tau_{\Gamma_n} < \tau_{\Gamma_4} \leq \tau_\Lambda \leq \tau_W \leq \tau_\Gamma.$$

By (10) and (11), the proof is finished in this case, and for $n = 7$ and $n = 8$; see Table 3.

- Assume that σ_∞ contains an affine component $\tilde{\sigma}$ of order 5. By Table 3, one has $7 \leq n \leq 9$. It is not difficult to list all possible extensions of $\tilde{\sigma}$. There are exactly 15 such extensions. It turns out that there are 11 extensions that encode Coxeter 5-simplex groups of finite covolume, whereas the remaining 4 extensions describe 5-simplex groups $\Delta_i, i = 1, \dots, 4$, of infinite covolume. These last four simplices arise by extending \tilde{B}_4, \tilde{C}_4 , and \tilde{F}_4 . They are given in Figure 7, together with their associated growth rates computed with CoxIter.

In view of (5), it turns out that

$$(12) \quad \tau_{\Gamma_5} < \tau_{\Delta_i}, \quad \text{for } i = 1, \dots, 4.$$

As above, the component $\tilde{\sigma}$ lies in a subgraph σ of order 6 in Σ , and the latter corresponds to a special subgroup W of Γ so that

$$\text{either } \tau_\Lambda \leq \tau_W \quad \text{or} \quad \tau_{\Delta_i} \leq \tau_W, \quad 1 \leq i \leq 4$$

where Λ is a Coxeter 5-simplex group of finite covolume. Since $\tau_{\Gamma_5} \leq \tau_{\Lambda}$, and by (5) and (12), one deduces that

$$(13) \quad \tau_{\Gamma_n} < \tau_{\Gamma_5} \leq \tau_W \leq \tau_{\Gamma}.$$

This finishes the proof of this case.

Finally, all the above considerations allow us to conclude the proof of the Theorem.

Acknowledgment The author would like to express her gratitude to her supervisor Ruth Kellerhals for all the expert advice and support throughout this project.

References

- [1] N. Bourbaki, *Groupes et algèbres de Lie: Chapitres 4 à 6*. Hermann, Paris, 1968.
- [2] N. Bredon and R. Kellerhals, *Hyperbolic Coxeter groups and minimal growth rates in dimensions four and five*. To appear in *Groups Geom. Dyn.*, 2021. [arXiv:2008.10961v3](https://arxiv.org/abs/2008.10961v3)
- [3] H. S. M. Coxeter, *Discrete groups generated by reflections*. *Ann. of Math. (2)* 35(1934), 588–621.
- [4] A. Felikson, *Hyperbolic Coxeter polytopes*.
<https://www.maths.dur.ac.uk/users/anna.felikson/Polytopes/polytopes.html>
- [5] A. Felikson and P. Tumarkin, *On hyperbolic Coxeter polytopes with mutually intersecting facets*. *J. Combin. Theory Ser. A* 115(2008), 121–146.
- [6] W. Floyd, *Growth of planar Coxeter groups, P.V. numbers, and Salem numbers*. *Math. Ann.* 293(1992), 475–483.
- [7] R. Guglielmetti, *CoxIter—Computing invariants of hyperbolic Coxeter groups*. *LMS J. Comput. Math.* 18(2015), 754–773.
- [8] R. Guglielmetti, *CoxIterWeb*. <https://coxiterweb.rafaelguglielmetti.ch/>
- [9] T. Hild, *The cusped hyperbolic orbifolds of minimal volume in dimensions less than ten*. *J. Algebra* 313(2007), 208–222.
- [10] T. Hild and R. Kellerhals, *The fcc lattice and the cusped hyperbolic 4-orbifold of minimal volume: In memoriam H. S. M. Coxeter*. *J. Lond. Math. Soc. (2)* 75(2007), 677–689.
- [11] J. Humphreys, *Reflection groups and Coxeter groups*, Cambridge Studies in Advanced Mathematics, 29, Cambridge University Press, Cambridge, 1990.
- [12] N. Johnson, R. Kellerhals, J. Ratcliffe, and S. Tschantz, *The size of a hyperbolic Coxeter simplex*. *Transform. Groups* 4(1999), 329–353.
- [13] R. Kellerhals, *Cofinite hyperbolic Coxeter groups, minimal growth rate and Pisot numbers*. *Algebr. Geom. Topol.* 13(2013), 1001–1025.
- [14] R. Kellerhals and G. Perren, *Growth of cocompact hyperbolic Coxeter groups and their rate*. *European J. Combin.* 32(2011), 1299–1316.
- [15] R. Meyerhoff, *The cusped hyperbolic 3-orbifold of minimum volume*. *Bull. Amer. Math. Soc.* 13(1985), 154–156.
- [16] C. L. Siegel, *Some remarks on discontinuous groups*. *Ann. of Math. (2)* 46(1945), 708–718.
- [17] T. Terragni, *On the growth of a Coxeter group (extended version)*. Preprint, 2015.
[arXiv:1312.3437v2](https://arxiv.org/abs/1312.3437v2)
- [18] T. Terragni, *On the growth of a Coxeter group*. *Groups Geom. Dyn.* 10(2016), 601–618.
- [19] È. Vinberg, *Hyperbolic reflection groups*. *Uspekhi Mat. Nauk* 40(1985), 29–66, 255.
- [20] È. Vinberg, *Geometry II*, Encyclopaedia of Mathematical Sciences, 29, Springer, Berlin, 1993.

Department of Mathematics, University of Fribourg, CH-1700 Fribourg, Switzerland
e-mail: naomi.bredon@unifr.ch

BIBLIOGRAPHY

- [1] D. Allcock, *Infinitely many hyperbolic Coxeter groups through dimension 19*, *Geom. Topol.* 10 (2006), 737–758.
- [2] E. M. Andreev, *On convex polyhedra of finite volume in Lobachevskii spaces*, *Math. USSR Sbornik* 12 (1970), 255–259.
- [3] M. Belolipetsky, *On volumes of arithmetic quotients of $SO(1,n)$* , *Ann. Sc. Norm. Super. Pisa Cl. Sci. (5)* 3 (2004), 749–770.
- [4] M. Belolipetsky, *On volumes of arithmetic quotients of $SO(1,n)$* , *Ann. Sc. Norm. Super. Pisa Cl. Sci. (5)* 6 (2007), 263–268.
- [5] R. E. Borcherds, *Automorphism groups of Lorentzian lattices*, *J. Algebra* 111 (1987), 133–153.
- [6] N. Bourbaki, *Groupes et algèbres de Lie*, Ch. 4-6. Hermann, Paris, 1968.
- [7] N. Bredon, R. Kellerhals, *Hyperbolic Coxeter groups and minimal growth rates in dimensions four and five*, *Groups Geom. Dynamics* 16 (2022), 725–741.
- [8] N. Bredon, *Hyperbolic Coxeter groups of minimal growth rates in higher dimensions*, *Canad. Math. Bull.* 66 (2023), 232–242.
- [9] N. Bredon, T. Yukita, *Coxeter systems with 2-dimensional Davis complexes, growth rates and Perron numbers*, to appear in *Algebraic & Geometric Topology*, 2022.
- [10] N. Bredon, *On ADEG-polyhedra in hyperbolic space*, Preprint in preparation, 2024.

-
- [11] V. O. Bugaenko, *Arithmetic crystallographic groups generated by reflections, and reflective hyperbolic lattices*, Advances in Soviet Mathematics 8 (1992), 33–55.
- [12] A. Burcroff, *Near classification of compact hyperbolic Coxeter d -polytopes with $d + 4$ facets and related dimension bounds*, Eur. J. Comb. 120 (2024), 103957.
- [13] J. W. Cannon, P. Wagreich, *Growth functions of surface groups*, Math. Ann. 293 (1992), 239–257.
- [14] R. Charney, M.W. Davis, *Reciprocity of growth functions of Coxeter groups*, Geom. Dedicata 39 (1991), 373–378.
- [15] M. Chein, *Recherche des graphes des matrices des Coxeter hyperboliques d'ordre ≤ 10* , Modélisation Mathématique et Analyse Numérique, Vol. 3 (1969), 3–16.
- [16] H. S. M. Coxeter, *Discrete groups generated by reflections*, Ann. Math. 35 (1934), 588–621.
- [17] P. de la Harpe, *Topics in geometric group theory*, Chicago Lect. in Math., The University of Chicago Press, Chicago, London, 2000.
- [18] V. Emery, R. Kellerhals, *The three smallest compact arithmetic hyperbolic 5-orbifolds*, Algebr. Geom. Topol. 13 (2013), 817–829.
- [19] V. Emery, *On volumes of quasi-arithmetic hyperbolic lattices*, Selecta Math. 23 (2017), 2849–2862.
- [20] F. Esselmann, *Über kompakte, hyperbolische Coxeter-Polytope mit wenigen Facetten*, SFB 343 preprint , Bielefeld (1994), 94–087.
- [21] F. Esselmann, *The classification of compact hyperbolic Coxeter d -polytopes with $d + 2$ facets*, Comment. Math. Helvetici 71 (1996), 229–242.
- [22] B. Everitt, *Coxeter groups and hyperbolic manifolds*, Math. Ann. 330 (2004), 127–150.
- [23] A. Felikson, *Hyperbolic Coxeter polytopes*, www.maths.dur.ac.uk/users/anna.felikson/Polytopes/polytopes.html
- [24] A. Felikson, P. Tumarkin, *On hyperbolic Coxeter polytopes with mutually intersecting facets*, J. Combin. Theory Ser. A 115 (2008), 121–146.

- [25] A. Felikson, P. Tumarkin, *Essential hyperbolic Coxeter polytopes*, Israel Journal of Mathematics 199 (2014), 113–161.
- [26] A. Felikson, P. Tumarkin, *Coxeter polytopes with a unique pair of non-intersecting facets*, J. Combin. Theory A 116 (2009), 875–902.
- [27] A. Felikson, P. Tumarkin, *On compact hyperbolic Coxeter d -polytopes with $d + 4$ facets*, Trans. Moscow Math. Soc. 69 (2008), 105–151.
- [28] W. Floyd, S. Plotnick, *Symmetries of planar growth functions*, Invent. Math. 93 (1988), 501–543.
- [29] W. Floyd, *Growth of planar Coxeter groups, PV numbers, and Salem numbers*, Math. Ann. 293 (1992), 475–483.
- [30] R. Guglielmetti, *CoxIter – computing invariants of hyperbolic Coxeter groups*, LMS J. Comput. Math. 18 (2015), 754–773.
- [31] R. Guglielmetti, *CoxIterWeb*, <https://coxiterweb.rafaelguglielmetti.ch/>
- [32] R. Guglielmetti, *Hyperbolic isometries in (in-)finite dimensions and discrete reflection groups: theory and computations*, Ph.D. thesis no. 2008, Université de Fribourg, 2017.
- [33] R. Guglielmetti, M. Jacquemet, R. Kellerhals, *Commensurability of hyperbolic Coxeter groups: theory and computation*, RIMS Kôkyûroku Bessatsu B66 (2017), 57–113.
- [34] T. Hild, R. Kellerhals, *The fcc lattice and the cusped hyperbolic 4-orbifold of minimal volume*, J. Lond. Math. Soc. 75 (2007), 677–689.
- [35] T. Hild, *The cusped hyperbolic orbifolds of minimal volume in dimensions less than ten*, J. Algebra 313 (2007), 208–222.
- [36] E. Hironaka, *The Lehmer polynomial and pretzel links*, Canad. Math. Bull. 44 (2001), 440–451.
- [37] J. Humphreys, *Reflection groups and Coxeter groups*, Cambridge Studies in Advanced Mathematics, vol. 29, Cambridge University Press, Cambridge, 1990.
- [38] H. Ch. Im Hof, *Napier cycles and hyperbolic Coxeter groups*, Bull. Soc. Math. de Belg. Serie A (1990), 523–545.
- [39] M. Jacquemet, S. Tschantz, *All hyperbolic Coxeter n -cubes*, J. Combin. Theory A 158 (2018), 387–406.

-
- [40] N. Johnson, R. Kellerhals, J. Ratcliffe, and S. Tschantz, *The size of a hyperbolic Coxeter simplex*, *Transform. Groups* 4 (1999), 329–353.
- [41] N. Johnson, R. Kellerhals, J. Ratcliffe, and S. Tschantz, *Commensurability classes of hyperbolic Coxeter simplex reflection groups*, *Linear Algebra Appl.* 345 (2002), 119–147.
- [42] I. M. Kaplinskaja, *The discrete groups generated by reflections in the faces of simplicial prisms in Lobachevskii spaces*, *Math. Notes* 15 (1974), 88–91.
- [43] R. Kellerhals, A. Kolpakov, *The minimal growth rate of cocompact Coxeter groups in hyperbolic 3-space*, *Canad. J. Math.* 66 (2014), 354–372.
- [44] R. Kellerhals, L. Liechti, *Salem numbers, spectral radius and growth rates of hyperbolic Coxeter groups*, *Transformation Groups* 28 (2023), 831–852.
- [45] R. Kellerhals, G. Perren, *Growth of cocompact hyperbolic Coxeter groups and their rate*, *European J. Combin.* 32 (2011), 1299–1316.
- [46] R. Kellerhals, *Cofinite hyperbolic Coxeter groups, minimal growth rate and Pisot numbers*, *Algebr. Geom. Topol.* 13 (2013), 1001–1025.
- [47] R. Kellerhals, *Hyperbolic orbifolds of minimal volume*, *Comput. Methods Funct. Theory* 14, no. 2-3 (2014), 465–481.
- [48] R. Kellerhals, *On minimal covolume hyperbolic lattices*, in: Special Issue “Geometry of Numbers”, MDPI Mathematics 2017, vol. 5, 16 pp.
- [49] A. G. Khovanskii, *Hyperplane sections of polyhedra, toric varieties and discrete groups in Lobachevsky space*, *Functional Analysis and its applications*, V. 20, N 1, 50–61, 1986; translation in *Funct. Anal. Appl.* V. 20 no. 1 (1986), 41–50.
- [50] A. Kolpakov, *Deformation of finite-volume hyperbolic Coxeter polyhedra, limiting growth rates and Pisot numbers*, *European J. Combin.* 33 (2012), 1709–1724
- [51] A. Kolpakov, A. Talambutsa, *Growth rates of Coxeter groups and Perron numbers*, *International Mathematics Research Notices* 19 (2022), 14675–14696.

Bibliography

- [52] Y. Komori, T. Yukita, *On the growth rate of ideal Coxeter groups in hyperbolic 3-space*, Proc. Japan Acad. Ser. A Math. Sci. 91 (2015), 155–159.
- [53] J.-L. Koszul, *Lectures on hyperbolic Coxeter groups*, University of Notre Dame, 1967.
- [54] F. Lannér, *On complexes with transitive groups of automorphisms*, Comm. Sem. Math. Univ. Lund 11 (1950), 1–71.
- [55] J. Ma, F. Zheng, *Compact hyperbolic Coxeter four-polytopes with eight facets*. J. Algebr. Comb. 59 (2024), 225–290.
- [56] J. Ma, F. Zheng, *Compact hyperbolic Coxeter five-dimensional polytopes with nine facets*. Transform. Groups (2024), 1–37.
- [57] C. Maclachlan, *Commensurability classes of discrete arithmetic hyperbolic groups*, Groups Geom. Dynamics 5 (2011), 767–785.
- [58] C. Maclachlan, A. W. Reid, *The arithmetic of hyperbolic 3-manifolds*, Graduate Texts in Mathematics Vol. 219 (2002) Springer, Berlin.
- [59] G. J. Martin, *Siegel’s problem in three dimensions*, Notices Amer. Math. Soc. 63 (2016), 1244–1247.
- [60] C. T. McMullen, *Coxeter groups, Salem numbers and the Hilbert metric*, Publ. Math. Inst. Hautes Etudes Sci. 95 (2002), 151–183.
- [61] J. Meleod, *Hyperbolic Coxeter pyramids*, Advances in Pure Mathematics 3 (2013), 78–82.
- [62] R. Meyerhoff, *The cusped hyperbolic 3-orbifold of minimum volume*, Bull. Amer. Math. Soc. 13 (1985), 154–156.
- [63] J. Milnor, *A note on curvature and fundamental group*, J. Differential Geometry 2 (1968), 1–7.
- [64] V. V. Nikulin, *Factor groups of groups of automorphisms of hyperbolic forms with respect to subgroups generated by 2-reflections*, Dokl. Akad. Nauk SSSR. Vol. 248 (1979), 1307–1309.
- [65] V. V. Nikulin, *Discrete reflection groups in Lobachevsky spaces and algebraic surfaces*, Proc. Intern. Congress of Math. Berkeley, 1986.
- [66] J. Nonaka, R. Kellerhals, *The growth rates of ideal Coxeter polyhedra in hyperbolic 3-space*, Tokyo J. Math. 40 (2017), 379–391.

-
- [67] W. Parry, *Growth series of Coxeter groups and Salem numbers*, J. Algebra, 154 (1993), 406–415.
- [68] H. Poincaré, *Théorie des groupes fuchsien*s, Acta Math. 1 (1882), 1–62.
- [69] M. N. Prokhorov, *The absence of discrete reflection groups with non-compact fundamental polyhedron of finite volume in Lobachevskij spaces of large dimension*, Math. USSR Izv. 28 (1987), 401–411.
- [70] M. N. Prokhorov, *On polyhedra of finite volume in Lobachevskij spaces with dihedral angle $\pi/2$ and $\pi/3$* , Lecture in mathematics and its applications, Vol 2, No.2 (Russian), Inst. Mat. im. Steklova (1988), 151–187.
- [71] J. G. Ratcliffe, *Foundations of hyperbolic manifolds*, Graduate Texts in Mathematics Vol. 149 (1994) Springer, Berlin.
- [72] M. Roberts, *A classification of non-compact Coxeter polytopes with $n+3$ facets and one non-simple vertex*, arXiv:1511.08451.
- [73] C. L. Siegel, *Some remarks on discontinuous groups*, Ann. Math. 46 (1945), 708–718.
- [74] L. Solomon, *The orders of the finite Chevalley groups*, J. Algebra 3 (1966), 376–393.
- [75] R. Steinberg, *Endomorphisms of linear algebraic groups*, Mem. Amer. Math. Soc. 80 (1968).
- [76] T. Terragni, *On the growth of a Coxeter group*, Groups Geom. Dyn. 10 (2016), 601–618.
- [77] T. Terragni, *On the growth of a Coxeter group (extended version)*, arXiv:1312.3437v2.
- [78] P. Tumarkin, *Hyperbolic Coxeter n -polytopes with $n+2$ facets*, Math. Notes 75 (2004), 848–854.
- [79] P. Tumarkin, *Non-compact hyperbolic Coxeter n -polytopes with $n+3$ facets*, Russian Math. Surveys 58 (2003), 805–806.
- [80] P. Tumarkin, *Compact hyperbolic Coxeter n -polytopes with $n+3$ facets*, Electron. J. Combin. 14 (2007), 36pp.
- [81] È. B. Vinberg, *Discrete groups generated by reflections in Lobachevskii space*, Math. USSR Sbornik 114 (1967), 429–444.

Bibliography

- [82] È. B. Vinberg, *Hyperbolic reflection groups*, Uspekhi Mat. Nauk 40 (1985), 29–66, 255.
- [83] È. B. Vinberg, *The absence of crystallographic groups of reflections in Lobachevsky spaces of large dimensions*, Trans. Moscow Math. Soc. 47 (1985), 75–112.
- [84] È. B. Vinberg, *Geometry II*, Encyclopaedia of Mathematical Sciences, vol. 29, Springer-Verlag, Berlin, 1993.
- [85] Wolfram Research, Inc. Mathematica, Champaign, IL, 2010.
- [86] T. Yukita, *Growth rates of 3-dimensional hyperbolic Coxeter groups are Perron numbers*, Canad. Math. Bull. 61 (2018), 405–422.
- [87] R. J. Zimmer, *Ergodic Theory and Semisimple Groups*, Monographs in Mathematics Vol. 81, Birkhäuser, Basel (1984).

Naomi Bredon

Birth: 11.10.1996
Citizenship: French
Gender: Female

Current Position

Since 12.19 **Graduate Assistant**, University of Fribourg.

Education

Since 12.19 **PhD Studies in Mathematics**, University of Fribourg.
Advisor: Prof. Dr. Ruth Kellerhals.
09.17 – 07.19 **Master of Science in Mathematics** ALGANT International,
University of Bordeaux.
03.15 – 07.17 **Bachelor of Science in Mathematics**, University of Bor-
deaux.
09.14 – 02.15 **Preparatory classes MPSI**, Lycée Camille Julian, Bor-
deaux.

Publications

[3] **Coxeter systems with 2-dimensional Davis complexes, growth rates and Perron numbers**, with T. Yukita. Accepted for publication in Algebraic & Geometric Topology, 2022.

[2] **Hyperbolic Coxeter groups of minimal growth rates in higher dimensions**, Can. Math. Bull. 66 (2023), 232–242.

[1] **Hyperbolic Coxeter groups and minimal growth rates in dimensions four and five**, with R. Kellerhals. Groups Geom. Dyn. 16 (2022), 725–741.

Invited Talks

04.24 **On the classification of hyperbolic Coxeter polyhedra**
Geometry Seminar, MPI for Mathematics in the Sciences, Leipzig.
03.24 **Hyperbolic Coxeter polyhedra with mutually intersecting facets**
Séminaire Groupes et Géométrie, University of Geneva.
01.24 **Sur la classification des groupes de Coxeter hyperboliques**
Séminaire de Géométrie et Topologie, University of Marseille.
11.23 **On the classification of hyperbolic Coxeter polyhedra**
Paroles aux jeunes chercheurs en géométrie et dynamique, GDR Platon,
University of Grenoble.
04.23 **Coxeter polyhedra and reflection groups**
Geometry graduate colloquium, ETH Zurich.
03.23 **Growth rates of Coxeter systems and Perron numbers**
SMS Doctoral day, University of Neuchâtel.
01.23 **Groupes de Coxeter hyperboliques et taux de croissance**
Séminaire virtuel francophone de groupes et géométrie.
12.22 **Minimal growth rates for hyperbolic Coxeter groups**
Geometry and Topology seminar, Israel Institute of Technology.
11.22 **Hyperbolic Coxeter groups and their growth rates**
Bern-Fribourg Graduate Seminar, University of Bern.

Departmental Talks

- 12.23 **Hyperbolic Coxeter polyhedra with dihedral angles $\frac{\pi}{2}$, $\frac{\pi}{3}$ and $\frac{\pi}{6}$**
Oberseminar Geometrie, University of Fribourg.
- 11.22 **Coxeter systems, growth rates and Perron numbers**
Oberseminar Geometrie, University of Fribourg.
- 05.22 **Hyperbolic manifolds and Coxeter groups**
Oberseminar Geometrie, University of Fribourg.
- 05.22 **Hyperbolic Coxeter groups of minimal growth rates**
SMS Doctoral day, University of Fribourg.
- 12.20 **Hyperbolic Coxeter groups and minimal growth rates – a follow up.** Oberseminar Geometrie, University of Fribourg.
- 11.20 **Hyperbolic Coxeter groups and minimal growth rates in $\text{Isom}\mathbb{H}^4$** Oberseminar Geometrie, University of Fribourg.

Conference Participation

- 11.23 **CUSO Graduate Colloquium**, University of Fribourg.
- 11.23 **Parole aux jeunes chercheuses et chercheurs du réseau Platon**,
Institut Fourier, Grenoble.
- 07.23 **Borel Seminar - Lattices in Negative Curvature**, SwissMAP Re-
search Station, Les Diablerets.
- 03.23 **Groups of Dynamical Origins, Automata and Spectra**,
SwissMAP Research Station, Les Diablerets.
- 11.22 **Discrete and locally compact groups**, ENS Lyon.
- 07.22 **Complex hyperbolic Geometry**, CIRM, Luminy.
- 07.21 **Swiss Knots**, University of Fribourg.

Attended Weekly Seminar

Oberseminar Geometrie (UniFr).
Bern-Fribourg Graduate Seminar (UniFr, UniBe).

Teaching Experience

Graduate Assistant at University of Fribourg for the following courses.

Linear Algebra	SP2020, SA2021-SP2022, SA2023-SP2024
Algebra and Geometry	SA2020-SP2021, SA2022-SP2023
Discrete Mathematics	From SP2020 to SP2024
Propedeutic Analysis	12.2019

Voluntary tutoring at University of Bordeaux from 2016 to 2019.

Outreach

- 2022 Active participation for the “Math Week”, University of Fribourg.
- 2017-2019 Contribution to the events “Filles et Maths”, University of Bordeaux.

Language skills

French: Native. English: Full professional proficiency.

Personal interests

Climbing, Hiking, Music.